

**NEW MINIMAL SUPERSYMMETRIC SO(10) GUT
PHENOMENOLOGY AND ITS COSMOLOGICAL
IMPLICATIONS**

A THESIS

Submitted to the
FACULTY OF SCIENCE
PANJAB UNIVERSITY, CHANDIGARH
for the degree of
DOCTOR OF PHILOSOPHY

2014

ILA GARG

DEPARTMENT OF PHYSICS
CENTRE OF ADVANCED STUDY IN PHYSICS
PANJAB UNIVERSITY
CHANDIGARH, INDIA

Dedicated To My Parents

Acknowledgements

I express my deep gratitude to my thesis supervisor Prof. C. S. Aulakh for his constant help and support during my Ph.D. His knowledge, vision and understanding in particle physics is invincible. He helped me to improve my personality as a scientist. I am also thankful to him for providing a healthy and open environment for research.

I am very thankful to my family members for their constant moral support, love, faith and prays for me. Without their support I won't be able to make it.

I would like to say thanks to my co-scholar Charanjit Kaur whom I know from my M.Sc. days. She is a part of this journey from the very beginning. Healthy discussions with her always helped me a pile to tackle even difficult problems.

I would like to recognize my friends Tanvi Vashisht, Jagdish Kaur, Rajni Jain, Simanpreet Kaur, Amandeep Chahal, Pankaj Verma, Rohit Sharma, Sukhjit Kaur, Sonika Goyal for having delightful moments during tough times and making life easy away from home. A special thanks to Anubha Jindal, Pranati Rath, Deepika Makkar, Aman Jindal for their constant support and encouragement.

I sincerely pay my regards to the Chairperson of our Department for the research facilities provided. I would like to say thank to all the members of this department for providing me all kind of help. I am also thankful to council of scientific and industrial research (CSIR) of India for providing me the generous funding during the course of my research work.

Above all I am grateful to God for providing me the strength and good health to accomplish this task. Last but not least I thank all who were directly or indirectly involved in the fulfillment of this project.

Date:01/04/2015

Ila Garg

Abstract

Supersymmetric GUTs based on $SO(10)$ gauge group are leading contenders to describe particle physics beyond the Standard Model. Among these the “New minimal supersymmetric $SO(10)$ grand unified theory” (NMSGUT) based on Higgs system $10+120+210+126+\overline{126}$ has been developing since 1982. It now successfully fits the whole standard Model gauge coupling, symmetry breaking and fermion mass-mixing data as well as the neutrino mass and mixing data in terms of NMSGUT parameters and just 6 soft supersymmetry breaking parameters defined at the GUT scale. In this thesis we study the phenomenology of NMSGUT, its implications for inflationary and Cold Dark matter cosmology and develop Renormalization group(RG) equations for the flow of NMSGUT couplings in the extreme ultraviolet.

We carry out a long calculation to show that threshold corrections due to heavy particle spectra to the matching condition between matter Yukawa couplings of the effective Minimal Supersymmetric Standard Model (MSSM) and the NMSGUT Yukawa vertex provide a generic mechanism to cure the long standing problem of fast Baryon decay rate due to dimension five operators. Incorporating these corrections we are able to find regions of the parameter space of NMSGUT superpotential where wave function renormalization of the effective MSSM Higgs doublets is close to the dissolution value ($Z_{H,\overline{H}} = 0$). The $SO(10)$ Yukawas required to match the MSSM fermion data are then lowered after the rescaling required to achieve canonical kinetic terms in the effective MSSM. It is these lowered $SO(10)$ Yukawas will also determine the dimension 5 Baryon number violation operator coefficients. Thus the associated rates can be suppressed to levels which are compatible with current experimental bounds.

Within the context of a supersymmetric model based on an extension of the MSSM gauge group we show that superpotential corresponding to supersymmetric Type-I seesaw for neutrino mass can provide inflection point inflation along a flat direction associated with a gauge invariant combination of the Higgs, slepton and right handed sneutrino superfields. The Majorana mass of a right handed neutrino

sets the scale of inflation. In this scenario the inflation parameters and fine-tuning required for flat inflaton potential is controlled by superpotential parameters rather than soft susy breaking terms which is in contrast to Dirac neutrino-inflation connection and therefore more stable under radiative corrections. Reheating after inflation is necessary for the success of big Bang nucleosynthesis. Reheating in context of supersymmetric seesaw inflation (SSI) via ‘instant preheating’ mechanism is presented. The high reheat temperature $\sim 10^{11}$ - 10^{13} GeV in this scenario requires large gravitino mass greater than 50 TeV to avoid a gravitino problem, pointing towards a high Susy breaking scale. The embedding of SSI in NMSGUT, which accommodates seesaw mechanism to explain neutrino masses and also predicts Susy breaking scale of O(10-100 TeV), is carried out. We discuss the obstacles that arose while embedding SSI in the NMSGUT and revisit the same in the light of new results of large value of tensor to scalar component ratio (r) of cosmic microwave background fluctuations by BICEP2 experiment. We find an improvement in the number of e-folds by 4-orders of magnitude but are still short by a factor of about 50.

In NMSGUT R-parity conservation down to weak scale facilitates Neutralino as lightest stable supersymmetric particle suitable for cold dark matter candidate. We evaluate the relic density of dark matter(DM) on NMSGUT parameter space (using the public DARKSUSY code) for the realistic parameter sets found using GUT scale threshold corrections. We find that solutions with light smuons can yield acceptable DM relic densities.

In addition we also calculated the 2-loop renormalization group equations (RGE) for the parameters of NMSGUT. We show that using RGEs of NMSGUT parameters in the energy range from Planck to GUT scale one can generate negative soft MSSM Higgs mass squared parameters : which were found to be essential for the explanation the distinctive normal hierarchy sparticle spectra found in the NMSGUT at the large $\tan\beta$ values so far investigated.

List of publications

1. C. S. Aulakh and **I. Garg**, “Supersymmetric Seesaw Inflation”, Phys. Rev. D. **86**, 065001 (2012) [arXiv:hep/ph-1201.0519v4]
2. C. S. Aulakh, **I. Garg** and C. K. Khosa, “Baryon stability on the Higgs dissolution edge: threshold corrections and suppression of baryon violation in the NMSGUT,” Nucl. Phys. B **882**, 397 (2014) [arXiv:1311.6100 [hep-ph]].

Contents

Acknowledgements	v
Abstract	vii
List of Publications	ix
List of Figures	xv
List of Tables	xvi

1 Introduction	1
1.1 Outline of thesis	4
2 New Minimal Supersymmetric SO(10) GUT	7
2.1 Introduction	7
2.2 NMSGUT superpotential and symmetry breaking	8
2.3 NMSGUT spectrum	10
2.4 Importance of NMSGUT spectrum	12
2.5 Fermion mass formulae	14
2.6 SM fermion fitting criteria in NMSGUT and its features	16
2.7 Dimension five operators for B,L violation	19

2.8	Problem of fast proton decay ($\tau \sim 10^{28}$ yrs)	22
2.9	Conclusion	23
3	Threshold Corrections and Suppression of d=5, $\Delta B \neq 0$ Operators	25
3.1	Introduction	25
3.2	One loop formula for GUT thresholds	27
3.3	Importance of threshold corrections	30
3.4	Suppression of d=5 operators for B,L violation	32
3.5	Search strategy and conditions imposed on fits	34
3.6	Example fit with description	35
3.7	Conclusions	38
3.8	Appendix A	40
3.9	Appendix B: Example fermion fit with threshold effects	46
4	Inflationary Cosmology	51
4.1	Introduction	51
4.2	Big Bang Cosmology	52
4.3	Shortcomings of Big Bang	54
4.4	The idea of Inflation	56
4.4.1	Standard Big Bang problems revisited	57
4.5	Ingredients of inflationary expansion	58
4.6	Inflection point Inflation Along MSSM Flat Directions	62
4.7	Dirac Neutrino Inflation connection and fine tuning issue	64
4.8	Discussions	66
5	Supersymmetric Seesaw Inflation	69
5.1	Introduction	69
5.2	Generic renormalizable inflection point inflation	71

5.3	Supersymmetric seesaw inflaton model	80
5.4	Conclusions and discussion	85
6	Reheating in Supersymmetric Seesaw Inflation Scenario	87
6.1	Introduction	87
6.2	Instant preheating	88
6.3	Supersymmetric seesaw inflaton	89
6.4	Finding the χ modes	89
6.4.1	Gauge interactions	90
6.4.2	Scalar interactions	94
6.4.3	Fermion interactions	96
6.5	Instant Preheating in context of SSI	97
6.6	Coupled evolution of energy density of χ modes	101
6.7	Conclusion	104
7	Susy Seesaw Inflation and NMSGUT	105
7.1	Introduction	105
7.2	Seesaw inflection and NMSGUT	107
7.3	BICEP2 experiment	111
7.4	Generic renormalizable inflation potential without fine tuning	112
7.5	NMSGUT inflation after BICEP2	115
7.6	Details of Example Fit With Inflation Parameters	118
7.7	Conclusions and discussion	119
7.8	Appendix A	120
8	Relic Density calculation for Neutralino Dark Matter	125
8.1	Introduction	125
8.2	Evidences for dark matter	126

8.2.1	Galactic clusters	126
8.2.2	Galactic rotation curve	127
8.2.3	Gravitational lensing	128
8.2.4	Cosmic microwave background	128
8.3	Detection mechanism	129
8.3.1	Direct detection experiments	129
8.3.2	Indirect detection experiments	130
8.4	Neutralino as a cold DM	131
8.5	Relic density	133
8.6	DarkSusy	138
8.7	NMSGUT and relic density calculation with DarkSusy	140
8.8	Conclusion and discussion	144
9	NMSGUT RGEs	145
9.1	Introduction	145
9.2	Generalized RGEs	147
9.3	SO(10) RGEs for soft parameters	150
9.4	Illustrative run down values of soft parameters at one loop	153
9.5	Discussion	155
9.6	Appendix A	158
10	Summary	175
	Bibliography	179

List of Figures

3.1	1-loop correction to SO(10) Yukawa vertex.	28
4.1	The variation of potential with ϕ . The potential is flat near inflection point at ϕ_0 where inflation occurs.	65
5.1	z_0 contours in the N_{CMB}, n_s plane. The variation shown contributes to the small range of permitted magnitudes for $h^2/M, \Delta/M^2$ etc. . . .	77
5.2	Variation of exponent of $\frac{h^2}{M}$ with N_{CMB} for different values of n_s, P_R .	78
5.3	Variation of exponent of $\frac{\Delta}{M^2}$ with N_{CMB} for different values of n_s, P_R .	79
6.1	Rolling of inflaton around minimum of its potential after inflaton. . .	90
6.2	Evolution of energy densities of inflaton, χ modes and relativistic particles normalized to initial energy density of inflaton (ρ_0) with Mt .	102
6.3	Evolution of energy densities of inflaton, χ modes and relativistic particles normalized to initial energy density of inflaton (ρ_0) with Mt when Hubble expansion rate is large and comparable to M	103
7.1	Plot of quartic coupling h and Number of e-folds for different values of ω at trilinear dimensionless parameter $\tilde{A}=1$. The contour line bears the constant value of ω and different colors of contour represent a range for ω . As we move towards higher values of ω number of e-folds increases and quartic coupling decreases.	115
7.2	Same as figure 7.1 with $\tilde{A}=0.1$	116
7.3	Same as figure 7.1 with $\tilde{A}=0.01$	116
7.4	Same as figure 7.1 with $\tilde{A}=0$	117
8.1	Rotation curve of a typical spiral galaxy. Predicted A and observed B.	127
8.2	The dashed line is the actual abundance, and the solid line is in equilibrium abundance which is boltzmann factor suppressed. . . .	138

- 8.3 Neutralino pair annihilation and Neutralino Smuon coannihilation.
See tables 8.3 and 8.4 for definitions of YZ,X. 142
- 9.1 Variation of Different Higgs masses squared (m_{Φ}^2 (purple), m_{Σ}^2 (red),
 m_{Σ}^2 (green), m_{Θ}^2 (blue), m_H^2 (orange)) from $t=\text{Log}_{10}(10^{18.38})$ to
 $t=\text{Log}_{10}(10^{16.33})$ 154

List of Tables

2.1	$d = 5$ operator mediated proton lifetimes $\tau_p(\text{yrs})$, decay rates $\Gamma(\text{yr}^{-1})$ and Branching ratios in the dominant Meson ⁺ + ν channels.	23
3.1	Examples showing the eigenvalues of the wavefunction renormalization matrices Z_f for fermion lines and for MSSM Higgs ($Z_{H,\bar{H}}$) for solutions found in [27]. In both solutions $Z_{H,\bar{H}}$ are so large that they imply the kinetic terms change sign and in Solution 2 even $Z_{f,\bar{f}}$ have large negative values!	31
3.2	$d = 5$ operator mediated proton lifetimes $\tau_p(\text{yrs})$, decay rates $\Gamma(\text{yr}^{-1})$ and Branching ratios in the dominant Meson ⁺ + ν channels.	38
3.3	Column 1 contains values of the NMSGUT-SUGRY-NUHM parameters at M_X derived from an accurate fit to all 18 fermion data and compatible with RG constraints. Unification parameters and mass spectrum of superheavy and superlight fields are also given. The values of $\mu(M_X), B(M_X)$ are determined by RG evolution from M_Z to M_X of the values determined by the EWRSB conditions.	47
3.4	Solution 2: Fit with $\chi_X = \sqrt{\sum_{i=1}^{17} (O_i - \bar{O}_i)^2 / \delta_i^2} = 0.1326$. Target values, at M_X of the fermion Yukawa couplings and mixing parameters, together with the estimated uncertainties, achieved values and pulls. The eigenvalues of the wavefunction renormalization increment matrices Z_i for fermion lines and the factors for Higgs lines are given. The Higgs fractions $\alpha_i, \bar{\alpha}_i$ which control the MSSM fermion Yukawa couplings are also given. Right handed neutrino threshold effects have been ignored. We have truncated numbers for display although all calculations are done at double precision.	48
3.5	Values of standard model fermion masses in GeV at M_Z compared with the masses obtained from values of GUT derived Yukawa couplings run down from M_X^0 to M_Z both before and after threshold corrections. Fit with $\chi_Z = \sqrt{\sum_{i=1}^9 (m_i^{MSSM} - m_i^{SM})^2 / (m_i^{MSSM})^2} = 0.0557$	49

3.6	Values (in GeV) of the soft Susy parameters at M_Z (evolved from the soft SUGRY-NUHM parameters at M_X). The values of soft Susy parameters at M_Z determine the Susy threshold corrections to the fermion Yukawas. The matching of run down fermion Yukawas in the MSSM to the SM parameters determines soft SUGRY parameters at M_X . Note the heavier third sgeneration. The values of $\mu(M_Z)$ and the corresponding soft Susy parameter $B(M_Z) = m_A^2 \sin 2\beta/2$ are determined by imposing electroweak symmetry breaking conditions. m_A is the mass of the CP odd scalar in the Doublet Higgs. The sign of μ is assumed positive.	49
3.7	Spectra of supersymmetric partners calculated ignoring generation mixing effects. Inclusion of such effects changes the spectra only marginally. Due to the large values of μ, B, A_0 the LSP and light chargino are essentially pure Bino and Wino(\tilde{W}_\pm). The light gauginos and light Higgs h^0 , are accompanied by a light smuon and sometimes selectron. The rest of the sfermions have multi-TeV masses. The mini-split supersymmetry spectrum and large μ, A_0 parameters help avoid problems with FCNC and CCB/UFB instability [56]. The sfermion masses are ordered by generation not magnitude. This is useful in understanding the spectrum calculated including generation mixing effects.	50
3.8	Spectra of supersymmetric partners calculated including generation mixing effects. Inclusion of such effects changes the spectra only marginally. Due to the large values of μ, B, A_0 the LSP and light chargino are essentially pure Bino and Wino(\tilde{W}_\pm). Note that the ordering of the eigenvalues in this table follows their magnitudes, comparison with the previous table is necessary to identify the sfermions.	50
6.1	The χ modes produced due to non-perturbative decay of inflaton. . .	97
7.1	Set of inflation parameters from [31].	111
7.2	Inflation parameters along with parameters b_A, c_A, a_m . Note that $ b_1 , c_1 , a_1 \approx 1$, and rest are very small.	120
7.3	Fit : Column 1 contains values of the NMSGUT-SUGRY-NUHM parameters at M_X derived from an accurate fit to all 18 fermion data and compatible with RG constraints. Unification parameters and mass spectrum of superheavy and superlight fields are also given. The values of $\mu(M_X), B(M_X)$ are determined by RG evolution from M_Z to M_X of the values determined by the EWRSB conditions.	121

- 7.4 Fit with $\chi_X = \sqrt{\sum_{i=1}^{17} (O_i - \bar{O}_i)^2 / \delta_i^2} = 0.9866$. Target values, at M_X of the fermion Yukawa couplings and mixing parameters, together with the estimated uncertainties, achieved values and pulls. The eigenvalues of the wavefunction renormalization increment matrices Z_i for fermion lines and the factors for Higgs lines are given. The Higgs fractions $\alpha_i, \bar{\alpha}_i$ which control the MSSM fermion Yukawa couplings are also given. Right handed neutrino threshold effects have been ignored. We have truncated numbers for display although all calculations are done at double precision. 122
- 7.5 Values of standard model fermion masses in GeV at M_Z compared with the masses obtained from values of GUT derived Yukawa couplings run down from M_X^0 to M_Z both before and after threshold corrections. Fit with $\chi_Z = \sqrt{\sum_{i=1}^9 (m_i^{MSSM} - m_i^{SM})^2 / (m_i^{MSSM})^2} = 0.4014$ 123
- 7.6 Values (GeV) in of the soft Susy parameters at M_Z (evolved from the soft SUGRY-NUHM parameters at M_X). The values of soft Susy parameters at M_Z determine the Susy threshold corrections to the fermion Yukawas. The matching of run down fermion Yukawas in the MSSM to the SM parameters determines soft SUGRY parameters at M_X . Note the heavier third sgeneration. The values of $\mu(M_Z)$ and the corresponding soft Susy parameter $B(M_Z) = m_A^2 \sin 2\beta / 2$ are determined by imposing electroweak symmetry breaking conditions. m_A is the mass of the CP odd scalar in the in the Doublet Higgs. The sign of μ is assumed positive. 123
- 7.7 Spectra of supersymmetric partners calculated ignoring generation mixing effects. Inclusion of such effects changes the spectra only marginally. Due to the large values of μ, B, A_0 the LSP and light chargino are essentially pure Bino and Wino(\tilde{W}_\pm). The light gauginos and light Higgs h^0 , are accompanied by a light smuon and sometimes selectron. The rest of the sfermions have multi-TeV masses. The mini-split supersymmetry spectrum and large μ, A_0 parameters help avoid problems with FCNC and CCB/UFB instability [56]. The sfermion masses are ordered by generation not magnitude. This is useful in understanding the spectrum calculated including generation mixing effects. 124
- 7.8 Spectra of supersymmetric partners calculated including generation mixing effects. Inclusion of such effects changes the spectra only marginally. Due to the large values of μ, B, A_0 the LSP and light chargino are essentially pure Bino and Wino(\tilde{W}_\pm). Note that the ordering of the eigenvalues in this table follows their magnitudes, comparison comparison with the previous table is necessary to identify the sfermions 124

8.1	The input sparticle spectrums in SLHA format to DarkSusy.	141
8.2	Relic Density of neutralino.	141
8.3	Thermally averaged annihilation cross section $\langle \sigma v \rangle$ for Neutralino pair-annihilation into tree level two body final states (YZ). The indices $i=1,..4.$ and $k=1,2.$	143
8.4	Thermally averaged annihilation cross section $\langle \sigma v \rangle$ for Neutralino Smuon coannihilation into tree level two body final states (YZ). The indices $i=1,..4.$ and $k=1,2.$	144
9.1	Dynkin index and Casimir invariant for different field representations of NMSGUT.	152
9.2	Variation of hard parameters of NMSGUT superpotential at 1-loop level. .	155
9.3	Variation of Soft Susy breaking parameters of NMSGUT at 1-loop level. .	156

Chapter 1

Introduction

With the advancement of technology and precision of experimental measurements, the last few decades have added a lot to our understanding of elementary particles and their interactions. The theory of strong, weak and electromagnetic interactions, i.e. the standard model (SM) of particle physics has been developed and established during this time. All the particles of SM (three complete families of elementary leptons and quarks) except Higgs boson (responsible for mass of massive particles in SM via Higgs mechanism) were known by the end of 20th century. In July, 2012, ATLAS and CMS, the two major experimental set-ups at Large Hadron Collider, jointly announced the discovery of a particle at 125 GeV [1, 2] which has properties of SM Higgs boson. This discovery completed the SM in terms of its particle content. The Standard Model now explains low energy phenomena to a precision of better than 1% [3]. But then the question arises, is it the ultimate theory or just a limit of some new theory at high scale? This question is all the more acute as SM is not able to answer some important questions which arise naturally. For example, in the SM without ad-hoc dimension 5 operators neutrinos are massless. However from neutrino oscillations [4, 5] it is well established that neutrinos are massive. SM has no explanation for hierarchial structure of fermion masses and number of generations restricted to three (Flavor problem). The structural instability is another issue i.e. electroweak masses are unstable to loop corrections from heavy particles in the region

between weak scale and Planck scale. It has problems in cosmological sector as well. SM doesn't contain a suitable candidate for dark matter and has no explanation for accelerated expansion of universe i.e. concept of dark energy.

All these limitations of SM led particle theorists to develop Grand Unified theories. The main insight of such theories is that the observed phenomena coded in the peculiar structure of the SM are the low energy manifestation of a fundamental unified theory with a larger gauge symmetry which like the SM symmetry is spontaneously broken (but at a high scale) resulting in the observed SM as the effective theory to an excellent approximation. Grand unification was proposed by J. Pati and Abdus Salam [6] in 1974 by considering a gauge group $SU(4)_c \times SU(2)_L \times SU(2)_R$ as symmetry of nature. The $SU(4)$ group unified the color $SU(3)$ group with $U(1)_{B-L}$ so that Lepton number becomes “fourth color” and the $SU(2)_R$ group parallels the chiral action of $SU(2)_L$ on left chiral fermions thus restoring parity. Thereafter H. Georgi and S. Glashow [7] gave a model which embeds the SM in a $SU(5)$ gauge theory with a SM fermion family in $\bar{\mathbf{5}} + \mathbf{10}$ of $SU(5)$. The other minimal possibility is $SO(10)$ [8]. More refined models are Supersymmetric GUT Models. Susy GUTs are strongly motivated by near exact unification of running gauge couplings at energy scale $\sim 10^{16.33}$ GeV in the minimal supersymmetric standard model (MSSM). Supersymmetry is crucial to maintain the large separation between Electroweak and GUT physics scales.

Supersymmetric Grand unified theories based on the $SO(10)$ gauge group have many attractive features:

- The fundamental **16** dimensional spinor representation of $SO(10)$ contains one family of 15 SM fermions and right handed neutrino necessary for neutrino mass (via Seesaw mechanism [9]).
- Third generation Yukawa unification in large $\tan\beta \simeq 50$ region [10, 11].
- Pati Salam group $SU(4) \times SU(2)_L \times SU(2)_R$ is subgroup of $SO(10)$ so it automatically embeds the minimal supersymmetric Left-Right models [12–14].

-
- B-L even vevs result in R-parity preservation down to the weak scale [15] and consequently a stable Lightest Supersymmetric Particle(LSP) which is the most suitable Weakly Interacting Massive Particle(WIMP) dark matter candidate in modern cosmology.
 - A specific SO(10) model [16–22] based on the $\mathbf{10}+\mathbf{210}+\mathbf{126}+\overline{\mathbf{126}}$ Higgs GUT system has the further remarkable virtues of:
 1. Solution of symmetry breaking at the GUT scale [19].
 2. An explicit calculations of superheavy spectra are available [20, 23–25].
 3. Such theories have intriguing gauge unification threshold effects which can raise the unification scale close to the Planck scale [24].
 4. An old conjecture regarding likely futility [26] of Susy SO(10) due to uncontrollable threshold corrections from GUT scale fields has been disproved [24]. Threshold corrections can emerge in a well controlled way and even lead to interesting mechanisms and phenomena which are characteristics of MSGUTs.

The so called New Minimal Supersymmetric SO(10) GUT (NMSGUT) [27, 28] based on the $\mathbf{10}+\mathbf{210}+\mathbf{120}+\mathbf{126}+\overline{\mathbf{126}}$ Higgs GUT system has all the above mentioned features. The main objective of this thesis is to contribute to making the NMSGUT a possibly viable and complete theory of particle physics and cosmology with the special emphasis on cosmology. The idea is to develop the theory on the same lines and as explicitly as the Standard Model. In order to do this, besides improvements of the computer codes already developed [27, 28] for calculating the effects of the NMSGUT at intermediate and low energies we need to confront the theory to various open problems of particle physics and cosmology. The specific objectives of this thesis are as follows:

1. Study of threshold effects of heavy fields appearing due to GUT scale symmetry breaking and consequently lowering of the strength of $d=5$, $\Delta B \neq 0$ operators resulting in natural suppression of proton decay rate.

2. The study of supersymmetric seesaw inflation (SSI).
3. The reheating mechanism in context of SSI.
4. BICEP2 revolution and NMSGUT inflation.
5. The testing of NMSGUT spectra in dark matter searches for neutralino as a dark matter candidate.
6. The study of NMSGUT RGEs in the region between Planck scale and GUT scale.

1.1 Outline of thesis

The outline of thesis is as follows:

In Chapter **2** we start by discussing the NMSGUT Higgs system, its superpotential and symmetry breaking scheme. We then discuss the crucial superheavy spectrum of NMSGUT and the corrections due to these superheavy fields to the unification scale M_X , the QCD coupling at M_Z ($\alpha_3(M_Z)$) and the gauge coupling at unification scale (α_G): at one loop order. We demonstrate the use of the fermion mass formulae and SM fermion fitting criteria in NMSGUT. Then we present formula for dimension 5 (“d=5”) baryon number violation operators and discuss the problem of fast proton decay in NMSGUT.

Having the tools described in Chapter 2 in hand we present the GUT threshold effects to SO(10) Yukawas in Chapter **3**. The extremely lengthy calculations involving the combination of several thousand terms were done separately by three collaborators: Myself, another Ph.D student C. K. Kaur and our thesis advisor Prof. C. S. Aulakh. This work is published as [29]. Such collaboration was essential to weed out errors over an iterative checking process lasting over one year. We have divided the presentation of results between the two theses since this work is the basis of both and is shared equally. We present the one loop formulas for threshold corrections and give illustrative examples to underline the significance of the GUT scale

threshold effects and the need to include them. We then discuss about lowering of strength of baryon violation $d=5$ operator due to inclusion of threshold corrections. We discuss various aspects of fitting criteria together with threshold effects and give an example solution of NMSGUT parameters which fit fermion mass-mixing data and are compatible with B decay limits. We also present full expression for correction factors to fermion(anti-fermion) line while those for Higgs line can be found in [29, 30].

In Chapter 4 we review early universe cosmology. Starting with the Big Bang and the puzzles of modern cosmology, we discuss the idea of inflation to solve these puzzles. We present the ingredients to have an inflationary epoch and constraints from observations on inflaton potential. We discuss in detail the inflation models based on MSSM flat directions (inflection point inflation) and the fine tuning problem in such models. Then we discuss an example of Dirac-neutrino-inflation connection in this context.

The nature of neutrino mass may be Dirac or Majorana with the latter carrying a special attraction because it allows for a neat explanation for the smallness of neutrino masses, we present the Majorana-neutrino-inflation connection in Chapter 5. We start with discussing about a generic renormalizable inflection point inflation (GRIPI) model followed by supersymmetric seesaw inflation (SSI) and present the conditions on inflationary potential parameters to achieve slow roll inflation conditions. We also discuss about the advantages of our scenario of inflation over Dirac-neutrino-inflation scenario. This work is published as [31].

In Chapter 6 we first discuss the necessity of the reheating after inflation. Then we present one of the mechanism of reheating called “instant preheating”. We present basic steps of how the inflaton energy is dumped into the MSSM degrees of freedom after the end of inflation in context of SSI. Then we present the evolution of densities of different χ modes and estimates of reheating temperature.

In Chapter 7 we discuss embedding of supersymmetric seesaw inflection point inflation in context of NMSGUT. Then in the light of BICEP2 results we present an

analysis of renormalizable inflation potential to achieve slow roll inflation without any fine tuning. Then we revisit Susy Seesaw inflation in NMSGUT. The obstacles and possible solutions to achieve inflation in NMSGUT are discussed.

In Chapter **8** we first review the main issues concerning Dark matter. Then we discuss about possibility of neutralino as candidate for cold dark matter. The relic density calculations for NMSGUT low energy MSSM spectrum using DARKSUSY package are presented. The results and constraints from relic density calculation on NMSGUT parameter space are discussed.

In Chapter **9** we present two loop renormalization group equations for soft parameters for NMSGUT superpotential. This calculation was also very lengthy and done in collaboration with C. K. Khosa and Prof. C. S. Aulakh and hence we present here half of the very extensive formulas. The exploitation of these RGEs has not been done fully but a qualitative view of how soft parameters will run in the region between Planck scale and NMSGUT scale is presented along with the explanation of why this running may play a crucial role in completing the NMSGUT.

In Chapter **10** we present a summary and direction of future research emerging from this thesis.

Chapter 2

New Minimal Supersymmetric SO(10) GUT

2.1 Introduction

The New Minimal Supersymmetric Grand Unified theory (NMSGUT) [27, 28] is based on $\mathbf{210} \oplus \mathbf{10} \oplus \mathbf{120} \oplus \mathbf{126} \oplus \overline{\mathbf{126}}$ Higgs system of SO(10) gauge group. The representations $\mathbf{10}(H_i)$, $\mathbf{120}(\Theta_{ijk})$ are real 1 and 3 index (totally antisymmetric (TAS)), $\mathbf{126}(\Sigma_{ijklm})$ is complex (5 index, TAS, self dual) and $\mathbf{210}(\Phi_{ijkl})$ is 4 index antisymmetric tensor. Here $i, j, k, l, m = 1, 2, \dots, 10$ run over the vector representation of SO(10). The fundamental spinor representation is $\mathbf{16}$ dimensional. The tensor product $\mathbf{16} \times \mathbf{16} = \mathbf{10} + \mathbf{120} + \mathbf{126}$, so there are 3 possible fermion mass generating (FM) Higgs: $\mathbf{10}$, $\mathbf{120}$, $\overline{\mathbf{126}}$. The $\overline{\mathbf{126}}$ plays a dual role i.e. it also acts as AM (adjoint multiplet type) which breaks the SO(10) gauge symmetry to MSSM together with $\mathbf{210}$ plet.

The original MSGUT (Minimal Susy GUT) [16–22] was the renormalizable globally supersymmetric theory (minimal in terms of parameter counting) in which $\mathbf{120}$ plet Higgs was not considered and $\mathbf{10}$ and $\mathbf{126}$ were used to fit fermion data. But MSGUT failed to fit the neutrino mass in the viable parameter space with the available seesaw mechanism (Type I and Type II). In MSGUT Type I is dominant

over Type II and Type I seesaw masses are one order of magnitude short [33, 34] of those required by atmospheric neutrino oscillations. To overcome this difficulty NMSGUT with **120** Higgs multiplet (which is quite naturally eligible since it is one of the three multiplets **10**, **120**, $\overline{\mathbf{126}}$ that have renormalizable SO(10) invariant couplings to the SO(10) fermion matter (**16**) bilinears) was proposed [27]. In NMSGUT the CKM structure and charged fermion hierarchy is generated by **120** along with **10**. The $\overline{\mathbf{126}}$ representation is eased from its duty to fit charged fermion masses. But it performs an important task to enhance the Type I seesaw neutrino masses via its ultra weak couplings (because Type I is inversely proportional to $\overline{\mathbf{126}}$ coupling). Type-II seesaw contribution is directly proportional to its coupling so gets further suppressed. It also lowers the right handed neutrino masses to $10^9 - 10^{13} GeV \ll M_X$ compatible with leptogenesis [35].

2.2 NMSGUT superpotential and symmetry breaking

The full superpotential of NMSGUT containing the mass terms and trilinear couplings is given schematically as

$$\begin{aligned}
W_{NMSGUT} = & m210^2 + M_H 10^2 + \lambda 210^3 + M 126 \cdot \overline{126} + \eta 210 \cdot 126 \cdot \overline{126} \\
& + 10 \cdot 210(\gamma 126 + \bar{\gamma} \overline{126}) + M_\Theta 120 \cdot 120 + k 10 \cdot 120 \cdot 210 \\
& + \rho 120 \cdot 120 \cdot 210 + \zeta 120 \cdot 126 \cdot 210 + \bar{\zeta} 120 \cdot \overline{126} \cdot 210 \\
& + h_{AB} 16_A \cdot 16_B \cdot 10 + f_{AB} 16_A \cdot 16_B \cdot \overline{126} + g_{AB} 16_A \cdot 16_B \cdot 120 \quad (2.1)
\end{aligned}$$

Details of tensor contractions can be found in [24, 27]. Here h_{AB}, f_{AB} are symmetric matrices of Yukawa couplings of the **10**, $\overline{\mathbf{126}}$ Higgs multiplets to the **16_A**, **16_B** matter bilinear and g_{AB} is antisymmetric matrix for the coupling of newly added Higgs representation **120** to **16_A**, **16_B**. One of the complex symmetric matrices can be made real and diagonal by a choice of SO(10) flavor basis. The complex Yukawas contain 3 real and 9 complex i.e 21 real parameters.

The symmetry breaking scheme of NMSGUT is same as MSGUT. If one looks at the Pati- Salam decomposition of **120** given below, it doesn't contain any SM singlet. So the 120-plet doesn't take part in GUT scale symmetry breaking where $SU(2)_L \times U(1)_Y$ is unbroken.

$$\begin{aligned} \Theta_{ijk}(120) = & \Theta_{\mu\nu}^{(s)}(10, 1, 1) + \Theta_{(s)}^{\mu\nu}(\overline{10}, 1, 1) + \Theta_{\nu\alpha\dot{\alpha}}^{\mu}(15, 2, 2) \\ & \Theta_{\mu\nu\dot{\alpha}\dot{\beta}}^{(a)}(6, 1, 3) + \Theta_{\mu\nu\alpha\beta}^{(a)}(6, 3, 1) + \Theta_{\alpha\dot{\alpha}}(1, 2, 2) \end{aligned} \quad (2.2)$$

The GUT scale vevs that break the $SO(10)$ gauge symmetry (one step symmetry breaking) down to SM symmetry are [16, 17, 32]

$$\langle (15, 1, 1) \rangle_{210} : \langle \phi_{abcd} \rangle = \frac{a}{2} \epsilon_{abcdef} \epsilon_{ef} \quad (2.3)$$

$$\langle (15, 1, 3) \rangle_{210} : \langle \phi_{ab\dot{\alpha}\dot{\beta}} \rangle = \omega \epsilon_{ab} \epsilon_{\dot{\alpha}\dot{\beta}} \quad (2.4)$$

$$\langle (1, 1, 1) \rangle_{210} : \langle \phi_{\dot{\alpha}\dot{\beta}\dot{\gamma}\dot{\delta}} \rangle = p \epsilon_{\dot{\alpha}\dot{\beta}\dot{\gamma}\dot{\delta}} \quad (2.5)$$

$$\langle (10, 1, 3) \rangle_{\overline{126}} : \langle \overline{\Sigma}_{\hat{1}\hat{3}\hat{5}\hat{8}\hat{0}} \rangle = \overline{\sigma} \quad (2.6)$$

$$\langle (\overline{10}, 1, 3) \rangle_{126} : \langle \Sigma_{\hat{2}\hat{4}\hat{6}\hat{7}\hat{9}} \rangle = \sigma \quad (2.7)$$

For preservation of Susy, vanishing of D-terms gives the condition $|\sigma| = |\overline{\sigma}|$.

An important simplification of this theory is that the GUT scale vevs and therefore the mass spectrum are all expressible in terms of a single complex parameter x which is a solution of the cubic equation [19].

$$8x^3 - 15x^2 + 14x - 3 = -\xi(1-x)^2 \quad (2.8)$$

where $\xi = \frac{\lambda M}{\eta m}$. Then the dimensionless vevs (denoted by tilde) in units of $(\frac{m}{\lambda})$ are $\tilde{\omega} = -x$ and

$$\tilde{a} = \frac{x^2 + 2x - 1}{1 - x} ; \tilde{p} = \frac{x(5x^2 - 1)}{(1 - x)^2} ; \tilde{\sigma}\tilde{\overline{\sigma}} = \frac{2\lambda x(1 - 3x)(1 + x^2)}{\eta(1 - x)^2} \quad (2.9)$$

Once one has all the superheavy vevs in terms of this parameter x the superheavy

mass spectrum which results due to the SO(10) symmetry breaking and responsible for all the GUT threshold effects can be calculated [20, 23, 24].

2.3 NMSGUT spectrum

The technique [23, 24] to find the heavy GUT spectrum is to decompose the SO(10) invariants of NMSGUT superpotential to Pati-Salam invariants. Then substituting the GUT vevs, one gets the superpotential in the MSSM vacuum in terms of MSSM invariants. The results for MSGUT are given in [23, 24] and for those extra terms corresponding to **120** can be found in [27]. These heavy fields fall into 26 MSSM irreducible representation (irreps) types which are named after 26 letters of alphabet [24, 27].

Gauge/gaugino masses: The massive gauge boson together with its longitudinal mode (Goldstone scalar) and real scalar partner of longitudinal mode as four bosonic degrees of freedom forms a massive supermultiplet. Its gaugino and the chiral fermion super-partner of Goldstone scalar pair form one Dirac fermion super-partner (with four degrees of freedom). These together form the so called massive vector gauge supermultiplet. Total 33 massive gauge/gauginos will appear due to symmetry breaking to MSSM. These gauge/gauginos lie in the PS representation $(6,2,2) \oplus (1,1,3)$ and in addition triplets and anti-triplets in $(15,1,1)$. These obtain mass by pairing with the AM Higgs fermion and their mass can be obtained by putting vevs of AM Higgs in the PS decomposition of gaugino Yukawa term given as:

$$g\sqrt{2}\left[\frac{1}{3!} \langle \tilde{\Phi}_{ijkl}^* \rangle \lambda_{im} \Phi_{mjkl}^F + \frac{1}{2.4!} (\langle \tilde{\Sigma}_{ijkln}^* \rangle \lambda_{im} \Sigma_{mjkl n}^F + \langle \tilde{\bar{\Sigma}}_{ijkln}^* \rangle \lambda_{im} \bar{\Sigma}_{mjkl n}^F)\right] \quad (2.10)$$

For example the $\bar{E}[3, 2, -\frac{1}{3}] \oplus E[3, 2, \frac{1}{3}]$ gauge field with mass $m_{\lambda_E} = g\sqrt{(4|a - \omega|^2 + 2|\omega - p|^2 + 2|\sigma|^2)}$. The complete mass matrix for E is 6×6 . The expression for full matrix is given in Eqn.(2.15).

AM chiral masses: The masses of chiral supermultiplets are calculated by putting AM Higgs vevs in the PS decomposition of the quadratic and trilinear terms in W_{AM} [23, 24, 27]. There are three types of mass terms involving fermions from chiral supermultiplets:

- **Unmixed chiral:** They don't mix with other massive chiral or gauge/gaugino fields. If the conjugate of chiral field exists then they form a Dirac field else the fermions have Majorana masses. In NMSGUT there are 11 ($A[1, 1, 4]$, $B[6, 2, \frac{5}{3}]$, $I[3, 1, \frac{10}{3}]$, $M[6, 1, \frac{8}{3}]$, $N[6, 1, \frac{-4}{3}]$, $O[1, 3, -2]$, $U[3, 3, \frac{4}{3}]$, $V[1, 2, -3]$, $W[6, 3, \frac{2}{3}]$, $Y[6, 2, \frac{-1}{3}]$, $Z[8, 1, 2]$) Dirac supermultiplets and 2 Majorana supermultiplets ($S[1, 3, 0]$, $Q[8, 3, 0]$). Here square brackets contain $SU(3)_C \times SU(2)_L \times U(1)_Y$ quantum number for respective fields, for example

$$O[1, 3, -2] = \frac{\vec{\Sigma}^{44(L)}}{\sqrt{2}} \quad \bar{O}[1, 3, 2] = \frac{\vec{\bar{\Sigma}}^{44(L)}}{\sqrt{2}} \quad (2.11)$$

form a Dirac supermultiplet with mass $2(M + \eta(3a - p))$.

- **Mixed pure chiral:** They mix with each other but not with massive gauge/gaugino fields. There are 8 ($R[8, 1, 0]$, $h[1, 2, 1]$, $t[3, 1, \frac{2}{3}]$, $C[8, 2, 1]$, $D[3, 2, \frac{7}{3}]$, $K[3, 1, \frac{8}{3}]$, $L[6, 1, \frac{2}{3}]$, $P[3, 3, \frac{2}{3}]$) fields of this type. Here we give the example of most important pure chiral field i.e NMSGUT Higgs field,

$$[1, 2, -1](\bar{h}_1, \bar{h}_2, \bar{h}_3, \bar{h}_4, \bar{h}_5, \bar{h}_6) \oplus [1, 2, 1](h_1, h_2, h_3, h_4, h_5, h_6) \equiv (H_2^\alpha, \bar{\Sigma}_2^{(15)\alpha}, \Sigma_2^{(15)\alpha}, \frac{\Phi_{44}^{2\alpha}}{\sqrt{2}}, O_2^\alpha, O_2^{(15)\alpha}) \oplus (H_{\alpha i}, \bar{\Sigma}_{\alpha i}^{(15)}, \Sigma_{\alpha i}^{(15)}, \frac{\Phi_\alpha^{44i}}{\sqrt{2}}, O_{\alpha i}, O_{\alpha i}^{(15)}) \quad (2.12)$$

In NMSGUT the Higgs mass matrix \mathcal{H} is 6×6 , two additional rows and columns (relative to the MSGUT) come from the 120-plet.

$$\begin{pmatrix} -M_H & \bar{\gamma}\sqrt{3}(\omega - a) & -\gamma\sqrt{3}(\omega + a) & -\bar{\gamma}\bar{\sigma} & kp & -\sqrt{3}ik\omega \\ -\bar{\gamma}\sqrt{3}(\omega + a) & 0 & -(2M + 4\eta(a + \omega)) & 0 & -\sqrt{3}\bar{\zeta}\omega & i(p + 2\omega)\bar{\zeta} \\ \gamma\sqrt{3}(\omega - a) & -(2M + 4\eta(a - \omega)) & 0 & -2\eta\bar{\sigma}\sqrt{3} & \sqrt{3}\zeta\omega & -i(p - 2\omega)\zeta \\ -\sigma\gamma & -2\eta\sigma\sqrt{3} & 0 & -2m + 6\lambda(\omega - a) & \zeta\sigma & \sqrt{3}i\zeta\sigma \\ pk & \sqrt{3}\bar{\zeta}\omega & -\sqrt{3}\omega\zeta & \bar{\zeta}\bar{\sigma} & -m_\Theta & \frac{p}{\sqrt{3}}i\omega \\ \sqrt{3}ik\omega & i(p - 2\omega)\bar{\zeta} & -i(p + 2\omega)\zeta & -\sqrt{3}i\bar{\zeta}\bar{\sigma} & -\frac{p}{\sqrt{3}}i\omega & -m_\Theta - \frac{2p}{3}a \end{pmatrix} \quad (2.13)$$

To get the masses, the above matrix is diagonalized after imposing the fine tuning condition $Det\mathcal{H} = 0$ (details in section 2.5).

- **Mixed chiral-gauge:** These mix with gauge fields as well as among themselves. There are 5 such types of fields $G[1, 1, 0]$ and $X[3, 2, \frac{4}{3}]$, $E[3, 2, \frac{1}{3}]$, $F[1, 1, 2]$, $J[3, 1, \frac{4}{3}]$. For example

$$[\bar{3}, 2, -\frac{1}{3}](\bar{E}_1, \bar{E}_2, \bar{E}_3, \bar{E}_4, \bar{E}_5, \bar{E}_6) \oplus [3, 2, \frac{1}{3}](E_1, E_2, E_3, E_4, E_5, E_6) \equiv (\Sigma_{4i}^{\bar{\mu}\alpha}, \bar{\Sigma}_{4i}^{\bar{\mu}\alpha}, \phi_{(s)2}^{\bar{\mu}4\alpha}, \phi_2^{(a)\bar{\mu}4\alpha}, \lambda_2^{\bar{\mu}4\alpha}, \Theta_{4i}^{\bar{\sigma}\alpha}) \oplus (\bar{\Sigma}_{\bar{\mu}\alpha 2}^4, \Sigma_{\bar{\mu}\alpha 2}^4, \phi_{\bar{\mu}4\alpha 1}^{(s)}, \phi_{\bar{\mu}4\alpha 1}^{(a)}, \lambda_{\bar{\mu}\alpha 1}, \Theta_{\bar{\sigma}\alpha}^{4i}) \quad (2.14)$$

The 6×6 mass matrix \mathcal{E} is

$$\begin{pmatrix} -2(M + \eta(a - \omega)) & 0 & 0 & 0 & 0 & (i\omega - ip + 2ia)\zeta \\ 0 & -2(M + \eta(a - 3\omega)) & -2\sqrt{2}i\eta\sigma & 2i\eta\sigma & ig\sqrt{2}\bar{\sigma}^* & (-3i\omega + ip + 2ia)\bar{\zeta} \\ 0 & 2i\sqrt{2}\eta\bar{\sigma} & -2(m + \lambda(a - \omega)) & -2\sqrt{2}\lambda\omega & 2g(a^* - \omega^*) & -\sqrt{2}\bar{\zeta}\bar{\sigma} \\ 0 & -2i\eta\bar{\sigma} & -2\sqrt{2}\lambda\omega & -2(m - \lambda\omega) & \sqrt{2}g(\omega^* - p^*) & \bar{\sigma}\bar{\zeta} \\ 0 & -ig\sqrt{2}\sigma^* & 2g(a^* - \omega^*) & g\sqrt{2}(\omega^* - p^*) & 0 & 0 \\ (-i\omega + ip - 2ia)\bar{\zeta} & (3i\omega - ip - 2ia)\zeta & -\sqrt{2}\zeta\sigma & \sigma\zeta & 0 & -(m_\Theta + \frac{\rho}{3}a - \frac{2}{3}\rho\omega) \end{pmatrix} \quad (2.15)$$

The mass matrix \mathcal{E} has the usual super-Higgs structure : complex conjugates of the 5th row and column after omitting the diagonal entry, provides left and right null eigenvectors of the chiral 5×5 submatrix \mathbf{E} obtained by omitting the fifth row and column. \mathcal{E} has non zero determinant although the determinant of \mathbf{E} vanishes.

2.4 Importance of NMSGUT spectrum

Due to these super heavy fields present in the theory there are corrections at one loop to unification scale M_X , the QCD coupling at M_Z ($\alpha_3(M_Z)$) and the gauge coupling at unification scale (α_G) as well as to fermion Yukawa couplings. We discuss here about the corrections to $\alpha_G, \alpha_3(M_Z), \text{Log}_{10}(M_X)$ and corrections to fermion Yukawa couplings in the next chapter. Here M_X is taken to be the mass of lightest gauge multiplet which mediates the proton decay and not a scale ($M_X^0 = 10^{16.33} \text{GeV}$) where

the three MSSM gauge couplings meet (since in general they do not at a point: due to threshold effects etc).

The threshold corrections due to heavy spectra on the matching relations of gauge couplings of low scale ($M_Z=91.1876$ GeV) and GUT scale (M_X) are done using the technique of Weinberg [36] and Hall [37]. The relation between two scale gauge couplings is given as:

$$\frac{1}{\hat{\alpha}_i(M_Z)} = \frac{1}{\alpha_G(M_X)} + 8\pi b_i \ln \frac{M_X}{M_Z} + 4\pi \sum_j \frac{b_{ij}}{b_j} \ln X_j - 4\pi \lambda_i(M_X) + \dots \quad (2.16)$$

Here $\hat{\alpha}_i = g_i^2/4\pi$ are MSSM gauge coupling in SU(5)GUT normalization. Second and third term corresponds to one and two loop gauge running with $X_j = 1 + 8\pi b_j \alpha_G(M_X^0) \ln(M_X^0/M_S)$. b_i and b_{ij} are coefficients of one and two loop gauge beta functions of MSSM [38]. λ_i is the leading one loop contribution of superheavy thresholds given as [36, 37] in $\overline{\text{MS}}$ scheme:

$$\lambda_i(\mu) = -\frac{2}{21}(b_{iV} + b_{iGB}) + 2(b_{iV} + b_{iGB}) \ln \frac{M_V}{\mu} + 2b_{iS} \ln \frac{M_V}{\mu} + 2b_{iF} \ln \frac{M_F}{\mu} \quad (2.17)$$

Where V, GB, S, F corresponds to vectors, Goldstone boson, scalar and fermions respectively. The formulas for threshold corrections are given [24, 34, 53] as:

$$\begin{aligned} \Delta^{(th)}(\ln M_X) &= \frac{\lambda_1(M_X) - \lambda_2(M_X)}{2(b_1 - b_2)} \\ \Delta_X &\equiv \Delta^{(th)}(\text{Log}_{10} M_X) = .0222 + 0.4873(\bar{b}'_1 - \bar{b}'_2) \text{Log}_{10} \frac{M'}{M_X} \\ \Delta_3 &\equiv \Delta^{(th)}(\alpha_3(M_Z)) \\ &= \frac{100\pi(b_1 - b_2)\alpha(M_Z)^2}{[(5b_1 + 3b_2 - 8b_3)\sin^2\theta_w(M_Z) - 3(b_2 - b_3)]^2} \sum_{ijk} \epsilon_{ijk}(b_i - b_j)\lambda_k(M_X) \\ &= .000311667 \sum_{M'} (5\bar{b}'_1 - 12\bar{b}'_2 + 7\bar{b}'_3) \text{Log}_{10} \frac{M'}{M_X} \end{aligned}$$

$$\begin{aligned}\Delta_G \equiv \Delta^{(th)}(\alpha_G^{-1}(M_X)) &= \frac{4\pi(b_1\lambda_2(M_X) - b_2\lambda_1(M_X))}{b_1 - b_2} \\ &= -1.27 + 0.1786 \sum_{M'} (6.6\bar{b}'_2 - \bar{b}'_1) \text{Log}_{10} \frac{M'}{M_X}\end{aligned}\quad (2.18)$$

Where $\bar{b}'_i = 16\pi^2 b'_i$ are 1-loop β function coefficients for different superheavy multiplets having mass M' .

To satisfy the perturbativity conditions the following limits were imposed on corrections:

$$\begin{aligned}-20.0 &\leq \Delta_G \equiv \Delta(\alpha_G^{-1}(M_X)) \leq 25 \\ 3.0 &\geq \Delta_X \equiv \Delta(\text{Log}_{10} M_X) \geq -0.03 \\ -0.017 &< \Delta_3 \equiv \Delta\alpha_3(M_Z) < -0.004\end{aligned}\quad (2.19)$$

An important point to mention is that the corrections depend only on ratios of masses and are independent of overall scale parameter which is chosen to be m (mass of **210** plet). The unification scale is defined as $M_X = M_X^0 10^{\Delta_X}$ and $M_X = m_{\lambda_X} = |m/\lambda| g_{10} \sqrt{4|\tilde{a} + \tilde{\omega}|^2 + 2|\tilde{p} + \tilde{\omega}|^2}$. The overall scale $|m|$ is then calculated by the RG analysis and given by

$$|m_{RG}| = 10^{16.33 + \Delta_X} \frac{|\lambda|}{g_{10} \sqrt{4|\tilde{a} + \tilde{\omega}|^2 + 2|\tilde{p} + \tilde{\omega}|^2}} \text{GeV}\quad (2.20)$$

Here g_{10} is the SO(10) gauge coupling (threshold corrected).

2.5 Fermion mass formulae

The 6×6 mass matrix H for MSSM Higgs type doublets is most important for fixing the tree level formulae for Yukawa couplings. The fine tuning condition $\text{Det}\mathcal{H} = 0$ is needed to keep a pair of Higgs doublets $H_{(1)}, \bar{H}_{(1)}$ (defined via left and right null eigenstates of the mass matrix \mathcal{H}) light. The composition of these null eigenstates in terms of the GUT scale doublets is specified by the so called ‘‘Higgs fractions’’

$\alpha_i, \bar{\alpha}_i$. The ‘‘Higgs fractions’’ are important as they determine how much different original GUT scale doublets will contribute to the EW symmetry breaking. They may be derived from the bi-unitary transformation ($h_i = U_{ij}H_j, \bar{h}_i = \bar{U}_{ij}\bar{H}_j$) that diagonalizes \mathcal{H} : $\bar{U}^T \mathcal{H} U = \Lambda_h$ then $U_{i1} = \alpha_i, \bar{U}_{i1} = \bar{\alpha}_i$.

To get the Dirac masses of fermion replace $\langle h_i \rangle \rightarrow \alpha_i v_u, \langle \bar{h}_i \rangle \rightarrow \bar{\alpha}_i v_d$ in Dirac mass matrices, where $v_{u,d}$ are the vevs of the light MSSM doublets H_1, \bar{H}_1 . The fermion Dirac masses can be calculated from the decomposition of $\mathbf{16} \cdot \mathbf{16} \cdot (\mathbf{10} \oplus \mathbf{120} \oplus \overline{\mathbf{126}})$ given in [23, 24, 33] and this yields [27]:

$$y^u = (\hat{h} + \hat{f} + \hat{g}) \quad ; \quad y^d = (\hat{r}_1 \hat{h} + \hat{r}_2 \hat{f} + \hat{r}_6 \hat{g}) \quad (2.21)$$

$$y^\nu = (\hat{h} - 3\hat{f} + (\hat{r}_5 - 3)\hat{g}) \quad ; \quad y^l = (\hat{r}_1 \hat{h} - 3\hat{r}_2 \hat{f} + (\hat{r}_5 - 3\hat{r}_6)\hat{g})$$

$$\hat{r}_1 = \frac{\bar{\alpha}_1}{\alpha_1}; \quad \hat{r}_2 = \frac{\bar{\alpha}_2}{\alpha_2}; \quad \hat{r}_5 = \frac{4i\sqrt{3}\alpha_5}{\alpha_6 + i\sqrt{3}\alpha_5}$$

$$\hat{r}_6 = \frac{\bar{\alpha}_6 + i\sqrt{3}\bar{\alpha}_5}{\alpha_6 + i\sqrt{3}\alpha_5}; \quad \hat{r}_5 = \frac{4i\sqrt{3}\bar{\alpha}_5}{\alpha_6 + i\sqrt{3}\alpha_5} \quad (2.22)$$

$$\hat{g} = 2ig\sqrt{\frac{2}{3}}(\alpha_6 + i\sqrt{\alpha_5}) \quad ; \quad \hat{h} = 2\sqrt{2}h\alpha_1 \quad ; \quad \hat{f} = -4\sqrt{\frac{2}{3}}if\alpha_2$$

The Yukawa couplings of matter fields with **120** Higgs field included give no additional contribution to the Majorana mass matrix of the superheavy neutrinos $\bar{\nu}_A$ so it remains same as MSGUT.

$$M_{AB}^{\bar{\nu}} = 8\sqrt{2}f_{AB}\bar{\sigma} \quad (2.23)$$

The Type I contribution is obtained by eliminating $\bar{\nu}_A$

$$W = \frac{1}{2}M_{AB}^{\bar{\nu}}\bar{\nu}_A\bar{\nu}_B + \bar{\nu}_A m_{AB}^{\nu}\nu_B + \dots \rightarrow \frac{1}{2}M_{AB}^{\nu(I)}\nu_A\nu_B + \dots$$

$$M_{AB}^{\nu(I)} = -((m^{\nu})^T(M^{\bar{\nu}})^{-1}m^{\nu})_{AB} \quad (2.24)$$

From the Type II seesaw (the **120** plet contributes new terms) one obtains [24, 27] contribution to the light neutrino Majorana mass :

$$M_{\nu}^{II} = 16if_{AB} \langle \bar{O}_- \rangle = 16if_{AB} \left(i\frac{\gamma}{\sqrt{2}}\alpha_1 + i\sqrt{6}\eta\alpha_2 - \sqrt{3}\zeta\alpha_6 + i\zeta\alpha_5 \right) \alpha_4 \left(\frac{v_u^2}{M_{\Theta}} \right) \quad (2.25)$$

where $M_\Theta = 2(M + \eta(3a - p))$. NMSGUT considers Type I and Type II mechanisms together. Then one does not have any freedom to switch one of them off at will.

2.6 SM fermion fitting criteria in NMSGUT and its features

Fitting to SM fermion data is done by χ^2 analysis. Fitting is done at two scales, M_X^0 and M_Z . The two scale fitting process is looped via 2-loop MSSM RGEs [38].

M_X^0 scale fitting: This requires us to find a set of superpotential parameters of NMSGUT such that the fermion Yukawas calculated from these parameters match the experimental data evolved to M_X^0 . The fitting at GUT scale is done in terms of 38 free superpotential parameters of NMSGUT. It includes 21 real parameters from the fermion Yukawa sector ($h_{AA}(3), f_{AB}(12), g_{AB}(6)$). One of the symmetric matrices is made real diagonal using the freedom to make U(3) rotations on the 16-plet kinetic terms (here h_{AB} is chosen to be real diagonal). 24 parameters come from scalar trilinear and quadratic terms ($\eta, \rho, \kappa, \gamma, \bar{\gamma}, \zeta, \bar{\zeta}, \lambda, m, M, \tilde{m}_\Theta, M_H$). Using phase redefinitions of 5 Higgs fields the number of parameters reduces to 24-5=19. M_H is kept fixed by fine tuning condition. m is also fixed by equation (2.20). So there are basically 37 free parameters. These parameters will determine the MSSM Yukawa and neutrino masses at M_X scale with the formula given in section 4. Then 2-loop RGEs extrapolate central values of SM data (it includes fermion Yukawas, CKM mixing angles, neutrino mass splitting and mixing data, total 18 parameters) to MSSM one loop corrected unification scale $M_X^0 = 10^{16.33}$ GeV (corrections from Right handed neutrino and Susy particles are not considered). The χ^2 function at M_X^0 is given as

$$\chi^2 = \sum_{i=1}^{18} \frac{(O_i - \bar{O}_i)^2}{\delta O_i^2} \quad (2.26)$$

Here O_i are calculated from NMSGUT parameters, \bar{O}_i are the target values and δO_i are the uncertainties in the target values based on extrapolating the fermion data uncertainties from the weak scale to GUT scale [39]. The downhill simplex method (AMOEBAsubroutine) given by Nelder and Mead [40] is used to do the χ^2 fit. The 37 parameters are thrown at random to start, then the subroutine AMOEBA search in 37 dimensional parameter space to find best fit.

Features of GUT scale fitting:

- Regions of NMSGUT parameter space exist where a fit for 18 SM parameters with $\chi < .1$ can be achieved.
- It successfully fits the Neutrino masses and large mixing angles.
- The tiny values of the $\overline{126}$ couplings results in three righthanded neutrino masses to be much lighter than M_X and having the range $\sim 10^8 - 10^{13} GeV$, required for Leptogenesis.
- The most striking feature of NMSGUT fitting at M_X is in fitting to down and strange quark. NMSGUT like other GUTs require large $\tan\beta \approx 50$ for t-b- τ Yukawa unification. The price to achieve that is that the down and strange quark Yukawa couplings come out to be 4-5 times smaller than the SM required central values at M_Z . However instead of taking this as a no-go [41] it was reinterpreted [27, 28] as necessity of Susy threshold corrections to d,s quark Yukawa couplings in large $\tan\beta$ region which are to be just what is required to allow the matching.

M_Z scale fitting: The best fit found at M_X scale along with five SUGRY-NUHM (Supergravity-Non universal Higgs mass) type soft Susy breaking parameters (m_0 (universal scalar mass), $m_{\frac{1}{2}}$ (universal gaugino mass), A_0 (universal trilinear coupling), m_{H^2, \bar{H}^2}) is run down to M_Z scale using two loop MSSM RGEs [38]. The χ^2 function at this scale is defined as:

$$\chi_{Susy}^2 = \sum_i \left(1 - \frac{y_i^{MSSM}}{y_i^{SM}}\right)^2 \quad (2.27)$$

Here $y_i^{MSSM} = y_i^{GUT} [\text{Sin}\beta(\text{cos}\beta)(1 + \eta_i)]$ is the susy threshold corrected Yukawa for up(**down**) type fermions. y_i^{GUT} is the value of the Yukawa coupling from the GUT fit run down to M_Z . η_i is the correction factor. The corrections include gluino, chargino [42] and bino [39] loop corrections. The corrections are applied in the absence of generation mixing. The leading contribution of Susy correction to top quark comes from the gluon and squark-gluino loop. In case of down type quarks, bottom quark Yukawa coupling receive corrections from gluino due to large $\tan\beta$. However it is cancelled or even dominated by chargino corrections due to large $A_0 y_t$. However for down and strange quark the gluino corrections (Yukawa is small for first two generations) reduce the SM Yukawa required to match with run down values of NMSGUT Yukawas. In case of charged leptons there are no gluino corrections. The fitting is again done throwing randomly the Susy breaking parameters at GUT scale (running them down to M_Z scale) using downhill simplex method. The s-particle spectra is calculated at tree level using subroutines from SPHENO [43]. Then Susy threshold corrections are calculated and applied to run down values of GUT fermion Yukawas to compare with SM Yukawas.

Features of M_Z scale fitting and Susy Spectra:

- The most striking feature of M_Z scale fitting is requirement of large μ, A_0 parameters required to have large Susy threshold corrections to fit down and strange quark.
- Large and negative value of $m_{H,\bar{H}}^2$ ensures that the third s-generation is heavier than first two independently from the value of A_0 . Thus NMSGUT predicts normal s-hierarchy opposite to most of other GUTs which predicts inverted s-hierarchy.
- Pure Bino is the lightest supersymmetric particle (LSP) which can be a suitable candidate for dark matter. Also in some cases NMSGUT provides light smuon close to the mass of Bino in some cases to provide co-annihilation channel as well as allow explanation of muon g-2 anomaly.

- An interesting feature is that the ratio of gaugino masses diverges significantly from the ratio 1:2:7 :: $M_1 : M_2 : M_3$ expected from the one loop running of the gauge couplings.
- S-particles are in range 2 TeV-50 TeV, gauginos ~ 0.1 -0.2 TeV, Higgsinos ~ 100 TeV and in some cases smuon can be as light as a few hundred GeV.
- The MSSM Higgs mass is calculated at 1-loop level (corrections from stop and sbottom quarks) and able to achieve mass value 124-126 GeV as dictated by experiments. Also the large value of A_0, μ (O(100 TeV)) parameter suggest large mass for light Higgs due to loop corrections. This feature of NMSGUT is known from 2008 [27], well before discovery of Higgs in 2012 made it a commonly acceptable assumption. Also these large values are quite natural for a decoupled/Mini Split type Susy s-spectra [44, 45].

2.7 Dimension five operators for B,L violation

Quarks and Leptons are grouped together in the same irreducible representation in Grand Unified theories. This leads to conversion of quarks into leptons e.g. proton decay via exchange of heavy gauge or Higgs fields. However non observation of the decay of proton put stringent constraints on Susy GUTs. The experiment at Super Kamiokande water Cherenkov radiation detector has given lower bound on the decay rate of proton to kaon and positron channel as [46]

$$\Gamma_{p \rightarrow K^+ \bar{\nu}} > (3.3 \times 10^{33} \text{yrs})^{-1}; \quad \Gamma_{p \rightarrow e^+ \pi^0} > (1.0 \times 10^{34} \text{yrs})^{-1} \quad (2.28)$$

In Non Susy GUTs the leading contribution to B violation comes from d=6 operators. The decay rate calculated from d=6 B violation operators is proportional to $\frac{1}{M_X^2}$, here M_X is mass of exchanged particle. In Non-Susy theories M_X is of O(10^{15} GeV) and in Susy theories it is O(10^{16} GeV). So the life time calculated from the d=6 operators comes out to be O(10^{36} yrs) or more.

However in Susy GUTs the d=5 and 4, B violation operator can also contribute. The d=4 (renormalizable) operators only arise in R-Parity violating theories. Since NMSGUT preserves R-parity so they are not relevant here. The d=5 operators involve two fermions and two sfermions with exchange of a color triplet Higgsino. In NMSGUT the effective superpotential for $B + L$ violating processes (although B-L preserving as it is a part of gauge symmetry) due to exchange of color triplet superheavy chiral supermultiplets contained in the $\mathbf{10}, \overline{\mathbf{126}}, \mathbf{120}$ Higgs multiplets are given in [23, 24] for $\mathbf{10}, \overline{\mathbf{126}}$ and [27] for $\mathbf{120}$. The complete d=4 superpotential in terms of MSSM decompositions is:

$$\begin{aligned}
W_{FM} = & 2\sqrt{2}h_{AB}[\bar{t}_1(\epsilon\bar{u}_Ad_B + Q_AL_B) + t_1(\frac{\epsilon}{2}Q_AQ_B + \bar{u}_A\bar{e}_B - \bar{d}_A\bar{\nu}_B)] \\
& -2\sqrt{2}h_{AB}[\bar{h}_1(\bar{d}_AQ_B + \bar{e}_AL_B) + h_1(\bar{u}_AQ_B + \bar{\nu}_AL_B)] \\
& +4\sqrt{2}f_{AB}[t_2(\frac{\epsilon}{2}Q_AQ_B - \bar{u}_A\bar{e}_B + \bar{\nu}_A\bar{d}_B) + \bar{t}_2(Q_AL_B - \epsilon\bar{u}_A\bar{d}_B)] \\
& +4\sqrt{2}f_{AB}[\frac{i}{\sqrt{3}}\{\bar{h}_2(\bar{d}_AQ_B - 3\bar{e}_AL_B) + h_2(\bar{u}_AQ_B - 3\bar{\nu}_AL_B)\}] \\
& +2(\bar{C}_1\bar{d}_AQ_B - C_2\bar{u}_AQ_B) + 2(E_1\bar{d}_AL_B - D_2\bar{u}_AL_B) \\
& +2(\bar{D}_2\bar{e}_AQ_B - \bar{E}_2\bar{\nu}_AQ_B)] \\
& +4f_{AB}[\bar{\Sigma}^{\dot{\alpha}\dot{\beta}}\bar{Q}_{A\dot{\alpha}}\bar{Q}_{B\dot{\beta}} + 2i(\bar{A}\bar{e}_A\bar{B} - G_5\bar{\nu}_A\bar{\nu}_B) - 2\sqrt{2}i\bar{F}_1\bar{e}_A\bar{\nu}_B \\
& +(\bar{W}Q_AQ_B + 2\bar{P}Q_AL_B + \sqrt{2}\bar{O}L_AL_B) \\
& -2it_4(\bar{d}_A\bar{\nu}_B + \bar{u}_A\bar{e}_B) + 2\sqrt{2}i(K\bar{d}_A\bar{e}_B - J_1\bar{u}_A\bar{\nu}_B)] \\
& +2\sqrt{2}g_{AB}[\bar{h}_5(\bar{d}_AQ_B + \bar{e}_AL_B) - h_5(\bar{u}_AQ_B + \bar{\nu}_AL_B)] \\
& -2\sqrt{2}g_{AB}[\sqrt{2}\bar{L}_2Q_AQ_B + F_4L_AL_B + \sqrt{2}\bar{t}_6Q_AL_B \\
& +2\sqrt{2}L_2\bar{u}_A\bar{d}_B + \sqrt{2}t_6(\bar{u}_A\bar{e}_B - \bar{d}_A\bar{\nu}_B) + 2\bar{F}_4\bar{\nu}_A\bar{e}_B] \\
& -2\sqrt{2}g_{AB}[2\bar{C}_3\bar{d}_AQ_B - 2C_3\bar{u}_AQ_B + \frac{i}{\sqrt{3}}\bar{h}_6(\bar{d}_AQ_B - 3\bar{e}_AL_B) \\
& -\frac{i}{\sqrt{3}}h_6(\bar{u}_AQ_B - 3\bar{\nu}_AL_B) + 2\bar{D}_3\bar{e}_AQ_B - 2\bar{E}_6\bar{\nu}_AQ_B \\
& +2E_6\bar{d}_AL_B - 2D_3\bar{u}_AL_B] - 2i\sqrt{2}g_{AB}[\epsilon\bar{J}_5\bar{d}_A\bar{d}_B \\
& +2K_2\bar{d}_A\bar{e}_B - \epsilon\bar{K}_2\bar{u}_A\bar{u}_B - 2J_5\bar{u}_A\bar{\nu}_B
\end{aligned}$$

$$-\sqrt{2}\epsilon\bar{t}_7\bar{d}_A\bar{u}_B - \sqrt{2}t_7(\bar{d}_A\bar{\nu}_B - \bar{e}_A\bar{u}_B)] - 2g_{AB}[\epsilon P_2 Q_A Q_B + 2\bar{P}_2 Q_A L_B] \quad (2.29)$$

The exchange of a Higgsino that couples to matter with a given $B + L$ will give rise to a $B + L$ violating effective $d = 5$ operator if it has a nonzero contraction with a conjugate (MSSM) representation Higgsino which couples to a matter chiral bilinear with a $B + L$ different from the conjugate of the first $B + L$ value. In NMSGUT in addition to familiar color triplets $[\bar{3}, 1, \pm\frac{2}{3}] \subset \mathbf{120}$ i.e $\{\bar{t}_{(6)}, \bar{t}_{(7)}\}[\bar{3}, 1, \frac{2}{3}]$ and $\{t_{(6)}, t_{(7)}\}$ but $P[3, 3, \pm\frac{2}{3}]$ and $K[3, 1, \pm\frac{8}{3}]$ multiplet types also contribute to baryon violation. Also due to mixing in $P(P_1, P_2)$, $K(K_1, K_2)$ a number of fresh contributions appear which were not there in MSGUT without $\mathbf{120}$.

After integrating out the heavy triplet Higgs supermultiplets the effective $d = 4$ Superpotential for Baryon Number violating processes in the NMSGUT [24, 27] is given (to leading order in m_W/M_X) by:

$$W_{eff}^{\Delta B \neq 0} = -L_{ABCD}(\frac{1}{2}\epsilon Q_A Q_B Q_C L_D) - R_{ABCD}(\epsilon \bar{e}_A \bar{u}_B \bar{u}_C \bar{d}_D) \quad (2.30)$$

where the coefficients are

and

$$\begin{aligned} R_{ABCD} = & \mathcal{S}_1^1 \tilde{h}_{AB} \tilde{h}_{CD} - \mathcal{S}_1^2 \tilde{h}_{AB} \tilde{f}_{CD} - \mathcal{S}_2^1 \tilde{f}_{AB} \tilde{h}_{CD} + \mathcal{S}_2^2 \tilde{f}_{AB} \tilde{f}_{CD} \\ & - i\sqrt{2}\mathcal{S}_4^1 \tilde{f}_{AB} \tilde{h}_{CD} + i\sqrt{2}\mathcal{S}_4^2 \tilde{f}_{AB} \tilde{f}_{CD} \\ & + \mathcal{S}_6^1 \tilde{g}_{AB} \tilde{h}_{CD} - i\mathcal{S}_7^1 \tilde{g}_{AB} \tilde{h}_{CD} - \mathcal{S}_6^2 \tilde{g}_{AB} \tilde{f}_{CD} + i\mathcal{S}_7^2 \tilde{g}_{AB} \tilde{f}_{CD} \\ & + i\mathcal{S}_1^7 \tilde{h}_{AB} \tilde{g}_{CD} - i\mathcal{S}_2^7 \tilde{f}_{AB} \tilde{g}_{CD} + \sqrt{2}\mathcal{S}_4^7 \tilde{f}_{AB} \tilde{g}_{CD} \\ & + i\mathcal{S}_6^7 \tilde{g}_{AB} \tilde{g}_{CD} + \mathcal{S}_7^7 \tilde{g}_{AB} \tilde{g}_{CD} - \sqrt{2}(\mathcal{K}^{-1})_1^2 \tilde{f}_{AD} \tilde{g}_{BC} \\ & - (\mathcal{K}^{-1})_2^2 \tilde{g}_{AD} \tilde{g}_{BC} \end{aligned} \quad (2.31)$$

$$\begin{aligned} L_{ABCD} = & \mathcal{S}_1^1 \tilde{h}_{AB} \tilde{h}_{CD} + \mathcal{S}_1^2 \tilde{h}_{AB} \tilde{f}_{CD} + \mathcal{S}_2^1 \tilde{f}_{AB} \tilde{h}_{CD} + \mathcal{S}_2^2 \tilde{f}_{AB} \tilde{f}_{CD} \\ & - \mathcal{S}_1^6 \tilde{h}_{AB} \tilde{g}_{CD} - \mathcal{S}_2^6 \tilde{f}_{AB} \tilde{g}_{CD} + \sqrt{2}(\mathcal{P}^{-1})_2^1 \tilde{g}_{AC} \tilde{f}_{BD} \\ & - (\mathcal{P}^{-1})_2^2 \tilde{g}_{AC} \tilde{g}_{BD} \end{aligned} \quad (2.32)$$

here $\mathcal{S} = \mathcal{T}^{-1}$ and \mathcal{T} is the mass matrix for $[3, 1, \pm 2/3]$ -sector triplets : $W = \bar{t}^i \mathcal{T}_i^j t_j + \dots$, and

$$\tilde{h}_{AB} = 2\sqrt{2}h_{AB} \quad \tilde{f}_{AB} = 4\sqrt{2}f_{AB} \quad \tilde{g}_{AB} = 4g_{AB} \quad (2.33)$$

Using these formulas the Baryon decay rates are estimated in NMSGUT on the basis of fits of fermion data. In the next section we will discuss about fits found in NMSGUT with baryon decay rates $\sim 10^{-28}\text{yrs}^{-1}$ which are faster than experimental value by six orders of magnitude.

2.8 Problem of fast proton decay ($\tau \sim 10^{28}$ yrs)

In NMSGUT, the raising of unification scale M_X near to Planck scale due to threshold effects leads to suppression of gauge mediated d=6 Baryon violation operators. A suppression of 4-6 orders of magnitude to 10^{36} yrs can be achieved relative to the non-Susy case. However the d=5 operators are a cause of concern. The effective dimension=4 operators are dressed with sparticles, which will eventually yield d=6 effective 4 fermion operators for baryon decay via exchange of gaugino/Higgsino. These operators are proportional to $\frac{1}{M_H M_{Susy}}$ (where M_{Susy} is the mass scale of s-particles) and give leading contribution to proton decay [47, 48]. So to calculate the decay rate the knowledge of sparticle spectrum and their mixing is required.

The formulas of [49, 50] are used to calculate the baryon decay rates. The (162 complex) operator coefficients (L_{ABCD}, R_{ABCD}) are run down from M_X to M_Z using RGEs and then along with the Susy spectrum calculated at this scale the run down values of these parameters are inserted into the formulas of [50]. The rates are calculated in terms of parameters of NMSGUT superpotential required for fermion fitting at GUT scale and 5 Susy breaking parameters required for fitting at M_Z scale. The two example sets [27] which account for viable SM fermion fits but fail to satisfy currents limits on baryon decay rates are given in Table 2.1.

parameter	Soln. 1	Soln. 2
$\tau_p(M^+\nu)$	8.1×10^{28}	1.7×10^{28}
$\Gamma(p \rightarrow \pi^+\nu)$	3.1×10^{-30}	7.2×10^{-30}
$\text{BR}(p \rightarrow \pi^+\nu_{e,\mu,\tau})$	$\{2.6 \times 10^{-5}, 0.09, 0.91\}$	$\{3.04 \times 10^{-5}, 0.01, 0.99\}$
$\Gamma(p \rightarrow K^+\nu)$	9.2×10^{-30}	5.2×10^{-29}
$\text{BR}(p \rightarrow K^+\nu_{e,\mu,\tau})$	$\{1.1 \times 10^{-4}, 0.27, 0.73\}$	$\{5.45 \times 10^{-5}, 0.01, 0.99\}$

Table 2.1: $d = 5$ operator mediated proton lifetimes $\tau_p(\text{yrs})$, decay rates $\Gamma(\text{yr}^{-1})$ and Branching ratios in the dominant Meson⁺ + ν channels.

2.9 Conclusion

Despite many attractive structural features and successes of NMSGUT the solutions found for complete fermion fits are unable to fulfill constraints from proton decay. However [28] proposed that in Minimal renormalizable Susy SO(10) theories, large wave function corrections are possible to light field propagators entering into the fermion Yukawa vertex due to large number of heavy fields. This suppresses the SO(10) Yukawa required to match with MSSM Yukawa. The suppressed SO(10) Yukawa will determine the $d=5$, $\Delta B \neq 0$ operators which will give the decay rate compatible with experimental limits. However in the work, while calculating the threshold corrections it was assumed that the MSSM Higgs is dominantly made from the h_1 i.e. α_1 is dominating. In this thesis and associated work, the complete 1-loop calculation is presented. In next chapter we will present full threshold corrections to SO(10) Yukawa vertex and the consequent lowering of the $d=5$, $\Delta B \neq 0$ operators.

Chapter 3

Threshold Corrections and Suppression of $d=5$, $\Delta B \neq 0$ Operators

3.1 Introduction

Threshold corrections at both M_X (Superheavy threshold corrections to M_X , $\alpha_3(M_Z)$, α_G) and M_S (Susy threshold corrections to fit down and strange quark Yukawas) played a central role in earlier NMSGUT calculations and fits of the fermion hierarchy [27, 28]. We discussed about threshold corrections to $M_X, \alpha_3(M_Z), \alpha_G, y_{d,b,s}$ in the previous chapter. In this chapter we will discuss about the importance of threshold corrections from dressing (by superheavy fields) of light Higgs, fermion and anti-fermion line leading into matter-Higgs Yukawa vertex in the NMSGUT. Again the claim of [26] about futility of threshold corrections by arguing that the large number of fields and their masses above or below the GUT scale can give rise to un-controllable uncertainty in low energy predictions is proved wrong. We argue that without performing any actual calculation one can't come to any conclusion. The most appealing feature of NMSGUT is that one has the full spectrum [23, 24, 27] of all the heavy fields appearing due to symmetry breaking. So

after having information about interactions and superheavy mass spectrum in hand one can calculate the threshold corrections. To start with, a preliminary calculation (with some defects) of the wave function renormalization of the Higgs line in the matter fermion-antifermion-MSSM Higgs vertex was done [28]. It was assumed a good approximation to take the MSSM Higgs to be dominantly made up of the **10**-plet so that one can ignore the admixture of the other 5 MSSM type Higgs doublets pairs present in the theory. However in practice it is found that viable parameter sets often imply sizable admixtures of Higgs multiplets other than **10**-plet. So to complete the threshold calculations we considered the other five remaining doublets (from **120**, **126**, $\overline{\mathbf{126}}$, **210**) too and applied the threshold corrections to each doublet [29]. The importance of these corrections can be counted from the observation that for the tree level fits found in [27], the wave function corrections (due to the large number of fields) violates even basic constraints such as positivity of wave function renormalization ($Z > 0$) very badly. While searching the parameter space for viable fermion fits, positivity of the wave function renormalization factors $Z_{f,H}$ is crucial. We found that despite the large number of fields involved in the calculation, the correction factors $Z_{f,H}$ can be reduced by a factor of several hundred keeping the positive sign undisturbed. Consequently it drastically reduces the magnitude of the SO(10) couplings required to fit the data at M_X relative to those found in [27]! The Baryon decay suppression mechanism we use relies on this very (large N facilitated) limiting value being approached i.e. $Z_{H,\overline{H}} \simeq 0$. The solutions found [29] respecting $1 \gg Z \simeq 0$ for light field renormalization also improved the perturbative status of the couplings so determined. With these small couplings (much smaller than before [27]) we are able to achieve tree level fermion fits and gauge unification [27]. The higher loop corrections will also behave the same way unless the theory has a pathologically ill defined perturbation expansion. The results from fits [29] have shown that the complexity of the spectra effectively enhances the possibilities for finding arrangements of parameters for which the feared breakdown does not take place. Our results favor the view that there is a natural tendency for a “Higgs dissolution edge” to form when implementing the unusual requirement of a fine tuned

light MSSM Higgs pair to separate out of a surplus of superheavy MSSM doublets. We found realistic fits of the earlier type [27] but now fully viable inasmuch as the $d = 5$, $\Delta B \neq 0$ lifetimes can be 10^{34} yrs or more.

3.2 One loop formula for GUT thresholds

The method of threshold corrections to gauge couplings is given by Weinberg and Hall [36, 37]. Its generalization was done by Wright [51] for calculating high scale threshold corrections to Yukawa couplings. It has been available for long time but not utilized fully, possibly due to the assumption that such corrections have negligible effect on the underlying theory. However in our opinion the GUT scale threshold corrections can be utilized in a favorable way without disturbing the already present features of theory under consideration. In this section we present the basic formalism to calculate the one loop thresholds in SO(10) NMSGUT.

As we know that due to non-renormalization theorem in supersymmetric theories the superpotential parameters are renormalized only due to wave function corrections [52]. So we need to calculate the correction factors for three legs (fermion, anti-fermion and Higgs) of SO(10) Yukawa vertex which will eventually give us the corrected Yukawa coupling (when we redefine the fields). However to calculate the corrections for the large number of heavy fields which couple to the light fermions and MSSM Higgs at SO(10) Yukawa and gauge vertices, though straightforward, is very laborious and time consuming. One needs to decompose the SO(10) superpotential terms into Pati-Salam labels which is already available in [23, 24, 27] and then to MSSM group. For calculation of fermion (anti-fermion) line correction factor we need to look at the trilinear invariants of the matter fields inside 16-plet with the Higgs (10,120,126, $\overline{126}$) and gauge field (45-plet). The calculation of correction factor to Higgs line is much more complicated than matter lines as it involves huge number of terms (~ 1100) due to mixing among different Higgs. To perform the calculation we need to change the weak basis of heavy field supermultiplet mass matrices to diagonal mass basis. For a given complete set of mass matrices and trilinear

coupling decompositions [23, 24, 27] one can easily compute this mass basis.

Let us first work out the expression for correction factor for generic scalar and fermion field. Then we present our explicit expressions (Appendix **A**). For a generic heavy field type Φ (conjugate $\bar{\Phi}$) the mass terms in the superpotential diagonalize as :

$$\bar{\Phi} = U^{\Phi} \bar{\Phi}' \quad ; \quad \Phi = V^{\Phi} \Phi' \quad \Rightarrow \quad \bar{\Phi}'^T M \Phi = \bar{\Phi}'^T M_{Diag} \Phi' \quad (3.1)$$

The circulation of heavy supermultiplets within the one loop insertions on each of the 3 chiral superfield lines ($f_c = \bar{f}, f, H_f = H, \bar{H}$) enters the matter Yukawa vertices (a pictorial view of it is shown in figure 3.1) :

$$\mathcal{L} = [f_c^T Y_f f H_f]_F + H.C. + \dots \quad (3.2)$$

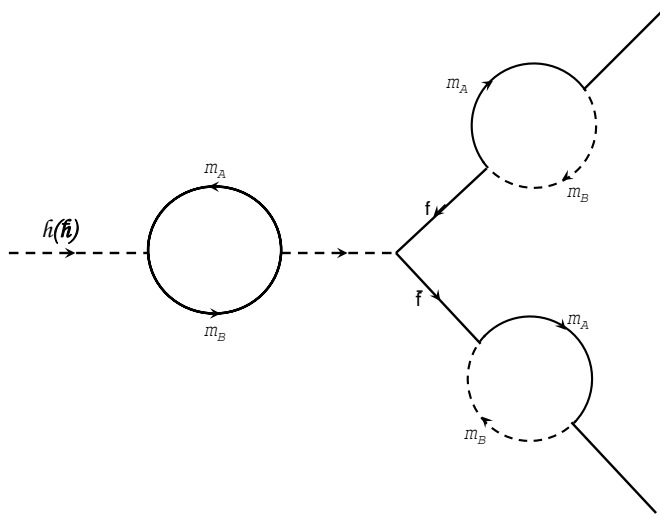


Figure 3.1: 1-loop correction to SO(10) Yukawa vertex.

From [51] one finds that a finite wave function renormalization in the Kinetic

terms :

$$\mathcal{L} = \left[\sum_{A,B} (\bar{f}_A^\dagger (Z_{\bar{f}})^B_A \bar{f}_B + f_A^\dagger (Z_f)^B_A f_B) + H^\dagger Z_H H + \bar{H}^\dagger Z_{\bar{H}} \bar{H} \right]_D + .. \quad (3.3)$$

Here $A, B = 1, 2, 3$ run over fermion generations and H, \bar{H} are the light Higgs doublets of the MSSM. As we discussed in the previous chapter that the light Higgs superfields are linear combinations of 6 Higgs doublets $h_i, \bar{h}_i, i = 1 \dots 6$ which come from the GUT multiplets:

$$H = \sum_i \alpha_i h_i \quad ; \quad \bar{H} = \sum_i \bar{\alpha}_i \bar{h}_i \quad (3.4)$$

where $\alpha_i, \bar{\alpha}_i$ are the usual Higgs fractions [19, 23, 24, 27].

Now we need the kinetic terms for the matter and Higgs field in canonical form. For that we need to diagonalize the correction factors $Z_{f, \bar{f}}$. Let $U_{Z_f}, \bar{U}_{Z_{\bar{f}}}$ be the unitary matrices which diagonalize $Z_{f, \bar{f}}$ to positive definite form $\Lambda_{Z_f, Z_{\bar{f}}}$ ($U^\dagger Z U = \Lambda_Z$). We thus have a new basis after performing this transformation as:

$$\begin{aligned} f &= U_{Z_f} \Lambda_{Z_f}^{-\frac{1}{2}} \tilde{f} = \tilde{U}_{Z_f} \tilde{f} \quad ; \quad \bar{f} = U_{Z_{\bar{f}}} \Lambda_{Z_{\bar{f}}}^{-\frac{1}{2}} \tilde{\bar{f}} = \tilde{U}_{Z_{\bar{f}}} \tilde{\bar{f}} \\ H &= \frac{\tilde{H}}{\sqrt{Z_H}} \quad ; \quad \bar{H} = \frac{\tilde{\bar{H}}}{\sqrt{Z_{\bar{H}}}} \end{aligned} \quad (3.5)$$

After substituting these expressions in eq. (3.5) and eq. (3.2) we get

$$\begin{aligned} \mathcal{L} &= \left[\sum_A (\tilde{f}_A^\dagger \tilde{f}_A + \tilde{f}_A^\dagger \tilde{f}_A) + \tilde{H}^\dagger \tilde{H} + \tilde{\bar{H}}^\dagger \tilde{\bar{H}} \right]_D + [\tilde{f}^T \tilde{Y}_f \tilde{f} \tilde{\bar{H}}]_F + H.c. + .. \\ \tilde{Y}_f &= \Lambda_{Z_{\bar{f}}}^{-\frac{1}{2}} U_{Z_{\bar{f}}}^T \frac{Y_f}{\sqrt{Z_{H_f}}} U_{Z_f} \Lambda_{Z_f}^{-\frac{1}{2}} = \tilde{U}_{Z_{\bar{f}}}^T \frac{Y_f}{\sqrt{Z_{H_f}}} \tilde{U}_{Z_f} \end{aligned} \quad (3.6)$$

Now it is \tilde{Y}_f different from original Y_f obtained [19, 23, 24] from the SO(10) Yukawas, should be compared with MSSM Yukawa while fitting at matching scale.

For any light Chiral field Φ_i the generic form of corrections is ($Z = 1 - \mathcal{K}$) :

$$\mathcal{K}_i^j = -\frac{g_{10}^2}{8\pi^2} \sum_{\alpha} Q_{ik}^{\alpha} Q_{kj}^{\alpha} F(m_{\alpha}, m_k) + \frac{1}{32\pi^2} \sum_{kl} Y_{ikl} Y_{jkl}^* F(m_k, m_l) \quad (3.7)$$

Here first term represent corrections from gauge sector and second term corresponds to Yukawa sector. $g_{10} = g_5/\sqrt{2}$ and g_5 are the $SO(10)$ and $SU(5)$ gauge couplings. The example of the terms for gauge coupling and Yukawa coupling has been given in previous chapter.

F is known as the symmetric 1-loop Passarino-Veltman function. When both the fields circulating inside the loop are heavy then $F(m_1, m_2)$ has form

$$F_{12}(M_A, M_B, Q) = \frac{1}{(M_A^2 - M_B^2)} \left(M_A^2 \ln \frac{M_A^2}{Q^2} - M_B^2 \ln \frac{M_B^2}{Q^2} \right) - 1 \quad (3.8)$$

When one field is light (say $M_B \rightarrow 0$) then it reduces to just

$$F_{11}(M_A, Q) = F_{12}(M_A, 0, Q) = \ln \frac{M_A^2}{Q^2} - 1 \quad (3.9)$$

One should keep in mind that if one of the heavy fields in the loop has MSSM doublet type G_{321} quantum numbers $[1, 2, \pm 1]$ then sum over light-light loops must be avoided because that calculations are part of MSSM scale radiative corrections.

3.3 Importance of threshold corrections

The importance of the threshold corrections at M_X for the matter fermion Yukawas can be counted from what values one obtains for $Z_{f,\bar{f},H,\bar{H}}$ using parameters from the previous fits found in [27] (obtained without including GUT scale threshold corrections) .

In the first solution of table (3.1) we see that the wave function corrections to Higgs line have large negative values so they can change the sign of kinetic terms thus violating unitarity condition. Moreover in Solution 2 fermion line corrections

SOLUTION 1			
Eigenvalues($Z_{\bar{u}}$)	0.928326	0.930946	1.031795
Eigenvalues($Z_{\bar{d}}$)	0.915317	0.917464	0.979132
Eigenvalues($Z_{\bar{\nu}}$)	0.870911	0.873470	0.975019
Eigenvalues($Z_{\bar{e}}$)	0.904179	0.908973	0.971322
Eigenvalues(Z_Q)	0.942772	0.946127	1.027745
Eigenvalues(Z_L)	0.911375	0.916329	0.997229
$Z_{\bar{H}}, Z_H$	-109.367	-193.755	
SOLUTION 2			
Eigenvalues($Z_{\bar{u}}$)	-7.526729	-7.416343	1.192789
Eigenvalues($Z_{\bar{d}}$)	-7.845885	-7.738424	1.191023
Eigenvalues($Z_{\bar{\nu}}$)	-8.830309	-8.681419	1.234923
Eigenvalues($Z_{\bar{e}}$)	-7.880892	-7.716853	1.238144
Eigenvalues(Z_Q)	-9.203739	-9.109832	1.171956
Eigenvalues(Z_L)	-9.797736	-9.698265	1.217620
$Z_{\bar{H}}, Z_H$	-264.776	-386.534	

Table 3.1: Examples showing the eigenvalues of the wavefunction renormalization matrices Z_f for fermion lines and for MSSM Higgs ($Z_{H,\bar{H}}$) for solutions found in [27]. In both solutions $Z_{H,\bar{H}}$ are so large that they imply the kinetic terms change sign and in Solution 2 even $Z_{f,\bar{f}}$ have large negative values!

also turn out to be negative along with Higgs correction. So we can say that the parameter sets (of superpotential) found previously in [27] as well as all previous GUTs that claim to account for observed charged fermion and neutrino data are doubtful. However we see that the problem suggests the solution as well: When the correction factors are imposed and we put a constraint on the correction factor to remain positive $Z > 0$, then not only finding the good fits like the previous ones [27], we are able to find regions of the parameter space where matter Yukawa couplings and other super potential parameters are lowered significantly thus improving the status of the model w.r.t. perturbativity conditions.

3.4 Suppression of $d=5$ operators for B,L violation

The important thing to notice is that the coefficients L_{ABCD}, R_{ABCD} of the $d = 5$ baryon decay operators are determined in terms of SO(10) Yukawa couplings $(h, f, g)_{AB}$ which also determine the MSSM yukawa. The effective superpotential can be obtained by integrating out the heavy chiral supermultiplets that is responsible for baryon decay (details are discussed in the previous chapter):

$$W_{eff}^{\Delta B \neq 0} = -L_{ABCD} \left(\frac{1}{2} \epsilon_{Q_A Q_B Q_C L_D} \right) - R_{ABCD} (\epsilon \bar{e}_A \bar{u}_B \bar{u}_C \bar{d}_D) \quad (3.10)$$

Now once we get the one loop corrected Yukawa \tilde{Y}_f (see equation (3.6), we need to diagonalize it to mass basis (let us denote it by primes) using bi-Unitary transformation. The unitary matrices $(U_f^{L,R})$ which will do it are made up of the left and right eigenvectors of \tilde{Y}_f . The phases must be fixed to make the diagonal form $(U_f^L)^T \tilde{Y}_f U_f^R = \Lambda_f$ positive definite :

$$\begin{aligned} W &= (\bar{f}')^T \Lambda_f f' \tilde{H}_f \\ f &= \tilde{U}_{Z_f} U_f^R f' = \tilde{U}'_f f' \\ \bar{f} &= \tilde{U}_{Z_{\bar{f}}} U_f^L \bar{f}' = \tilde{U}'_{\bar{f}} \bar{f}' \end{aligned} \quad (3.11)$$

Due to these transformations the $d = 5, \Delta B = \pm 1$ operator coefficients in terms of primed basis become

$$\begin{aligned} L'_{ABCD} &= \sum_{a,b,c,d} L_{abcd} (\tilde{U}'_Q)_{aA} (\tilde{U}'_Q)_{bB} (\tilde{U}'_Q)_{cC} (\tilde{U}'_L)_{dD} \\ R'_{ABCD} &= \sum_{a,b,c,d} R_{abcd} (\tilde{U}'_{\bar{e}})_{aA} (\tilde{U}'_{\bar{u}})_{bB} (\tilde{U}'_{\bar{u}})_{cC} (\tilde{U}'_{\bar{d}})_{dD} \end{aligned} \quad (3.12)$$

Now while searching with the additional requirement of suppression of $d = 5, \Delta B = \pm 1$ operator coefficients L'_{ABCD}, R'_{ABCD} (so that they give proton lifetime proton lifetime $\tau_p > 10^{34}$ yrs), we find that the search engine inevitably target those re-

gions of $SO(10)$ parameter space where $Z_{H,\bar{H}} \ll 1$. This results into lowering of $SO(10)$ Yukawa couplings required to match the MSSM. They are lowered to such a significant extent [29] that they become much smaller than those [27] when threshold corrections were not included. Now these suppressed Yukawa couplings will enter into L'_{ABCD}, R'_{ABCD} to make them lower. An important point to note is that L'_{ABCD}, R'_{ABCD} are not boosted by $Z_{H,\bar{H}}$ as they don't have an external Higgs line and $Z_{f,\bar{f}}$ have very small effect as they are close to one. The condition to achieve the required baryon decay rates during search for fits is discussed in the next section along with the other features of fitting criteria.

The effect of GUT scale threshold corrections on the MSSM and other GUT parameters is also illuminating and worth mentioning. The MSSM superpotential μ parameter is larger than that derived from the GUT parameters by the factor $(Z_H Z_{\bar{H}})^{-1/2}$. The factor also appears for the soft Susy breaking parameter B . The matter sfermion soft masses are affected by Z_f^{-1} which will be very close to 1 so as to make no difference. However the soft Higgs masses will be enhanced by $Z_{H/\bar{H}}^{-1}$. The trilinear coupling parameter A_0 does not change because the change of wave function corrections are absorbed by the Yukawa coupling which defines it ($A = A_0 \tilde{Y}$). While searching it is these corrected parameters that are found in our fits.

Now an important part of calculations at M_X are the masses of right handed neutrino $(M_{\bar{\nu}})_{AB} \sim f_{AB} \langle \bar{\sigma} \rangle$. However the vev $\langle \bar{\sigma} \rangle$ is protected by the non-renormalization theorem. It is fixed since it is defined in terms of the parameters m, λ, M, η and the corresponding field fluctuation is not a part of the low energy effective theory. The heavy loops will redefine $f_{AB} \rightarrow \tilde{f}_{AB} = (\tilde{U}_{\bar{\nu}}^T f \tilde{U}_{\bar{\nu}})_{AB}$ along with $Y_{AB}^{\nu} \rightarrow \tilde{Y}_{AB}^{\nu}$ (eqn(3.6)). So in Type I Seesaw when the right handed neutrinos $\bar{\nu}$ are integrated out the factors $\tilde{U}_{\bar{\nu}}$ actually cancel out and we are left with $\tilde{U}_{\nu} Z_H^{-1}$ that changes the formula obtained without threshold corrections. So we have considered the effect of one-loop GUT threshold corrections to the gauge, Yukawa, Seesaw, B-decay operators and GUT scale Susy breaking parameters.

3.5 Search strategy and conditions imposed on fits

In this section we discuss the search strategy and conditions imposed on the search engine while doing SM data fit. These conditions includes the requirement of lowering of B-decay as well as constraints from current experimental data [3].

1. Strict positivity condition is imposed on the wave function renormalization factor:

$$Z_{f,\bar{f},H,\bar{H}} > 0 \quad (3.13)$$

Without this the kinetic terms would become ghost like.

2. The suppression of $d = 5, \Delta B \neq 0$ operators (which consists of LLLL and RRRR operators) is achieved by putting a penalty on the maximum value of these operators as $Max(\tilde{O}^{(4)}) < 10^{-5}$ (\tilde{O} is the dimensionless operator in units of $|m/\lambda|$ so in dimensionful terms $Max(O^{(4)}) < 10^{-22} GeV^{-1}$). It results into proton lifetimes above 10^{34} yrs. When threshold corrections were not included the maximal absolute value of $O^{(4)}$ was of $O(10^{-17} GeV^{-1})$ which leads to decay rates $\sim 10^{-27} yr^{-1}$ [27]. The interesting fact is that while looking for fits along with this condition we find those parameter regions where $Z_{H,\bar{H}} \approx 0$. However $Z_{f,\bar{f}}$ undergo minor changes since the **16**-plet Yukawas are suppressed.
3. Along with the contribution of GUT threshold corrections, we incorporated as an improvement the contribution of Susy threshold effects on gauge unification parameters $\alpha_3(M_Z), M_X, \alpha(M_X)$. This is important in the sense that NMSGUT generated Susy spectrum is highly spread out so then can contribute to a significant amount. The correction factors are :

$$\Delta_{\alpha_s}^{Susy} \approx \frac{-19\alpha_s^2}{28\pi} \ln \frac{M_{Susy}}{M_Z} \quad (3.14)$$

Here

$$M_{Susy} = \prod_i m_i^{-\frac{5}{38}(4b_i^4 - 9.6b_i^2 + 5.6b_i^3)} \quad (3.15)$$

is the weighted sum over Susy particles as given in [53].

$$\Delta_X^{Susy} = \frac{1}{11.2\pi} \sum_i (b_1 - b_2) \text{Log}_{10} \frac{m_i}{M_Z} \quad (3.16)$$

$$\Delta_G^{Susy} = \frac{1}{11.2\pi} \sum_i (6.6 b_2 - b_1) \ln \frac{m_i}{M_Z} \quad (3.17)$$

Here b_1, b_2, b_3 are the 1-loop β function coefficients of U(1), SU(2), SU(3) in the MSSM respectively. Among these $\Delta_{\alpha_s}^{Susy}$ can have significant value to change the allowed range at GUT scale. So we limit our search program for following range of $\Delta_{\alpha_s}^{Susy}$.

$$-0.0146 < \Delta_{\alpha_s}^{Susy} < -0.0102 \quad (3.18)$$

4. All the Susy particle masses are calculated at tree level except Higgs mass. The Higgs masses are calculated using the 1-loop corrected electroweak symmetry breaking conditions and 1-loop effective potential using a subroutine [43] based on [54]. The Higgs(h^0) mass in range $124 \text{ GeV} < m_{h^0} < 126 \text{ GeV}$ are ensured via a penalty.
5. The LHC Susy searches have put [55] lower limit of 1200 GeV for the Gluino mass which is quite model independent. So a tolerable Gluino mass is achieved via penalty as $M_{\tilde{G}} > 1 \text{ TeV}$.

3.6 Example fit with description

In this section we present an example fermion fit after including GUT threshold effects. We give a detailed description of the model parameters. Some of the old features of NMSGUT are still there along with some new features which we will

discuss here. The complete set of tables (3.3-3.8) of example fit is given in Appendix B.

In Table 3.3 the complete set of NMSGUT parameters defined at the one loop unification scale $M_X^0 = 10^{16.33}$ GeV-which is the GUT-MSSM matching scale- along with the soft Susy breaking parameters ($m_0, m_{1/2}, A_0, B, M_{H,\bar{H}}^2$) values and the superpotential parameter μ are given. The soft Susy breaking parameters are of N=1 Supergravity GUT type. However Non-universal soft Higgs masses (NUHM) for the MSSM Higgs are allowed as they originate from the mixture of different SO(10) irreps which have their own soft masses and renormalization of Supergravity induced masses by RG flows from M_{Planck} to M_{GUT} . Just like the previous fits found in [27], negative values for these soft masses are found. It can be possible if the soft masses of at least some of the SO(10) representations are negative themselves. From the values of SO(10) matter Yukawa couplings (h_{AA}, f_{AB}, g_{AB}) it is clear that they are suppressed and the superpotential couplings are reduced (η undergoes a large reduction). The mass spectrum of superheavy fields is less spread in magnitude which improves the status of the NMSGUT on the scale of perturbation. The Type I and Type II neutrino seesaw masses along with right handed Majorana neutrino masses are also given. In the second block of the same table are the soft Susy breaking parameters at M_X scale. The universal gaugino parameter $|m_{1/2}|$ is quite small (0-100 GeV) compared to other soft parameters $m_0, A_0, M_{H,\bar{H}}$ which are of O(100 TeV). In this solution it is approximately 0. The values of B and μ at M_X scale are determined by RGE running from M_Z to M_X of values calculated from electroweak symmetry breaking conditions [27, 42]. In the third block the changes ($\Delta_{X,G,3}^{Susy}$) in gauge unification parameters from Susy breaking scale threshold corrections are given. The benefit of imposing $1 \gg Z > 0$ condition can be best appreciated if one compares the solutions found in [27] with solution given here and in [29]. The effective Susy breaking scale defined in Eqn. (3.15) is found to be $M_{Susy} = 2.887$ TeV.

In Table 3.4 the values of the target fermion parameters i.e two loop RGE extrapolated, Susy threshold corrected MSSM Yukawas, mixing angles, neutrino

mixing angles and their mass squared differences are given. The uncertainties in their values are calculated as in [39] along with the achieved values and pulls. It represents an excellent fit with most of the fractional errors $O(1.0\%)$. Next is the eigenvalues of the GUT scale threshold correction factors for fermion, anti-fermion and Higgs lines $Z_{f,\bar{f},H,\bar{H}}$ of Yukawa vertices. It is clear from the table that amoeba search engine has found that region where $Z_{H,\bar{H}} \approx 0$. As the magnitude of SO(10) matter Yukawas is reduced so the $Z_{f,\bar{f}}$ are close to one and almost same for the three generations. Then come ‘‘Higgs fractions’’ [19, 24, 27] $\alpha_i, \bar{\alpha}_i$ which play a crucial role in the fermion mass formulae [24, 27, 33, 34]. We note that the values of the $\alpha_1, \bar{\alpha}_1$ given in the table are taken real by convention although phases are used in threshold corrections. Because the overall phase of the $\alpha, \bar{\alpha}$ does’nt affect the other physical parameters of NMSGUT so we continue to take it real as in [28].

In Table 3.5 the first column contains the running values of the SM masses at M_Z scale. Next column contains mass values calculated from run down values of GUT scale threshold corrected Yukawas from M_X to M_Z using two loop RGEs [38]. Then large $\tan \beta$ driven Susy radiative correction are applied to these masses (third column) which are then compared with the SM values.

Table 3.6 contains the values of the soft supersymmetry breaking parameters at M_Z scale. The kind of soft parameter set the NMSGUT prefers is one of its distinct and remarkable features. The survival of the NMSGUT is linked to a rarely considered and different kind of soft Susy spectrum with large $\mu, A_0, B > 100$ TeV and third generation sfermion masses heavier than first two generations and in the 10-50 TeV range. However in some cases *right chiral* sfermions especially the smuon (see Solution 1 of [29]) emerges at $O(100)$ GeV which is close to experimental lower limits on sfermion masses. Light smuon solutions are interesting in the sense that they allow a significant supersymmetric contribution to the muon $g - 2$ anomaly and they can also provide a coannihilation channel with the LSP (pure Bino in this case) and so reduce the relic density to levels required to validate it as a dark matter candidate. We will discuss this feature in Chapter 8 in detail. An important point worth mentioning is that despite the very small value of $M_{1/2} \approx 0$ at M_X we are able

to get the reasonable gaugino mass parameters because the large A_0 driven two loop RGEs are capable of generating acceptable gaugino masses of $O(1 \text{ TeV})$. Also the correlation between M_1, M_2, M_3 deviates significantly from 1:2:7 just like previous fits [27, 28].

In Table 3.7 the Susy particle masses determined using two loop RGEs parameters given in the previous table without generation mixing and in Table 3.8 masses with generation mixing are given. Since they are so similar they justify the use of diagonal values to estimate the Susy threshold corrections.

The values of B-decay rates for our example solution are given in Table 3.2. The details of contribution from different channels (gluino, neutralino and chargino) can be found in [30].

$\tau_p(M^+\nu)$	$\Gamma(p \rightarrow \pi^+\nu)$	$\text{BR}(p \rightarrow \pi^+\nu_{e,\mu,\tau})$	$\Gamma(p \rightarrow K^+\nu)$	$\text{BR}(p \rightarrow K^+\nu_{e,\mu,\tau})$
3.5×10^{34}	2.1×10^{-36}	$\{1.7 \times 10^{-3}, 0.18, 0.81\}$	2.6×10^{-35}	$\{1.8 \times 10^{-3}, 0.2, 0.8\}$

Table 3.2: $d = 5$ operator mediated proton lifetimes $\tau_p(\text{yrs})$, decay rates $\Gamma(\text{yr}^{-1})$ and Branching ratios in the dominant Meson $^+ + \nu$ channels.

3.7 Conclusions

We showed that the superheavy threshold corrections to Higgs (and matter) kinetic terms and thus to the Yukawa couplings play a critical role due to the large number of fields involved in dressing each line entering the effective MSSM vertices. In fact care must be taken to maintain positivity of the kinetic terms after renormalization which is otherwise generically badly violated : in particular by the fits found earlier. As a result we find that searches incorporating threshold corrected Yukawa couplings, and a constraint to respect B-decay limits, naturally flow to region of parameter space that has weak Yukawa couplings and $Z_{H,\bar{H}}$ close to zero and hence imply strong lowering of the required SO(10) matter Yukawa couplings. The mechanism that we demonstrate is likely to work in any realistic GUT since the features

required are so generic and the necessity of implementation of threshold corrections while maintaining unitarity undeniable. Since its success depends on Z_H approaching zero while remaining positive rather than fine tuning to some specific parameter values our mechanism is likely to be robust against 2 and higher loop corrections. Moreover the large wave function renormalization driven threshold/matching effects can also have notable influence on soft supersymmetry breaking parameters, enhancing $\mu, M_{H,\bar{H}}^2$ relative to their GUT scale values consistent with the patterns found in our fits here and before. The central result of this work is that close attention must be paid to the consequences of the fact that MSSM Higgs multiplets derive from multiple GUT sources. Analyses of GUT models that neglect the multiple GUT level origin of MSSM Higgs and the resulting large threshold corrections to tree level effective MSSM couplings should no longer be accepted uncritically.

3.8 Appendix A

Here we present the explicit form of expressions for correction factors to fermion, anti-fermion lines. As we mentioned that great care must be taken while doing these calculations. so we did many consistency checks to make sure that we have considered contributions from all members of multiplets.

The correction factor to fermion (anti-fermion) line is given as $Z_{f,(\bar{f})} = 1 - \mathcal{K}_{\Phi}^{f,(\bar{f})}$. \mathcal{K}_{Φ}^f signifies the loop corrections on the matter fermion (f) line with loop containing heavy multiplet Φ . Using the formulae in Section 2 gives:

$$(16\pi^2)\mathcal{K}_{\bar{T}}^{\bar{u}} = K_{\bar{T}}^{\bar{u}} + K_T^{\bar{u}} + 2K_H^{\bar{u}} + \frac{16}{3}K_C^{\bar{u}} + 2K_D^{\bar{u}} + K_J^{\bar{u}} + 4K_L^{\bar{u}} + 4K_{\bar{K}}^{\bar{u}} + 16K_M^{\bar{u}} \\ - 2g_{10}^2(0.05F_{11}(m_{\lambda_G}, Q) + F_{11}(m_{\lambda_J}, Q) + F_{11}(m_{\lambda_F}, Q) + 4F_{11}(m_{\lambda_X}, Q) \\ + 2F_{11}(m_{\lambda_E}, Q)) \quad (3.19)$$

$$K_T^{\bar{u}} = 2 \sum_{a=1}^7 \left(\bar{h}U_{1a}^T - 2\bar{f}U_{2a}^T - \sqrt{2}i\bar{g}U_{7a}^T \right)^* \left(\bar{h}U_{1a}^T - 2\bar{f}U_{2a}^T \\ + \sqrt{2}i\bar{g}U_{7a}^T \right) F_{11}(m_a^T, Q) \quad (3.20)$$

$$K_T^{\bar{u}} = \sum_{a=1}^7 \left(\bar{h}V_{1a}^T - 2\bar{f}V_{2a}^T - 2\sqrt{2}i\bar{f}V_{4a}^T - \sqrt{2}\bar{g}V_{6a}^T + \sqrt{2}i\bar{g}V_{7a}^T \right)^* \left(\bar{h}V_{1a}^T - 2\bar{f}V_{2a}^T \\ - 2\sqrt{2}i\bar{f}V_{4a}^T + \sqrt{2}\bar{g}V_{6a}^T - \sqrt{2}i\bar{g}V_{7a}^T \right) F_{11}(m_a^T, Q) \quad (3.21)$$

$$K_H^{\bar{u}} = \sum_{a=2}^6 \left(\bar{h}V_{1a}^H - \frac{2i}{\sqrt{3}}\bar{f}V_{2a}^H - \bar{g}V_{5a}^H + \frac{i}{\sqrt{3}}\bar{g}V_{6a}^H \right)^* \left(\bar{h}V_{1a}^H - \frac{2i}{\sqrt{3}}\bar{f}V_{2a}^H + \bar{g}V_{5a}^H \\ - \frac{i}{\sqrt{3}}\bar{g}V_{6a}^H \right) F_{11}(m_a^H, Q) \quad (3.22)$$

$$K_C^{\bar{u}} = \sum_{a=1}^3 \left(-4\bar{f}V_{2a}^C + 2\bar{g}V_{3a}^C \right)^* \left(-4\bar{f}V_{2a}^C - 2\bar{g}V_{3a}^C \right) F_{11}(m_a^C, Q) \quad (3.23)$$

$$K_D^{\bar{u}} = \sum_{a=1}^3 \left(-4\bar{f}V_{1a}^D + 2\bar{g}V_{3a}^D \right)^* \left(-4\bar{f}V_{1a}^D - 2\bar{g}V_{3a}^D \right) F_{11}(m_a^D, Q) \quad (3.24)$$

$$K_J^{\bar{u}} = \sum_{a=1, a \neq 4}^5 \left(-4i\bar{f}V_{1a}^J + 2i\bar{g}V_{5a}^J \right)^* \left(-4i\bar{f}V_{1a}^J - 2i\bar{g}V_{5a}^J \right) F_{11}(m_a^J, Q) \quad (3.25)$$

$$K_L^{\bar{u}} = \sum_{a=1}^2 \left(2\sqrt{2}i\bar{f}V_{1a}^L + \sqrt{2}\bar{g}V_{2a}^L \right)^* \left(2\sqrt{2}i\bar{f}V_{1a}^L - \sqrt{2}\bar{g}V_{2a}^L \right) F_{11}(m_a^L, Q) \quad (3.26)$$

$$K_K^{\bar{u}} = 2 \sum_{a=1}^2 (-i\bar{g})^* (i\bar{g}) |U_{2a}^K|^2 F_{11}(m_a^K, Q) \quad (3.27)$$

$$K_M^{\bar{u}} = (2i\bar{f})^* (2i\bar{f}) F_{11}(m^M, Q) \quad (3.28)$$

$$\begin{aligned} (16\pi^2)\mathcal{K}^{\bar{d}} &= K_T^{\bar{d}} + K_T^{\bar{d}} + 2K_H^{\bar{d}} + \frac{16}{3}K_C^{\bar{d}} + 2K_E^{\bar{d}} + K_K^{\bar{d}} + 4K_L^{\bar{d}} + 4K_J^{\bar{d}} + 16K_N^{\bar{d}} \\ &\quad - 2g_{10}^2(0.45F_{11}(m_{\lambda_G}, Q) + F_{11}(m_{\lambda_J}, Q) + F_{11}(m_{\lambda_F}, Q) \\ &\quad + 2F_{11}(m_{\lambda_X}, Q) + 4F_{11}(m_{\lambda_E}, Q)) \end{aligned} \quad (3.29)$$

$$\begin{aligned} K_T^{\bar{d}} &= 2 \sum_{a=1}^7 \left(\bar{h}U_{1a}^T - 2\bar{f}U_{2a}^T + \sqrt{2}i\bar{g}U_{7a}^T \right)^* \left(\bar{h}U_{1a}^T - 2\bar{f}U_{2a}^T \right. \\ &\quad \left. - \sqrt{2}i\bar{g}U_{7a}^T \right) F_{11}(m_a^T, Q) \end{aligned} \quad (3.30)$$

$$\begin{aligned} K_T^{\bar{d}} &= \sum_{a=1}^7 \left(-\bar{h}V_{1a}^T + 2\bar{f}V_{2a}^T - 2\sqrt{2}i\bar{f}V_{4a}^T + \sqrt{2}\bar{g}V_{6a}^T + \sqrt{2}i\bar{g}V_{7a}^T \right)^* \left(-\bar{h}V_{1a}^T \right. \\ &\quad \left. + 2\bar{f}V_{2a}^T - 2\sqrt{2}i\bar{f}V_{4a}^T - \sqrt{2}\bar{g}V_{6a}^T - \sqrt{2}i\bar{g}V_{7a}^T \right) F_{11}(m_a^T, Q) \end{aligned} \quad (3.31)$$

$$\begin{aligned} K_H^{\bar{d}} &= \sum_{a=2}^6 \left(-\bar{h}U_{1a}^H + \frac{2i}{\sqrt{3}}\bar{f}U_{2a}^H + \bar{g}U_{5a}^H - \frac{i}{\sqrt{3}}\bar{g}U_{6a}^H \right)^* \left(-\bar{h}U_{1a}^H + \frac{2i}{\sqrt{3}}\bar{f}U_{2a}^H \right. \\ &\quad \left. - \bar{g}U_{5a}^H + \frac{i}{\sqrt{3}}\bar{g}U_{6a}^H \right) F_{11}(m_a^H, Q) \end{aligned} \quad (3.32)$$

$$K_C^{\bar{d}} = \sum_{a=1}^3 \left(4\bar{f}U_{1a}^C - 2\bar{g}U_{3a}^C \right)^* \left(4\bar{f}U_{1a}^C + 2\bar{g}U_{3a}^C \right) F_{11}(m_a^C, Q) \quad (3.33)$$

$$K_E^{\bar{d}} = \sum_{a=1, a \neq 5}^6 \left(4\bar{f}V_{1a}^E - 2\bar{g}V_{6a}^E \right)^* \left(4\bar{f}V_{1a}^E + 2\bar{g}V_{6a}^E \right) F_{11}(m_a^E, Q) \quad (3.34)$$

$$K_K^{\bar{d}} = \sum_{a=1}^2 \left(4i\bar{f}V_{1a}^K - 2i\bar{g}V_{2a}^K \right)^* \left(4i\bar{f}V_{1a}^K + 2i\bar{g}V_{2a}^K \right) F_{11}(m_a^K, Q) \quad (3.35)$$

$$K_L^{\bar{d}} = \sum_{a=1}^2 \left(2\sqrt{2}i\bar{f}V_{1a}^L - \sqrt{2}\bar{g}V_{2a}^L \right)^* \left(2\sqrt{2}i\bar{f}V_{1a}^L + \sqrt{2}\bar{g}V_{2a}^L \right) F_{11}(m_a^L, Q) \quad (3.36)$$

$$K_J^{\bar{d}} = 2 \sum_{a=1, a \neq 4}^5 (i\bar{g})^* (-i\bar{g}) |U_{5a}^J|^2 F_{11}(m_a^J, Q) \quad (3.37)$$

$$K_N^{\bar{d}} = (2i\bar{f})^* (2i\bar{f}) F_{11}(m^N, Q) \quad (3.38)$$

$$(16\pi^2)\mathcal{K}^{\bar{e}} = 3K_T^{\bar{e}} + 2K_H^{\bar{e}} + K_F^{\bar{e}} + 6K_D^{\bar{e}} + 3K_K^{\bar{e}} + 4K_A^{\bar{e}} - 2g_{10}^2(0.05F_{11}(m_{\lambda_G}, Q) \\ + 3F_{11}(m_{\lambda_J}, Q) + F_{11}(m_{\lambda_F}, Q) + 6F_{11}(m_{\lambda_X}, Q)) \quad (3.39)$$

$$K_T^{\bar{e}} = \sum_{a=1}^7 \left(\bar{h}V_{1a}^T - 2\bar{f}V_{2a}^T - 2\sqrt{2}i\bar{f}V_{4a}^T + \sqrt{2}\bar{g}V_{6a}^T - \sqrt{2}i\bar{g}V_{7a}^T \right)^* \left(\bar{h}V_{1a}^T - 2\bar{f}V_{2a}^T \\ - 2\sqrt{2}i\bar{f}V_{4a}^T - \sqrt{2}\bar{g}V_{6a}^T + \sqrt{2}i\bar{g}V_{7a}^T \right) F_{11}(m_a^T, Q) \quad (3.40)$$

$$K_H^{\bar{e}} = \sum_{a=2}^6 \left(-\bar{h}U_{1a}^H - 2\sqrt{3}i\bar{f}U_{2a}^H + \bar{g}U_{5a}^H + \sqrt{3}i\bar{g}U_{6a}^H \right)^* \left(-\bar{h}U_{1a}^H - 2\sqrt{3}i\bar{f}U_{2a}^H \\ - \bar{g}U_{5a}^H - \sqrt{3}i\bar{g}U_{6a}^H \right) F_{11}(m_a^H, Q) \quad (3.41)$$

$$K_F^{\bar{e}} = \sum_{a=1, a \neq 3}^4 \left(4i\bar{f}U_{1a}^F - 2\bar{g}U_{4a}^F \right)^* \left(4i\bar{f}U_{1a}^F + 2\bar{g}U_{4a}^F \right) F_{11}(m_a^F, Q) \quad (3.42)$$

$$K_D^{\bar{e}} = \sum_{a=1}^3 \left(4\bar{f}U_{2a}^D - 2\bar{g}U_{3a}^D \right)^* \left(4\bar{f}U_{2a}^D + 2\bar{g}U_{3a}^D \right) F_{11}(m_a^D, Q) \quad (3.43)$$

$$K_K^{\bar{e}} = \sum_{a=1}^2 \left(4i\bar{f}V_{1a}^K + 2i\bar{g}V_{2a}^K \right)^* \left(4i\bar{f}V_{1a}^K - 2i\bar{g}V_{2a}^K \right) F_{11}(m_a^K, Q) \quad (3.44)$$

$$K_A^{\bar{e}} = (2\sqrt{2}i\bar{f})^* (2\sqrt{2}i\bar{f}) F_{11}(m^A, Q) \quad (3.45)$$

$$(16\pi^2)\mathcal{K}^{\bar{v}} = 3K_T^{\bar{v}} + 2K_H^{\bar{v}} + K_F^{\bar{v}} + 6K_E^{\bar{v}} + 3K_J^{\bar{v}} + 4K_G^{\bar{v}} - 2g_{10}^2(1.25F_{11}(m_{\lambda_G}, Q) \\ + 3F_{11}(m_{\lambda_J}, Q) + F_{11}(m_{\lambda_F}, Q) + 6F_{11}(m_{\lambda_E}, Q)) \quad (3.46)$$

$$K_T^{\bar{\nu}} = \sum_{a=1}^7 \left(-\bar{h}V_{1a}^T + 2\bar{f}V_{2a}^T - 2\sqrt{2}i\bar{f}V_{4a}^T - \sqrt{2}\bar{g}V_{6a}^T - \sqrt{2}i\bar{g}V_{7a}^T \right)^* \left(-\bar{h}V_{1a}^T + 2\bar{f}V_{2a}^T - 2\sqrt{2}i\bar{f}V_{4a}^T + \sqrt{2}\bar{g}V_{6a}^T + \sqrt{2}i\bar{g}V_{7a}^T \right) F_{11}(m_a^T, Q) \quad (3.47)$$

$$K_H^{\bar{\nu}} = \sum_{a=2}^6 \left(\bar{h}V_{1a}^H + 2\sqrt{3}i\bar{f}V_{2a}^H - \bar{g}V_{5a}^H - \sqrt{3}i\bar{g}V_{6a}^H \right)^* \left(\bar{h}V_{1a}^H + 2\sqrt{3}i\bar{f}V_{2a}^H + \bar{g}V_{5a}^H + \sqrt{3}i\bar{g}V_{6a}^H \right) F_{11}(m_a^H, Q) \quad (3.48)$$

$$K_F^{\bar{\nu}} = \sum_{a=1, a \neq 3}^4 \left(-4i\bar{f}U_{1a}^F + 2\bar{g}U_{4a}^F \right)^* \left(-4i\bar{f}U_{1a}^F - 2\bar{g}U_{4a}^F \right) F_{11}(m_a^F, Q) \quad (3.49)$$

$$K_E^{\bar{\nu}} = \sum_{a=1, a \neq 5}^6 \left(-4i\bar{f}U_{2a}^E + 2\bar{g}U_{6a}^E \right)^* \left(-4i\bar{f}U_{2a}^E - 2\bar{g}U_{6a}^E \right) F_{11}(m_a^E, Q) \quad (3.50)$$

$$K_J^{\bar{\nu}} = \sum_{a=1, a \neq 4}^5 \left(-4i\bar{f}V_{1a}^J - 2i\bar{g}V_{5a}^J \right)^* \left(-4i\bar{f}V_{1a}^J + 2i\bar{g}V_{5a}^J \right) F_{11}(m_a^J, Q) \quad (3.51)$$

$$K_G^{\bar{\nu}} = \sum_{a=1}^5 (-2\sqrt{2}i\bar{f})^* (-2\sqrt{2}i\bar{f}) |U_{5a}^G|^2 F_{11}(m_a^G, Q)$$

$$\begin{aligned} (16\pi^2)\mathcal{K}^u &= K_T^u + K_T^u + K_H^u + K_H^u + \frac{8}{3}K_C^u + \frac{8}{3}K_C^u + K_E^u + K_D^u + 3K_P^u \\ &\quad + 12K_P^u + 48K_W^{\bar{u}} + 4K_L^{\bar{u}} - 2g_{10}^2(0.05F_{11}(m_{\lambda_G}, Q) + F_{11}(m_{\lambda_J}, Q) \\ &\quad + 3F_{11}(m_{\lambda_X}, Q) + 3F_{11}(m_{\lambda_E}, Q)) = (16\pi^2)\mathcal{K}^d \end{aligned} \quad (3.52)$$

$$K_T^u = \sum_{a=1}^7 \left(-\bar{h}U_{1a}^T - 2\bar{f}U_{2a}^T + \sqrt{2}\bar{g}U_{6a}^T \right)^* \left(-\bar{h}U_{1a}^T - 2\bar{f}U_{2a}^T - \sqrt{2}\bar{g}U_{6a}^T \right) F_{11}(m_a^T, Q) \quad (3.53)$$

$$K_T^u = 2 \sum_{a=1}^7 \left(\bar{h}V_{1a}^T + 2\bar{f}V_{2a}^T \right)^* \left(\bar{h}V_{1a}^T + 2\bar{f}V_{2a}^T \right) F_{11}(m_a^T, Q) \quad (3.54)$$

$$K_H^u = \sum_{a=2}^6 \left(-\bar{h}U_{1a}^H + \frac{2i}{\sqrt{3}}\bar{f}U_{2a}^H - \bar{g}U_{5a}^H + \frac{i}{\sqrt{3}}\bar{g}U_{6a}^H \right)^* \left(-\bar{h}U_{1a}^H + \frac{2i}{\sqrt{3}}\bar{f}U_{2a}^H + \bar{g}U_{5a}^H - \frac{i}{\sqrt{3}}\bar{g}U_{6a}^H \right) F_{11}(m_a^H, Q) \quad (3.55)$$

$$K_H^u = \sum_{a=2}^6 \left(\bar{h}V_{1a}^H - \frac{2i}{\sqrt{3}}\bar{f}V_{2a}^H + \bar{g}V_{5a}^H - \frac{i\bar{g}}{\sqrt{3}}V_{6a}^H \right)^* \left(\bar{h}V_{1a}^H - \frac{2i}{\sqrt{3}}\bar{f}V_{2a}^H - \bar{g}V_{5a}^H + \frac{i\bar{g}}{\sqrt{3}}V_{6a}^H \right) F_{11}(m_a^H, Q) \quad (3.56)$$

$$K_C^u = \sum_{a=1}^3 \left(-4\bar{f}V_{2a}^C - 2\bar{g}V_{3a}^C \right)^* \left(-4\bar{f}V_{2a}^C + 2\bar{g}V_{3a}^C \right) F_{11}(m_a^C, Q) \quad (3.57)$$

$$K_C^u = \sum_{a=1}^3 \left(4\bar{f}U_{1a}^C + 2\bar{g}U_{3a}^C \right)^* \left(4\bar{f}U_{1a}^C - 2\bar{g}U_{3a}^C \right) F_{11}(m_a^C, Q) \quad (3.58)$$

$$K_E^u = \sum_{a=1, a \neq 5}^6 \left(-4\bar{f}U_{2a}^E - 2\bar{g}U_{6a}^E \right)^* \left(-4\bar{f}U_{2a}^E + 2\bar{g}U_{6a}^E \right) F_{11}(m_a^E, Q) \quad (3.59)$$

$$K_D^u = \sum_{a=1}^3 \left(4\bar{f}U_{2a}^D + 2\bar{g}U_{3a}^D \right)^* \left(4\bar{f}U_{2a}^D - 2\bar{g}U_{3a}^D \right) F_{11}(m_a^D, Q) \quad (3.60)$$

$$K_P^u = \sum_{a=1}^2 \left(2\sqrt{2}\bar{f}U_{1a}^P - \sqrt{2}\bar{g}U_{2a}^P \right)^* \left(2\sqrt{2}\bar{f}U_{1a}^P + \sqrt{2}\bar{g}U_{2a}^P \right) F_{11}(m_a^P, Q) \quad (3.61)$$

$$K_P^u = 2 \sum_{a=1}^2 \left(-\frac{\bar{g}}{\sqrt{2}} \right)^* \left(\frac{\bar{g}}{\sqrt{2}} \right) |V_{2a}^P|^2 F_{11}(m_a^P, Q) \quad (3.62)$$

$$K_W^u = (\sqrt{2}\bar{f})^* (\sqrt{2}\bar{f}) F_{11}(m^W, Q) \quad (3.63)$$

$$K_L^u = \sum_{a=1}^2 (-\sqrt{2}\bar{g})^* (\sqrt{2}\bar{g}) |U_{2a}^L|^2 F_{11}(m_a^L, Q) \quad (3.64)$$

$$\begin{aligned} (16\pi^2)\mathcal{K}^e &= 3K_T^e + K_H^e + K_H^e + 3K_D^e + 3K_E^e + 9K_P^e + K_F^e + 12K_O^e \\ &\quad - 2g_{10}^2(0.45F_{11}(m_{\lambda_G}, Q) + 3F_{11}(m_{\lambda_J}, Q) + 3F_{11}(m_{\lambda_X}, Q) + 3F_{11}(m_{\lambda_E}, Q)) \\ &= (16\pi^2)\mathcal{K}^\nu \end{aligned} \quad (3.65)$$

$$K_T^e = \sum_{a=1}^7 \left(-\bar{h}U_{1a}^T - 2\bar{f}U_{2a}^T - \sqrt{2}\bar{g}U_{6a}^T \right)^* \left(-\bar{h}U_{1a}^T - 2\bar{f}U_{2a}^T + \sqrt{2}\bar{g}U_{6a}^T \right) F_{11}(m_a^T, Q) \quad (3.66)$$

$$K_H^e = \sum_{a=2}^6 \left(\bar{h}U_{1a}^H + 2\sqrt{3}i\bar{f}U_{2a}^H + \bar{g}U_{5a}^H + \sqrt{3}i\bar{g}U_{6a}^H \right)^* \left(\bar{h}U_{1a}^H + 2\sqrt{3}i\bar{f}U_{2a}^H - \bar{g}U_{5a}^H - \sqrt{3}i\bar{g}U_{6a}^H \right) F_{11}(m_a^H, Q) \quad (3.67)$$

$$K_H^e = \sum_{a=2}^6 \left(-\bar{h}V_{1a}^H - 2\sqrt{3}i\bar{f}V_{2a}^H - \bar{g}V_{5a}^H - i\sqrt{3}\bar{g}V_{6a}^H \right)^* \left(-\bar{h}V_{1a}^H - 2\sqrt{3}i\bar{f}V_{2a}^H + \bar{g}V_{5a}^H + i\sqrt{3}\bar{g}V_{6a}^H \right) F_{11}(m_a^F, Q) \quad (3.68)$$

$$K_D^e = \sum_{a=1}^3 \left(4\bar{f}V_{1a}^D + 2\bar{g}V_{3a}^D \right)^* \left(4\bar{f}V_{1a}^D - 2\bar{g}V_{3a}^D \right) F_{11}(m_a^D, Q) \quad (3.69)$$

$$K_E^e = \sum_{a=1, a \neq 5}^6 \left(-4\bar{f}V_{1a}^E - 2\bar{g}V_{6a}^E \right)^* \left(-4\bar{f}V_{1a}^E + 2\bar{g}V_{6a}^E \right) F_{11}(m_a^E, Q) \quad (3.70)$$

$$K_P^e = \sum_{a=1}^2 \left(2\sqrt{2}\bar{f}U_{1a}^P + \sqrt{2}\bar{g}U_{2a}^P \right)^* \left(2\sqrt{2}\bar{f}U_{1a}^P - \sqrt{2}\bar{g}U_{2a}^P \right) F_{11}(m_a^P, Q) \quad (3.71)$$

$$K_F^e = \sum_{a=1, a \neq 3}^4 (-2\bar{g})^*(2\bar{g})|V_{4a}^F|^2 F_{11}(m_a^F, Q) \quad (3.72)$$

$$K_O^e = (2i\bar{f})^*(2i\bar{f})F_{11}(m^O, Q) \quad (3.73)$$

Here g_{10} is the SO(10) gauge coupling and

$$\bar{h} = 2\sqrt{2}h \quad ; \quad \bar{g} = 2\sqrt{2}g \quad ; \quad \bar{f} = 2\sqrt{2}f$$

Due to mixing among the several Higgs (6 pairs) from **10**, **120**(2 pairs) $\overline{\mathbf{126}}$, **126**, **210** SO(10) Higgs multiplets calculation for the correction factor to the light Higgs doublet lines H, \overline{H} is much more tedious than the matter lines. The MSSM Higgs is linear combination of SO(10) Higgs multiplets. The couplings of the GUT field doublets. Having the Pati-Salam decomposition of trilinear Yukawa terms [23, 24, 27] in hand we need to do MSSM decomposition. The we need to recognize those terms

which forms singlet with the MSSM Higgs field. The NMSGUT spectra is named after 26 letters of alphabet [23, 24] and there are precisely 26 different combinations of GUT multiplets which form singlets with the MSSM $H[1, 2, 1]$ and similarly 26 with $\bar{H}[1, 2, -1]$. After summing them we get

$$\begin{aligned}
(16\pi^2)\mathcal{K}_H = & 8K_{R\bar{C}} + 3K_{J\bar{D}} + 3K_{E\bar{J}} + 9K_{X\bar{P}} + 3K_{X\bar{T}} + 9K_{P\bar{E}} + 3K_{T\bar{E}} + 6K_{Y\bar{L}} \\
& + K_{V\bar{F}} + 8K_{C\bar{Z}} + 3K_{D\bar{I}} + 24K_{Q\bar{C}} + 9K_{E\bar{U}} + 9K_{U\bar{D}} + 6K_{L\bar{B}} + 3K_{K\bar{X}} \\
& + 6K_{B\bar{M}} + 18K_{W\bar{B}} + 18K_{Y\bar{W}} + 3K_{V\bar{O}} + 6K_{N\bar{Y}} + K_{\bar{V}\bar{A}} + 3K_{H\bar{O}} \\
& + 3K_{S\bar{H}} + K_{H\bar{F}} + K_{G\bar{H}} \tag{3.74}
\end{aligned}$$

Here the number in front of correction factor K is the multiplicity factor (color, $SU(2)$ multiplicity etc.). Similarly for \bar{H} conjugated pairs run inside the loop (unless it is a real irrep). Here we present the expression for one of these and rest of the expressions for correction factors to Higgs line can be found in [29, 30].

$$\begin{aligned}
K_{R\bar{C}} = & \sum_{a=1}^{d(R)} \sum_{a'=1}^{d(C)} \left| \left(\frac{i\kappa}{\sqrt{2}} V_{2a}^R U_{3a'}^C - \gamma V_{1a}^R U_{2a'}^C + \frac{\gamma}{\sqrt{2}} V_{2a}^R U_{2a'}^C - \bar{\gamma} V_{1a}^R U_{1a'}^C - \frac{\bar{\gamma}}{\sqrt{2}} V_{2a}^R U_{1a'}^C \right) V_{11}^H \right. \\
& + \left(\frac{2\eta}{\sqrt{3}} V_{1a}^R U_{2a'}^C - \sqrt{\frac{2}{3}} \eta V_{2a}^R U_{2a'}^C + \frac{i\bar{\zeta}}{\sqrt{6}} V_{2a}^R U_{3a'}^C \right) V_{21}^H + \left(\frac{2\eta}{\sqrt{3}} V_{1a}^R U_{1a'}^C + \sqrt{\frac{2}{3}} \eta V_{2a}^R U_{1a'}^C \right. \\
& + \left. \frac{i\zeta}{\sqrt{6}} V_{2a}^R U_{3a'}^C \right) V_{31}^H + \left(\frac{\zeta}{\sqrt{2}} V_{2a}^R U_{2a'}^C - \frac{i\rho}{3\sqrt{2}} V_{2a}^R U_{3a'}^C + \frac{\bar{\zeta}}{\sqrt{2}} V_{2a}^R U_{1a'}^C \right) V_{51}^H - \left(\frac{i\zeta}{\sqrt{6}} V_{2a}^R U_{2a'}^C \right. \\
& + \left. \frac{i\bar{\zeta}}{\sqrt{6}} V_{2a}^R U_{1a'}^C - \frac{\rho}{3\sqrt{3}} V_{1a}^R U_{3a'}^C \right) V_{61}^H \Big|^2 F_{12}(m_a^R, m_{a'}^C, Q) \tag{3.75}
\end{aligned}$$

3.9 Appendix B: Example fermion fit with threshold effects

Parameter	Value	Field [$SU(3), SU(2), Y$]	Masses (Units of 10^{16}GeV)
χ_X	0.133	$A[1, 1, 4]$	1.36
χ_Z	0.056	$B[6, 2, 5/3]$	0.097
$h_{11}/10^{-6}$	3.96	$C[8, 2, 1]$	0.93, 5.17, 7.45
$h_{22}/10^{-4}$	3.61	$D[3, 2, 7/3]$	0.29, 6.07, 9.09
h_{33}	0.018	$E[3, 2, 1/3]$	0.11, 0.75, 2.60
$f_{11}/10^{-6}$	$-0.013 + 0.159i$		2.60, 4.85, 8.23
$f_{12}/10^{-6}$	$-1.022 - 1.812i$	$F[1, 1, 2]$	0.19, 0.65
$f_{13}/10^{-5}$	$0.072 + 0.339i$		0.65, 4.30
$f_{22}/10^{-5}$	$6.554 + 4.376i$	$G[1, 1, 0]$	0.025, 0.20, 0.76
$f_{23}/10^{-4}$	$-0.734 + 2.351i$		0.77, 0.77, 0.85
$f_{33}/10^{-3}$	$-1.273 + 0.516i$	$h[1, 2, 1]$	0.33, 2.67, 5.57
$g_{12}/10^{-4}$	$0.128 + 0.19i$		7.65, 17.54
$g_{13}/10^{-5}$	$-9.543 + 2.823i$	$I[3, 1, 10/3]$	0.36
$g_{23}/10^{-4}$	$-1.64 - 0.628i$	$J[3, 1, 4/3]$	0.30, 0.39, 1.44
$\lambda/10^{-2}$	$-4.691 - 0.149i$		1.44, 5.01
η	$-0.249 + 0.068i$	$K[3, 1, 8/3]$	1.73, 5.14
ρ	$1.175 - 0.297i$	$L[6, 1, 2/3]$	1.79, 2.60
k	$-0.018 + 0.058i$	$M[6, 1, 8/3]$	1.95
ζ	$1.296 + 0.951i$	$N[6, 1, 4/3]$	1.88
$\bar{\zeta}$	$0.224 + 0.589i$	$O[1, 3, 2]$	3.14
$m/10^{16}\text{GeV}$	0.010	$P[3, 3, 2/3]$	0.49, 4.65
$m_\Theta/10^{16}\text{GeV}$	$-2.55e^{-i\text{Arg}(\lambda)}$	$Q[8, 3, 0]$	0.31
γ	0.39	$R[8, 1, 0]$	0.10, 0.38
$\bar{\gamma}$	-2.45	$S[1, 3, 0]$	0.44
x	$0.85 + 0.51i$	$t[3, 1, 2/3]$	0.38, 1.16, 1.67, 3.05
$\Delta_X^{tot}, \Delta_X^{GUT}$	0.80, 0.86		5.18, 5.70, 20.56
$\Delta_G^{tot}, \Delta_G^{GUT}$	-20.52, -23.43	$U[3, 3, 4/3]$	0.38
$\Delta\alpha_3^{tot}(M_Z), \Delta\alpha_3^{GUT}(M_Z)$	-0.012, -0.002	$V[1, 2, 3]$	0.26
$\{M^{\nu^c}/10^{12}\text{GeV}\}$	0.0002, 2.33, 81.40	$W[6, 3, 2/3]$	2.50
$\{M_{II}^\nu/10^{-8}\text{eV}\}$	0.005, 42.93, 1496.83	$X[3, 2, 5/3]$	0.09, 2.83, 2.83
$M_\nu(\text{meV})$	1.171, 7.11, 40.21	$Y[6, 2, 1/3]$	0.11
$\{\text{Evals}[f]\}/10^{-6}$	0.004, 40.69, 1418.7	$Z[8, 1, 2]$	0.38
Soft parameters at M_X	$m_{\frac{1}{2}} = 0.000$ $\mu = 1.72 \times 10^5$ $M_H^2 = -2.9 \times 10^{10}$	$m_0 = 12860.4$ $B = -1.5 \times 10^{10}$ $M_H^2 = -2.9 \times 10^{10}$	$A_0 = -1.98 \times 10^5$ $\tan\beta = 50.0$ $R_{\frac{b\tau}{s\mu}} = 5.64$
$\text{Max}(L_{ABCD} , R_{ABCD})$	$7.7 \times 10^{-22} \text{GeV}^{-1}$		
Susy contribution to $\Delta_{X,G,3}$	$\Delta_X^{\text{Susy}} = -0.053$	$\Delta_G^{\text{Susy}} = 2.91$	$\Delta_3^{\text{Susy}} = -0.01$

Table 3.3: Column 1 contains values of the NMSGUT-SUGRY-NUHM parameters at M_X derived from an accurate fit to all 18 fermion data and compatible with RG constraints. Unification parameters and mass spectrum of superheavy and superlight fields are also given. The values of $\mu(M_X), B(M_X)$ are determined by RG evolution from M_Z to M_X of the values determined by the EWRSB conditions.

Parameter	Target = \bar{O}_i	Uncert. = δ_i	Achieved = O_i	Pull = $\frac{(O_i - \bar{O}_i)}{\delta_i}$
$y_u/10^{-6}$	2.035847	0.777694	2.035834	-0.000017
$y_c/10^{-3}$	0.992361	0.163740	0.994253	0.011560
y_t	0.350010	0.014000	0.350076	0.004715
$y_d/10^{-5}$	10.674802	6.223410	10.374090	-0.048320
$y_s/10^{-3}$	2.024872	0.955740	2.118158	0.097606
y_b	0.340427	0.176682	0.349778	0.052924
$y_e/10^{-4}$	1.121867	0.168280	1.122417	0.003267
$y_\mu/10^{-2}$	2.369435	0.355415	2.364688	-0.013356
y_τ	0.474000	0.090060	0.471211	-0.030967
$\sin \theta_{12}^q$	0.2210	0.001600	0.2210	0.0009
$\sin \theta_{13}^q/10^{-4}$	30.0759	5.000000	30.0765	0.0001
$\sin \theta_{23}^q/10^{-3}$	35.3864	1.300000	35.3924	0.0046
δ^q	60.0215	14.000000	60.0469	0.0018
$(m_{12}^2)/10^{-5}(eV)^2$	4.9239	0.521931	4.9233	-0.0012
$(m_{23}^2)/10^{-3}(eV)^2$	1.5660	0.313209	1.5664	0.0011
$\sin^2 \theta_{12}^L$	0.2944	0.058878	0.2931	-0.0217
$\sin^2 \theta_{23}^L$	0.4652	0.139567	0.4622	-0.0220
$\sin^2 \theta_{13}^L$	0.0255	0.019000	0.0260	0.0252
$(Z_{\bar{u}})$	0.972582	0.972763	0.972764	
$(Z_{\bar{d}})$	0.967473	0.967657	0.967659	
$(Z_{\bar{\nu}})$	0.946651	0.946835	0.946838	
$(Z_{\bar{e}})$	0.961973	0.962151	0.962154	
(Z_Q)	0.983138	0.983334	0.983336	
(Z_L)	0.967422	0.967617	0.967619	
$Z_{\bar{H}}, Z_H$	0.000480	0.001284		
α_1	$0.202 + 0.000i$	$\bar{\alpha}_1$	$0.134 - 0.000i$	
α_2	$-0.481 - 0.632i$	$\bar{\alpha}_2$	$-0.518 - 0.285i$	
α_3	$0.011 - 0.356i$	$\bar{\alpha}_3$	$-0.360 - 0.286i$	
α_4	$0.362 - 0.147i$	$\bar{\alpha}_4$	$0.497 + 0.328i$	
α_5	$-0.0160 - 0.045i$	$\bar{\alpha}_5$	$0.054 - 0.229i$	
α_6	$-0.001 - 0.217i$	$\bar{\alpha}_6$	$0.019 - 0.105i$	

Table 3.4: Solution 2: Fit with $\chi_X = \sqrt{\sum_{i=1}^{17} (O_i - \bar{O}_i)^2 / \delta_i^2} = 0.1326$. Target values, at M_X of the fermion Yukawa couplings and mixing parameters, together with the estimated uncertainties, achieved values and pulls. The eigenvalues of the wavefunction renormalization increment matrices Z_i for fermion lines and the factors for Higgs lines are given. The Higgs fractions $\alpha_i, \bar{\alpha}_i$ which control the MSSM fermion Yukawa couplings are also given. Right handed neutrino threshold effects have been ignored. We have truncated numbers for display although all calculations are done at double precision.

Parameter	SM(M_Z)	$m^{\text{GUT}}(M_Z)$	$m^{\text{MSSM}} = (m + \Delta m)^{\text{GUT}}(M_Z)$
$m_d/10^{-3}$	2.90000	1.05215	2.80332
$m_s/10^{-3}$	55.00000	21.48237	57.23281
m_b	2.90000	2.77488	2.94586
$m_e/10^{-3}$	0.48657	0.48189	0.48468
m_μ	0.10272	0.10148	0.10207
m_τ	1.74624	1.73337	1.73251
$m_u/10^{-3}$	1.27000	1.09833	1.27302
m_c	0.61900	0.53640	0.62171
m_t	172.50000	146.22372	172.58158

Table 3.5: Values of standard model fermion masses in GeV at M_Z compared with the masses obtained from values of GUT derived Yukawa couplings run down from M_X^0 to M_Z both before and after threshold corrections. Fit with $\chi_Z = \sqrt{\sum_{i=1}^9 (m_i^{\text{MSSM}} - m_i^{\text{SM}})^2 / (m_i^{\text{MSSM}})^2} = 0.0557$.

Parameter	Value	Parameter	Value
M_1	246.41	$M_{\tilde{u}_1}$	12822.53
M_2	590.18	$M_{\tilde{u}_2}$	12822.49
M_3	1200.01	$M_{\tilde{u}_3}$	48248.96
$M_{\tilde{l}_1}$	11957.95	$A_{11}^{0(l)}$	-137311.14
$M_{\tilde{l}_2}$	11961.97	$A_{22}^{0(l)}$	-137158.88
$M_{\tilde{l}_3}$	38556.41	$A_{33}^{0(l)}$	-93057.53
$M_{\tilde{L}_1}$	15324.76	$A_{11}^{0(u)}$	-147185.28
$M_{\tilde{L}_2}$	15326.33	$A_{22}^{0(u)}$	-147183.69
$M_{\tilde{L}_3}$	30130.38	$A_{33}^{0(u)}$	-81454.63
$M_{\tilde{d}_1}$	11245.04	$A_{11}^{0(d)}$	-138168.65
$M_{\tilde{d}_2}$	11246.12	$A_{22}^{0(d)}$	-138165.70
$M_{\tilde{d}_3}$	49308.99	$A_{33}^{0(d)}$	-76263.17
$M_{\tilde{Q}_1}$	13440.51	$\tan \beta$	50.00
$M_{\tilde{Q}_2}$	13440.94	$\mu(M_Z)$	155715.41
$M_{\tilde{Q}_3}$	48976.61	$B(M_Z)$	4.1869×10^9
M_H^2	-2.5331×10^{10}	M_H^2	-2.5545×10^{10}

Table 3.6: Values (in GeV) of the soft Susy parameters at M_Z (evolved from the soft SUGRY-NUHM parameters at M_X). The values of soft Susy parameters at M_Z determine the Susy threshold corrections to the fermion Yukawas. The matching of run down fermion Yukawas in the MSSM to the SM parameters determines soft SUGRY parameters at M_X . Note the heavier third sgeneration. The values of $\mu(M_Z)$ and the corresponding soft Susy parameter $B(M_Z) = m_A^2 \sin 2\beta/2$ are determined by imposing electroweak symmetry breaking conditions. m_A is the mass of the CP odd scalar in the Doublet Higgs. The sign of μ is assumed positive.

Field	Mass(GeV)
$M_{\tilde{G}}$	1200.01
M_{χ^\pm}	590.18, 155715.46
M_{χ^0}	246.41, 590.18, 155715.44, 155715.44
$M_{\tilde{\nu}}$	15324.618, 15326.183, 30130.304
$M_{\tilde{e}}$	11958.03, 15324.84, 11961.76, 15326.63, 30125.09, 38560.60
$M_{\tilde{u}}$	12822.48, 13440.40, 12822.42, 13440.85, 48227.49, 48998.14
$M_{\tilde{d}}$	11245.07, 13440.65, 11246.13, 13441.10, 48865.41, 49419.24
M_A	457636.54
M_{H^\pm}	457636.55
M_{H^0}	457636.54
M_{h^0}	125.00

Table 3.7: Spectra of supersymmetric partners calculated ignoring generation mixing effects. Inclusion of such effects changes the spectra only marginally. Due to the large values of μ, B, A_0 the LSP and light chargino are essentially pure Bino and Wino(\tilde{W}_\pm). The light gauginos and light Higgs h^0 , are accompanied by a light smuon and sometimes selectron. The rest of the sfermions have multi-TeV masses. The mini-split supersymmetry spectrum and large μ, A_0 parameters help avoid problems with FCNC and CCB/UFB instability [56]. The sfermion masses are ordered by generation not magnitude. This is useful in understanding the spectrum calculated including generation mixing effects.

Field	Mass(GeV)
$M_{\tilde{G}}$	1200.22
M_{χ^\pm}	590.28, 155704.39
M_{χ^0}	246.44, 590.28, 155704.37, 155704.37
$M_{\tilde{\nu}}$	15324.61, 15326.19, 30133.937
$M_{\tilde{e}}$	11958.04, 11961.80, 15324.83, 15326.64, 30128.73, 38566.31
$M_{\tilde{u}}$	12822.35, 12822.41, 13440.35, 13459.00, 48229.64, 48995.86
$M_{\tilde{d}}$	11245.00, 11246.06, 13440.60, 13459.25, 48864.06, 49420.94
M_A	457783.97
M_{H^\pm}	457783.98
M_{H^0}	457783.97
M_{h^0}	125.02

Table 3.8: Spectra of supersymmetric partners calculated including generation mixing effects. Inclusion of such effects changes the spectra only marginally. Due to the large values of μ, B, A_0 the LSP and light chargino are essentially pure Bino and Wino(\tilde{W}_\pm). Note that the ordering of the eigenvalues in this table follows their magnitudes, comparison with the previous table is necessary to identify the sfermions.

Chapter 4

Inflationary Cosmology

4.1 Introduction

According to standard Big Bang theory our universe was born 15 billion years ago in a extremely hot and infinite dense state. With rapid expansion it became cold. It has many surprising and remarkable predictions e.g. the formation of nuclei which results in primordial abundances of light elements. Later formation of neutral atoms which results in the free motion of the cosmic background photons. When neutral atoms formed the universe became transparent to photons so they are traveling to us from the time of recombination till today. This is also known as surface of last scattering. Big Bang theory became popular with the observation [64, 65] of cosmic microwave background radiation (CMBR). However on closer examination it was realized that there are problems in the Big Bang scenario such as existence of unwanted relics expected from the particle physics theories and relevant at big bang times (gravitinos, monopoles, domain walls etc.) and very robust initial condition problems (flatness problem, horizon problem etc.).

The idea of inflation [58, 59] was introduced to solve the problems of standard Big Bang. Inflationary cosmology is widely accepted and vastly studied now a days. It has become one of the cornerstones of modern cosmology. Not only solving the puzzles of Big Bang, inflation can also make predictions on the large scale

structure [60–62] of our universe on the basis of quantum fluctuations which grew via gravitational instability and are the seeds for the large scale structure of present day universe.

4.2 Big Bang Cosmology

The Big Bang theory is based upon the cosmological principle which states that the our universe is almost homogeneous and isotropic at least on large scales (> 1 Megaparsec $\approx 10^{24}$ cm). It is also confirmed from observations on CMB temperature which is almost same at different parts of the sky. However if we look at the sky on smaller scales, they are highly inhomogeneous i.e. the material is clumped into stars, galaxies and clusters of galaxies. It can be thought to have originated from a distribution which was homogeneous in past but after progressive clumping due to gravitational attraction over time becomes inhomogeneous. So the dynamics of observable universe can be broken into two parts. The large scale behavior is homogeneous and isotropic and on this background are imposed small scale irregularities which act as small perturbations on the evolution of the universe which looks homogeneous on scales greater than Megaparsec.

The homogeneous and isotropic universe on large scale can be described by Friedmann-Robertson-Walker (FRW) metric [63]:

$$ds^2 = -dt^2 + a^2(t) \left[\frac{dr^2}{1 - kr^2} + r^2(d\theta^2 + \sin^2\theta d\phi^2) \right] \quad (4.1)$$

Here t is time coordinate. r, θ, ϕ are polar coordinates. k is spatial curvature constant. The values $k = +1, 0, -1$ correspond to closed, flat and open universes respectively. $a(t)$ is scale factor which determines the rate of expansion. It distinguishes between the physical distance (it changes due to expansion) and comoving distance (remains same during expansion) between two points as:

$$d_{physical} = a(t) d_{comoving} \quad (4.2)$$

The expansion of the universe depends upon the material contained in it and governed by the Friedmann equations:

$$H^2 = \frac{8\pi\rho}{3M_{pl}^2} - \frac{k}{a^2} \quad (4.3)$$

Here $H = \frac{\dot{a}}{a}$ is Hubble parameter and ρ is the density of material. $M_{pl} = 2.43 \times 10^{18}$ GeV is Planck scale. However this equation can be best utilized if we know the evolution of density of material in the universe. This is given by the fluid equation derived from the first law of thermodynamics relating the rate of change of the density $\dot{\rho}$ to the density ρ and pressure p and Hubble parameter $H(t)$.

$$\dot{\rho} + 3H(\rho + p) = 0 \quad (4.4)$$

The first term of bracket denotes decrease in energy density due to expansion and second term denotes decrease in energy due to work done by pressure for expansion. The two equations (4.3), (4.4) can be combined to form a more convenient equation known as the acceleration equation:

$$\frac{\ddot{a}}{a} = -\frac{4\pi}{3M_{pl}^2}(\rho + 3p) \quad (4.5)$$

Notice that the acceleration equation doesn't contain k .

For flat universe ($k=0$) the Friedmann equation can be solved to yield classical cosmological solutions which corresponds to universe dominated by matter, radiation and cosmological constant.

$$\begin{aligned} p = 0; \quad \rho \propto a^{-3}; \quad a(t) \propto t^{\frac{2}{3}} \quad \text{Matter domination} \\ p = -\frac{\rho}{3}; \quad \rho \propto a^{-4}; \quad a(t) \propto t^{\frac{1}{2}} \quad \text{Radiation domination} \\ p = -\rho; \quad \rho \propto a^0; \quad a(t) \propto \exp^{Ht}; \quad \text{Cosmological constant } \lambda \end{aligned} \quad (4.6)$$

For flat universe and given H , the density of universe equals to critical density

given as:

$$\rho_c = \frac{3M_{pl}^2 H^2}{8\pi} \quad (4.7)$$

and density of universe expressed as fraction of critical density is known as density parameter Ω_c :

$$\Omega_c \equiv \frac{\rho}{\rho_c} \quad (4.8)$$

The present value of Hubble parameter is given as

$$H_0 = 100h \text{ Km s}^{-1} \text{ Mpc}^{-1} \quad (4.9)$$

Where the current measured value of h lie in range (0.70-0.76). Hubble parameter is an important scale parameter of Big Bang theory. H^{-1} gives the Hubble time and $cH^{-1}=H^{-1}$ (in natural units $c=1$) is Hubble length or radius. Hubble time is the time taken by universe to expand appreciably and distance traveled by light during that time is Hubble radius. Thus Hubble radius now determines the size of observable universe. The present critical density is

$$\rho(t_0) = 1.88h^2 \times 10^{-29} \text{ gm cm}^{-3} \quad (4.10)$$

4.3 Shortcomings of Big Bang

Despite various successes of Big Bang model it is plagued with some basic initial condition problems which are:

- **Flatness Problem:** This one is easiest to understand. From equation (4.3), the total density parameter is given as:

$$|\Omega_{tot} - 1| = \frac{|k|}{a^2 H^2} \quad (4.11)$$

Present density of universe is close to critical density, so $\Omega_{tot} \approx 1$. But during Big Bang evolution $a^2 H^2$ decreases with time, so Ω_{tot} moves away from one. This can be understood in the following way. During radiation domination $a^2 H^2 \propto t^{-1}$ and in matter domination $a^2 H^2 \propto t^{-2/3}$. So we have

$$\begin{aligned} |\Omega_{tot} - 1| &\propto t && \text{radiation domination} \\ |\Omega_{tot} - 1| &\propto t^{2/3} && \text{matter domination} \end{aligned} \quad (4.12)$$

So in both cases $|\Omega_{tot} - 1|$ is an increasing function of time. For example to obtain the present day density of universe we require $|\Omega_{tot} - 1| < 10^{-16}$ at the time of nucleosynthesis. Such a fine tuned initial condition seems very implausible and the necessity of assuming it is known as the flatness problem.

- **Horizon Problem:** The horizon problem refers to the communication between different regions of universe which are casually disconnected. The cosmic microwave radiation from two distant places are found to be at nearly equal temperature (to a precision of one part in 100,000 [65]). It implies universe came into thermal equilibrium due to interaction between different regions of universe which have been causally separated through out the Big Bang. Thus Big Bang has no explanation for such homogeneity and thermal equilibrium. The light we see from the opposite sides of the sky has been traveling towards us since the time very close to the time of Big Bang itself. Since the light has only just reached us, so it can not possibly have made it all the way across to the opposite side of the sky. Therefore, there has not been time for two regions on opposite sides of the sky to interact in any way, and so one can not claim that the regions have come to the same temperature by interaction.

Another important issue which adds to this problem is that the microwave background radiation is not perfectly isotropic, but instead exhibits small fluctuations, as observed by COBE [64] and WMAP [65] satellite. These irregularities are thought to represent the ‘seeds’ from which the structure in the Universe grows. In the standard Big Bang theory one does not have a

mechanism allowing the generation of such kinds of seed perturbation.

- **Relic Particles problem:** Another important issue with Big Bang is production of unwanted relic (quasi-stable) particles e.g. magnetic monopoles, supersymmetric particles like gravitinos, moduli fields related to superstrings, domain walls etc. which particle theories predict at high energy. The idea is that if these are produced in early universe then they are expected to decay or annihilate so slowly that relic populations should be detectable or even dominate the energy density today. Current Universe is far too cold to produce the reactions required to make these particles but if they had been produced in the early Universe we would expect some of them to still be detectable today. This is contrary to the observations, so we need a mechanism to get rid of these unwanted particles.

4.4 The idea of Inflation

The two major problems of flatness and horizon come from the fact that the comoving Hubble radius $(aH)^{-1}$ is strictly increasing during Big Bang expansion. So what will happen if one inverts this behavior? The concept of inflation is based upon the idea that the comoving Hubble radius is decreasing during expansion of the universe. To achieve this one can define inflation as an era when $\ddot{a} > 0$ i.e. accelerating expansion.

$$\ddot{a} > 0 \quad \Rightarrow \quad \frac{d\dot{a}}{dt} > 0 \quad \Rightarrow \quad \frac{d(aH)^{-1}}{dt} = \frac{\ddot{a}}{\dot{a}^2} < 0 \quad (4.13)$$

So according to above equation the Hubble radius, measured in comoving coordinates, which determines the size of observable universe decreases during inflation. Also from equation (4.5), we have

$$p < -\frac{\rho}{3} \quad (4.14)$$

Evolution dominated by a cosmological constant with equation of state $p=-\rho$ and giving exponential expansion $a(t) \propto e^{Ht}$.

The successes of Big Bang theory depend upon conventional evolution which is non inflationary so one can not allow inflation to go on forever. Inflation must come to an end followed by conventional Big Bang behavior, so it acts as an add-in to the standard Big Bang theory for its better performance.

4.4.1 Standard Big Bang problems revisited

- **Flatness Problem:** The solution for this problem lies in the definition of inflation more or less. As it is clear from Friedmann equation,

$$|\Omega_{tot} - 1| = \frac{|k|}{a^2 H^2} \quad (4.15)$$

the condition for inflation is to achieve an initial evolution which drives Ω_{tot} very close to 1 rather than away from one. The aim is to use inflation not just to force Ω_{tot} close to one but in fact to make it so extraordinarily close to 1 that the post inflationary period can't make it move away from 1. Another way to understand it is that during inflation the size of the portion of the Universe we can observe, given roughly by the Hubble length cH^{-1} (or H^{-1} in natural units $c=1$) does not change while it inflates. So, we are unable to notice the curvature of the surface. This is in contrast to the Big Bang scenario where the distance we see increases more quickly so we can see more of the curvature as time passes.

- **Horizon Problem:** Inflation increases the size of the Universe so fast that it keeps the Hubble scale fixed. This means that small patch of the Universe expanded to much larger than the size of our presently observable Universe. Then microwaves coming from two opposite sides of the sky really are at same temperature because the distance between these two regions of the Universe we see after (even long after) inflation is much smaller than the distance before

inflation started i.e. they were once causally connected in past. Equally, these causal processes provide the opportunity to generate irregularities in the Universe which can lead to structure formation.

- **Relic Particles problem:** The inflationary solution to this problem is that the rapid expansion of the inflationary period dilutes the unnecessary relic particles, because the energy density during inflation decreases more slowly than the relic particle density. But the idea can only work if after inflation, the energy density of the Universe can be converted into ordinary matter (via a process known as reheating) without recreating these relics. But reheating should be such that the temperature of the universe never gets so high that these unwanted particles are created again. The reheating process should generate only those particles that the present universe contains. A successful reheating scenario will allow us to get back into the standard hot big bang conditions required for the success of nucleosynthesis and the microwave background radiation.

4.5 Ingredients of inflationary expansion

In the previous section we discussed about how inflation is successful in curing the diseases of Big Bang theory. But we need to have a mechanism to generate such kind of expansion. This can be provided by scalar fields. Scalar fields describe spin zero particles in particle physics and play an important role in symmetry breaking e.g. Higgs scalar field is responsible for electroweak symmetry breaking. But it can be any other scalar responsible for breaking of other symmetries like GUT or Supersymmetry etc.

Let us take any general scalar field ϕ and call it inflaton field. The energy density and pressure for the inflaton can be calculated from its energy momentum tensor by considering it a perfect fluid.

$$\rho_\phi = \frac{1}{2}\dot{\phi}^2 + V(\phi) \tag{4.16}$$

$$p_\phi = \frac{1}{2}\dot{\phi}^2 - V(\phi) \quad (4.17)$$

In both equations the first term is kinetic energy and second term is potential energy.

Some simple examples of inflationary potentials are:

$$V(\phi) = \frac{1}{2}m^2\phi^2 \quad \text{massive scalar} \quad (4.18)$$

$$V(\phi) = \lambda\phi^4 \quad \text{self interacting scalar field} \quad (4.19)$$

The inflationary literature contains literally thousands of suggestions for inflaton candidates and inflation potential. We discuss a class of models in next section.

Here we will consider the general form of $V(\phi)$.

The dynamics of scalar field can be obtained by substituting equations (4.16) and (4.17) into Friedmann equation (4.3) and fluid equation (4.4). It yields,

$$H^2 = \frac{8\pi}{3M_{pl}^2} \left[V(\phi) + \frac{1}{2}\dot{\phi}^2 \right] \quad (4.20)$$

$$\ddot{\phi} + 3H\dot{\phi} = -\frac{dV}{d\phi} \quad (4.21)$$

Here the curvature term is ignored as it becomes insignificant once inflation starts. From the equation (4.14), the condition for inflation in terms of K.E. and P.E. is given as that for negative pressure

$$\frac{\dot{\phi}^2}{2} < V(\phi) \quad (4.22)$$

So basically the potential energy is responsible for inflation. It is a measure of internal energy associated with the inflaton. A crucial ingredient which permits inflation is that the inflaton field configuration is far from the minimum in potential energy configuration during inflation.

When potential term dominates, inflation is assured. However a sufficient number of e-folds is possible only if potential is flat enough so that inflaton rolls

slowly thus allowing sufficient inflation. Also potential must have some minimum where inflaton can settle down after the end of inflation.

To solve the equations (4.20,4.21) a standard scheme is followed known as Slow Roll approximation (SRA). It assumes that the kinetic term in Eqn. (4.20) and acceleration term in Eqn. (4.21) can be neglected to obtain a set of simpler equations,

$$H^2 \simeq \frac{8\pi}{3M_{pl}^2} V(\phi) \quad (4.23)$$

$$3H\dot{\phi} \simeq -\frac{dV}{d\phi} \quad (4.24)$$

the most important slow roll parameters are defined as:

$$\epsilon(\phi) = \frac{M_{pl}^2}{2} \left(\frac{V'}{V}\right)^2 \quad ; \quad \eta(\phi) = M_{pl}^2 \left(\frac{V''}{V}\right) \quad (4.25)$$

ϵ measures the slope of potential and η measures the curvature of inflationary potential. The required conditions for slow roll are

$$\epsilon \ll 1 \quad ; \quad |\eta| \ll 1 \quad (4.26)$$

Inflation comes to an end when $|\eta| \approx 1$.

However whether the inflaton has produced enough inflation or not is a question of concern. The amount of inflation is measured in terms of logarithm of amount of expansion termed as “number of e-folds” given as:

$$N = \ln \frac{a(t_{end})}{a(t_{initial})} = \int_{t_i}^{t_e} H dt = -\frac{2}{M_{pl}^2} \int_{\phi_i}^{\phi_e} \frac{V}{V'} d\phi \quad (4.27)$$

Here ϕ_i, ϕ_e are the inflaton field value at the starting of inflation (when $\epsilon, |\eta| \ll 1$) and at the end of inflation (when $|\eta| \approx 1$) and can be calculated using equation of motion. However the number of efolds of importance are the number left when representative scale of the present day cosmos (pivot scale $k \sim .002 \text{ Mpc}^{-1}$ [65]) leaves the comoving horizon. The importance of this scale lies in the fact that the CMB observations are made with least uncertainty at this scale. The minimum number of

efolds required to have sufficient inflation is 50-70. It corresponds to an expansion by a factor 10^{16} . However it should be noted that the number of ‘observable efolds’ spanning the conceivably observable scale is limited to about 9. The rest are inferred from the necessity of flatness and causal connection.

The simple picture of inflation driven by single scalar field makes a definite set of predictions for the form of primordial cosmological fluctuations. The quantum fluctuations generated by a single scale scalar field should be gaussian, adiabatic and scale invariant i.e. n_s (spectral index)=1. Scale invariance comes from the fact that in the limit of de-Sitter space, Hubble radius remains constant during inflation. However the slow roll inflation is quasi de-Sitter, so the perturbation spectra is partly, not exactly scale invariant. The expression for spectral index and power spectrum of scalar perturbations is given by

$$n_s = 1 - 6\epsilon(\phi_{CMB}) + 2\eta(\phi_{CMB}) \quad (4.28)$$

$$P_R = \frac{H}{m_{pl}\sqrt{\pi\epsilon}} \Big|_{\phi=\phi_{CMB}} \quad (4.29)$$

Here ϕ_{CMB} is the field value at which perturbations relevant to the CMB spectrum are observed today. From the WMAP 7-year data [65] the values of spectral index and power spectrum are

$$P_R = (2.43 \pm 0.11) \times 10^{-9} \quad ; \quad n_s = 0.967 \pm 0.014 \quad (4.30)$$

Another contribution to CMB spectrum perturbation comes from gravitational waves which is known as tensor mode of perturbations. Although their contribution was usually considered negligible as compared to scalar perturbation, after announcement of BICEP2 result [66], a large value of $r \approx .20 \pm 0.05$ is now under active consideration. We will discuss it in Chapter 6. The ratio of scalar to tensor perturbation is defined as

$$r = \frac{P_R}{P_T} = 16\epsilon(\phi_{CMB}) \quad (4.31)$$

So one must also calculate the value of r while considering constraints from power spectrum and spectral index values from observational data.

4.6 Inflection point Inflation Along MSSM Flat Directions

Many types of inflationary models exist in literature. But most of them explain inflation considering a generic scalar field and are not connected to the SM of particle physics. Models where inflation is driven not by a generic scalar field, but by an inflaton which is tied to the Standard Model gauge group and spectrum are important and carry an obvious appeal. These models can explain reheating into the Standard Model degrees of freedom as required for the success of Big Bang Nucleosynthesis, after the end of inflation. In this section we focus on the inflation models based on inflection points in the inflationary potential. The idea of inflection point inflation relies on the fact that at an inflection point the inflationary potential is flat required for the achievement of slow roll inflation. In this context the suggestion [67–72] that inflation can be embedded within the Minimal Supersymmetric Standard Model (MSSM) is an attractive scenario. These types of models are based on slow roll inflation associated with “flat directions” in the MSSM field space along which the D-term potential vanishes. A well known theorem [73–76] allows one to use holomorphic gauge invariants formed from chiral superfields as coordinates for the D-flat manifold of the scalar field space of SUSY gauge theories. The flat directions are lifted by supergravity generated soft supersymmetry breaking terms and by non renormalizable terms in the MSSM effective superpotential.

At renormalizable level, supersymmetric theories can have large number of directions in the space (known as moduli space collectively) of scalar fields, where the D-term contribution to the scalar potential is zero identically. These degeneracies are protected from quantum perturbations due to non-renormalization theorem but can be lifted by non-perturbative effects. In MSSM the flat directions are conden-

sates of sleptons, squarks and Higgs fields.

There are two types of flat directions in MSSM, D-flat and F-flat directions. The field values where the potential will vanish can be calculated by solving the equations for D and F term vanishing conditions:

$$D^a = \Phi_i^* T^a \Phi_i = 0 \quad ; \quad F_i = \frac{\partial W}{\partial \Phi_i} = 0 \quad (4.32)$$

Here Φ_i is chiral superfield. T^a are generators for the MSSM gauge group. The field condensate which obeys these equations simultaneously are called D and F-flat direction. Important thing is correspondence between the flat direction and gauge invariant holomorphic monomials in term of chiral superfield Φ_i . The parameter which moves along flat direction is the scalar component of the gauge invariant polynomial of chiral superfields.

Now we discuss a D-flat direction which is our interest. Consider a flat direction from leptonic sector. The potential in this sector in the absence of Susy breaking terms is given as

$$V = \frac{g^2}{2} \sum_{i=1}^3 \left(\sum_A \tilde{L}_A^\dagger T_i \tilde{L}_A \right)^2 + \frac{g'^2}{2} \left(\sum_A \left(\tilde{L}_A^\dagger \frac{Y}{2} \tilde{L}_A \right)^2 + \left(\tilde{e}_A^\dagger \frac{Y}{2} \tilde{e}_A \right)^2 \right) \quad (4.33)$$

Where T_i are usual Pauli generators for SU(2) and Y is hypercharge. One can easily check that the potential vanishes for a set of flat directions of the form

$$\tilde{L}_1 = \begin{pmatrix} \phi \\ 0 \end{pmatrix}; \quad \tilde{L}_2 = \begin{pmatrix} 0 \\ \phi \end{pmatrix}; \quad \tilde{e}_3 = \phi \quad (4.34)$$

Where ϕ is the vev along flat direction (it will act as inflaton in case of inflation along flat direction). Each such type of flat direction is labelled by gauge invariant polynomial $\tilde{L}_i \tilde{L}_j \tilde{e}_k$. In the next section we discuss the inflection point inflation along one such gauge invariant flat direction of MSSM extended with $U(1)_{B-L}$ gauge group.

4.7 Dirac Neutrino Inflation connection and fine tuning issue

In [77, 78] a connection between smallness of neutrino mass and inflation has been made. They considered the inflaton to be a gauge invariant combination of righthanded sneutrino, left handed slepton and Higgs field, which generates a flat direction along which inflation will take place on the condition of neutrino Yukawa being very small $h_\nu \sim 10^{-12}$. Such types of models are able to produce the observed anisotropy and power spectrum of CMB.

They considered MSSM with right handed neutrino and gauge symmetry extended to $SU(3)_C \times SU(2)_L \times U(1)_Y \times U(1)_{B-L}$. Here B and L are baryon and lepton number. Neutrino is considered to be a Dirac particle. Recall that the nature of neutrino i.e. whether it is a Dirac or Majorana fermion is still under debate. One can introduce small masses of O(0.1 eV) corresponding to the atmospheric neutrino oscillations detected by Super-Kamiokande experiment [5] by two way. Either by a seesaw mechanism with large right handed neutrino Majorana masses and neutrino Yukawa couplings of same magnitude as charged fermions or by Dirac masses with small right handed neutrino Majorana masses and small Yukawa couplings. Here we review the second case as considered by [77, 78].

In the previous section we noted that MSSM has many flat directions made up of squarks, slepton and Higgs fields. In [77, 78] it was proposed that the D-flat direction along which inflation will take place is NH_uL (where N is the conjugate neutrino of left chiral superfield) as it is gauge invariant under the gauge group considered. Taking neutrinos in mass diagonal basis the flat direction NH_uL is specified by the field configuration

$$H_u = \begin{pmatrix} 0 \\ \frac{\phi}{\sqrt{3}} \end{pmatrix}; \quad \tilde{L} = \begin{pmatrix} \frac{\phi}{\sqrt{3}} \\ 0 \end{pmatrix}; \quad \tilde{\nu}^C = \frac{\phi}{\sqrt{3}} \quad (4.35)$$

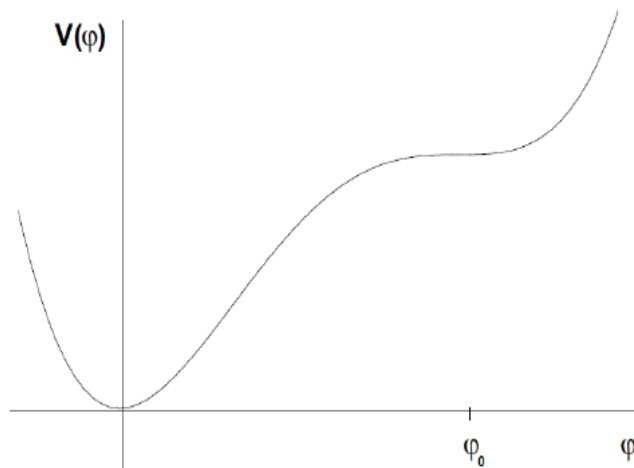


Figure 4.1: The variation of potential with ϕ . The potential is flat near inflection point at ϕ_0 where inflation occurs.

After including the soft terms (mass terms and trilinear terms), the renormalizable inflation potential along flat direction has form

$$V(\phi) = \frac{m_\phi^2}{2}\phi^2 + \frac{Ah}{6\sqrt{3}}\cos(\theta + \theta_h + \theta_A)\phi^3 + \frac{h^2}{12}\phi^4 \quad (4.36)$$

Here $m_\phi^2 = (m_N^2 + m_{H_u}^2 + m_L^2)/3$. Let ϕ, θ denotes the radial and angular component of flat direction: $\phi = \phi_R + i\phi_I = \sqrt{2}\phi \exp(i\theta)$. θ_h and θ_A are phases of Yukawa coupling h and the A-term respectively. The potential can be minimized when $\cos(\theta + \theta_h + \theta_A) = -1$. The potential has global minima at $\phi=0$ and local minima at $\phi_0 \sim m_\phi/h$. Successful inflation around ϕ_0 and a graceful exit from this local minima after the end of inflation is only possible if

$$A = 4m_\phi \quad (4.37)$$

Then at ϕ_0 the first and second derivative of $V(\phi)$ vanishes (inflection point) and potential becomes extremely flat (shown in figure 4.1). However at low scale symmetry breaking, the condition given by equation (4.37) needs to be achieved to a great accuracy and is thus a challenge to overcome. At higher scale of supersymmetry

breaking severity of fine tuning can be reduced but is still potentially problematic. This problem is known as fine tuning problem in inflection point inflation models [79]. In [78] the constraints on inflation potential parameters are formulated on the basis of WMAP 7-Year data. The fine tuning parameter β is defined as

$$\delta = \frac{A^2}{16m_\phi^2} = 1 - \frac{\beta^2}{4} \quad (4.38)$$

Here β can be real or imaginary according to $\delta < 1$ or $\delta > 1$.

Authors of [78] showed the allowed range of parameters m_ϕ and h along with the allowed values of fine tuning parameters, imposing constraint that the inflaton VEV should be sub-Planckian i.e $\phi_0 < 0.1 M_{Pl}$ via drawing contour plots between m_ϕ and h .

The conclusions drawn are that for low inflaton masses, the coupling h is required to be very small $\sim 10^{-12}$ for the model to simultaneously match the spectrum and e-fold constraints. Such small coupling then gives small masses ~ 100 MeV to the third neutrino through Dirac term in superpotential. The inflaton mass is controlled by soft term masses which are in range 1-10 TeV. Then the required value of fine tuning parameter is $\Delta \leq 10^{-20}$. This is a severe tuning of Susy breaking parameters and also unstable since the A terms violates Susy and are thus not protected from the large radiative corrections.

4.8 Discussions

In this chapter starting from the Big bang theory and introduction of inflation, we discussed recipe for successful inflation. The inflection point inflationary models based on gauge invariant flat directions of MSSM or extended MSSM present an attractive scenario for inflation linked to known physics of MSSM particles. However these models are plagued with the fine tuning problems. To reduce the fine tuning issues several mechanisms have been suggested which involves invocation of dynamics of other scalar fields [78]. However we found in [31] that the Majorana-neutrino

inflation can be a better scenario compared to Dirac-neutrino-inflation case. The fine tuning conditions are less severe in Majorana-neutrino inflation and are imposed on the superpotential parameters rather than soft Susy breaking parameters. So they are radiatively stable . We present the details in next Chapter.

Chapter 5

Supersymmetric Seesaw Inflation

5.1 Introduction

The seesaw mechanism [9] provides an attractive alternative to a fine tuned Yukawa coupling for explaining small observed active neutrino masses. Supersymmetric Unified theories which contain a renormalizable Type I seesaw mechanism for small neutrino masses compatible with neutrino oscillations, can also provide slow roll inflection point inflation along a flat direction associated with a gauge invariant combination of the Higgs, slepton and right handed sneutrino superfields. Non zero neutrino masses in the milli-eV range are interpreted as a strong signal of physics beyond the SM. In the Dirac case light neutrino masses can be understood by taking highly suppressed Yukawa couplings, ($\mathcal{L} = y_\nu \bar{N} H_u L + \dots$; $y_\nu \sim m_\nu/M_W \sim 10^{-12}$) which are seven or more orders of magnitude smaller than the charged fermion Yukawa couplings. Also these masses should be accompanied by highly suppressed right handed Majorana neutrino masses, $M_{\nu^c} \sim 0.1eV$ or less. In contrast to it, the Majorana case, where one can generate small effective (Type I seesaw) neutrino Majorana masses ($m_\nu \sim (m_\nu^D)^2/M_{\nu^c}$) for the left handed neutrinos does not require such unnatural assumptions. This is possible only if the right handed neutrino masses M_{ν^c} take the large values allowed by their vanishing SM gauge charges. In this case the large Majorana mass of right handed neutrino will give required small

masses of the neutrinos (due to inverse dependence) rather than ultra small Yukawa couplings as required in the Dirac mass case.

In the last section of the previous chapter we discussed about a connection [77, 78] made between the smallness of the (Dirac) neutrino masses and flatness of the inflaton potential within the MSSM extended by the addition of $U(1)_{B-L}$ gauge group and right handed neutrinos. The inflaton field was a gauge invariant D -flat direction, NH_uL , where N is the right handed sneutrino, H_u is the MSSM Higgs which gives masses to the up-type quarks, and L is the slepton field. The gauge invariant superpotential term $y_\nu NH_uL$ generates the tiny (Dirac) neutrino masses due to the tiny neutrino Yukawa coupling ($y_\nu \sim 10^{-12}$). Along with soft trilinear and bilinear supersymmetry breaking terms of mass scale $\sim 100 \text{ GeV}$ to 10 TeV , the associated renormalizable inflaton potential can then be fine tuned to achieve inflection point inflation consistent with WMAP 7 year data [65].

Given the attractiveness of the seesaw scenario relative to tuned Yukawas for Dirac neutrino masses, it is natural to ask whether it too supports inflectionary inflation. At first sight, it seems difficult to achieve conditions of the neutrino-inflaton scenario in this prospect i.e ultra small superpotential couplings, and TeV scale trilinear/mass terms. Generic Type I seesaw are based upon a mechanism where large right handed neutrino Majorana masses are generated by breaking of $B - L$ symmetry by vevs $V_{B-L} \gg \text{TeV}$. An inflaton involving the right handed sneutrino will then have (supersymmetric) mass as large as the righthanded neutrino mass since Susy breaking scale is smaller than $B - L$ symmetry breaking scale. If one considers normal hierarchy for neutrino masses, then the third generation light neutrino masses $m_\nu \sim y_3^2 v_{EW}^2 / M_{\nu^c} \sim 0.1 \text{ eV}$ can be achieved for $y_3 \sim 1$, $M_{\nu^c} \sim 10^{15} \text{ GeV}$. At first glance it seems that such large couplings and masses would completely finish the needed flatness of the inflationary potential. But there is a way out of it. Three generations of neutrinos and their superpartners are in play, so there is wide scope for much smaller superpotential couplings. One possibility that we considered is that the neutrino Yukawa coupling eigenvalues can have the typical values associated with up type fermions while off diagonal components matched the

tiny Majorana couplings in smallness. Off diagonal flat directions ($N_A H L_B, A \neq B=1,2,3$) can serve just as well as diagonal ones. Later we will discuss others allowed by high scale inflation.

The famous Leptogenesis [35] scenario strongly favors right handed neutrino masses in the range 10^6 to 10^{12} GeV. So for B-L breaking scale $V_{B-L} \sim M_X > 10^{16}$ GeV the superpotential couplings $f_A, A = 1, 2, 3$ (we work in a basis where these couplings are diagonal associated with the superpotential terms), which generate right handed neutrino masses $M_{\nu_A^c} \sim f_A V_{B-L}$ [12–14], come out to be very small ($f_A \sim 10^{-9}$ to 10^{-4}). Thus the essential ingredients for an inflation in the Type I seesaw scenario are potentially present justifying detailed analysis.

5.2 Generic renormalizable inflection point inflation

In this section we present our analytic formulae for the relations required among the parameters of the generic renormalizable inflection point inflation (GRIPI) potential for successful inflation and fulfilling constraints from WMAP 7-year data. In contrast to the previous analysis [78] (opaque graphical methods) our calculations are more rigorous and can easily be interpreted. The results are viable for any GRIPI model. A GRIPI model can be formulated in terms of a single complex field φ . After extremizing with respect to the angular degree of freedom (which has positive curvature and cannot support inflation) one is left with the potential for a real degree of freedom ϕ in the complex scalar inflaton field φ

$$V = \frac{h^2}{12}\phi^4 - \frac{Ah}{6\sqrt{3}}\phi^3 + \frac{M^2}{2}\phi^2 \quad (5.1)$$

Here A, h, ϕ are real and A, h positive without loss of generality.

The fine tuning condition between A and M can be expressed in terms a parameter Δ given as $A = 4M\sqrt{1 - \Delta}$ ($\Delta = \beta^2/4$ in the notation of [78]). The

inflection point at

$$\phi_0 = \frac{\sqrt{3}M}{h}(1 - \Delta + O(\Delta^2)) \quad : \quad V''(\phi_0) = 0 \quad (5.2)$$

is also a saddle point ($V'(\phi_0) = 0$) when $\Delta = 0$. For small Δ

$$\begin{aligned} V(\phi_0) = V_0 &= \frac{M^4}{4h^2}(1 + 4\Delta) \quad ; \quad V'(\phi_0) = \alpha = \frac{\sqrt{3}M^3\Delta}{h} \\ V'''(\phi_0) = \gamma &= \frac{2Mh}{\sqrt{3}}(1 - 2\Delta) \end{aligned} \quad (5.3)$$

For a tiny coupling h , $V_0 \gg M^4$ and $\phi_0 \gg M$. The γ is quite small due to the smallness of h and α is small (but non-zero [79]) because of the tuning condition. So with such a large vacuum energy flatness of potential around ϕ_0 will allow the inflaton ϕ to roll slowly with small field velocity in the vicinity of ϕ_0 . The small change in the field value during this expansion is given as $\Delta\phi \sim V_0/\gamma M_p^2$ below ϕ_0 . Around the inflection point ϕ_0 , we can write the inflection point inflation potential in the form

$$V(\phi) = V_0 + \alpha(\phi - \phi_0) + \frac{\gamma}{6}(\phi - \phi_0)^3 + \frac{h^2}{12}(\phi - \phi_0)^4 \quad (5.4)$$

The last term is necessarily negligible, since h^2 is very small by assumption.

The slow roll parameters are defined as ($M_p = 2.43 \times 10^{18} \text{ GeV}$)

$$\begin{aligned} \eta(\phi) &= \frac{M_p^2 V''}{V} \simeq \frac{M_p^2}{V_0} \gamma (\phi - \phi_0) \\ \epsilon(\phi) &= \frac{M_p^2}{2} \left(\frac{V'}{V}\right)^2 \simeq \left(\alpha + \frac{\gamma}{2}(\phi - \phi_0)^2\right)^2 \left(\frac{M_p^2}{2V_0^2}\right) \\ \xi &= \frac{M_p^4 V' V'''}{V^2} \simeq \frac{M_p^4 \alpha \gamma}{V_0^2} \end{aligned} \quad (5.5)$$

The small first and third Taylor coefficients α, γ determine [79–81] the measured inflation parameters (P_R, n_s) at the field value ϕ_{CMB} at the time of horizon entry of the “pivot” momentum scale ($k_{pivot} = 0.002 \text{ Mpc}^{-1}$). The termination of the slow roll [79, 81] is fixed on the basis of an overall cosmogonic scenario and the

consistency of the slow roll approximation ($\eta(\phi_{end}) \approx 1$). The field value ϕ_{cmb} has theoretical importance only. It is the number ($N_{CMB} = N(\phi_{CMB})$) of e-folds of inflation which are left to occur after field value ϕ_{CMB} is reached at the time when the fluctuation scale of interest (k_{pivot}) left the comoving horizon (i.e $k = a_k H_k$) during inflation that has physical significance. This number is determined by the overall history (inflation, reheating, radiation dominance, matter dominance, BBN etc.) of the Universe from primordial times [81]. The observed perturbations in CMB require $40 < N_{CMB} < 60$ and this restricts the inflation exponents to a great extent.

The field value at the end of slow roll inflation ϕ_{end} is defined as the value where

$$\eta(\phi_{end}) \simeq \frac{\gamma(\phi_{end} - \phi_0)M_p^2}{V(\phi_0)} \simeq 1 \quad (5.6)$$

which gives

$$\phi_0 - \phi_{end} = \frac{V_0}{\gamma M_p^2}, \quad (5.7)$$

Then in the slow roll approx $\ddot{\phi} \simeq 0$, $\dot{\phi} = -V'(\phi)/3H$, where $H = \sqrt{V(\phi_0)/(3M_p^2)}$ is the (constant) inflation rate during slow roll inflation, one has

$$\begin{aligned} N(\phi) &= -3 \int_{\phi}^{\phi_{end}} \frac{H^2}{V'(\phi)} d\phi \\ &= \sqrt{\frac{2}{\alpha\gamma}} \frac{V_0}{M_p^2} \left(\arctan \sqrt{\frac{\gamma}{2\alpha}}(\phi_0 - \phi_{end}) - \arctan \sqrt{\frac{\gamma}{2\alpha}}(\phi_0 - \phi) \right) \end{aligned} \quad (5.8)$$

and conversely

$$\phi(N) = \frac{\phi_{end} + \phi_0(\phi_0 - \phi_{end})\sqrt{\frac{\gamma}{2\alpha}} \tan \sqrt{\frac{\alpha\gamma}{2}} \frac{NM_p^2}{V_0} + \sqrt{\frac{2\alpha}{\gamma}} \tan \sqrt{\frac{\alpha\gamma}{2}} \frac{NM_p^2}{V_0}}{1 + (\phi_0 - \phi_{end})\sqrt{\frac{\gamma}{2\alpha}} \tan \sqrt{\frac{\alpha\gamma}{2}} \frac{NM_p^2}{V_0}} \quad (5.9)$$

This inversion of the function $N(\phi)$ is derived without assuming that $\phi_{end} \ll \phi(N)$ [79].

The observed CMB data [65] put constraints on the power spectrum and spectral index for modes around the pivot scale. However the number of e-folds remaining at the time when pivot scale left the comoving horizon during inflation can be estimated using the standard Big Bang thermal cosmogony along with estimates from the reheating behavior. This gives [81]

$$N_{\text{pivot}} = 65.5 + \ln \frac{\rho_{rh}^{\frac{1}{12}} V_0^{\frac{1}{6}}}{M_{\text{p}}} \quad (5.10)$$

where ρ_{rh} is the energy density after reheating and V_0 the potential value during inflation.

The analysis is done following the steps mentioned in the 4th section of the previous chapter. For the sake of completeness we present the formula for power spectrum and spectral index in terms of our parameterizations. The slow roll inflation formula for the power spectrum of the mode that is leaving horizon when the inflaton rolls to ϕ is([80])

$$P_R(\phi) = \frac{V_0}{24\pi^2 M_{\text{p}}^4 \epsilon(\phi)}, \quad (5.11)$$

and the corresponding spectral index and it's variation with momentum is

$$\begin{aligned} n_s(\phi) &\equiv 1 + 2\eta(\phi) - 6\epsilon(\phi) \\ \mathcal{D}_k(n_s) &= \frac{kd n_s(\phi)}{dk} = -16\epsilon\eta + 24\epsilon^2 + 2\xi^2 \end{aligned} \quad (5.12)$$

The ratio of tensor to scalar perturbations $r = \frac{P_T}{P_R} = 16\epsilon$.

In practice, ϵ, ξ are so tiny in the small region around ϕ_0 where slow-roll inflation occurs, that their contribution to n_s is negligible. Thus $\mathcal{D}_k(n_s)$ is negligible i.e. the spectral index is scale invariant in the observed range, as is allowed by observation so far.

To search for sets of potential parameters M, h, Δ compatible with P_R, n_S, N_{CMB} in their allowed ranges one may proceed as follows. First one uses the

chosen (within experimental range) values of P_R, n_s and given M, h to define

$$\begin{aligned}\epsilon_{CMB} &= \frac{V_0}{24\pi^2 M_p^4 P_R} \\ \eta_{CMB} &= \frac{(n_s - 1)}{2}\end{aligned}\quad (5.13)$$

From $\epsilon_{CMB}, \eta_{CMB}$ one may deduce α_{CMB}, ϕ_{CMB} using the eqns.(5.5)

$$\begin{aligned}\phi_{CMB} &= \phi_0 + \frac{V_0 \eta_{CMB}}{\gamma M_p^2} \\ \alpha_{CMB} &= \sqrt{2\epsilon_{CMB}} \frac{V_0}{M_p} - \frac{V_0^2 \eta_{CMB}^2}{2\gamma M_p^4}\end{aligned}\quad (5.14)$$

The required fine-tuning Δ is then

$$\Delta = \frac{h\alpha_{CMB}}{\sqrt{3}M^3} = \left(\frac{M}{4hM_p}\right)^4 \left(\frac{16h^2 M_p}{3\pi M \sqrt{P_R}} - (1 - n_s)^2\right)\quad (5.15)$$

α_{CMB}, Δ should emerge real and positive and using $\{\alpha_{CMB}, \phi_{CMB}\}$ in the formula for N_{CMB} one should obtain a sensible value in the range $N_{CMB} = 51 \pm 5$. Positivity of Δ (a local minimum develops if Δ is negative leading to eternal inflation) requires

$$h^2 \geq M \frac{3\pi(1 - n_s)^2 \sqrt{P_R}}{16M_p}\quad (5.16)$$

Using eqns.(5.3,5.75.13) in eqn(5.8) we have

$$N_{CMB} = \frac{1}{z} \arctan \frac{2z(1 + n_s)}{8z^2 + 1 - n_s}\quad (5.17)$$

$$z = \left(\frac{h^2 M_p}{3\pi M \sqrt{P_R}} - \frac{(1 - n_s)^2}{16}\right)^{\frac{1}{2}}\quad (5.18)$$

By solving eqn.(5.17) for $z = z_0(N_{CMB}, n_s)$ one obtains the general relation between h and M :

$$\frac{h^2}{M} = \frac{3\pi\sqrt{P_R}}{M_p} \left(z_0^2(N_{CMB}, n_s) + \frac{(1 - n_s)^2}{16}\right)\quad (5.19)$$

and then

$$\Delta = \frac{16M^2 z_0^2(N_{CMB}, n_s)}{9\pi^2 M_P^2 P_R((1 - n_s)^2 + 16z_0^2(N_{CMB}, n_s))^2} \quad (5.20)$$

Where $z_0(N_{CMB}, n_s)$ is the solution of eqn (5.17). An excellent approximation to the required function in the region of interest in the N_{CMB}, n_s plane is given by the Taylor series around $n_s^0 = 0.967, N_C^0 = 50.006$:

$$\begin{aligned} z_0(N_{CMB}, n_s) = & .0238 - 0.0006(N_{CMB} - N_C^0) + 0.2407(n_s - n_s^0) \\ & + 0.000022 \frac{(N_{CMB} - N_C^0)^2}{2} - 3.70875 \frac{(n_s - n_s^0)^2}{2} + 0.002353(N_{CMB} - N_C^0)(n_s - n_s^0) \\ & - .0000015 \frac{(N_{CMB} - N_C^0)^3}{6} + 8.79982 \frac{(n_s - n_s^0)^3}{6} - 0.000788 \frac{(N_{CMB} - N_C^0)^2(n_s - n_s^0)}{2} \\ & - 0.7536 \frac{(N_{CMB} - N_C^0)(n_s - n_s^0)^2}{2} \end{aligned} \quad (5.21)$$

In Fig. 5.1 we plot the contours of $z_0(N_{CMB}, n_s)$ in the N_{CMB}, n_s plane. It is clear that the variation of z_0 is rather small scaled. So for the plausible range $46 < N_{CMB} < 56$ one obtains a tight constraint on the exponents in the relation between h, Δ and M :

$$h^2 \sim 10^{-24.95 \pm 0.17} \left(\frac{M}{GeV}\right) ; \quad \Delta \sim 10^{-28.17 \pm 0.13} \left(\frac{M}{GeV}\right)^2 \quad (5.22)$$

Notice that the approximate expressions give $\frac{h^2}{M} \approx \frac{10^{-21.8}}{N_{CMB}^2}$ which is effectively the same! We estimate the maximum variations in the exponents which corresponds to the quoted errors in the WMAP 7- year data [65] from the graphs in Fig. 5.2 and Fig. 5.3. The formulae we derive are applicable to any single inflaton theory with a renormalizable potential.

However a clearer qualitative understanding results from noticing that for $N_{CMB} \sim 50, Z_0 \approx \frac{1.2}{N_{CMB}}$ solves eqn.(5.17) to a good approximation. Then eqn.(5.18) gives

$$\frac{h^2}{M} \approx \frac{3\pi}{M_P} \frac{\sqrt{P_R}}{N_{CMB}^2} \approx \frac{2.75 \times 10^{-22}}{N_{CMB}^2} \approx 10^{-25} GeV^{-1} \quad (5.23)$$

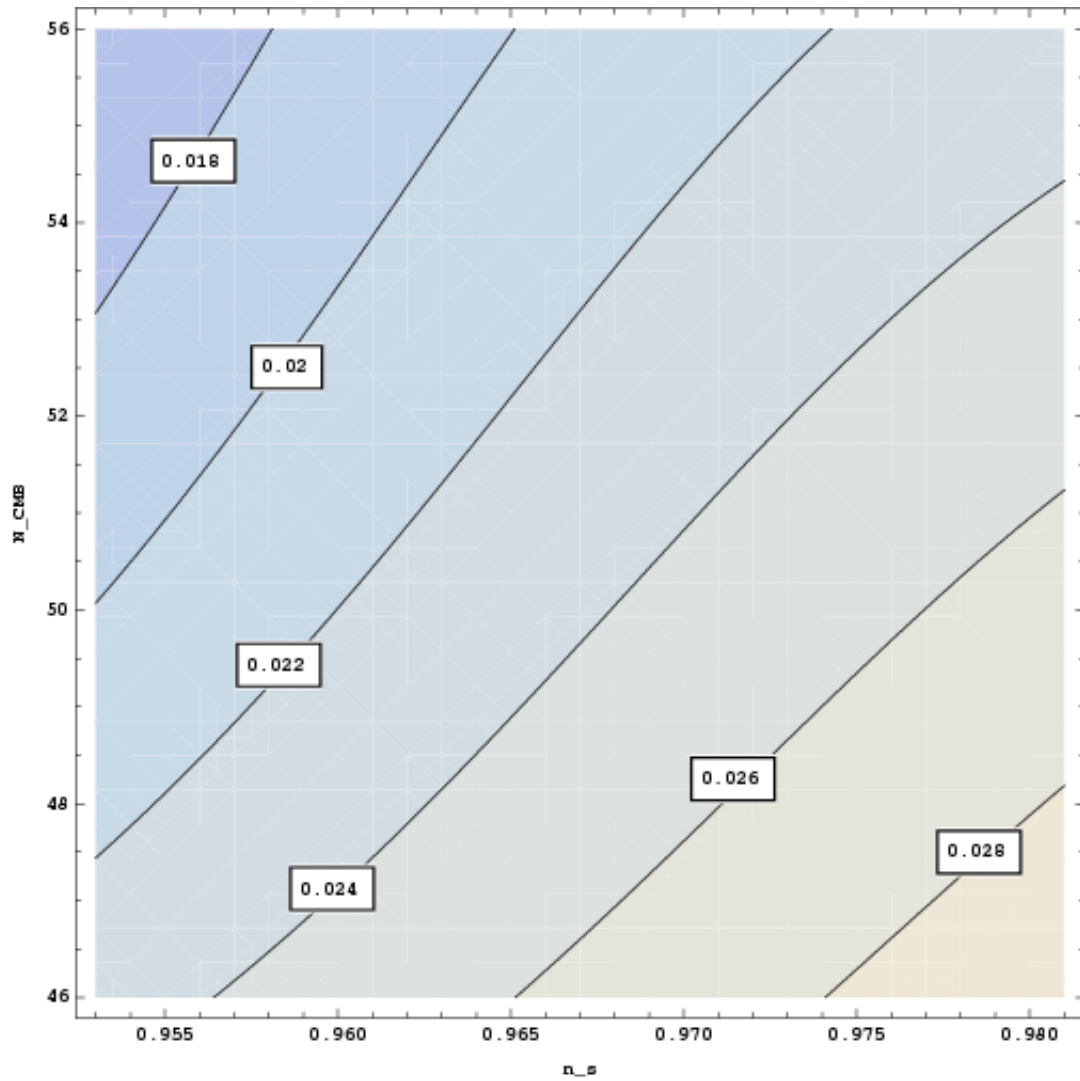


Figure 5.1: z_0 contours in the N_{CMB}, n_s plane. The variation shown contributes to the small range of permitted magnitudes for $h^2/M, \Delta/M^2$ etc.

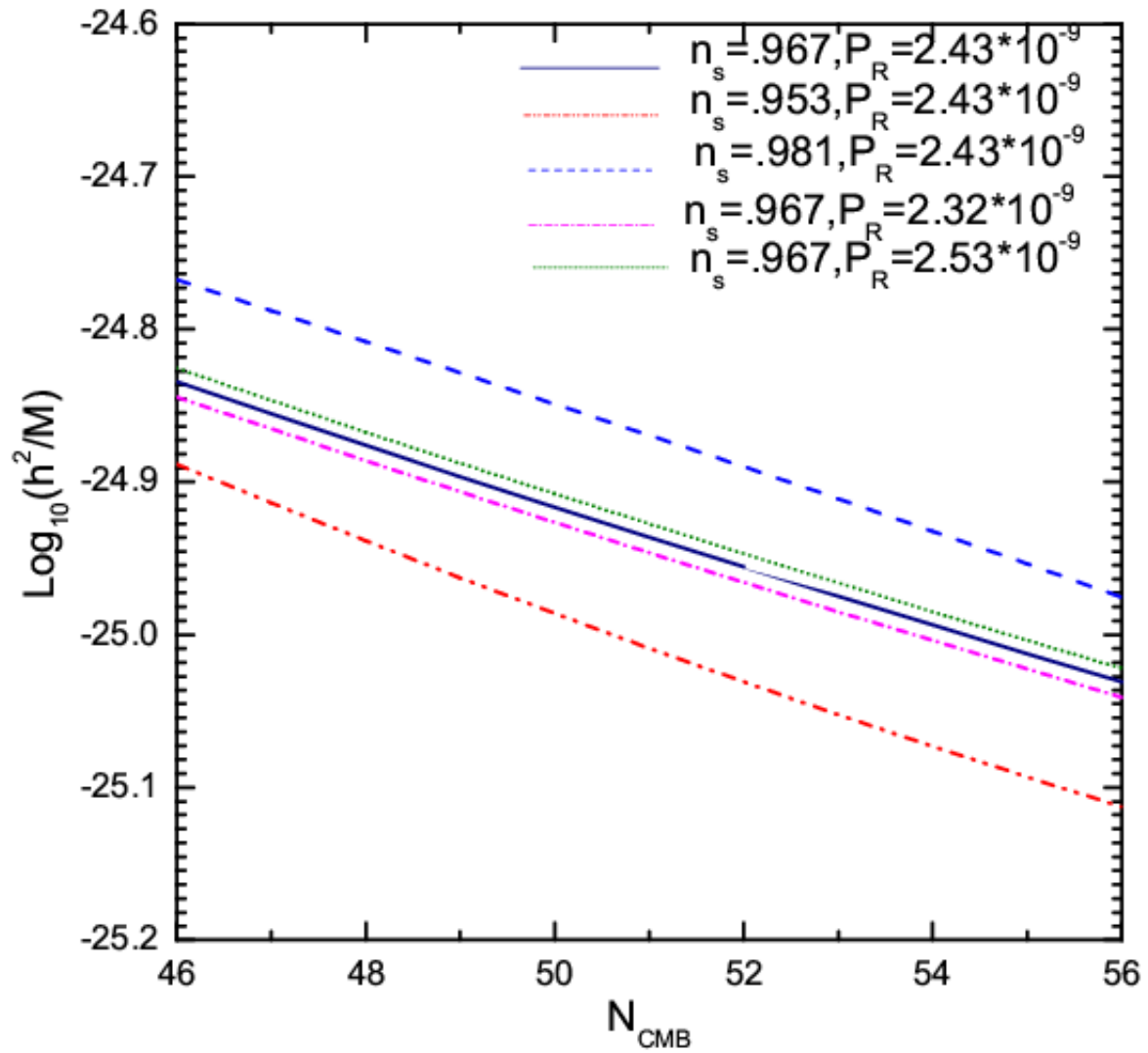


Figure 5.2: Variation of exponent of $\frac{h^2}{M}$ with N_{CMB} for different values of n_s, P_R .

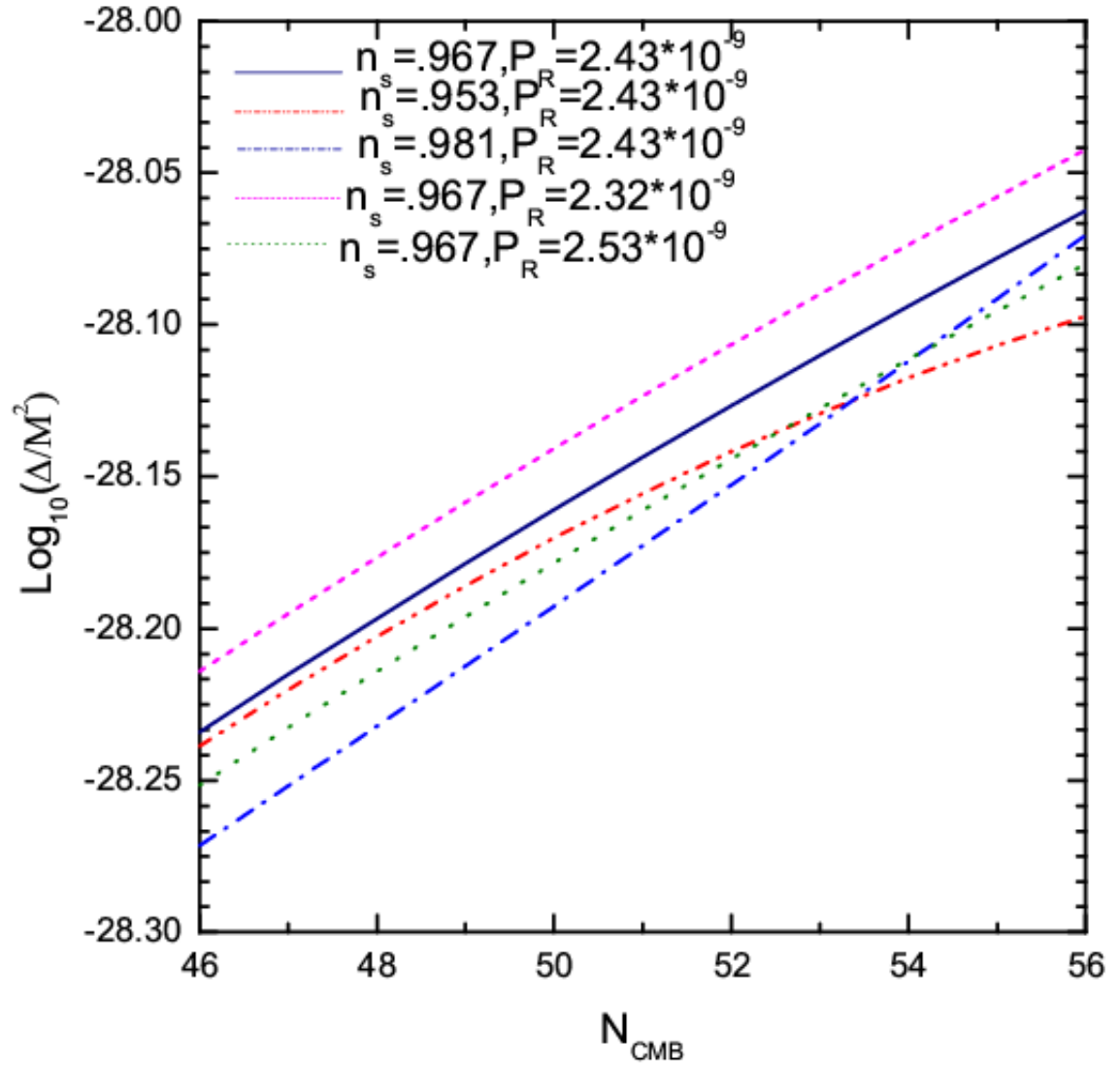


Figure 5.3: Variation of exponent of $\frac{\Delta}{M^2}$ with N_{CMB} for different values of n_s, P_R .

$$\frac{\Delta}{M^2} \approx \frac{4.14 \times 10^{-34}}{N_{CMB}^2 P_R} \approx 10^{-28.2} \text{GeV}^{-2} \quad (5.24)$$

These are effectively the same results that we derive from eq. 5.22.

Using these results on parameters of GRIPI, we can find constraints on the parameters of potential required for Susy seesaw inflation. The details are presented in next section.

5.3 Supersymmetric seesaw inflaton model

The requirements of the Supersymmetric seesaw inflation scenario can be fulfilled by considering a model with gauge group $SU(3) \times SU(2) \times U(1)_R \times U(1)_{B-L}$ and the field content of the MSSM with some additional superfields, right handed Neutrino chiral multiplet $N[1, 1, -1/2, 1]$ and a field $S[1, 1, 1, -2]$. The vev of S field generates the large Majorana masses M_ν ($10^6 - 10^{14}$ GeV) for the conjugate neutrinos $\nu_A^c \equiv N_A$ through a renormalizable superpotential coupling $3\sqrt{2}f_{AB}S\nu_A^c\nu_B^c$. Additional fields Ω_i are required which helps to fix the vev of S as present in Minimal Supersymmetric Left Right Models (MSLRMs) [12–14] and in GUTs that embed them [12–15, 27, 28]. Soft supersymmetry breaking terms are of the supergravity type (i.e universal trilinear couplings, scalar masses, gaugino masses except for Higgs (Non Universal Higgs Masses(NUHM) scenario). The other essential component of the scenario are neutrino Dirac mass generating Yukawa couplings y_{AB} , $A, B = 1, 2, 3$ in the superpotential. These couple the right handed neutrinos to the Left chiral lepton doublets $L_A = \begin{pmatrix} \nu \\ e \end{pmatrix}_A^T$, $A = 1, 2, 3$. L_A transform as $L[1, 2, 0, -1]$ and the up type Higgs doublet type field as $H[1, 2, 1/2, 0]$ so that $y_{AB}NL_AH_B$ is a gauge invariant term in the Superpotential. Each doublet of this type present in the underlying theory must have its complementary doublet transforming as e.g. $\bar{H}[1, 2, -1/2, 0]$ to cancel anomalies. The relevant flat direction is assumed to extend out of the minimum of the supersymmetric potential corresponding to the breaking of the

gauge group down to the MSSM symmetry

$$SU(3) \times SU(2) \times U(1)_R \times U(1)_{B-L} \rightarrow SU(3) \times SU(2) \times U(1)_Y \quad (5.25)$$

This leads to a Type I seesaw plus MSSM (SIMSSM) effective theory.

The fields \tilde{N} (the chosen conjugate sneutrino), $\tilde{\nu}$ (chosen left sneutrino flavor from a Lepton doublet L with suitable Yukawa couplings) and the light neutral Higgs field (from the doublet H with $Y = +1$) may be parameterized in terms of the flat-direction associated with the gauge invariant NLH as

$$\tilde{N} = \tilde{\nu} = h_0 = \frac{\varphi}{\sqrt{3}} = \phi e^{i\theta}; \quad \phi \geq 0, \quad \theta \in [0, 2\pi) \quad (5.26)$$

The additional fields Ω_i , (for example a, ω, p in NMSGUT (discussed in chapter 2)), are assumed to be coupled to S in such a way that extremization of the SUSY potential using $F_{\Omega_i} = 0$, $D_\alpha|_{\phi=0} = 0$ fixes the vev of S : $\langle S \rangle = \bar{\sigma}/\sqrt{2}$ without constraining the inflaton field φ . This is also true in the Minimal Susy LR models [12–14].

The vanishing of the D -term for the $B-L$ generator requires Ω_i to include the conjugate field(s) $\bar{S}[1, 1, -1, 2]$ which have a vev of equal magnitude as S in order to preserve SUSY through the symmetry breaking down to the MSSM symmetry at high scales. This is also a feature of MSLRMs and R-parity preserving GUTs [12–17, 19, 20, 23, 27, 28]. The gauge invariance of NLH ensures that the D -terms for the flat direction vanish. Thus at scales $\phi \sim \bar{\sigma} \gg M_S$ where SUSY is exact and the relevant superpotential is given by:

$$W = 3\sqrt{3}yN\nu h + 3f\sqrt{2}SNN + \dots = y\varphi^3 + f\sqrt{2}S\varphi^2 + \dots \quad (5.27)$$

where $h, f, \bar{\sigma}$ can be taken real without loss of generality. The right handed neutrino Majorana mass will be $M_\nu = 6f\bar{\sigma}$.

Since the equations of motion of the unperturbed vacuum imply $\langle F_S \rangle = 0$,

$\langle S \rangle = \bar{\sigma}/\sqrt{2}$ this superpotential leads to a flat direction potential

$$\begin{aligned} V_{susy} &= |3y\varphi^2 + 2f\bar{\sigma}\varphi|^2 + 2|f\bar{\varphi}^2|^2 \\ &= f^2 [(2 + 9\tilde{y}^2)\phi^4 + 12\tilde{y}\phi^3\bar{\sigma}\cos\theta + 4\bar{\sigma}^2\phi^2] \end{aligned} \quad (5.28)$$

Here $\tilde{y} = y/f$ and it is clear from the potential that $\bar{\sigma}$ sets the inflaton mass scale. Minimizing with respect to θ gives $\theta = \pi$. As long as we are interested only in the dynamics of inflationary (once parameters are tuned to ensure an inflection point in the flat region where $|\varphi| \sim \bar{\sigma}$), we can concentrate on just the real part of φ and set $\varphi = -\phi$ with ϕ real and positive near the inflection point but free to fall into the well around $\phi = 0$ and oscillate around that value. The reason of taking real value is that the imaginary part ϕ' of φ has a large curvature $V_{\phi'\phi'} \sim \bar{\sigma}^2$ in the flat region. Since $V_{\phi'}|_{\phi'=0} = 0$ it is viable to consider the dynamics in the real φ plane alone as a leading approximation. The effect of disturbance in the ϕ' direction when the dynamics is initiated with $\phi' \neq 0$ can be studied numerically as a correction to the dynamics of the inflaton field ϕ .

The susy breaking potential from the μ term for the Higgs doublets together soft quadratic and cubic terms, which we assume to be of the type generated by supergravity, but with non universal Higgs masses, has form:

$$\begin{aligned} V_{soft} &= [A_0(y\varphi^3 + f\sqrt{2}S\varphi^2) + h.c.] + m_{\tilde{f}}^2 \sum_{\tilde{f}} |\tilde{f}|^2 + m_H^2 |H|^2 + m_{\bar{H}}^2 |\bar{H}|^2 \\ &= f^2 \left[\tilde{y}\tilde{A}_0\phi^3\bar{\sigma}\cos 3\theta + \tilde{A}_0\bar{\sigma}^2\phi^2\cos 2\theta + \tilde{m}_0^2\bar{\sigma}^2\phi^2 \right] \end{aligned} \quad (5.29)$$

here $\tilde{m}_0 = m_0/f\bar{\sigma}$, $\tilde{A}_0 = 2A_0/f\bar{\sigma}$. The soft mass m_0 receives contributions from the sfermion and Higgs soft masses as well as the μ term

$$m_0^2 = \frac{2m_{\tilde{f}}^2 + \bar{m}_H^2}{3} \quad (5.30)$$

$m_{\tilde{f},H}$ are the sfermion and up type Higgs soft effective masses at the unification scale ($\bar{m}_H^2 = m_H^2 + |\mu|^2$). Since these masses and A_0 should be in the range $10^2 - 10^5$ GeV

while the righthanded neutrino masses lie in the range $10^6 - 10^{12}$ GeV, it is clear that \tilde{m}_0, \tilde{A}_0 are small parameters. Thus these terms cannot significantly change $\theta = \pi$ assumed earlier. The total inflaton potential is then

$$V_{tot} = f^2 \left((2 + 9\tilde{y}^2)\phi^4 - (\tilde{A}_0 + 12)\tilde{y}\bar{\sigma}\phi^3 + (\tilde{A}_0 + \tilde{m}_0^2 + 4)\bar{\sigma}^2\phi^2 \right). \quad (5.31)$$

Thus we have a generic quartic inflaton potential of the same type as in Section 2 but the parameter values in the case of Type I seesaw are quite different from the light Dirac neutrino case. We have the identification of parameters

$$\begin{aligned} h &= f\sqrt{12(2 + 9\tilde{y}^2)} \\ A &= \frac{3f(\tilde{A}_0 + 12)\tilde{y}\bar{\sigma}}{\sqrt{(2 + 9\tilde{y}^2)}} \\ M^2 &= 2f^2\bar{\sigma}^2(4 + \tilde{A}_0 + \tilde{m}_0^2) \\ \Delta &= \left(1 - \frac{A^2}{16M^2}\right) \\ &= \left(1 - \frac{9\tilde{y}^2(\tilde{A}_0 + 12)^2}{32(2 + 9\tilde{y}^2)(\tilde{A}_0 + \tilde{m}_0^2 + 4)}\right) \end{aligned} \quad (5.32)$$

For seesaw models the natural magnitude for the neutrino Dirac mass is, $m_\nu^D > 1\text{MeV}$ i.e $|y_\nu^D| > 10^{-5}$ and then the limit $m_\nu \ll 0.01\text{eV}$ for the lightest neutrino (assuming direct hierarchy) implies $M_{\nu^c} > 10^6$ GeV. The preferred values for the Susy breaking scale are smaller than 100 TeV (at most) it follows that the maximum value of $|\tilde{A}_0|, |\tilde{m}_0| \sim 0.1$ and they could be much smaller for more typical larger values of the conjugate neutrino masses $M_{\nu^c} \sim 10^8$ to 10^{12} GeV. It is then clear from the corresponding range $\Delta \sim 10^{-12}$ to 10^{-4} that the coupling ratio $\tilde{y} = y/f$ becomes ever closer to exactly $\tilde{y} = 4/3$ as M increases and even for $M \sim 10^6$ GeV differs from 1.333 only at the second decimal place. Thus to a good approximation

$h = 6\sqrt{6}f$. Then it follows from the Eqs.(5.22)and (5.32) that

$$\begin{aligned} f &\simeq 10^{-26.83\pm 0.17} \left(\frac{\bar{\sigma}}{\text{GeV}}\right) \quad ; \quad M \simeq 10^{-25.38\pm 0.17} \left(\frac{\bar{\sigma}}{\text{GeV}}\right)^2 \\ \Delta &\simeq 10^{-78.93\pm 0.47} \left(\frac{\bar{\sigma}}{\text{GeV}}\right)^4 \end{aligned} \quad (5.33)$$

The range $M \sim 10^{6.6}$ to $10^{10.6}$ GeV corresponds nicely to $10^{16} \text{ GeV} < \bar{\sigma} < 10^{18} \text{ GeV}$: as is natural in single scale Susy SO(10) GUTs [15–17, 19, 20, 23, 27, 28]. f increases with $\bar{\sigma}$ with values above 10^{-11} for $\bar{\sigma} > 10^{16} \text{ GeV}$ (which is however achievable in the NMSGUT only with difficulty). However in MSLRMs, since there are no GUT constraints on $\bar{\sigma}$, so one can have somewhat broad ranges for these parameters.

In all relevant cases $\Delta < 10^{-8}$ is required. Thus the above equations imply that \tilde{y}^2 must be close to the value

$$\tilde{y}_0^2 = \frac{64}{9} \frac{4 + \tilde{A}_0 + \tilde{m}_0^2}{16 - 8\tilde{A}_0 - 32\tilde{m}_0^2 + \tilde{A}_0^2} \quad (5.34)$$

Here $\tilde{A}_0, \tilde{m}_0 \sim O(M_S/M_{\nu c}) \ll 1$, hence \tilde{y}_0 is rather close to $4/3$ and the equality is very close for larger $M \sim f\bar{\sigma}$ since then \tilde{A}_0, \tilde{m}_0 are very small. So this is the type of fine tuning that supports the advancement of inflation in SIMSSM models. We see that the of severity of fine tuning $\beta = \sqrt{\Delta} \sim 10^{-4} - 10^{-6}$ is much less than the case of the MSSM Dirac neutrino inflaton since there $\beta \sim 10^{-12}$ to 10^{-10} due to the low values of the inflaton mass. Moreover the fine tuning condition is determined in terms of superpotential parameters, which are radiatively stable due to non renormalization theorems. Specially for large $\bar{\sigma} > 10^{16} \text{ GeV}$ the Type I Susy seesaw can provide a rather attractive inflationary seesaw with a natural explanation for neutrino masses and demands weaker tuning conditions on the radiatively unstable Susy breaking parameters. Also unlike the chaotic sneutrino inflaton scenario [82, 83], no trans-Planckian vevs are invoked.

We have viable inflation with M in range $10^6 - 10^{12}$ GeV as

$$V_0 \sim \frac{M^4}{h^2} \sim (M)^3 \times 10^{25} \text{ GeV} \sim 10^{43} - 10^{61} \text{ GeV}^4 \quad (5.35)$$

$$H_0 \sim \sqrt{\frac{V_0}{M_P^2}} \sim 10^3 - 10^{12} \text{ GeV} \quad ; \quad T_{max} \sim V_0^{\frac{1}{4}} \sim 10^{11} - 10^{15} \text{ GeV} \quad (5.36)$$

It is important to note that with maximum value of inflaton mass $M=10^{12}$ GeV the ratio of tensor to scalar perturbations $r=16 \epsilon \simeq 2(M/10^{14}\text{GeV})^3$ can be less than 10^{-6} . It is not compatible with the measurement of the tensor perturbations via CMB polarization at $r \sim 10^{-3}$ level or larger. However as M is raised above 10^{13} GeV the assumptions of our analysis break down and the question of compatibility with BICEP2 results [66] must be analyzed afresh. This will be discussed in later Chapters.

5.4 Conclusions and discussion

In this chapter we showed how Supersymmetric Type-I seesaw models with the typical superpotential couplings found in MSLRMs and MSGUTs (NMSGUT) allow an attractive and natural implementation of renormalizable inflection point inflation. Inflation parameters are tied to seesaw parameter values and the required fine tuning is less severe and more stable than in the Dirac neutrino case since it is essentially independent of the supersymmetry breaking parameters and is governed by the physics of intermediate scales $\sim 10^6 - 10^{12}\text{GeV}$. In the Dirac neutrino case [77] the opposite it is true and the inflation occurs at low scales.

The post-inflationary reheating behavior (to be discussed in next chapter in details) in the our model differs from the Dirac neutrino case. In our case (unlike [77], where $B-L$ is just broken above the susy scale) $B-L$ is not a gauge symmetry down to low energies. This can have important consequences for nucleosynthesis and matter domination since the heavy right handed neutrinos must find a non-gauge channel to decay through. This channel can be a Yukawa coupling since the right-handed neutrinos are singlets of the low energy (SM) gauge group. The reheating can occur via a mechanism of “instant preheating” [84]. It ensures efficient transfer of all the inflaton energy into thermalized MSSM plasma within few Hubble times after the end of inflation through oscillations around its true minimum after slow

roll of a flat direction. However a high reheat temperature $T_{rh} \sim 10^{11} - 10^{15}$ GeV requires a gravitino mass larger than about 50 TeV. This is necessary to make the inflation consistent with Nucleosynthesis. Such large Supersymmetry breaking scales are also required by the NMSGUT to fit all the fermion data [27]. The high reheat temperatures and the presence of the Higgs in the inflaton sit comfortably with the requirements of thermal [83] and non thermal Leptogenesis [85].

Chapter 6

Reheating in Supersymmetric Seesaw Inflation Scenario

6.1 Introduction

Inhomogeneities produced during inflation are proposed to have been the seeds for the growth of large scale inhomogeneities such as galaxies observed today [60–62]. After the inflation the universe undergoes a phase of cooling. But we know the present matter content can be explained very well by hot Big Bang theory and its modelling of nucleosynthesis (helium formation from hydrogen). So there must be some way that after the end of inflation the inflaton dumps its energy into radiation and massive particles. The process of converting inflaton energy into the matter content is known as reheating (it involves particle creation as well as thermalization). The resulting temperature of the universe is called “reheating temperature”. The success of any inflationary model depends on whether it can lead to Big-Bang nucleosynthesis and explain the matter content of universe. For this purpose one needs a reheating mechanism for inflaton to decay into known particles in the inflationary model considered.

In our model of Supersymmetric seesaw inflation [31] the inflaton is a gauge invariant D -flat direction, NH_uL , where N is the right handed sneutrino, H_u is the

MSSM Higgs which gives masses to the up-type quarks, and L is the slepton field. So their couplings (gauge and Yukawa) to the visible sector are known. The mechanism of instant preheating [84] can work very well in such types of inflation scenarios. We followed the procedure of previous work [86], where authors have studied the instant preheating in case of inflation along LLe flat direction. Our scenario is very different in the sense that in our case inflaton mass scale $\sim 10^6 - 10^{12}$ GeV (right handed neutrino mass) while in their case inflaton mass is $\sim 0.1-10$ TeV (Susy breaking scale). Large inflaton mass in our case results into high reheat temperature $\sim 10^{11} - 10^{13}$ GeV.

6.2 Instant preheating

The idea of instant preheating [84] is based upon the non-perturbative decay of inflaton (into the bosons and fermions -collectively called χ particles-) it is directly coupled to when it is close to the minimum of the potential (at $\phi = 0$). The χ particles decay further to other light MSSM modes not coupled directly to the inflaton. This happens before the inflaton reaches its minimum again because of the large decay width of the χ particles when ϕ is near maximum magnitude in its oscillation. A well known mechanism of non-perturbative particle production called parametric resonance was given in [87, 88]. In the case of parametric resonance several oscillations are required to increase the energy transfer from inflaton to decay products as only a very tiny fraction of inflaton energy $\sim 10^{-2}g^2$ is transferred in each oscillation. But in case of instant preheating, if the χ particles have strong interaction with light modes which are not directly coupled to inflaton (i.e other MSSM particles collectively called ψ modes) then they can decay before the inflaton returns to the potential minimum and the parametric resonance will not occur. This does happen because the mass of χ modes depends upon the instantaneous inflaton field vev. At the time of their production, their mass is zero as $\phi=0$, but as inflaton rolls back to its maximum value the χ modes become heavy. When they have maximum decay width they decay rapidly into ψ modes. With this kind of

chain reaction one has an efficient way to transfer the whole energy of inflaton into relativistic particles within few oscillations. This process called “instant preheating”. ψ particle creation is followed by their thermalization, resulting the final “reheated” state.

6.3 Supersymmetric seesaw inflaton

In Supersymmetric Seesaw inflation (SSI) the flat direction is gauge invariant combination of \tilde{L}_1 , H_u , $\tilde{\nu}_3^c$. The flat direction corresponds to

$$H_u = \begin{pmatrix} 0 \\ \varphi \end{pmatrix}; \quad \tilde{L} = \begin{pmatrix} \varphi \\ 0 \end{pmatrix}; \quad \tilde{\nu}^c = \varphi \quad (6.1)$$

Here φ is complex scalar field and inflaton ϕ corresponds to its real part. The inflationary potential has form given in [31]:

$$V(\phi) = \frac{M^2}{2}\phi^2 - \frac{2h}{3\sqrt{3}}\phi^3 + \frac{h^2}{12}\phi^4 \quad (6.2)$$

Here ϕ is the inflaton field. At inflection point the value of field is $\phi_0 = \frac{\sqrt{3}M}{h}$ if $A \approx 4M$. The potential given above can be reparameterized as

$$\tilde{V} = \frac{V}{V_0} = \frac{3}{2}\tilde{\phi}^2 - 2\tilde{\phi}^3 + \frac{3}{4}\tilde{\phi}^4 \quad (6.3)$$

Where $\tilde{\phi} = \frac{\phi}{\phi_0}$ and $V_0 = \frac{M^4}{h^2}$ is value of potential energy at inflection point. A pictorial view of the inflaton rolling towards its minimum after inflation is shown in figure 6.1.

6.4 Finding the χ modes

The χ modes have both gauge and Yukawa couplings but except for the top Yukawa (and not even that when $\tan\beta$ is large) the gauge couplings dominate the Yukawa

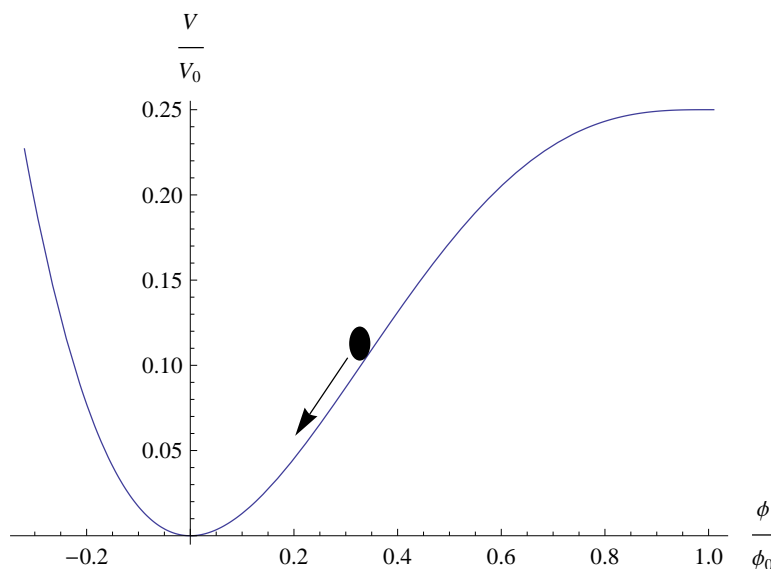


Figure 6.1: Rolling of inflaton around minimum of its potential after inflation.

couplings. So for simplicity we ignore the Yukawa coupling contributions and consider only gauge terms. The first step is to calculate the spectrum in which inflaton field will decay whenever it crosses the origin i.e. when $\phi = 0$. To calculate this spectrum we need all the terms from MSSM lagrangian which contains \tilde{L} , H_u , $\tilde{\nu}^c$ fields. These include interaction with gauge bosons, fermions and scalars. We calculate them one by one as follows:

$$H_u = \begin{pmatrix} H_u^+ \\ H_u^0 \end{pmatrix} = \begin{pmatrix} \phi_1 \\ \phi_2 \end{pmatrix}; \quad \tilde{L} = \begin{pmatrix} \tilde{\nu} \\ \tilde{e} \end{pmatrix} = \begin{pmatrix} \phi_3 \\ \phi_4 \end{pmatrix}; \quad \tilde{\nu}^c = \phi_5 \quad (6.4)$$

Here all the ϕ 's are complex fields given by $\phi = \frac{\phi_R + i\phi_I}{\sqrt{2}}$. The inflaton is given by

$$\varphi = \frac{\phi_{2R} + \phi_{3R} + \phi_{5R}}{\sqrt{3}} \quad (6.5)$$

6.4.1 Gauge interactions

The gauge interaction terms come from the gauge terms of fields \tilde{L} , $H_u, \tilde{\nu}^c$ which form the inflaton. If we recall the field content of SSI then the required fields along

with these are $S[1,1,1-2]$ and $\bar{S}[1,1,-1,2]$. In this case symmetry breaks as:

$$SU(3)_C \times SU(2)_L \times U(1)_R \times U(1)_{B-L} \rightarrow SU(3)_C \times U(1)_Q \quad (6.6)$$

Here S field gets vev σ which breaks the $U(1)_{B-L}$ symmetry. The background inflaton field breaks the $SU(2)_L$ symmetry. The relevant kinetic terms are:

$$L_{kinetic} = (D_\mu H_u)^\dagger D^\mu H_u + (D_\mu \tilde{L}_1)^\dagger D^\mu \tilde{L}_1 + (D_\mu \tilde{\nu}_3^c)^\dagger D^\mu \tilde{\nu}_3^c + (D_\mu S)^\dagger D^\mu S + (D_\mu \bar{S})^\dagger D^\mu \bar{S}$$

Where

$$\begin{aligned} D_\mu H_u &= \left(\partial_\mu - \frac{i}{2} g_R C_\mu - \frac{i}{2} g_W \sum_{a=1}^3 W_\mu^a T^a \right) H_u \\ D_\mu \tilde{L}_1 &= \left(\partial_\mu + \frac{i}{2} g_{B-L} E_\mu - \frac{i}{2} g_W \sum_{a=1}^3 W_\mu^a T^a \right) \tilde{L}_1 \\ D_\mu \tilde{\nu}_3^c &= \left(\partial_\mu + \frac{i}{2} g_R C_\mu - \frac{i}{2} g_{B-L} E_\mu \right) \tilde{\nu}_3^c \\ D_\mu S &= \left(\partial_\mu - i g_R C_\mu + i g_{B-L} E_\mu \right) S \\ D_\mu \bar{S} &= \left(\partial_\mu + i g_R C_\mu - i g_{B-L} E_\mu \right) \bar{S} \end{aligned} \quad (6.7)$$

Here g_w, g_{B-L}, g_R are the gauge couplings and W_μ^a, E_μ, C_μ are gauge fields corresponding to gauge group $SU(2)_L, U(1)_{B-L}, U(1)_R$ respectively. T^a are $SU(2)$ generators:

$$T_1 = \frac{1}{2} \begin{pmatrix} 0 & 1 \\ 1 & 0 \end{pmatrix}; \quad T_2 = \frac{1}{2} \begin{pmatrix} 0 & -i \\ i & 0 \end{pmatrix}; \quad T_3 = \frac{1}{2} \begin{pmatrix} 1 & 0 \\ 0 & -1 \end{pmatrix}$$

In terms of inflaton vev and vev for S and \bar{S} fields given,

$$\begin{aligned} \langle H_u \rangle &= \begin{pmatrix} 0 \\ \frac{\varphi}{\sqrt{3}} \end{pmatrix}; \quad \langle \tilde{L}_1 \rangle = \begin{pmatrix} \frac{\varphi}{\sqrt{3}} \\ 0 \end{pmatrix}; \quad \langle \tilde{\nu}_3^c \rangle = \frac{\varphi}{\sqrt{3}} \\ \langle S \rangle &= \frac{\sigma}{\sqrt{2}}; \quad \langle \bar{S} \rangle = \frac{\bar{\sigma}}{\sqrt{2}} \end{aligned} \quad (6.8)$$

one can find the massive gauge modes which will appear due to symmetry breaking. According to Higgs mechanism four massive gauge bosons will appear. One gets the following mass terms:

$$L_{kinetic} = \frac{1}{12}(g_R C_\mu - g_W W_\mu^3)^2 \varphi^2 + \frac{1}{3}g_W^2 W_\mu^+ W_\mu^- \varphi^2 + \frac{1}{12}(g_{B-L} E_\mu - g_W W_\mu^3)^2 \varphi^2 \\ + (g_R C_\mu - g_{B-L} E_\mu)^2 \left(\frac{\varphi^2}{12} + |\sigma|^2 \right)$$

However in this basis of gauge fields, they mix with each other. Since the mass matrix is symmetric so one needs to find a orthogonal matrix which diagonalize the mass matrix of gauge bosons. We found that for three different gauge couplings the expressions for gauge fields in mass basis are quite complicated. For simplification we chose NMSGUT relation between gauge couplings: $g_W = g_R = g$ and $g_{B-L} = \sqrt{\frac{3}{2}}g$. Here g is the $SO(10)$ gauge coupling in the standard unitary normalization. After taking these relations eq. (6.9) can be written as

$$L_{kinetic} = \frac{1}{3}g^2 W_\mu^+ W_\mu^- \varphi^2 + \frac{1}{2}M_{X'}^2 X'^2 + \frac{1}{2}M_{Z'}^2 Z'^2 \quad (6.9)$$

Where

$$M_{X'}^2 = (14 + 5a + p)g^2 \frac{\varphi^2}{24}; \quad M_{Z'}^2 = (14 + 5a - p)g^2 \frac{\varphi^2}{24} \quad (6.10)$$

Where $a = \frac{12|\sigma|^2}{\varphi^2}$ and $p = \sqrt{14 + 5a + 25a^2}$. X'_μ and Z'_μ are liner combination of X_μ , Z_μ with coefficients which are functions of a and p .

$$X'_\mu = \cos\theta X_\mu + \sin\theta Z_\mu \\ Z'_\mu = -\sin\theta X_\mu + \cos\theta Z_\mu \quad (6.11)$$

Where $\tan\theta = (6 + 25a - 5p)/8$. $X_\mu = \sqrt{2/5}C_\mu - \sqrt{3/5}E_\mu$ is the gauge field which gets a large mass when S and \bar{S} field get vevs. The orthogonal combination of X_μ , say B_μ (represents gauge field for hypercharge $Y/2$) mixes with W_μ^3 to give the $Z_\mu = \sqrt{\frac{3}{8}}B_\mu - \sqrt{\frac{5}{8}}W_\mu^3$. The orthogonal combination to Z_μ is the photon field A_μ

which remains massless.

$$A_\mu = \sqrt{\frac{5}{8}}B_\mu + \sqrt{\frac{3}{8}}W_\mu^3 \quad (6.12)$$

Now the masses of X' and Z' contain terms with $|\sigma|^2$. In the SSI scenario $|\sigma|$ doesn't vary with time, so these fields will remain heavy during the oscillation of inflaton. They don't participate in the preheating, so only the charged gauge bosons are of interest to us.

The massive charged W_\pm gauge fields have interaction terms with scalars through their kinetic terms. The gauge fields decay into squarks, sleptons and Higgs fields. The relevant terms are:

$$\begin{aligned} L \supset & \frac{i}{\sqrt{2}}g(\partial\tilde{u}_iW_\mu^+\tilde{d}_i^* - \partial\tilde{d}_i^*W_\mu^+\tilde{u}_i) + h.c. \\ & + \frac{i}{\sqrt{2}}g(\partial\tilde{\nu}_iW_\mu^+\tilde{e}_i^* - \partial\tilde{e}_i^*W_\mu^+\tilde{\nu}_i) + h.c. \\ & + \frac{i}{\sqrt{2}}g(\partial H_d^0W_\mu^+H_d^{-*} - \partial H_d^{-*}W_\mu^+H_d^0) + h.c. \\ & + \frac{i}{\sqrt{2}}g(\partial H_u^+W_\mu^+H_u^{0*} - \partial H_u^{0*}W_\mu^+H_u^+) + h.c. \end{aligned}$$

Here i runs over the family index. The decay rate for decay of a gauge boson with mass M to a pair of massless scalars coupled as above is $g^2M/96\pi$.

Similarly the interaction terms of massive gauge fields with fermions are given by:

$$\begin{aligned} L \supset & \frac{i}{\sqrt{2}}g(u_i^\dagger\bar{\sigma}^\mu W_\mu^+d_i + \nu_i^\dagger\bar{\sigma}^\mu W_\mu^+e_i) + h.c. \\ & + \frac{i}{\sqrt{2}}g(\tilde{H}_d^0\bar{\sigma}^\mu W_\mu^+\tilde{H}_d^- + \tilde{H}_u^+\bar{\sigma}^\mu W_\mu^+\tilde{H}_u^0) + h.c. \end{aligned}$$

The decay rate for decay of a gauge boson with mass M to a pair of massless fermions is $g^2M/48\pi$. The decay rates for W_μ^\pm after summing over all channels is given by

$$\Gamma_{W_\mu^\pm} = \frac{7g^3\phi(t)}{16\sqrt{3}\pi} \quad (6.13)$$

6.4.2 Scalar interactions

Due to breaking of symmetry 2 degrees of freedom of neutral and 2 charged scalars are eaten by gauge modes so we are left with four massive scalar fields whose masses can be obtained from D-terms of the MSSM potential:

$$\begin{aligned} V_D(\phi, \phi^*) &= \frac{1}{2} \sum_a D^a D^a = \frac{1}{2} \left(\sum_{a=1}^3 D^a D^a + D^R D^R + D^{B-L} D^{B-L} \right) \quad (6.14) \\ &= \frac{1}{2} \sum_{a=1}^3 g_a^2 (\phi^* T^a \phi)^2 + g_R^2 (\phi^* T^R \phi)^2 + g_{B-L}^2 (\phi^* T^{B-L} \phi)^2 \end{aligned}$$

Now from the D-terms we concentrate on terms linear in the inflaton so that square of this term gives us the mass of scalar field and cross terms with bilinears give the couplings responsible for the decay of this massive scalar to massless scalars. We consider only trilinear terms as they are dominant over the quartic ones. For example D_1 is given as

$$\begin{aligned} D_1 &= H_u^* T^1 H_u + \tilde{L}_1^* T^1 \tilde{L}_1 + \tilde{Q}_i^* T^1 \tilde{Q}_i + \tilde{L}_{2,3}^* T^1 \tilde{L}_{2,3} + \tilde{H}_d^* T^1 \tilde{H}_d \quad (6.15) \\ &= \frac{1}{2} (\phi_2^* \phi_1 + \phi_1^* \phi_2 + \phi_4^* \phi_3 + \phi_3^* \phi_4) + \tilde{Q}_i^* T^1 \tilde{Q}_i + \tilde{L}_{2,3}^* T^1 \tilde{L}_{2,3} + H_d^* T^1 H_d \end{aligned}$$

After substituting $\phi_2 = \hat{\phi}_2 + \phi$ and $\phi_3 = \hat{\phi}_3 + \phi$, where fields with “hat” represent the fluctuation part, we get:

$$D_1 = \frac{1}{2} (\hat{\phi}_1^- + \hat{\phi}_1^+ + \hat{\phi}_4^- + \hat{\phi}_4^+) \frac{\varphi}{\sqrt{3}} + \tilde{Q}_i^* T^1 \tilde{Q}_i + \tilde{L}_i^* T^1 \tilde{L}_i + H_d^* T^1 H_d + H_u^* T^1 H_u$$

Similarly from other D-terms

$$\begin{aligned} D_2 &= \frac{-i}{2} (\hat{\phi}_1^- - \hat{\phi}_1^+ + \hat{\phi}_4^- - \hat{\phi}_4^+) \frac{\varphi}{\sqrt{3}} + \tilde{Q}_i^* T^2 \tilde{Q}_i + \tilde{L}_i^* T^2 \tilde{L}_i + H_d^* T^2 H_d + H_u^* T^2 H_u \\ D_3 &= \frac{(\hat{\phi}_{3R} - \hat{\phi}_{2R})}{\sqrt{2}} \frac{\varphi}{\sqrt{3}} + \tilde{Q}_i^* T^3 \tilde{Q}_i + \tilde{L}_i^* T^3 \tilde{L}_i + H_d^* T^3 H_d + H_u^* T^3 H_u \end{aligned}$$

$$D_R = \frac{(\hat{\phi}_{2R} - \hat{\phi}_{5R})}{\sqrt{2}} \frac{\varphi}{\sqrt{3}} + \frac{1}{2} (|H_u|^2 - |H_d|^2 - |\tilde{\nu}_i^c|^2 - |\tilde{u}_i^c|^2 + |\tilde{d}_i^c|^2 + |\tilde{e}_i^c|^2)$$

$$D_{B-L} = \frac{(\hat{\phi}_{5R} - \hat{\phi}_{3R})}{\sqrt{2}} \frac{\varphi}{\sqrt{3}} - \frac{1}{2} (|L_i|^2 - |\tilde{\nu}_i^c|^2 - \frac{1}{3} |\tilde{Q}_i|^2 + \frac{1}{3} |\tilde{u}_i^c|^2 + \frac{1}{3} |\tilde{d}_i^c|^2 - \mathbf{6}_i^c \mathbf{1}_i^c)$$

The MSSM potential corresponding to these D-terms is given by

$$V = g^2 \left(\varphi^2 \frac{\chi^+ \chi^-}{3} + \varphi^2 \frac{\chi_1^2}{4} + \varphi^2 \frac{\chi_2^2}{3} \right.$$

$$+ \frac{\varphi \chi^+}{\sqrt{6}} (\tilde{Q}_i^* (T^1 + iT^2) \tilde{Q}_i + \tilde{L}_i^* (T^1 + iT^2) \tilde{L}_i + H_d^* (T^1 + iT^2) H_d + H_u^* (T^1 + iT^2) H_u)$$

$$+ \frac{\varphi \chi^-}{\sqrt{6}} (\tilde{Q}_i^* (T^1 - iT^2) \tilde{Q}_i + \tilde{L}_i^* (T^1 - iT^2) \tilde{L}_i + H_d^* (T^1 - iT^2) H_d + H_u^* (T^1 - iT^2) H_u)$$

$$- \frac{\varphi \chi_1}{\sqrt{3}} (\tilde{Q}_i^* T^3 \tilde{Q}_i + \tilde{L}_i^* T^3 \tilde{L}_i + H_d^* T^3 H_d + H_u^* T^3 H_u)$$

$$- \frac{\varphi \chi_1}{4\sqrt{3}} (|H_d|^2 - |H_u|^2 + |\tilde{L}_i|^2 + \frac{4}{3} |\tilde{u}_i^c|^2 - \frac{2}{3} |\tilde{d}_i^c|^2 - \frac{1}{3} |\tilde{Q}_i|^2 - 2|\tilde{e}_i^c|^2)$$

$$- \frac{\varphi \chi_2}{2\sqrt{3}} (|H_d|^2 - |H_u|^2 - |\tilde{L}_i|^2 + \frac{2}{3} |\tilde{u}_i^c|^2 - \frac{4}{3} |\tilde{d}_i^c|^2 + \frac{1}{3} |\tilde{Q}_i|^2 + 2|\tilde{\nu}_i^c|^2)$$

$$+ \frac{1}{4} \chi_1^2 (-|H_d|^2 - 2|\tilde{\nu}_i^c|^2 + |\tilde{L}_i|^2 - \frac{2}{3} |\tilde{u}_i^c|^2 + \frac{4}{3} |\tilde{d}_i^c|^2 - \frac{1}{3} |\tilde{Q}_i|^2)$$

$$+ \frac{5}{16} \chi_2^2 (|H_d|^2 + 2|\tilde{\nu}_i^c|^2 - |\tilde{L}_i|^2 + \frac{2}{3} |\tilde{u}_i^c|^2 - \frac{4}{3} |\tilde{d}_i^c|^2 + \frac{1}{3} |\tilde{Q}_i|^2) \Big) \quad (6.17)$$

where

$$\chi^- = \frac{\hat{\phi}_1^- + \hat{\phi}_4^-}{\sqrt{2}}, \quad \chi^+ = \frac{\hat{\phi}_1^+ + \hat{\phi}_4^+}{\sqrt{2}}, \quad \chi_1 = \frac{(\hat{\phi}_{2R} - \hat{\phi}_{3R})}{\sqrt{2}}, \quad \chi_2 = \frac{\hat{\phi}_{2R} + \hat{\phi}_{3R} - \sqrt{6}\hat{\phi}_{5R}}{\sqrt{8}}$$

The decay rate for decay of a massive scalar with mass M into a pair of massless scalars is $\sigma^2/16\pi M$. Here σ is the coupling of massive scalar with massless scalar.

The decay rates for χ^\pm, χ_1, χ_2 after summing over all channels is given by

$$\Gamma_{\chi^\pm} = \frac{7g^3\phi(t)}{16\sqrt{3}\pi}; \quad \Gamma_{\chi_1} = \frac{67g^3\phi(t)}{96\sqrt{2}\pi} \quad \Gamma_{\chi_2} = \frac{11g^3\phi(t)}{16\sqrt{6}\pi} \quad (6.18)$$

6.4.3 Fermion interactions

The fermion interactions of inflaton can be found from the following part of MSSM lagrangian

$$\begin{aligned}
L \supset & -\sqrt{2}g_W \sum_{a=1}^3 (\tilde{L}_1^* \tilde{W}_a T^a L_1 + H_u^* \tilde{W}_a T^a \tilde{H}_u) - \sqrt{2}g_R (S^* \tilde{C} \tilde{S} - \bar{S}^* \tilde{C} \tilde{S} - \frac{1}{2} \tilde{\nu}_3^{c*} \tilde{C} \nu_3^c \\
& + \frac{1}{2} H_u^* \tilde{C} \tilde{H}_u) - \sqrt{2}g_{B-L} (-S^* \tilde{E} \tilde{S} + \bar{S}^* \tilde{E} \tilde{S} + \frac{1}{2} \tilde{\nu}_3^{c*} \tilde{E} \nu_3^c - \frac{1}{2} \tilde{L}_1^* \tilde{E} L_1) \quad (6.19)
\end{aligned}$$

Putting vevs for inflaton fields, S and \bar{S} , we get the mass terms for fermions.

$$\begin{aligned}
L \supset & -\frac{g_W \varphi}{\sqrt{6}} (\tilde{W}^3 \nu_1 + \sqrt{2} \tilde{W}^+ e_1 + \sqrt{2} \tilde{W}^- \tilde{H}_u^+ - \tilde{W}^3 \tilde{H}_u^0) - \frac{g_R \varphi}{\sqrt{6}} (\tilde{H}_u^0 - \nu_3^c) \tilde{C} \\
& - g_{B-L} (\nu_3^c - \nu_1) \tilde{E} \frac{\varphi}{\sqrt{6}} - g_R (\tilde{S} - \tilde{\bar{S}}) \tilde{C} |\bar{\sigma}| - g_{B-L} (-\tilde{S} + \tilde{\bar{S}}) \tilde{E} |\bar{\sigma}| \\
= & -\frac{g_W \varphi}{\sqrt{3}} (\tilde{W}^+ e_1 + \tilde{W}^- \tilde{H}_u^+) - (g_W \tilde{W}^3 - g_{B-L} \tilde{E}) \nu_1 \frac{\varphi}{\sqrt{6}} - (g_R \tilde{C} - g_W \tilde{W}^3) \tilde{H}_u^0 \frac{\varphi}{\sqrt{6}} \\
& - (g_{B-L} \tilde{E} - g_R \tilde{C}) \nu_3^c \frac{\varphi}{\sqrt{6}} - (g_R \tilde{C} - g_{B-L} \tilde{E}) |\bar{\sigma}| (\tilde{S} - \tilde{\bar{S}}) + H.C. \\
= & -\frac{g \varphi}{\sqrt{3}} (\tilde{W}^+ e_1 + \tilde{W}^- \tilde{H}_u^+) + g \frac{\varphi}{\sqrt{6}} \frac{\alpha^2 + 2\sqrt{a}}{4\sqrt{3a}} \tilde{X}' \psi_3 + g \frac{\varphi}{\sqrt{6}} \frac{\alpha^2 - 2\sqrt{a}}{4\sqrt{3a}} \tilde{Z}' \psi_4
\end{aligned}$$

Where

$$\begin{aligned}
\psi_3 &= \nu_1 - \frac{2\sqrt{3}}{\alpha + 2\sqrt{a}} \tilde{H}_u^0 + \frac{4\sqrt{3a}}{\alpha^2 + 2\sqrt{a}\alpha} \nu_3^c + \frac{2\sqrt{6a}}{\alpha^2 + 2\sqrt{a}\alpha} (\tilde{S} - \tilde{\bar{S}}) \\
\psi_4 &= \nu_1 - \frac{2\sqrt{3}}{\alpha - 2\sqrt{a}} \tilde{H}_u^0 + \frac{4\sqrt{3a}}{\alpha^2 - 2\sqrt{a}\alpha} \nu_3^c + \frac{2\sqrt{6a}}{\alpha^2 - 2\sqrt{a}\alpha} (\tilde{S} - \tilde{\bar{S}})
\end{aligned}$$

With $\alpha = 2\sqrt{\sqrt{3a} + a}$. In form of Dirac spinor the χ modes are

$$\Psi_1 = \begin{pmatrix} e_1 \\ \tilde{W}_\mu^{+*} \end{pmatrix}; \quad \Psi_2 = \begin{pmatrix} \tilde{H}_u^+ \\ \tilde{W}_\mu^{-*} \end{pmatrix}; \quad \Psi_3 = \begin{pmatrix} \psi_3 \\ \tilde{Z} \end{pmatrix}; \quad \Psi_4 = \begin{pmatrix} \psi_4 \\ \tilde{Z}' \end{pmatrix} \quad (6.20)$$

The Dirac fermions Ψ_3, Ψ_4 are heavy as their masses contain $|\sigma|$ which doesn't vary during oscillations, so they don't participate in reheating. So we are left with Ψ_1, Ψ_2

only and the interaction terms for these fermion χ particles are given as:

$$L \supset -\sqrt{2}g \left(\tilde{U}_i^* \Psi_1 P_L D_i + \tilde{L}_i^* \Psi_1 P_L N_i + H_d^{0*} \Psi_1 \tilde{H}_d^- + H_u^{+*} \Psi_1 \tilde{H}_u^0 + h.c. \right. \\ \left. + \tilde{D}_i^* \Psi_2 P_L U_i + \tilde{N}_i^* \Psi_2 P_L L_i + H_d^{-*} \Psi_2 \tilde{H}_d^0 + H_u^{0*} \Psi_2 \tilde{H}_u^+ + h.c. \right)$$

The decay rate for decay of a massive fermion with mass M into a massless scalar and its fermionic partner is $g^2 M/32\pi$. The decay rates for $\Psi_{1,2}$ after summing over all channels are

$$\Gamma_{\Psi_{1,2}} = \frac{7g^3 \phi(t)}{16\sqrt{3}\pi} \quad (6.21)$$

Once we have all the χ modes and their decay rates (given in table 6.1) we can estimate instant preheating in our model.

χ mode	Mass	Decay Rate	Degrees of freedom
W_μ^\pm	$1/\sqrt{3}g\phi(t)$	$7g^3\phi(t)/16\sqrt{3}\pi$	6
χ^\pm	$1/\sqrt{3}g\phi(t)$	$7g^3\phi(t)/16\sqrt{3}\pi$	2
χ_1	$1/\sqrt{2}g\phi(t)$	$67g^3\phi(t)/96\sqrt{2}\pi$	1
χ_2	$\sqrt{2/3}g\phi(t)$	$11g^3\phi(t)/16\sqrt{6}\pi$	1
Ψ^\pm	$1/\sqrt{3}g\phi(t)$	$7g^3\phi(t)/16\sqrt{3}\pi$	8

Table 6.1: The χ modes produced due to non-perturbative decay of inflaton.

6.5 Instant Preheating in context of SSI

After the end of inflation the inflaton starts oscillating around the minimum of potential and decays to the χ modes we calculated in the previous section. The mass of these χ modes is proportional to time dependent value of the inflaton. Let us first consider the charged χ type modes which include charged scalars, fermions and gauge bosons (we collectively called them χ_1 modes). The energy of such fields

is given by

$$\omega_k = \sqrt{k^2 + \frac{g^2 \phi(t)^2}{3}} \quad (6.22)$$

It is convenient to write this equation in terms a of parameter Q_1 (resonance parameter)

$$\omega_k = \sqrt{k^2 + 4M^2 \tau^2 Q_1}; \quad Q_1 = \frac{g^2 \dot{\phi}_0^2}{12M^4} \quad (6.23)$$

and $\tau = MT$ measures the time period of each oscillation in the units of M^{-1} . Here $\dot{\phi}_0$ is the velocity of inflaton at the time of zero crossing. The χ_1 modes are produced as inflaton moves towards origin and adiabaticity condition is violated i.e. $\dot{\omega}_k \gg \omega_k^2$. This condition is true for those modes having momentum less than,

$$k_{max}^2 \simeq g \frac{\dot{\phi}_0}{\sqrt{3}} \quad (6.24)$$

The number density of χ_1 modes with momentum k is [87]

$$\begin{aligned} n_{\chi_1, k} &= \exp\left[\frac{-\pi\sqrt{3}k^2}{g\dot{\phi}(t)}\right] \\ &= \exp\left[\frac{-\pi k^2}{2M^2\sqrt{Q_1}}\right] \end{aligned} \quad (6.25)$$

The total number density is given as

$$\begin{aligned} n_{\chi_1} &= \int_0^\infty \frac{d^3k}{(2\pi)^3} \exp\left[\frac{-\pi\sqrt{3}k^2}{g\dot{\phi}(t)}\right] \\ &= \frac{M^3}{2\sqrt{2}\pi^3} Q_1^{\frac{3}{4}} \end{aligned} \quad (6.26)$$

As soon as the adiabaticity condition is restored the χ_1 modes can decay further to the light particles which are not coupled to inflaton directly. The decay time of χ_1

modes is given as $t_{dec}^{\chi_1} = \Gamma_{\chi_1}^{-1}$. In terms of variable τ it is be given as

$$\tau_{dec}^{\chi_1} = \left(\frac{8\pi}{7g^2}\right)^{\frac{1}{2}} Q_1^{-\frac{1}{4}} \quad (6.27)$$

The energy density of χ modes after zero crossing is given by

$$\begin{aligned} \rho_{\chi_1}(\tau^{\chi_1}) &= \int_0^\infty \frac{k^2 dk}{(2\pi^2)} n_{\chi_1, k} \omega_k(\tau) \\ &= \frac{Q_1 M^4}{\pi^4} A_1 \exp A_1 K_1(A_1) \end{aligned} \quad (6.28)$$

Where

$$A_1 = \pi \sqrt{Q_1} \tau^2 \quad (6.29)$$

and K_1 is the modified Bessel function of second kind. As the χ_1 modes decay when the time reaches to their time of decay, so their energy density also decreases.

$$\rho_{\chi_1}(\tau) = \rho_{\chi_1} \exp\left[-\int_0^\tau \Gamma_{\chi_1} dt'\right] = \frac{Q_1 M^4}{\pi^4} A_1 \exp A_1 K_1(A_1) \exp\left[-\frac{7g^2 A_1}{16\pi^2}\right] \quad (6.30)$$

The amount of energy transferred to light MSSM fields every time the inflaton crosses the origin is (calculated at $\tau = \tau_{dec}^{\chi_1}$)

$$\bar{\rho}_{\chi_1} = \rho_{\chi_1}(\tau_{\chi_1}) = 3.606 \frac{Q_1 M^4}{\pi^4} \quad (6.31)$$

If $\rho_\phi = \frac{\dot{\phi}_0^2}{2}$ is the inflaton energy when it crosses zero, then the fraction of inflaton energy transferred by χ_1 modes to relativistic degrees of freedom is

$$\frac{\bar{\rho}_{\chi_1}}{\rho_\phi} = .0062g^2 \quad (6.32)$$

Similarly for χ_2, χ_3 modes we have,

$$Q_2 = \frac{g^2 \dot{\phi}_0^2}{8M^4}; \quad Q_3 = \frac{g^2 \dot{\phi}_0^2}{6M^4} \quad (6.33)$$

$$\tau_{dec,2} = \left(\frac{48\pi}{67g^2}\right)^{\frac{1}{2}} Q_2^{-\frac{1}{4}}; \quad \tau_{dec,3} = \left(\frac{16\pi}{11g^2}\right)^{\frac{1}{2}} Q_3^{-\frac{1}{4}} \quad (6.34)$$

The expressions for number density and energy transferred are given as

$$n_{\chi_2} = \frac{M^3}{2\sqrt{2}\pi^3} Q_2^{\frac{3}{4}}; \quad n_{\chi_3} = \frac{M^3}{2\sqrt{2}\pi^3} Q_3^{\frac{3}{4}} \quad (6.35)$$

$$\bar{\rho}_{\chi_2} = 2.883 \frac{Q_2 M^4}{\pi^4}; \quad \bar{\rho}_{\chi_3} = 4.054 \frac{Q_3 M^4}{\pi^4} \quad (6.36)$$

$$\frac{\bar{\rho}_{\chi_2}}{\rho_\phi} = .0074g^2; \quad \frac{\bar{\rho}_{\chi_3}}{\rho_\phi} = .0138g^2 \quad (6.37)$$

To find out total energy transferred to MSSM degrees of freedom we need to add contributions from all decay channels into light final states. It includes 6 degrees of freedom from gauge bosons (W_μ^\pm), four degrees of freedom from scalar (χ^\pm, χ_1, χ_2) and 8 from fermions ($\Psi_{1,2}$). The charged degrees of freedom χ_1 which sum to a total of 16 d.o.f lose energy according to equation (6.32) and χ_2, χ_3 according to eq. 6.37 respectively. So the total amount of energy transferred to MSSM degrees of freedom is

$$\rho_{rel} = 16\rho_{\chi_1} + \rho_{\chi_2} + \rho_{\chi_3} \quad (6.38)$$

For $g = .72$, the amount of energy loss per zero crossing is

$$\frac{\rho_{rel}}{\rho_\phi} \sim 6.22\% \quad (6.39)$$

Thus every time the inflaton crosses zero (i.e. twice in each cycle) it losses about 6% of its energy to relativistic particles. After N oscillations the ρ_ϕ and ρ_{rel} are given by

$$\rho_\phi = 0.88^N \rho_0; \quad \rho_{rel} = (1 - 0.88^N) \rho_0 \quad (6.40)$$

Here ρ_0 is the initial energy density of inflaton before it starts oscillating.

6.6 Coupled evolution of energy density of χ modes

The transfer of energy from inflaton to χ modes and then to the MSSM degrees of freedom can be depicted with the study of coupled differential equations for energy densities of ϕ field, χ modes and relativistic particles.

To illustrate the kind of picture that emerges we first take $M \sim 10^6$ GeV (i.e mass of inflaton is determined by Majorana mass of first generation right handed neutrino). Then the Hubble rate comes out to be is very small:

$$H = \sqrt{\frac{M^3}{10^{12}}} GeV^{-1} \approx 10^{-3} M \quad (6.41)$$

In other words the Hubble time is much greater than the inflaton oscillation time. So inflaton undergoes many oscillations in one Hubble time and the Hubble expansion can be ignored while studying the energy density evolution.

$$\begin{aligned} \dot{\rho}_\phi &= -(\Gamma_\phi^1 + \Gamma_\phi^2 + \Gamma_\phi^3)\rho_\phi \\ \dot{\rho}_{\chi_1} &= \Gamma_\phi^1\rho_\phi - \Gamma_{\chi_1}\rho_{\chi_1}\rho_\phi^{1/4} \\ \dot{\rho}_{\chi_2} &= \Gamma_\phi^2\rho_\phi - \Gamma_{\chi_2}\rho_{\chi_2}\rho_\phi^{1/4} \\ \dot{\rho}_{\chi_3} &= \Gamma_\phi^3\rho_\phi - \Gamma_{\chi_3}\rho_{\chi_3}\rho_\phi^{1/4} \\ \dot{\rho}_{rel} &= (\Gamma_{\chi_1}\rho_{\chi_1} + \Gamma_{\chi_2}\rho_{\chi_2} + \Gamma_{\chi_3}\rho_{\chi_3})\rho_\phi^{1/4} \end{aligned} \quad (6.42)$$

Here $\Gamma_\phi^1=0.105 M$ represents the effective decay rate of inflaton due to loss of energy to χ_1 and estimated by

$$\frac{\Gamma}{M} = -\frac{\text{Log}(\rho_\phi(N+1)) - \text{Log}(\rho_\phi(N))}{M(t_{N+1} - t_N)} \quad (6.43)$$

For half of the oscillation $M(t_{N+1} - t_N)= 0.5$. Similarly $\Gamma_\phi^2=.008 M$ and $\Gamma_\phi^3=.014 M$ are the effective rates due to decay into χ_2 and χ_3 respectively. $\Gamma_{\chi_1} = 1.16 \times 10^4 \rho_\phi^{1/4} M$ is the effective decay rate of χ_1 particles into MSSM particles (estimated from equa-

tion (6.27) and taking $(\dot{\phi}_0)^{1/2}=(2\rho_\phi)^{1/4}$. Similarly $\Gamma_{\chi_2}=1.62\times 10^4\rho_\phi^{1/4}M$ and $\Gamma_{\chi_3}=1.22\times 10^4\rho_\phi^{1/4}M$ are the effective decay rates for the χ_2 and χ_3 particles respectively. The differential equations are solved with the initial conditions $\rho_\phi/\rho_0=1$, $\rho_{\chi_1}/\rho_0=\rho_{\chi_2}/\rho_0=\rho_{\chi_3}/\rho_0=0$ and $\rho_{rel}/\rho_0=0$.

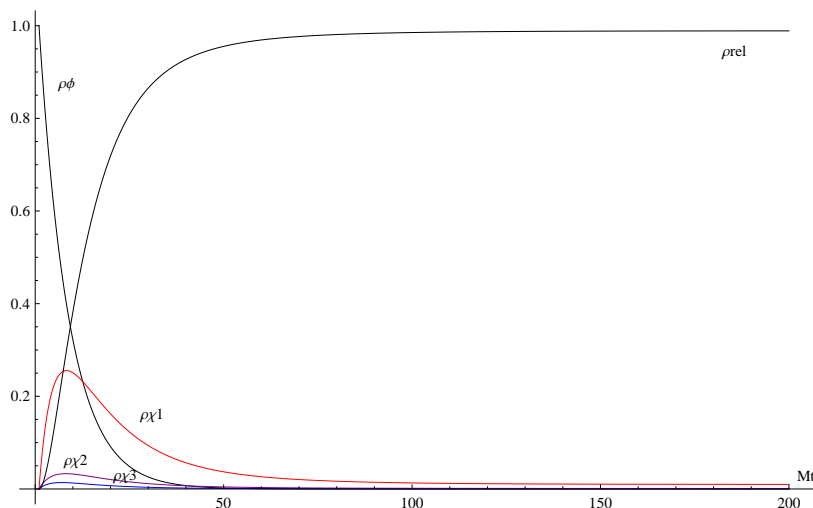


Figure 6.2: Evolution of energy densities of inflaton, χ modes and relativistic particles normalized to initial energy density of inflaton (ρ_0) with Mt .

However If we take inflaton mass $\geq 10^{10}$ GeV, the Hubble rate comes out to be much larger: $H \geq 10^{-1}M$ i.e. $H^{-1} \leq 10 T_{osc}$. In this case the oscillations are strongly damped due to Hubble expansion only. The whole inflaton energy is not converted into χ modes and then to relativistic particles (see Figure 6.3). However the initial energy density is so large ($\sim 10^{55} GeV^4$) even the small fraction of it transferred to MSSM degrees of freedom can still give us large reheat temperature ($T_{rh} \propto \rho^{1/4}$).

For $M=10^6$ GeV we see from Figure 6.2 that within 100 oscillations the inflaton loses all of its energy into the relativistic MSSM degrees of freedom. The relativistic particles produced by this chain process are not in thermal equilibrium at the time of their production. We study here the preheating part of the scenario, the complete reheating will take place when the relativistic particles come into equilibrium by undergoing subsequent scattering and collision. After their thermalization one can obtain the reheat temperature of the universe. The ultimate symmetry left in this case is $SU(3)_C \times U(1)_Q$. So we have gluons and photons as massless particles which

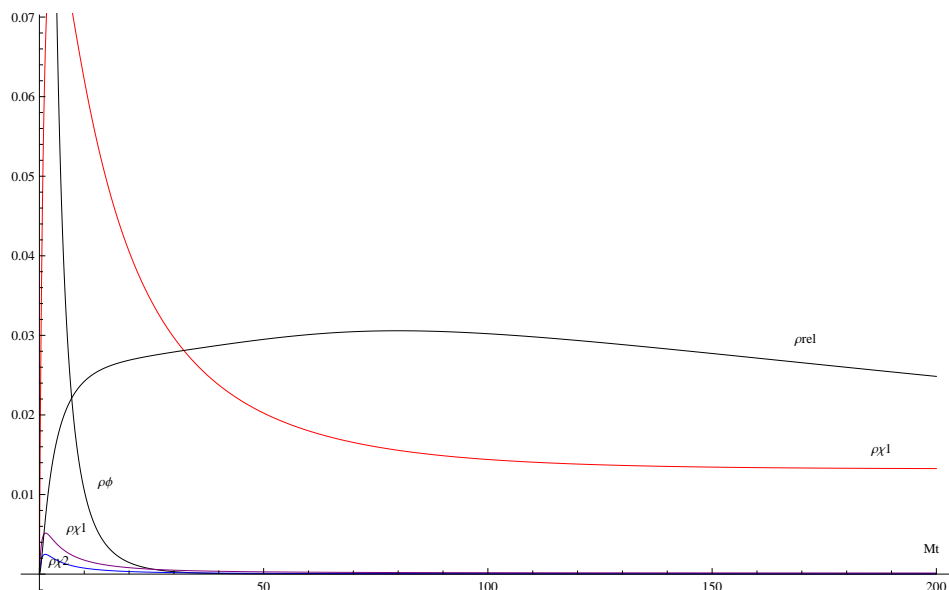


Figure 6.3: Evolution of energy densities of inflaton, χ modes and relativistic particles normalized to initial energy density of inflaton (ρ_0) with Mt when Hubble expansion rate is large and comparable to M .

are exchanged during the scattering of MSSM particles to bring them in thermal equilibrium. The dominant processes are $2 \rightarrow 3$ scattering process via gluon and photon exchange [89]. The rate of scattering via exchange of massive gauge bosons is suppressed because of large inflaton vev induced mass. Their exchange becomes effective when the amplitude of inflaton oscillation is quite small i.e. just near to the origin. When all the MSSM degrees of freedom get thermalized, it results in a reheating temperature of the universe, given by

$$T_{rh} = \frac{30}{\pi^2 g_*} \rho_{rel}^{1/4} \simeq 10^{11} - 10^{13} GeV \quad (6.44)$$

Here $g_* = 228.75$ are total effective MSSM degrees of freedom in thermal bath. $\rho_{rel} \approx \rho_0 = \frac{M^4}{h^2}$ is the initial energy density of inflaton. Such a high reheat temperature can lead to overproduction of gravitinos. For successful nucleosynthesis, they should decay before the time of nucleosynthesis $\tau_N \sim 1$ otherwise their late decay will destroy the created nucleons. The solution to this problem is if gravitino is massive

enough to decay before nucleosynthesis [90].

$$\tau_{grav} \sim 10^5 \text{ sec} \left(\frac{1 \text{ TeV}}{m_{3/2}} \right)^3 \ll \tau_N \sim 1 \text{ sec} \quad (6.45)$$

We see that the reheating in SSI scenario favors the scale of supersymmetry breaking -as indicated by the gravitino mass- should be above 50 TeV. It is interesting that such large supersymmetry breaking scales are preferred by both the NMSGUT [27–29] and the latest data indicating [1, 2] light Higgs mass $M_h \sim 125 \text{ GeV}$.

6.7 Conclusion

The idea of instant preheating works well in SSI scenario. For small inflaton mass the Hubble expansion rate is $\sim 10^{-3} M$ so inflaton undergoes many oscillations in one Hubble time and within 100 oscillations it loses all of its energy into the relativistic MSSM degrees of freedom which then undergo collisions and thermalize. In this way inflaton can efficiently transfer its whole energy to relativistic particles which after thermalization results into the reheat temperature $\sim 10^{11} \text{ GeV}$. For large inflaton mass the Hubble rate is comparable to the inflaton mass then only a very small fraction of inflaton energy is converted into the relativistic degrees of freedom. But the resulting reheat temperature is still very large $\sim 10^{13} \text{ GeV}$. Such large reheat temperature points to a high scale of Susy breaking which is favored in NMSGUT. So it points towards the idea of embedding of SSI in NMSGUT. We will discuss this idea in detail in the next Chapter.

Chapter 7

Susy Seesaw Inflation and NMSGUT

7.1 Introduction

In Chapter 5 we discussed the properties of generic inflection point inflation potential of the Susy Seesaw inflection (SSI) model. Since $SO(10)$ NMSGUT is a natural home for Seesaw so we can embed our SSI model in it. In [31] we presented the conditions on NMSGUT superpotential parameters consistent with the slow roll inflation conditions and results of inflation parameters along with fermion fit. Although we failed to achieve the required number of e-folds in NMSGUT inflation and also the required fine tuning together with a viable fermion fit, but results in [31] did not include high scale threshold corrections [29] which are crucial determining the $SO(10)$ Yukawas and hence inflation parameters. During our study of inflation conditions in NMSGUT after implementing GUT threshold conditions, the startling announcement from BICEP2 experiment arrived. The BICEP2 collaboration [66] claimed the observation of B-mode polarization in CMB. If confirmed then it is a direct evidence of primordial inflation and quantum gravitational effects [91, 92] because the large B-mode polarization they claim to have detected could only be due to primordial gravitational waves which were produced during inflation via quantum

effects. They claim a large value of tensor to scalar fluctuations parameter $r = .2_{-.05}^{+.07}$ which indicates a very high scale of inflation for single field inflation models. Later doubts were raised regarding their treatment of contamination of polarization data by foreground dust [93–95]. More polarization data is required to resolve the issue. A final word is awaited from the PLANCK collaboration. Now for a non zero value of r , from [96] we have

$$V_0^{\frac{1}{4}} = \left(\frac{r}{0.1} \right)^{1/4} \times 2 \times 10^{16} \text{GeV} \quad (7.1)$$

Thus the BICEP2 claim favors single field inflation models at precisely the MSSM gauge coupling unification scale ! Also the inflation takes place over a field interval $\delta\phi \sim 5M_{Pl}$ [96, 97]. Previously almost all inflation models were designed to avoid such a large value of r since there appeared little chance of finding $r \sim 0.1$ as reported by the PLANCK collaboration [98]. A large value of r will change the whole scenario of inflection point inflation models. For such a large field digression one needs a steep potential rather than a flat potential. The condition found on the trilinear-Mass term tuning parameter ($\Delta \approx 10^{-28} M^2 \text{GeV}^{-2}$) in [31] stops being a fine tuning condition for $M > 10^{13}$ GeV and the assumptions of our previous analysis break down.

In this chapter after discussing our first attempt to embed SSI in NMSGUT (with $M \leq 10^{12}$ GeV when fine tuning is required and the generic analysis of Chapter 5 holds) we revisit the issue of supersymmetric seesaw inflation in NMSGUT without any fine tuning of inflation potential and without making any assumption on the family index of matter fields in the inflaton LHN condensate. We derive the new conditions for inflation parameters for slow roll inflation conditions for a generic renormalizable potential for such large r .

7.2 Seesaw inflection and NMSGUT

To study the NLH flat direction in NMSGUT we need to consider this flat direction in full GUT potential in terms of light (SIMSSM) field vevs. Then this flat direction rolls out of the MSGUT vacuum with SIMSSM as effective theory. The required fields are the GUT scale vev fields $\Omega(p, a, \omega, \sigma, \bar{\sigma})$ and the (6) possible components $h_i, \bar{h}_i; i = 1 \dots 6$ of the light MSSM Higgs doublet pair H, \bar{H} along with the chiral lepton fields $L_A, \nu_A^c, A = 1, 2, 3$. The relevant superpotential is then [16, 17, 19, 20, 23]

$$W = 2\sqrt{2}(h_{AB}h_1 - 2\sqrt{3}f_{AB}h_2 - g_{AB}(h_5 + i\sqrt{3}h_6)) + \bar{h}^T \mathcal{H}(\langle \Omega \rangle) h + 4\sqrt{2}f_{AB}\bar{\sigma}\bar{\nu}_A\bar{\nu}_B + W_\Omega(\Omega) \quad (7.2)$$

where

$$W_\Omega(\Omega) = m(p^2 + 3a^2 + 6\omega^2) + 2\lambda(a^3 + 3p\omega^2) + (M + \eta(p + 3a - 6\omega))\sigma\bar{\sigma} \quad (7.3)$$

and

$$\frac{\partial W_\Omega}{\partial \Omega}|_{h, \bar{\nu}, L=0} = 0 \quad D_\alpha(\Omega)|_{h, \bar{\nu}, L=0} = 0 \quad (7.4)$$

Here h_{AB}, f_{AB}, g_{AB} are the usual Yukawa coupling matrices of the three matter 16-plets to the **10**, **120**, $\overline{\mathbf{126}}$ Higgs multiplets in NMSGUT. Equation (7.4) represents the MSGUT vacuum [16, 17, 19, 20, 23]. Out of the 5 diagonal D-terms of SO(10) the charge and color neutral vevs for Ω and ν, ν^c, h_0 correspond to breaking of the generators $T_{3L}, T_{3R}, B - L$. The vevs Ω do not contribute to the D terms for their generators, so their values are

$$D_{3L} = \frac{g_u}{2} \left(- \sum_{i=1}^6 |h_{i0}|^2 + \sum_A |\tilde{\nu}_A|^2 \right) \quad (7.5)$$

$$D_{3R} = \frac{g_u}{2} \left(\sum_{i=1}^6 |h_{i0}|^2 - 2|h_{40}|^2 - \sum_A |\tilde{\nu}_A|^2 \right) \quad (7.6)$$

$$D_{B-L} = \sqrt{\frac{3}{8}} g_u \left(\sum_A (|\tilde{\nu}_A| - |\bar{\nu}_A|^2) + 2|h_{40}|^2 \right) \quad (7.7)$$

Where from [16, 17, 19, 20, 23] only $h_{4\alpha} = \Phi_{2\alpha}^{44}$ has $B-L = +2, T_{3R} = -1/2$ and thus $T_{3L} = 1/2$ while all others have $T_{3R} = 1/2$ and $B-L = 0$. g_u is the SO(10) gauge coupling in the standard unitary normalization. Thus the D-flatness conditions give

$$\sum_A |\tilde{\nu}_A|^2 = \sum_i |h_{i0}^2| = \sum_A |\bar{\nu}_A|^2 + 2|h_{40}|^2 \quad (7.8)$$

We know from the previous discussion that in MSGUTs the MSSM Higgs doublet pair is defined by fine tuning $Det(\mathcal{H}) \simeq 0$ so that its lightest eigenvalue $\mu \sim 1 - 100$ TeV specifies the μ term in the superpotential of the SIMSSM : $W = \mu \bar{H}H + \dots$ Here the doublet pair H, \bar{H} is a linear combination [16, 17, 19, 20, 23] of the 6 doublet pairs of the NMSGUT:

$$h_i = U_{ij} H_j \quad \bar{h}_i = \bar{U}_{ij} \bar{H}_j \quad (7.9)$$

where U, \bar{U} are the unitary matrices that diagonalize the doublet mass matrix \mathcal{H} such that $\bar{U} \mathcal{H} U = \text{Diag}\{\mu, M_2^H, \dots, M_6^H\}$. To obtain the tree level Yukawa couplings replace $h_i, \bar{h}_i \rightarrow \alpha_i H, \bar{\alpha}_i \bar{H}$ in the GUT Higgs doublets (h_i, \bar{h}_i) couplings to the matter fermions of the SIMSSM. Thus in particular the neutrino Dirac coupling is

$$y_{AB}^\nu = \tilde{h}_{AB} \alpha_1 - 2\sqrt{3} \tilde{f}_{AB} \alpha_2 - \tilde{g}_{AB} (\alpha_5 + i\sqrt{3} \alpha_6) \quad (7.10)$$

Here $((\tilde{h}_{AB}, \tilde{g}_{AB}, \tilde{f}_{AB}) = 2\sqrt{2}(h_{AB}, g_{AB}, f_{AB}))$ We assumed that only light Higgs doublets will contribute to inflaton flat direction since from the $|F_{\tilde{h}}|^2$ terms of the potential it is evident that the involvement of any other Higgs doublet would lead to GUT scale rather than conjugate neutrino scale mass for the inflaton. Also only one generation of sneutrinos ν_A and conjugate sneutrinos $\bar{\nu}_B$ contribute to the inflaton flat direction with $A \neq B$. In view of the tight upper bounds on the fermion Yukawas

(see eqn.(5.22)) we need to involve the lightest generation of sfermion. Thus we take $\nu_A = \nu_1$. On the other hand we take $\nu_A^c = \nu_3^c$ to satisfy the fine tuning condition. So the ansatz for the inflaton flat direction is

$$\tilde{\nu}_1 = \frac{\phi}{\sqrt{3-2|\alpha_4|^2}} \quad H_1^0 = \frac{\phi}{\sqrt{3-2|\alpha_4|^2}} \quad \tilde{\nu}_3 = \frac{\phi\sqrt{1-2|\alpha_4|^2}}{\sqrt{3-2|\alpha_4|^2}} \quad (7.11)$$

Now the F-term potential corresponding to fields under consideration is

$$\begin{aligned} V_{hard} = & [(y^{\nu\dagger}y^\nu)_{11} + \Gamma(|\tilde{h}_{31}|^2 + 4|\tilde{g}_{31}|^2 + (y^\nu y^{\nu\dagger})_{33}) + 4|\tilde{f}_{33}|^2\Gamma^2] \frac{|\phi|^4}{9} \\ & + \frac{8}{3\sqrt{3}}\tilde{f}_{33}|y_{31}^\nu||\bar{\sigma}|\sqrt{\Gamma}\text{Cos}(\theta_\phi + \theta_{y_{31}^\nu} - \theta_{\bar{\sigma}})|\phi|^3 + \\ & \left(\frac{|\mu|^2}{3} + \frac{16}{3}|\tilde{f}_{33}|^2|\bar{\sigma}|^2\Gamma\right)|\phi|^2 \end{aligned} \quad (7.12)$$

Here $\Gamma = 1 - 2|\alpha_4|^2$. The corresponding Supergravity(SUGRA)-NUHM type soft terms in terms of a common trilinear parameter A_0 but different soft mass parameters $\tilde{m}_{\tilde{f}}^2, \tilde{m}_{h_i}^2$ for the 16 plets and the different Higgs is given as

$$\begin{aligned} V_{soft} = & A_0W + c.c. + \tilde{m}_{16}^2|\tilde{\Psi}|^2 + \sum_i \tilde{m}_{h_i}^2|h_i|^2 \\ = & 2A_0\sqrt{\Gamma}|y_{31}^\nu|\frac{|\phi|^3}{3\sqrt{3}}\text{Cos}(3\theta_\phi + \theta_{y_{31}^\nu}) + \frac{4}{3}A_0\tilde{f}_{33}|\bar{\sigma}|\Gamma|\phi|^2\text{Cos}(2\theta_\phi + \theta_{\bar{\sigma}}) \\ & + (\hat{m}_0^2 - \frac{|\mu|^2}{3})|\phi|^2 \end{aligned} \quad (7.13)$$

where

$$\hat{m}_0^2 = \frac{\tilde{m}_{16}^2}{3}(1 + \Gamma) + \sum_i \frac{\tilde{m}_{h_i}^2|\alpha_i|^2}{3} + \frac{|\mu|^2}{3} \quad (7.14)$$

Since $\tilde{m}_{16}, \tilde{m}_{h_i}, A_0$ are all $\sim O(M_S)$, so $f_{33}|\bar{\sigma}| \gg M_S$. It implies that the phase θ_ϕ can be fixed by minimizing the term in V_{hard} :

$$\theta_\phi = \pi + \theta_{\bar{\sigma}} - \theta_{y_{31}^\nu} \quad (7.15)$$

We assume that θ_ϕ is fixed at this value. Since the inflationary dynamics is at large values of $|\phi|$ and θ_ϕ is fixed so we can work with a real field ϕ . Now adding the hard and soft potentials and then comparing with the generic renormalizable inflaton potential, we can identify the parameters (M, h, A) . However for simplicity we can drop the soft term contribution (in trilinear and quadratic terms) since they play a negligible role in fine tuning and inflaton mass being completely determined by $m_{\nu c} \geq 10^6$ GeV. Inflation parameters can be deduced from superpotential:

$$h = \frac{2\sqrt{3}}{(3 - 2|\alpha_4|^2)} [(y^{\nu\dagger} y^\nu)_{11} + (|\tilde{h}_{31}|^2 + 4|\tilde{g}_{31}|^2 + (y^\nu y^{\nu\dagger})_{33})\Gamma + 4|\tilde{f}_{33}|^2\Gamma^2]^{\frac{1}{2}} \quad (7.16)$$

$$A = \frac{48\sqrt{3}|\tilde{f}_{33}||y_{31}^\nu||\bar{\sigma}|\sqrt{\Gamma}}{h(3 - 2|\alpha_4|^2)^{\frac{3}{2}}} \quad (7.17)$$

$$M^2 = 32|\tilde{f}_{33}|^2|\bar{\sigma}|^2 \frac{\Gamma}{(3 - 2|\alpha_4|^2)} + 2\mu^2 \quad (7.18)$$

The fine tuning condition is now determined to be:

$$\begin{aligned} |y_{31}^\nu|^2 &= \frac{8}{1 - 8\Gamma} (\Gamma(|\tilde{h}_{31}|^2 + 4|\tilde{g}_{31}|^2 + |y_{32}^\nu|^2 + |y_{33}^\nu|^2) \\ &\quad + |y_{11}^\nu|^2 + |y_{21}^\nu|^2 + 4|\tilde{f}_{33}|^2\Gamma^2) \end{aligned} \quad (7.19)$$

If we tune

$$\Gamma \approx 0 \quad \text{i.e} \quad |\alpha_4| = \frac{1}{\sqrt{2}} \quad (7.20)$$

then it may be possible to satisfy it to a good accuracy. This means that the MSSM doublet H is almost exactly 50% derived from the doublet in the 210 plet ! If this condition can be achieved the remaining tuning condition is only

$$|y_{31}^\nu|^2 = 8(|y_{11}^\nu|^2 + |y_{21}^\nu|^2) \quad (7.21)$$

We found that this fine tuning condition is achievable in NMSGUT along fermion fitting. But to achieve the required number of efolds, the stringent condition [31] on quartic coupling and inflaton Mass $\frac{h^2}{M} \sim (y^{\nu\dagger} y^\nu)_{11}/M_3 \approx 10^{-25}$ is quite hard to

satisfy. In the present case the third generation right handed sneutrino mass $\sim |f_{33}|\bar{\sigma}|$ determines the inflaton mass. In Table 7.1 we have given the important

Parameter	Value
h	2.44×10^{-4}
M	$3.043 \times 10^{11} GeV$
Δ	10^{-2}
Γ	4.343×10^{-5}
$M_3^{\nu^c}$	$4.86 \times 10^{13} GeV$
$Log_{10}(h^2/M)$	$-18.706 GeV^{-1}$
N_{CMB}	4.78×10^{-4}

Table 7.1: Set of inflation parameters from [31].

set of inflation parameters from the table given in [31]. The third generation right handed neutrino mass comes out to be $\sim 10^{13} GeV$ and inflaton mass is $\sim 10^{11} GeV$. The value of quartic coupling in eq(7.16) is controlled by the second and third terms since they are the largest ($O(10^{-3})$) [27]. However we can lower them with the help of factor $\Gamma \approx 0$. Then the controlling term will be the first one ($(y^{\nu^\dagger} y^\nu)_{11}$). But the same factor appears in the formula for inflaton mass Eqn.(7.18) (determined by Majorana mass term ($\sim |f_{33}|\bar{\sigma}|$) for 3rd generation right handed neutrino), so it will reduce the value of M (from $O(10^{13} GeV)$ to $O(10^{11} GeV)$). Corresponding to this value of M we need quartic coupling $O(10^{-7})$ and $\Delta \approx 10^{-6}$ (approximated using eqn. (5.22)). But the actual value of quartic coupling as well as fine-tuning parameter is quite large as compared to the required values. Hence it results in a very small value of $N_{CMB} \sim 10^{-4}$. So this simple embedding of SSI in NMSGUT doesn't work.

7.3 BICEP2 experiment

BICEP2 is a telescope mounted at the south pole for background imaging of cosmic extragalactic polarization. This experiment is specially designed to detect the signal of primordial gravitational waves. The gravitational waves active during the inflationary epoch produce polarization in cosmic background radiation. They leave

their imprint on the CMB in terms of a curl or rotation which is known as primordial B-mode polarization or tensor component. However this type of polarization can also be produced via gravitational lensing and foreground dust (non-primordial B-mode polarization detected by South pole telescope (SPT) [99]). Scalar density fluctuations also produce polarization in CMB known as E-mode polarization or scalar component. The difference in two modes cannot be detected simply by looking at the variation of CMB temperature. Moreover the B-mode is weaker than E-mode and thus difficult to detect. However certain angles in polarization can be measured and allow one to distinguish between the two modes. The BICEP2 experiment claimed to measure this difference and has given their results in terms of tensor to scalar component ratio $r = .2_{-.05}^{+.07}$ at 3σ [66] level. They also discarded the possibility of $r=0$ at 7σ level. The central value (0.2) of r is quite large as compared to those found by WMAP [65] and PLANCK [98]. However the contamination of the polarization data by foreground dust may not have been correctly accounted for which can reduce this value. So to confirm the results great scrutiny is required. If BICEP2 results are confirmed, it will be a big blow to a huge class of inflationary models and start a new era of modern cosmology. The PLANCK collaboration will report on this issue soon using their original data on the foreground dust.

7.4 Generic renormalizable inflation potential without fine tuning

The GUT scale of inflation doesn't require fine tuned flat potential. Also for the inflaton mass $\geq 10^{13}$ GeV the analysis done in chapter 5 does not hold. So first we will find out the condition on inflation parameters of generic renormalizable potential for slow roll inflation without any fine tuning. The general renormalizable inflationary potential is :

$$V(\phi) = M^2 \frac{\phi^2}{2} - \frac{Ah}{6\sqrt{3}} \phi^3 + h^4 \frac{\phi^4}{12} \quad (7.22)$$

Here M, A, h are real without loss of generality. It's dimensionless form

$$\tilde{V} = \frac{V}{V_0} = \frac{x^2}{2} - \frac{\tilde{A}x^3}{6\sqrt{3}} + \frac{x^4}{12} \quad (7.23)$$

where $x = \frac{\phi}{\phi_0}$, $V_0 = \frac{M^4}{h^2}$, $\tilde{A} = \frac{A}{M}$ and $\phi_0 = \frac{M}{h}$ is inflaton vev is more convenient for numerical work.

If we define a new parameter $\omega = \frac{M}{hM_{Pl}}$, then for a given potential the slow roll parameters ϵ and η are given by:

$$\epsilon = \frac{\tilde{V}_x^2}{2\omega^2\tilde{V}}; \quad \eta = \frac{\tilde{V}_{xx}}{\omega^2\tilde{V}} \quad (7.24)$$

Where $M_{Pl} = 2.43 \times 10^{18}$ GeV. The slow roll inflation formula for Power spectrum, spectral index and tensor to scalar ratio are given by:

$$P_R = \frac{\omega^4 h^2 \tilde{V}}{24\pi^2 \epsilon}; \quad n_s = 1 + 2\eta - 6\epsilon; \quad r = 16\epsilon \quad (7.25)$$

The values for Power spectrum, spectral index given by PLANCK [98] are

$$P_R = (2.1977 \pm .103) \times 10^{-9}; \quad n_s = .958 \pm .008 \quad (7.26)$$

and BICEP2 value [66] for tensor to scalar ratio, r

$$r = 0.2_{-.05}^{+.07} \quad (7.27)$$

The number of e-folds of inflation remaining when pivot scale crosses the horizon can be found from equation of motion of inflaton field

$$N = \omega^2 \int_{x_{cmb}}^{x_{end}} \frac{\tilde{V}}{\tilde{V}_x} dx \quad (7.28)$$

Integrating this equation gives

$$N = \frac{\omega^2}{128}(-3(\tilde{A}^2 - 16) \log(-3\tilde{A}x + 4x^2 + 12) - \frac{2\tilde{A}(3\tilde{A}^2 - 80) \tan^{-1}\left(\frac{3\tilde{A}-8x}{\sqrt{192-9\tilde{A}^2}}\right)}{\sqrt{\frac{64}{3} - \tilde{A}^2}} + 8x(2x - \tilde{A})) \Bigg|_{x_{cmb}}^{x_{end}} \quad (7.29)$$

Now we need to find the viable parameter values of M , h and \tilde{A} to achieve values given in equation (7.26) and $N_{efolds} \approx 50$. The procedure we follow is:

1. Take some value of r and n_s in the allowed range given by Eqn. (7.26).
2. Calculate the value of ϵ and η by Eqns. (7.25).
3. Then define a ratio $\theta = \eta/\epsilon$ and solve for x . It gives one real root for x which we take as x_{cmb} (Note that it does not give real root for whole range of values given in (7.26))
4. Then the field value (x_{end}) is calculated from $\eta \approx 0.8$.
5. Throwing the values of M, h, A we calculate the value of $P_R, V_0^{1/4}$ and $N_{e-folds}$.

In figures 7.1-7.4 we have shown contour plots between quartic coupling h and number of efolds with contour lines bearing constant value of ω . We have kept the value of $r=.2$ fixed and three set of values of spectral index $n_s=0.954, 0.958, 0.962$. So each figure contains three contour plots. For each figure we vary the trilinear term parameter \tilde{A} over the values(.1,.01,.001, 0). We accepted only those values of M and h for which the value of P_R falls in range $(1.0947-1.3007) \times 10^{-9}$ and the value of $V_0^{1/4}$ as given by Eqn. (7.1). By comparing Figures 7.1,7.2, parameter \tilde{A} has only a small effect: when we change \tilde{A} from .1 to .01, the plots shift little bit towards higher values of N_{CMB} . However reducing \tilde{A} further doesn't make any difference. For $n_s=.962$, we need $h \sim 10^{-6.1}$ and $\omega \approx 9$ to have $N_{efolds} \approx 50$. This corresponds to inflaton mass of order $10^{13.1}$ GeV. For $n_s=.958$, to achieve $N_{efolds} \approx 50$ we need smaller $h \sim 10^{-6.35}$ and $\omega \approx 15$. For $n_s=.954$, the required quartic

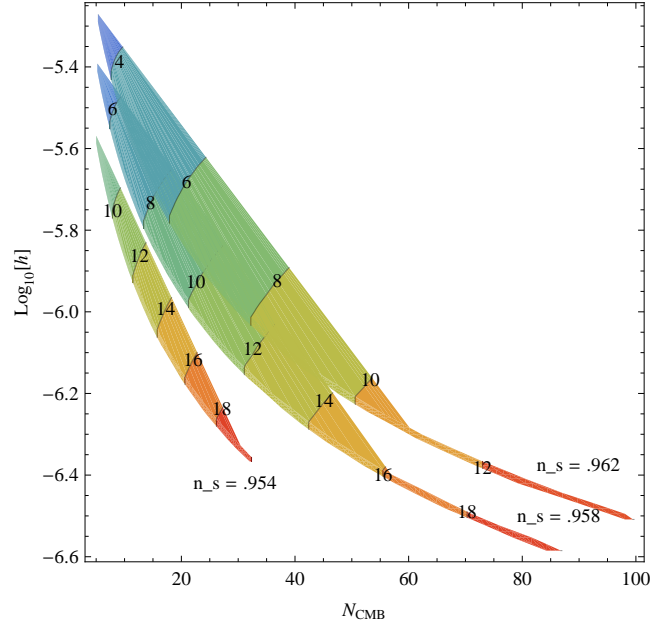


Figure 7.1: Plot of quartic coupling h and Number of e-folds for different values of ω at trilinear dimensionless parameter $\tilde{A}=1$. The contour line bears the constant value of ω and different colors of contour represent a range for ω . As we move towards higher values of ω number of e-folds increases and quartic coupling decreases.

coupling is less than $10^{-6.4}$ and ω more than 20. These estimates thus provide a revised rule of thumb replacing the rule $h^2 \sim 10^{-25}(M/GeV)$ derived earlier in the fine tuned case. Note that ω is controlled by M/h so that for $\omega \approx 20$, $h \approx 10^{-6.35}$ corresponds to $M \approx 10^{13.1}$ GeV and $h^2/M \sim 10^{-26} GeV^{-1}$. Which is about an order of magnitude smaller than for $M \ll 10^{13}$ GeV.

7.5 NMSGUT inflation after BICEP2

In Section 7.3 we assumed that only the light Higgs will contribute to inflaton flat direction so as to keep $M < 10^{13}$ GeV. With M allowed to be large the 5 heavy Higgs pair with GUT scale masses in the NMSGUT can also be allowed to contribute i.e. the strong condition that only the light Higgs corresponding to MSSM contributes to the inflaton condensate can be relaxed. So in this case the heavy Higgs having masses $O(10^{16}$ GEV) will control the mass of the inflaton. Also no assumption

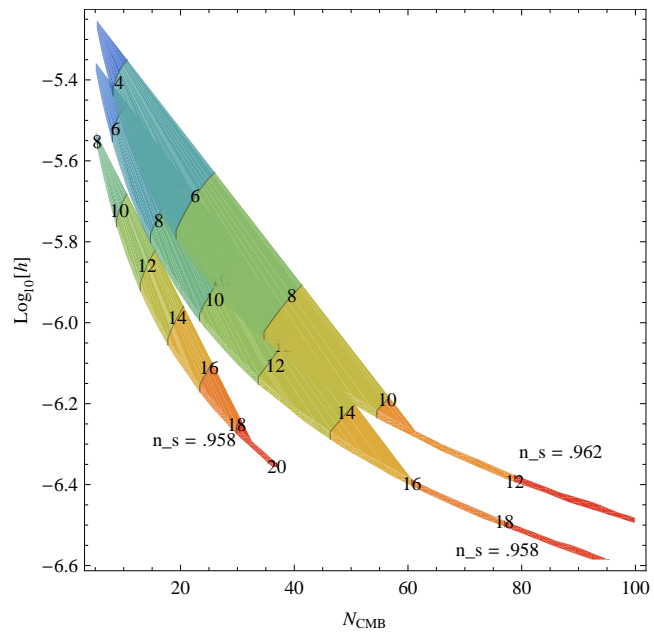


Figure 7.2: Same as figure 7.1 with $\tilde{A}=.01$

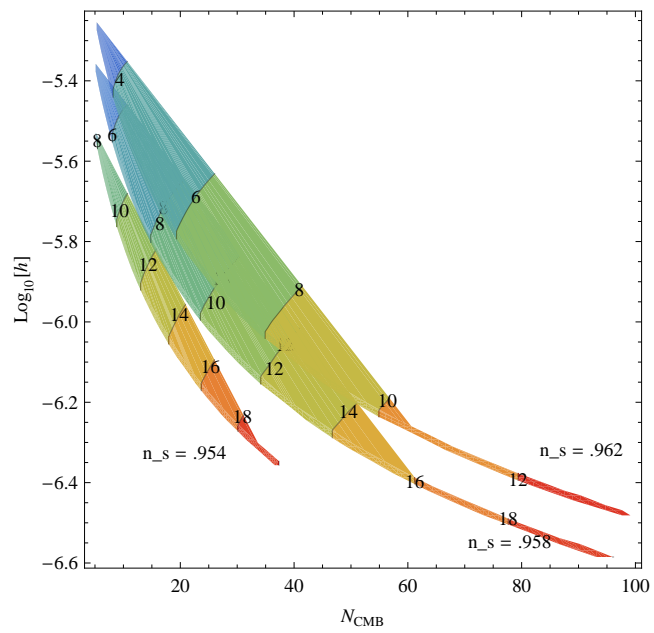
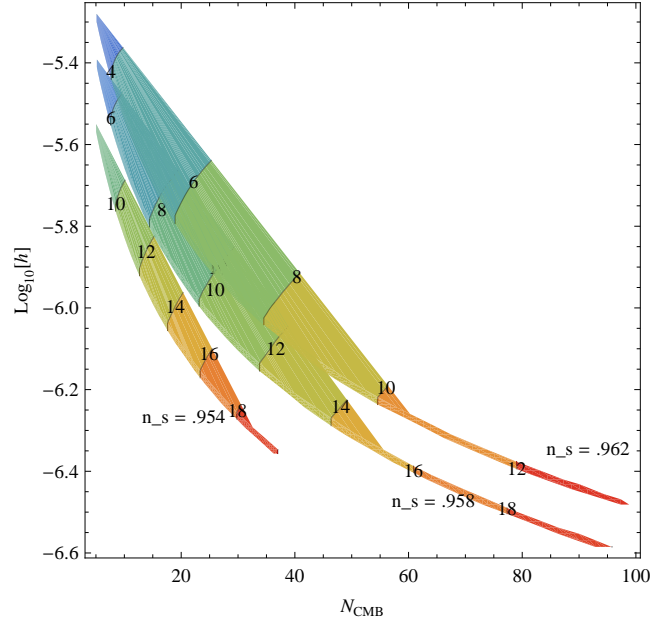


Figure 7.3: Same as figure 7.1 with $\tilde{A}=.001$

Figure 7.4: Same as figure 7.1 with $\tilde{A}=0$

on family index for s-fermion components of inflaton is made. Our new ansatz for inflaton is

$$\tilde{\nu}_A = b_A \frac{\phi}{\sqrt{3}} ; \tilde{\nu}_A = c_A \frac{\phi}{\sqrt{3}} ; h_l = U_{lm} H_m = U_{lm} a_m \frac{\phi}{\sqrt{3}} \quad (7.30)$$

Here $A=1,2,3$ (family index) and $l, m =1-6$ (types of different Higgs). The parameters b_A , c_A and a_m are complex numbers which decide the fraction each field contributes to the inflaton. From D-flatness condition we have

$$\sum_A |c_A|^2 = \sum_l |a_l|^2 = \sum_A |b_A|^2 + \sum_l 2|U_{4l} a_l|^2 \quad (7.31)$$

To achieve canonically normalized kinetic term for inflaton field we need:

$$\sum_A |b_A|^2 + \sum_A |c_A|^2 + \sum_l |a_l|^2 = 1 \quad (7.32)$$

And this can be achieved in this scenario in the following way:

$$\sum_A |b_A|^2 = \sum_A |c_A|^2 = \sum_l |a_m|^2 = \frac{1}{3} \quad (7.33)$$

With $\sum_l U_{4l} a_l = 0$. Now y^ν is replaced by this new matrix given by

$$Z_{AB} = \tilde{h}_{AB} V_{1l} a_l - 2\sqrt{3} \tilde{f}_{AB} V_{2l} a_l - \tilde{g}_{AB} (V_{5l} a_l + i\sqrt{3} V_{6l} a_l) \quad (7.34)$$

The inflation parameters are given by

$$h^2 = \frac{4}{3} (|b_A \tilde{h}_{AB} c_B|^2 + 12 |b_A \tilde{f}_{AB} c_B|^2 + 4 |b_A \tilde{g}_{AB} c_B|^2 + |b_A Z_{AB}|^2 + 4 |b_A \tilde{f}_{AB} b_B|^2 + |Z_{AB} c_B|^2) \quad (7.35)$$

$$M^2 = \frac{32}{3} |\tilde{f}_{AB} b_B|^2 |\bar{\sigma}|^2 + \frac{2}{3} |a_l|^2 m_{H_l}^2 \quad (7.36)$$

$$A = \frac{16}{h} |c_A^* Z_{AB}^\dagger \tilde{f}_{BC} b_C \bar{\sigma}| \quad (7.37)$$

Now we throw the $24=6(b_A)+6(c_A)+12(a_m)$ real numbers randomly along with 38 parameters of NMSGUT superpotential at M_X while fitting. The dimensionality of space in which our search engine will look for the solution is thus 62. The basic idea is that there can be an interplay between b_A, c_A, a_m and SO(10) Yukawas h_{AB}, f_{AB}, g_{AB} such that they can give us small quartic coupling $h \sim 10^{-6.1}$ or less required for 50 e-folds along with fermion fitting. Also the mass of inflaton of $O(10^{13} \text{ GeV})$ can be achieved with heavy higgs fields of GUT scale masses. An important point worth mentioning is that GUT scale threshold corrections which lower the required SO(10) Yukawas so much that $\Gamma_{d=5}^{\Delta B \neq 0}$ is suppressed to less than 10^{-34} yrs will also control the quartic coupling $h \sim 10^{-6.3}$. In this way NMSGUT may connect the Baryon stability with the primordial inflation.

7.6 Details of Example Fit With Inflation Parameters

With these new formulas we tried to find a good fermion fit along with sufficient inflation. In Appendix A we give the complete set of tables. In Table (7.2) we quote the inflation parameters. We are able to achieve quartic coupling value $h=1.78 \times 10^{-5}$

and $N_{efolds} \approx 1$. Note that this is an improvement over our earlier attempt by a factor of 10^4 . The quartic coupling as well as the mass of inflaton is somewhat larger than required for successful inflation. The value of ω (≈ 2) achieved is still smaller than required. The rest of the parameters are in an acceptable range.

However the search for inflation conditions along with fermion fitting led us to completely new kind of NMSGUT fitting solution! We provide an example fermion fit in Tables (7.3-7.8). If we look at Table (7.3) the value of $\tan\beta=2.58$ (which we didn't keep fixed but threw randomly along with soft parameters) given along with the soft Susy breaking parameters at scale M_X is quite small. NMSGUT was never hitherto able to achieve fitting with small $\tan\beta$! This accidental discovery motivates new searches for low $\tan\beta$ solutions in NMSGUT. If we switch off the inflation penalties then it should be easier to find solutions. The play of GUT scale thresholds [29] might be responsible for such type of behavior as they were not applied before [27]. Along with it one of the Higgs mass square parameter $M_H^2=7.0208 \times 10^{10} GeV^2$ comes out positive, which is also a new feature. It results into the more commonly encountered inverted s-fermion hierarchy given in Table (7.5). It is notable that all the s-particles are still very heavy of $O(100 \text{ TeV})$. The rest of the features are already explained in Chapter 3.

7.7 Conclusions and discussion

In the present scenario of inflation in NMSGUT we can achieve $M = 10^{13.0-13.2}$ GeV. The quartic coupling $h^2 = 10^{-12.2} - 10^{-12.7}$ seems harder to achieve but not impossible. Because to search in such a high dimensional parameter space one needs patience for running of code for months. For such a large value of inflaton mass the trilinear term comes out to be very small and plays a minor role. Thus one can even drop that term from inflation potential. Super Planckian vev defined in terms of parameter $\omega = \frac{\phi_0}{M_{pl}} \sim 15$ is required to achieve sufficient e-folds. However in NMSGUT the number of e-folds increased from 10^{-4} to 1 but is still not realistic. The BICEP2 results favor inflation at GUT scale and if BICEP2 results stand scrutiny then

NMSGUT can be a desirable candidate to explain inflation. Apart from SSI inflation, NMSGUT superpotential can have many other flat directions along which inflation can take place to evaluate which a detailed study is required. One needs to explore the NMSGUT potential to study evolution with different field configurations. An important conclusion that comes out from this study is that fitting of fermion data is possible in NMSGUT even with small $\tan\beta \approx 2.5$. It implies that NMSGUT is viable on the entire range of $\tan\beta$, thus overturning some assumptions of our previous work [27–29].

7.8 Appendix A

Inflation Parameter	Value
M	$7.8826 \times 10^{13} GeV$
h	1.7736×10^{-5}
N_{efolds}	.73
ϵ	1.25×10^{-2}
η	1.85×10^{-2}
n_s	.962
P_R	2.1977×10^{-9}
r	.20
A_0	1.277×10^{-4}
$V_0^{1/4}$	$2.1825 \times 10^{16} GeV$
ω	1.82
$ a_m $	0.999, 4.295×10^{-2} , 6.287×10^{-4} , 3.049×10^{-4} , 2.752×10^{-4} , 5.439×10^{-5}
$ b_A $	0.999, 3.601×10^{-2} , 4.119×10^{-3}
$ c_A $	0.999, 4.325×10^{-2} , 3.209×10^{-3}

Table 7.2: Inflation parameters along with parameters b_A, c_A, a_m . Note that $|b_1|, |c_1|, |a_1| \approx 1$, and rest are very small.

Parameter	Value	Field [SU(3), SU(2), Y]	Masses (Units of 10^{16} GeV)
χ_X	0.98	$A[1, 1, 4]$	0.69
χ_Z	0.40	$B[6, 2, 5/3]$	0.05
$h_{11}/10^{-6}$	-5.49	$C[8, 2, 1]$	0.78, 3.55, 4.33
$h_{22}/10^{-4}$	4.45	$D[3, 2, 7/3]$	0.35, 4.02, 5.10
h_{33}	-0.02	$E[3, 2, 1/3]$	0.05, 0.51, 1.64
$f_{11}/10^{-6}$	$0.05 - 0.03i$		1.6, 3.41, 4.61
$f_{12}/10^{-6}$	$-2.51 - 0.86i$	$F[1, 1, 2]$	0.03, 0.33
$f_{13}/10^{-5}$	$0.15 - 0.095i$		0.33, 1.98
$f_{22}/10^{-5}$	$5.17 + 5.76i$	$G[1, 1, 0]$	0.02, 0.12, 0.43
$f_{23}/10^{-4}$	$-1.23 + 1.05i$		0.44, 0.44, 0.51
$f_{33}/10^{-3}$	$-0.42 - 0.24i$	$h[1, 2, 1]$	0.22, 1.21, 3.68
$g_{12}/10^{-4}$	$0.11 - 0.06i$		4.38, 18.50
$g_{13}/10^{-5}$	$1.79 + 4.67i$	$I[3, 1, 10/3]$	0.22
$g_{23}/10^{-4}$	$-0.93 - 0.02i$	$J[3, 1, 4/3]$	0.19, 0.28, 0.80
$\lambda/10^{-2}$	$-4.38 - 1.01i$		0.80, 2.76
η	$-0.26 - 0.04i$	$K[3, 1, 8/3]$	0.95, 2.69
ρ	$1.08 - 0.38i$	$L[6, 1, 2/3]$	0.97, 1.28
k	$0.25 - 0.03i$	$M[6, 1, 8/3]$	1.16
ζ	$1.08 + 1.11i$	$N[6, 1, 4/3]$	1.11
$\bar{\zeta}$	$-0.03 + 0.65i$	$O[1, 3, 2]$	2.07
$m/10^{16} GeV$	0.005	$P[3, 3, 2/3]$	0.16, 2.65
$m_\Theta/10^{16} GeV$	$-1.11e^{-iArg(\lambda)}$	$Q[8, 3, 0]$	0.20
γ	0.20	$R[8, 1, 0]$	0.05, 0.22
$\bar{\gamma}$	-4.05	$S[1, 3, 0]$	0.25
x	$0.85 + 0.41i$	$t[3, 1, 2/3]$	0.20, 0.75, 0.99, 1.91
$\Delta_X^{tot}, \Delta_X^{GUT}$	0.86, 0.93		3.13, 4.28, 21.76
$\Delta_G^{tot}, \Delta_G^{GUT}$	-19.96, -24.02	$U[3, 3, 4/3]$	0.23
$\Delta\alpha_3^{tot}(M_Z), \Delta\alpha_3^{GUT}(M_Z)$	-0.012, 0.002	$V[1, 2, 3]$	0.14
$\{M^{\nu^c}/10^{12} GeV\}$	0.004271, 1.02, 18.34	$W[6, 3, 2/3]$	1.93
$\{M_{II}^\nu/10^{-8} eV\}$.025, 6.03, 108.54	$X[3, 2, 5/3]$	0.05, 1.77, 1.77
$M_\nu(meV)$	2.29, 7.21, 38.59	$Y[6, 2, 1/3]$	0.06
$\{Evals[f]\}/10^{-6}$	0.13, 29.93, 538.95	$Z[8, 1, 2]$	0.22
Soft parameters at M_X	$m_{\frac{1}{2}} = 0.000$ $\mu = 1.53 \times 10^5$ $M_H^2 = -5.47 \times 10^{10}$	$m_0 = 278926.8$ $B = -2.68 \times 10^{10}$ $M_H^2 = 7.02 \times 10^{10}$	$A_0 = -6.74 \times 10^5$ $\tan\beta = 2.5842$ $R_{\frac{b\tau}{s\mu}} = 7.9039$
$Max(L_{ABCD} , R_{ABCD})$	$5.95 \times 10^{-22} GeV^{-1}$		
Susy contribution to $\Delta_{X,G,3}$	$\Delta_X^{Susy} = -0.07$	$\Delta_G^{Susy} = 4.05$	$\Delta\alpha_3^{Susy} = -0.014$

Table 7.3: Fit : Column 1 contains values of the NMSGUT-SUGRY-NUHM parameters at M_X derived from an accurate fit to all 18 fermion data and compatible with RG constraints. Unification parameters and mass spectrum of superheavy and superlight fields are also given. The values of $\mu(M_X)$, $B(M_X)$ are determined by RG evolution from M_Z to M_X of the values determined by the EWRSB conditions.

Parameter	Target = \bar{O}_i	Uncert. = δ_i	Achieved = O_i	Pull = $\frac{(O_i - \bar{O}_i)}{\delta_i}$
$y_u/10^{-6}$	2.054931	0.784984	2.049459	-0.006971
$y_c/10^{-3}$	1.001645	0.165271	0.971159	-0.184458
y_t	0.348829	0.013953	0.350779	0.139806
$y_d/10^{-5}$	1.120978	0.653530	0.788682	-0.508463
$y_s/10^{-3}$	0.212620	0.100356	0.186201	-0.263246
y_b	0.012296	0.006381	0.013778	0.232372
$y_e/10^{-4}$	0.053871	0.008081	0.053091	-0.096439
$y_\mu/10^{-2}$	0.113725	0.017059	0.109655	-0.238555
y_τ	0.019341	0.003675	0.020974	0.444360
$\sin \theta_{12}^q$	0.2210	0.001600	0.2210	0.0045
$\sin \theta_{13}^q/10^{-4}$	31.7661	5.000000	31.9197	0.0307
$\sin \theta_{23}^q/10^{-3}$	37.3725	1.300000	37.3109	-0.0474
δ^q	60.0259	14.000000	59.9487	-0.0055
$(m_{12}^2)/10^{-5}(eV)^2$	4.6513	0.493035	4.6699	0.0378
$(m_{23}^2)/10^{-3}(eV)^2$	1.4536	0.290712	1.4369	-0.0573
$\sin^2 \theta_{12}^L$	0.2999	0.059990	0.3001	0.0017
$\sin^2 \theta_{23}^L$	0.5002	0.150065	0.4875	-0.0844
$\sin^2 \theta_{13}^L$	0.0286	0.019000	0.0190	-0.5077
<i>Eigenvalues</i> ($Z_{\bar{u}}$)	0.945693	0.946064	0.946065	
<i>Eigenvalues</i> ($Z_{\bar{d}}$)	0.939238	0.939606	0.939607	
<i>Eigenvalues</i> ($Z_{\bar{\nu}}$)	0.907891	0.908263	0.908264	
<i>Eigenvalues</i> ($Z_{\bar{e}}$)	0.927277	0.927638	0.927640	
<i>Eigenvalues</i> (Z_Q)	0.960652	0.961036	0.961036	
<i>Eigenvalues</i> (Z_L)	0.935785	0.936151	0.936152	
$Z_{\bar{H}}, Z_H$	0.112304	0.000850		
α_1	0.176 + 0.000 <i>i</i>	$\bar{\alpha}_1$	0.078 + 0.0000 <i>i</i>	
α_2	-0.676 - 0.535 <i>i</i>	$\bar{\alpha}_2$	-0.409 - 0.125 <i>i</i>	
α_3	-0.048 - 0.376 <i>i</i>	$\bar{\alpha}_3$	-0.290 - 0.269 <i>i</i>	
α_4	0.006 + 0.042 <i>i</i>	$\bar{\alpha}_4$	0.517 + 0.527 <i>i</i>	
α_5	0.088 + 0.068 <i>i</i>	$\bar{\alpha}_5$	0.166 - 0.283 <i>i</i>	
α_6	-0.044 - 0.259 <i>i</i>	$\bar{\alpha}_6$	-0.003 - 0.071 <i>i</i>	

Table 7.4: Fit with $\chi_X = \sqrt{\sum_{i=1}^{17} (O_i - \bar{O}_i)^2 / \delta_i^2} = 0.9866$. Target values, at M_X of the fermion Yukawa couplings and mixing parameters, together with the estimated uncertainties, achieved values and pulls. The eigenvalues of the wavefunction renormalization increment matrices Z_i for fermion lines and the factors for Higgs lines are given. The Higgs fractions $\alpha_i, \bar{\alpha}_i$ which control the MSSM fermion Yukawa couplings are also given. Right handed neutrino threshold effects have been ignored. We have truncated numbers for display although all calculations are done at double precision.

Parameter	SM(M_Z)	$m^{\text{GUT}}(M_Z)$	$m^{\text{MSSM}} = (m + \Delta m)^{\text{GUT}}(M_Z)$
$m_d/10^{-3}$	2.90000	1.84864	2.23856
$m_s/10^{-3}$	55.00000	43.64483	52.85039
m_b	2.90000	3.01506	3.57003
$m_e/10^{-3}$	0.48657	0.52627	0.52626
m_μ	0.10272	0.10870	0.10869
m_τ	1.74624	2.07812	2.07807
$m_u/10^{-3}$	1.27000	1.02974	1.24699
m_c	0.61900	0.48791	0.59087
m_t	172.50000	143.37063	170.87710

Table 7.5: Values of standard model fermion masses in GeV at M_Z compared with the masses obtained from values of GUT derived Yukawa couplings run down from M_X^0 to M_Z both before and after threshold corrections. Fit with $\chi_Z = \sqrt{\sum_{i=1}^9 (m_i^{\text{MSSM}} - m_i^{\text{SM}})^2 / (m_i^{\text{MSSM}})^2} = 0.4014$.

Parameter	Value	Parameter	Value
M_1	437.38	$M_{\tilde{u}_1}$	278803.51
M_2	1000.00	$M_{\tilde{u}_2}$	278801.41
M_3	2350.15	$M_{\tilde{u}_3}$	25640.30
$M_{\tilde{l}_1}$	265890.12	$A_{11}^{0(l)}$	-673734.44
$M_{\tilde{l}_2}$	265888.42	$A_{22}^{0(l)}$	-673732.79
$M_{\tilde{l}_3}$	265267.68	$A_{33}^{0(l)}$	-673131.35
$M_{\tilde{L}_1}$	283496.59	$A_{11}^{0(u)}$	-482870.96
$M_{\tilde{L}_2}$	283495.79	$A_{22}^{0(u)}$	-482868.74
$M_{\tilde{L}_3}$	283206.48	$A_{33}^{0(u)}$	-295397.84
$M_{\tilde{d}_1}$	266537.97	$A_{11}^{0(d)}$	-675378.37
$M_{\tilde{d}_2}$	266537.84	$A_{22}^{0(d)}$	-675377.52
$M_{\tilde{d}_3}$	266010.83	$A_{33}^{0(d)}$	-612876.05
$M_{\tilde{Q}_1}$	267304.87	$\tan \beta$	2.58
$M_{\tilde{Q}_2}$	267303.72	$\mu(M_Z)$	173486.65
$M_{\tilde{Q}_3}$	182583.24	$B(M_Z)$	3.3063×10^9
$M_{\tilde{H}}^2$	-5.2721×10^{10}	$M_{\tilde{H}}^2$	-5.2812×10^{10}

Table 7.6: Values (GeV) in of the soft Susy parameters at M_Z (evolved from the soft SUGRY-NUHM parameters at M_X). The values of soft Susy parameters at M_Z determine the Susy threshold corrections to the fermion Yukawas. The matching of run down fermion Yukawas in the MSSM to the SM parameters determines soft SUGRY parameters at M_X . Note the heavier third sgeneration. The values of $\mu(M_Z)$ and the corresponding soft Susy parameter $B(M_Z) = m_A^2 \sin 2\beta/2$ are determined by imposing electroweak symmetry breaking conditions. m_A is the mass of the CP odd scalar in the in the Doublet Higgs. The sign of μ is assumed positive.

Field	Mass(GeV)
$M_{\tilde{G}}$	2350.15
M_{χ^\pm}	999.97, 173486.70
M_{χ^0}	437.37, 999.97, 173486.66, 173486.70
$M_{\tilde{\nu}}$	283496.581, 283495.788, 283206.471
$M_{\tilde{e}}$	265890.12, 283496.59, 265888.42, 283495.80, 265267.68, 283206.48
$M_{\tilde{u}}$	267304.86, 278803.51, 267303.71, 278801.40, 25639.07, 182583.52
$M_{\tilde{d}}$	266537.97, 267304.87, 266537.84, 267303.72, 182583.25, 266010.83
M_A	99112.92
M_{H^\pm}	99112.96
M_{H^0}	99112.94
M_{h^0}	125.00

Table 7.7: Spectra of supersymmetric partners calculated ignoring generation mixing effects. Inclusion of such effects changes the spectra only marginally. Due to the large values of μ, B, A_0 the LSP and light chargino are essentially pure Bino and Wino(\tilde{W}_\pm). The light gauginos and light Higgs h^0 , are accompanied by a light smuon and sometimes selectron. The rest of the sfermions have multi-TeV masses. The mini-split supersymmetry spectrum and large μ, A_0 parameters help avoid problems with FCNC and CCB/UFB instability [56]. The sfermion masses are ordered by generation not magnitude. This is useful in understanding the spectrum calculated including generation mixing effects.

Field	Mass(GeV)
$M_{\tilde{G}}$	2352.37
M_{χ^\pm}	1000.91, 173433.06
M_{χ^0}	437.78, 1000.91, 173433.02, 173433.06
$M_{\tilde{\nu}}$	283206.72, 283496.04, 283496.832
$M_{\tilde{e}}$	265267.64, 265888.38, 265890.08, 283206.73, 283496.05, 283496.84
$M_{\tilde{u}}$	25103.10, 182549.16, 267304.28, 267305.88, 278802.29, 278804.40
$M_{\tilde{d}}$	182548.89, 266011.59, 266538.66, 266538.78, 267304.29, 267305.89
M_A	99562.44
M_{H^\pm}	99562.47
M_{H^0}	99562.46
M_{h^0}	124.66

Table 7.8: Spectra of supersymmetric partners calculated including generation mixing effects. Inclusion of such effects changes the spectra only marginally. Due to the large values of μ, B, A_0 the LSP and light chargino are essentially pure Bino and Wino(\tilde{W}_\pm). Note that the ordering of the eigenvalues in this table follows their magnitudes, comparison comparison with the previous table is necessary to identify the sfermions

Chapter 8

Relic Density calculation for Neutralino Dark Matter

8.1 Introduction

The astrophysical evidences of dark matter are well known now a days. From the observations of COBE [64], WMAP [65], PLANCK [98] it is evident that our universe is filled with non baryonic matter other than proton and neutrons. The total matter density of universe is $\Omega_m h^2 \simeq 0.133$ and baryonic density is $\Omega_b h^2 \simeq 0.022$, which implies the $\Omega_{dm} h^2 \simeq 0.11$. The amount of this invisible matter is 4-5 times the visible matter. Although evidence for existence of dark matter is strong, its nature is still unknown. Particle physics should provide some suitable candidate for dark matter and its interactions with Standard Model particles. Dark matter can't be baryonic. The CMB structure that we see today would look different in case of baryonic DM. Also the abundance of light elements during BBN (big bang nucleosynthesis) era gives similar constraints on baryonic content. Another constraint is that DM should be neutral, weakly interacting and massive. DM candidates with masses $\sim 0.1-1$ TeV are popularly known as WIMPs (weakly interacting massive particle) in astro-particle physics terminology. The Standard Model (SM) contains left handed neutrino which is stable and neutral. But WMAP has constrained the

neutrino masses to be $\leq .23$ eV, which gives the $\Omega_\nu h^2 \simeq 0.0072$. So it cannot account for the whole missing matter content. The Minimal Supersymmetric Standard Model (MSSM), an appealing candidate for new physics, provides a suitable WIMP candidate for dark matter namely the lightest supersymmetric particle (LSP). In MSSM the assumed symmetry R-parity (introduced to eliminate the terms in Lagrangian which lead to fast proton decay) makes the LSP stable. We studied the possibility of neutralino as dark matter candidate in context of SO(10) NMSGUT. Since NMSGUT preserves R parity down to weak scale it leads to LSP as suitable candidate for DM. In NMSGUT the LSP is pure Bino. In this chapter we present tests of NMSGUT generated s-spectra by evaluating the associated relic density for LSP. The relic density for LSP is calculated using publicly available package DarkSusy [100].

8.2 Evidences for dark matter

There are many strong and convincing evidences for dark matter from the study of galactic clusters, gravitational lensing and CMB. We briefly review each of these.

8.2.1 Galactic clusters

Jan Oort [101], while observing stellar motions in the galactic neighborhood, calculated the velocities of stars by Doppler Shift. He observed that the galaxies should be three times more massive than the mass of visible matter contained to hold the stars from escaping. So there is some missing matter.

In astronomy, the mass and size of galaxy can be determined by the Virial theorem. While studying galaxy dynamics to find mass of galaxy, the rotational velocity of gas and stars is used. Then the K.E. and P.E of a galactic cluster of radius R and mass M_c can be related as

$$T = -\frac{1}{2}V \Rightarrow \frac{3\sigma^2}{2} = \frac{GM_c}{R} \Rightarrow M_c = \frac{3\sigma^2 R}{2G} \quad (8.1)$$

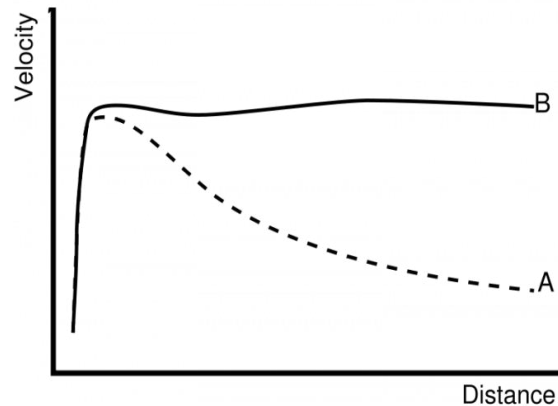


Figure 8.1: Rotation curve of a typical spiral galaxy. Predicted A and observed B.

Here σ represent dispersion of galactic velocities using Doppler shift of light from its galaxies, G =gravitational constant. Fritz Zwicky [102] in his study of Coma cluster independently estimated the mass of each galaxy in the cluster based on their luminosity and added up all of galaxy masses to get a total luminous cluster mass i.e. M_L and obtained $M_c = 400M_L$. Thus majority of the mass on the coma cluster is non luminous.

8.2.2 Galactic rotation curve

The presence of dark matter in spiral galaxies can be studied from galactic rotation curves [103]. According to Newton's law of gravity, the stellar velocity should decrease with increasing distance from center if the mass in the galaxy is confined to its central region.

$$v = \sqrt{\frac{GM}{R}} \quad (8.2)$$

But from galactic rotation curves (fig. 8.1) it is found that stellar velocity remains constant with increasing distance. Thus from flat galactic rotation curves one can say that there must be some non luminous mass associated with each galaxy extending out to a great distance beyond the central luminous region of the galaxy which is still undiscovered.

8.2.3 Gravitational lensing

The most recent evidence of dark matter came from gravitational lensing by Bullet cluster [104]. The Bullet Cluster(IE0657-56) consists of two colliding clusters of galaxies. The speed and shape of the 'Bullet' and other information from various telescopes suggests that the smaller cluster passed through the core of the larger one about 150 million years ago. These two enormous objects collided at speeds of several million miles an hour. The force of this event was so great that it separated the normal matter in the form of hot gas away from dark matter.

Gravitational lensing by Bullet cluster can be the best evidence of dark matter to present date. This technique can be used to determine the location of mass in a galaxy cluster. Gravity from mass in the galaxy cluster distorts light from background galaxies. Due to lensing, two distorted images of one background galaxy are seen above and below the real location of the galaxy. By looking at the shapes of many different background galaxies, it is possible to make a map showing where the gravity and therefore the mass in the cluster is located. Largest lensing is in the region where dark matter is present. Bullet cluster contain galaxies($\sim 2\%$ of the mass), intergalactic plasma($\sim 10\%$ of the mass), and dark matter($\sim 88\%$ of the mass).

8.2.4 Cosmic microwave background

The above observations give strong evidence of localized dark matter but not of its total amount in the universe. However this information can be extracted from the study of cosmic microwave background radiation. CMB radiation was emitted 13.7 billion years ago, only a few thousand years after the big bang. As the Universe cooled, neutral hydrogen atoms formed and photons decoupled from matter. CMB photons interact weakly with the hydrogen allowing them to travel long distances($\sim Mpc$) in straight lines i.e. without scattering (surface of last scattering). The WMAP data [65] of CMB put constraints on the baryonic and matter content of

universe:

$$\Omega_m h^2 = 0.14 \pm 0.02; \quad \Omega_b h^2 = 0.024 \pm 0.001 \quad (8.3)$$

During the Big-bang nucleosynthesis (BBN) period (from a few seconds to a few minutes after the Big Bang in the early hot universe) neutrons and protons fused together to form deuterium, Helium and trace amounts of lithium and other light elements. Other heavy elements were produced later in stars. BBN limits the average baryonic content of the universe. BBN is the largest source of deuterium in the universe as any deuterium found or produced in stars immediately fused to helium. By considering the deuterium to hydrogen ratio of regions with low levels of elements heavier than lithium, we are able to determine the D/H abundance directly after BBN. D/H ratio is heavily dependent on the overall density of baryons in the universe so measuring the D/H abundance gives the overall baryon abundance which is consistent with the CMB observations. The global dark matter density can be found by subtracting the baryon density from the total matter density.

$$\Omega_{dm} h^2 = 0.11 \pm 0.021 \quad (8.4)$$

8.3 Detection mechanism

8.3.1 Direct detection experiments

The idea of direct detection is simple. If our galaxy is filled with some non luminous matter then motion of our planet through this matter will cause a recoil of nuclei of detector due to elastic scattering of dark matter with the detector material. The basic goal of direct detection experiments is to measure the energy deposited after the recoil of WIMPs. The detectors, located far underground to reduce the effect of background cosmic rays, are sensitive to WIMP's that stream through the earth and interact with nuclei in the detector. The recoiling nucleus deposits energy in the form of ionization, heat and light, that is detected. After an elastic collision

with WIMPs of mass m , a nucleus of mass M recoils with energy given as

$$E = \left(\frac{\mu^2 v^2}{M} \right) (1 - \cos \theta) \quad (8.5)$$

where $\mu = \frac{mM}{m+M}$ is the reduced mass, v is the relative velocity of WIMPs w.r.t nucleus and θ is the scattering angle in the center of mass frame. Some experiments [105] find annual modulation in the dark matter signal because of the relative motion of the earth through the dark matter halo. For the simplified assumptions about the distribution of dark matter in the halo, flux is maximum in June and minimum in December. Annual modulation is a powerful signature for dark matter because most background signals e.g radioactivity don't exhibit such time dependence. Another method is to detect directional dependence of nucleus recoil (away from the direction of Earth motion) which is more powerful than annual modulation.

8.3.2 Indirect detection experiments

Indirect detection experiments are based on detection of the particles produced due to annihilation of dark matter. These include neutrinos, gamma rays and antimatter (positrons).

Gamma rays from WIMPs annihilation are more readily produced in galactic center. These can be produced by two processes. First is WIMPs annihilates into quark and anti quark pair, which further produced a particle jet from which stream of gamma rays is released. Second is the direct annihilation of WIMPs into gamma rays. Typical WIMPs masses of $O(100)$ GeV produce very high energy gamma rays. Such a gamma ray line would be a direct indication of the dark matter but the detection is not that easy since the production of gamma rays from other sources is not well understood. The Fermi Gamma Ray Space Telescope (NASA's) [106], designed to capture gamma rays from the center of our own galaxy can provide the best evidence for the existence of Dark Matter.

If the galactic halo is filled with the dark matter then it will scatter off nuclei in

the sun and the earth. The probability of scattering is small and the recoil velocity is smaller than the escape velocity so they get gravitationally bound to sun or earth. With time they will undergo multiple scattering and get settled inside the core and can annihilate with another WIMPs to quarks, leptons and Higgs bosons. But these particles get absorbed almost immediately. However if annihilation of WIMPs produces energetic muon neutrinos then they can travel long distances and can be detected by neutrino detectors. Inside the detector muon neutrino suffers a charged current event and produces a muon. These neutrinos can easily be distinguished from solar, atmospheric neutrinos as they are more massive ($O(\text{GeV})$ because they are produced from WIMPs) than the previous ones ($O(\text{MeV})$). Moreover the background signal from solar, atmospheric neutrinos over from the WIMP annihilation can easily be removed.

Antimatter can be an excellent signal of DM because production of antimatter by WIMP annihilation. For example: WIMP annihilation can produce positrons through secondary processes such as W^+, W^- and ZZ where $W^+ \rightarrow e^+ \nu_e$. One needs to study the flux of antimatter particles over the entire galactic halo rather than on particular areas because the products are charged and affected by magnetic fields within space and lose energy very soon so we can't say where the annihilation took place unlike gamma rays and neutrinos.

8.4 Neutralino as a cold DM

Beyond Standard Model theory, Supersymmetry gives us a leading cold dark matter candidate. In Minimal Supersymmetric Standard Model(MSSM) to eliminate new B,L violating Yukawa couplings in the renormalizable superpotential we add a new discrete(Z_2)symmetry. This new symmetry is called R parity which gives us the best possible cold dark matter candidate i.e. Light Supersymmetric Particle(LSP) [107]. R parity is defined as:

$$R = (-1)^{3(B-L)+2s} \quad (8.6)$$

where s is spin of particle. All SM particles have $R=1$ while all supersymmetric particles have $R=-1$. Because of this R parity, single SUSY particles cannot decay into just standard model particles. If R parity is conserved, all the supersymmetric particle will eventually decay into lightest susy particle (LSP). The LSP can't decay further but it can annihilate. This makes supersymmetry an interesting theory from astrophysical point of view. In MSSM we have three color and charge neutral particles sneutrino, gravitino and neutralino. Here we will discuss only about the possibility of neutralino only. In MSSM the neutral higgsinos ($\tilde{H}_u^0, \tilde{H}_d^0$) and the neutral gauginos (\tilde{B}, \tilde{W}^0) combine to form four mass eigenstates called neutralinos. In general neutralinos can be expressed as:

$$\chi = a\tilde{B} + b\tilde{W}^0 + c\tilde{H}_u^0 + d\tilde{H}_d^0 \quad (8.7)$$

The coefficients a,b,c,d can be found by diagonalizing the mass matrix for neutralinos:

$$M_{\tilde{N}} = \begin{pmatrix} M_1 & 0 & \frac{-g'v_d}{\sqrt{2}} & \frac{g'v_u}{\sqrt{2}} \\ 0 & M_2 & \frac{gv_d}{\sqrt{2}} & \frac{-gv_u}{\sqrt{2}} \\ \frac{-g'v_d}{\sqrt{2}} & \frac{gv_d}{\sqrt{2}} & 0 & -\mu \\ \frac{g'v_u}{\sqrt{2}} & \frac{-gv_u}{\sqrt{2}} & -\mu & 0 \end{pmatrix} \quad (8.8)$$

Here M_1 and M_2 (deduced from $m_{1/2}$ by RG evolution from the Planck/GUT scale to to Susy scale \sim TeV) are the soft susy breaking terms giving mass to the U(1) and SU(2) gauginos respectively. g' and g are gauge coupling corresponding to U(1) and SU(2) group. μ is electroweak symmetry breaking parameter. v_u, v_d are Higgs vevs determined by $\tan\beta$. So the mixing and masses of the neutralinos depend upon $m_{\frac{1}{2}}, \mu$ and $\tan\beta$. After diagonalizing, by convention the mass eigen-values can be labelled in ascending order so that $m_{\chi_1^0} < m_{\chi_2^0} < m_{\chi_3^0} < m_{\chi_4^0}$. The lightest neutralino χ_1^0 is assumed to be the desired candidate for dark matter. If it is produced in the early universe, then it may exist in the present day universe with sufficient density (relic density) to act as dark matter.

8.5 Relic density

The study of thermodynamics of early universe is necessary to understand the particle creation. Then solution of Boltzmann equations which governs the evolution of the different particle densities, tell us the relic density for any particular species today. The most important quantity to calculate is the interaction rate. If we consider WIMP (LSP) to be dark matter then due to assumed conservation of R-parity it cannot decay but it can annihilate or co-annihilate (i.e. produce normal matter by collision with other R-parity odd superparticle). So we are interested in the calculation of relic density of LSP dark matter whose number density varies due to annihilation (coannihilation). The annihilation rate is given as

$$\Gamma = n\sigma v. \quad (8.9)$$

Here n is the number density, σ is annihilation cross section and v is relative velocity of particles. As long as $\Gamma > H$ (Hubble constant), the particles remain in thermal equilibrium with the rest of the universe. But when $\Gamma < H$, the particles are said to be decoupled i.e. they move freely. The evolution of number density of a particle in early universe is governed by its Boltzmann equation:

$$\frac{dn}{dt} + 3Hn = - \langle \sigma v \rangle [n^2 - n_{eq}^2] \quad (8.10)$$

One can solve this equation by standard approximation methods however [108] pointed out 3 major improvements required while calculating the relic density from this equation:

1. **Relic density from coannihilation** If the supersymmetric theory contains a superparticle slightly more massive than the LSP then the relic density of LSP is not determined by only annihilation rates but one must also consider the coannihilation channels wherein the LSP and the nearly degenerate superparticle “co-annihilate” to ordinary matter.

2. **Annihilation into forbidden channels** This case deals with the annihilation of LSP into particles which are more massive than the LSP. Since at the time of freeze out LSPs are thermally distributed and annihilation into heavier particle can occur. [108] showed that if the heavier supersymmetric particles are only 5-15% more massive, then these channels can dominate the annihilation cross section and determine the relic density. for example, annihilation into higgs, $b\bar{b}$, $t\bar{t}$, W^+W^- etc.
3. **Annihilation near poles** In this case the relic density is greatly affected if the annihilation occurs near a pole. This can happen if the mass of neutralino is just near to half of the mass of exchanged particle during annihilation. These exceptions basically alter the way one calculates the thermal averaging of cross-section and hence the relic density.

We review here the calculation of relic density as given in [109, 110] considering all the factors mentioned above.

Let us consider that N supersymmetric particles χ_i ($i=1,\dots,N$) with masses m_i annihilate. Assume that χ_1 with mass m_1 is lightest, χ_2 is the second lightest and so on. Evolution of the χ_i can be determined by set of N Boltzmann equations:

$$\begin{aligned}
\frac{dn_i}{dt} = & -3Hn_i - \sum_{j=1}^N [\langle \sigma_{ij} v_{ij} \rangle (n_i n_j - n_i^{eq} n_j^{eq}) \\
& - \sum_{j \neq i} (\langle \sigma'_{Xij} v_{ij} \rangle (n_i n_X - n_i^{eq} n_X^{eq}) - \langle \sigma'_{ij} v_{ij} \rangle (n_j n'_X - n_j^{eq} n_X^{eq})) \quad (8.11) \\
& - \sum_{j \neq i} [\Gamma_{ij}(n_i - n_i^{eq}) - \Gamma_{ji}(n_j - n_j^{eq})]
\end{aligned}$$

The term with Hubble rate H on the R.H.S represents decrease in density due to the expansion of the universe. The second term describes $\chi_i \chi_j$ annihilations into standard model particles $\chi_i \chi_j \rightarrow XX'$ with cross section

$$\sigma_{ij} = \sigma(\chi_i \chi_j \rightarrow XX') \quad (8.12)$$

The third term represents conversions with the cosmic backgrounds ($\chi_i \rightarrow \chi_j$) which changes n_i if $i \neq j$ and have cross section

$$\sigma'_{ij} = \sigma(\chi_i X \rightarrow \chi_j X') \quad (8.13)$$

The last term represents decay of χ_i particles with decay rate

$$\Gamma_{ij} \rightarrow \Gamma(\chi_i \rightarrow \chi_j X X') \quad (8.14)$$

v_{ij} is the relative velocity defined as:

$$v_{ij} = \frac{\sqrt{(P_i \cdot P_j)^2 - m_i^2 m_j^2}}{E_i E_j} \quad (8.15)$$

n_i^{eq} is the equilibrium number density for i^{th} particle given as:

$$n_i^{eq} = \frac{g_i}{2\pi} \int d^3 p_i f_i \quad (8.16)$$

Here p_i is the three-momentum of particle and f_i is the phase space distribution function defined in Maxwell-Boltzmann approximation as

$$f_i = e^{-\frac{E_i}{T}} \quad (8.17)$$

And finally the $\langle \sigma_{ij} v_{ij} \rangle$ in this thermal distribution is defined as

$$\langle \sigma_{ij} v_{ij} \rangle = \frac{\int d^3 p_i d^3 p_j f_i f_j \sigma_{ij} v_{ij}}{\int d^3 p_i d^3 p_j f_i f_j} \quad (8.18)$$

Since all the χ_i , which are heavier than LSP will eventually decay into χ_1 , the total density of χ_i particles is, $n = \sum_{i=1}^N n_i$. Therefore the sum of equation (8.11) over i gives:

$$\frac{dn}{dt} = -3Hn - \sum_{ij=1}^N \langle \sigma_{ij} v_{ij} \rangle (n_i n_j - n_i^{eq} n_j^{eq}) \quad (8.19)$$

Since the scattering rate of supersymmetric particles in thermal background is much faster than their annihilation rate because $\sigma'_{ij} \sim \sigma_{ij}$ and when $n_X \gg n_i$, then due to relativistic nature of X particles and non relativistic nature of χ particles lead them to suppressed by Boltzmann factor. So χ_i distribution remain in thermal equilibrium and we have

$$\frac{n_i}{n} \simeq \frac{n_i^{eq}}{n^{eq}} \quad (8.20)$$

After putting it in equation (8.19), we get

$$\frac{dn}{dt} = -3Hn - \langle \sigma_{eff} v \rangle (n^2 - n_{eq}^2) \quad (8.21)$$

Where

$$\langle \sigma_{eff} v \rangle = \sum_{ij} \langle \sigma_{ij} v_{ij} \rangle \frac{n_i^{eq} n_j^{eq}}{n^{eq} n^{eq}} \quad (8.22)$$

The numerator (let us denote it by A) in the above equation is the annihilation rate per unit volume and it can be written in a more convenient way as

$$A = \sum_{ij} \langle \sigma_{ij} v_{ij} \rangle n_i^{eq} n_j^{eq} = \sum_{ij} \int W_{ij} \frac{g_i f_i d^3 p_i}{(2\pi)^3} \frac{g_j f_j d^3 p_j}{(2\pi)^3} \quad (8.23)$$

Here g_i are internal degrees of freedom of particle. W_{ij} is Lorentz invariant and related to cross section as

$$W_{ij} = 4p_{ij} \sqrt{s} \sigma_{ij} = 4E_i E_j \sigma_{ij} v_{ij} \quad (8.24)$$

Here p_{ij} is the momentum of i^{th} particle w.r.t j^{th} or vice versa in the center of mass frame of both particles and given as

$$p_{ij} = \frac{[s - (m_i + m_j)^2]^{1/2} [s - (m_i - m_j)^2]^{1/2}}{2\sqrt{s}} \quad (8.25)$$

After following steps given in [109] one can find effective form of $\langle \sigma_{eff} v \rangle$ given as

$$\langle \sigma_{eff} v \rangle = \frac{\int_0^\infty dp_{eff} p_{eff}^2 W_{eff} K_1\left(\frac{\sqrt{s}}{T}\right)}{m_1^4 T [\sum_i \frac{g_i}{g_1} \frac{m_i^2}{m_1^2} K_2\left(\frac{\sqrt{m_i}}{T}\right)]^2} \quad (8.26)$$

Here $p_{eff} = \sqrt{s - 4m_1^2}/2$ and T is the temperature. K_1 is the modified Bessel function of second kind of order 1 and k_2 is of order 2. W_{eff} has form

$$W_{eff} = \sum_{ij} \frac{p_{ij}}{p_{eff}} \frac{g_i g_j}{g_1^2} W_{ij} \quad (8.27)$$

The eq. (8.21) can be written in a more convenient way if we put $Y = \frac{n}{s}$ in this equation. Here s is entropy density. We have

$$\frac{dY}{dt} = - \langle \sigma v \rangle s [Y^2 - Y_{eq}^2] \quad (8.28)$$

Since the right hand side depends upon temperature T so it is convenient to make the T as a independent variable instead of time. Define a new variable $x_{f=m_1/T}$ then this equation can be written as

$$\frac{dY}{dx} = - \sqrt{\frac{\pi}{45G}} \frac{g_*^{1/2} m_1}{x^2} \langle \sigma_{eff} v \rangle [Y^2 - Y_{eq}^2] \quad (8.29)$$

Where

$$Y_{eq} = \frac{45x^2}{4\pi^4 h_{eff}(T)} \sum_i g_i \left(\frac{m_i}{m_1}\right)^2 K_2\left(x \frac{m_i}{m_1}\right) \quad (8.30)$$

and g_* is the total number of relativistic degrees of freedom given as

$$g_*^{1/2} = \frac{h_{eff}}{\sqrt{g_{eff}}} \left(1 + \frac{T}{3h_{eff}} \frac{dh_{eff}}{dT}\right) \quad (8.31)$$

g_{eff} and h_{eff} are the effective energy and entropy degrees of freedom. g_{eff} , h_{eff} and $g_*^{1/2}$ are function of temperature and can be calculated at QCD phase transition temperature $T_{QCD}=150$ MeV as given in [109].

Fig.8.2 plots an analytic approximation to the Boltzmann equation and illustrates several key points. At freeze out, the actual abundance leaves the equilibrium value, and remains essentially constant, the equilibrium value continues to decrease. The larger the annihilation cross section, lower the value of relic abundance Y . Using freeze-out approximation and integrating this differential equation between $x=0$ to

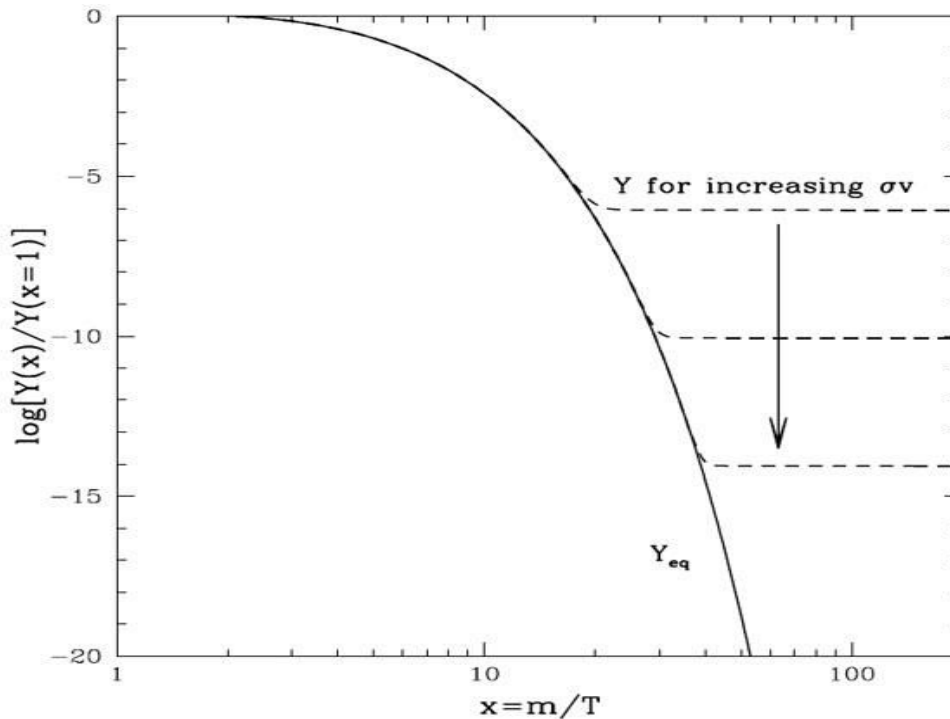


Figure 8.2: The dashed line is the actual abundance, and the solid line is in equilibrium abundance which is boltzmann factor suppressed.

$x = m_1/T_0$, where T_0 is the present day CMB temperature, leads to the formula for the relic density [109]:

$$\Omega h^2 = 2.755 \times 10^8 \frac{m_1}{\text{GeV}} Y_0 \quad (8.32)$$

8.6 DarkSusy

DarkSusy [100] is a publicly available package for the neutralino dark matter calculations. It is a code written in FORTRAN 77. With the help of DarkSUSY one can calculate the present relic density for neutralino. While calculating the relic density DarkSUSY takes care of resonances, annihilation thresholds and coannihilations which can have large effect on the value of relic density. Also it provides the rates from direct and indirect detection methods. Our interest in this study is calculation of relic density for NMSGUT generated spectra. We use version 5.1.1 of DarkSusy for this purpose. It basically provides a library which can be interfaced with one's own code. However for testing it can also be used by giving it sample set of model

parameters. Let us discuss the various steps how it calculates the relic density for a particular model.

The main function is DSMAIN inside the test directory. One can enter model parameters during interactive run by hand (for MSSM, mSUGRA model) or can provide a SLHA file [111]. Then it calls ISASUGRA (from ISAJET) to calculate s-particle spectrum and checks whether the model parameters are consistent or not. However one can give the low energy spectrum. In our case, we gave it the tree level spectrum (with loop corrected Higgs mass) which NMSGUT calculates and directly perform the task of calculating relic density. The subroutine which calculates relic density is the function DSRDOMEGA. All the main routine files which form the DarkSusy library are given inside the SRC directory. The steps how it calls main subroutines and uses functions while calculation of relic density in DarkSusy are given below.

1. **DSRDOMEGA** It is function which returns relic density Ωh^2 for MSSM neutralino using subroutine DSRDENS. It uses a switch which controls whether one wants to include co-annihilation channels or not. It also checks for resonances and thresholds looking at the mass of each particle which need to be included .
2. **DSRDENS** It is a subroutine which calculates the relic density in the units of critical density time h^2 . To calculate relic density it requires invariant annihilation rates for which it requires function DSANWX.
3. **DSANWX** It is a function which calculates the neutralino annihilation invariant rates. It requires the value of momentum (p_{eff}) of two annihilating particles in their center of momentum frame.

DarkSusy takes care of thresholds and resonances through variation of W_{eff} and p_{eff} . Since the equation (8.26) is independent of the temperature so W_{eff} and p_{eff} can be tabulated for each model. The value of p_{eff} should be such that it includes all resonances, thresholds and coannihilation. The thermal average of W_{eff} is adjusted

by factor $K_1 p_{eff}^2$ and at resonances and thresholds there is exponential decay of K_1 for large p_{eff} . DarkSusy calculates the thermal average via integrating over p_{eff} using adaptive Gaussian integration, using spline interpolation in (p_{eff}, W_{eff}) table and splits the integration interval at sharp thresholds.

8.7 NMSGUT and relic density calculation with DarkSusy

In this section, we present results for relic density of lightest neutralino (Bino in this case) calculated with DarkSusy for two example sets of mass spectra taken from [27] compatible with SM fermion data. The sparticles are mostly heavy O(10-50 TeV) except for gauginos and in one of these spectra Smuon is also light O(100GeV). The input i.e. low energy MSSM data is given in SLHA (Susy Les Houches Accord) [111] format. The input spectrum is shown in Table 8.1 and outputs are shown in Table 8.2.

Results for the relic density with and without including coannihilation channels are shown. From the output it is clear that we got large value of relic density for Soln.1 and reasonable value for Soln.2. Also in Soln.1 all the particles have masses much heavier than Neutralino 1(χ_1^0), so no coannihilation channels are possible, so relic density with and without co-annihilation is almost same. In Soln.2 there is one particle right handed Smuon($\tilde{\mu}_R$) whose mass is comparable to that of χ_1^0 , So coannihilation channels are possible which result into further decrease in relic density.

Approximate value of relic density given in [112] by taking $g_*^{1/2} = 10$, $x_f = 25$, $M_{pl} = 10^{19}$ gives us:

$$\Omega h^2 = \frac{3 \times 10^{-27} cm^3 s^{-1}}{\langle \sigma v \rangle} \quad (8.33)$$

The values of $\langle \sigma v \rangle$ for individual annihilation channels are given in Table 8.3 and for coannihilation channels are given in Table 8.4.

The reason for large value of relic density in the first solution can be explained

PDG code	Mass(Soln.1)	Mass(Soln.2)	Particles
24	80.32	80.326	W^+
25	125.000	123.99	h_0
35	457636.54	377025.28	H_0
36	457636.54	377025.29	A_0
37	457636.55	377025.30	H^+
1000021	1200.000	1000.13	\tilde{g}
1000022	246.4066	210.0974	χ_1^0
1000023	590.178	569.808	χ_2^0
1000024	590.178	569.8083	χ_1^+
1000025	155715.44	125591.2	χ_3^0
1000035	155715.44	125591.2	χ_4^0
1000037	155715.46	125591.22	χ_2^+
1000001	11245.066	8402.9938	\tilde{d}_L
1000002	12822.48	11271.798	\tilde{u}_L
1000003	11246.13	8401.4765	\tilde{s}_L
1000004	12822.424	11270.628	\tilde{c}_L
1000005	48865.409	40269.187	\tilde{b}_L
1000006	48227.493	24607.508	\tilde{t}_L
1000011	11958.032	1761.88	\tilde{e}_L
1000012	15324.618	11270.946	$\tilde{\nu}_{eL}$
1000013	11961.759	15258.60	$\tilde{\mu}_L$
1000014	15326.183	15258.32	$\tilde{\nu}_{\mu L}$
1000015	30125.093	20674.71	$\tilde{\tau}_L$
1000016	30130.304	21320.059	$\tilde{\nu}_{\tau L}$
2000001	13440.651	11272.10	\tilde{d}_R
2000002	13440.398	14446.76	\tilde{u}_R
2000003	13441.103	11270.09	\tilde{s}_R
2000004	13440.845	14445.80	\tilde{c}_R
2000005	49419.242	51845.90	\tilde{b}_R
2000006	48998.142	40275.875	\tilde{t}_R
2000011	15324.839	15308.291	\tilde{e}_R
2000013	15326.634	211.56859	$\tilde{\mu}_R$
2000015	38560.601	21419.559	$\tilde{\tau}_R$

Table 8.1: The input sparticle spectrums in SLHA format to DarkSusy.

Ωh^2	Soln.1	Soln.2
With coannihilation	97182.8934	0.051
Without coannihilation	97182.8934	1.285

Table 8.2: Relic Density of neutralino.

from the diagrams of neutralino annihilation. Feynmann diagrams for the $\chi_1^0\chi_1^0 \rightarrow YZ$ are given in Fig. 8.3 If we calculate the relic density by eq(8.33) and put the

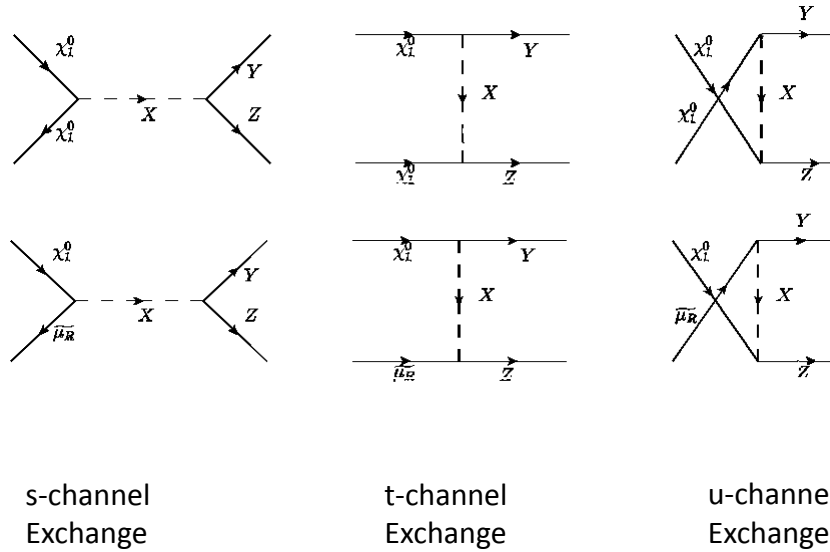


Figure 8.3: Neutralino pair annihilation and Neutralino Smuon coannihilation. See tables 8.3 and 8.4 for definitions of YZ,X.

value of the thermally averaged annihilation cross section for the dominating channel ($\langle \sigma v \rangle$) and compare it with the relic density calculated by DarkSusy, we find the results comparable.

For Soln.2, first we calculate the relic density when there is no coannihilation. If we take $\langle \sigma v \rangle = \langle \sigma v \rangle_{\chi_1^0 \tilde{\mu}_R \rightarrow \mu^+ \mu^-}$ which is the dominating channel and calculate Ωh^2 , we get $\Omega h^2 \simeq 0.8$ Similarly, we calculate the relic density including coannihilation channels. Here, also if we take $\langle \sigma v \rangle = \langle \sigma v \rangle_{\chi_1^0 \tilde{\mu}_R \rightarrow \gamma \mu_R}$ then we get $\Omega h^2 \simeq .09$ from the approximate formulae. In both the cases for soln.2 the values of relic density are nearly equal to relic density calculated by Dark Susy considering all channels. So we can say that it is the cross section for dominant channel which gives us the final relic density for neutralino. Relic density is less when coannihilation channels are included, it is due to the reason that $\langle \sigma_{\chi_1^0 \chi_1^0} v \rangle$ is much less than

$\langle \sigma_{\chi_1^0 \tilde{\mu}_R} v \rangle$. For Soln. 1 the total cross section is very small (10^{-5} times smaller than the maximum cross-section of Soln. 2) hence the relic density is 5 orders of magnitude higher. Although we did not perform searches of NMSGUT parameter space including dark matter constraints, it is clear from the above examples that such searches are perfectly feasible. When we have complete incorporation of loop effects on sparticle masses in our searches as well as $\tan\beta$ variation we intend to interface the DarkSusy Library with our code and search for realistic solutions compatible with DM cosmology. The preliminary exploratory survey of this chapter has laid the basis for future work in this direction.

Process: $\chi_1^0\chi_1^0 \rightarrow YZ$	Exchanged Particles(X)		$\langle \sigma v \rangle (cm^3 s^{-1})$	
YZ	s channel	t and u channel	Soln.1	Soln.2
HH,hH,AA,HA,ZA	h,H	χ_i^0	0.00000	0.00000
hh	h,H	χ_i^0	6.61712×10^{-34}	2.8868×10^{-34}
hA,ZH	A,Z	χ_i^0	0.00000	0.000000
Zh	A,Z	χ_i^0	2.5789×10^{-38}	3.0151×10^{-38}
W^-, H^+	h,H,A	χ_k^\pm	0.00000	0.0000
Z^0, Z^0	h,H	χ_i^0	8.37763×10^{-39}	9.70311×10^{-40}
W^+, W^-	h,H,Z	χ_k^\pm	4.33936×10^{-38}	1.509256×10^{-38}
$\nu_e \bar{\nu}_e$	h,H,A,Z	$\tilde{\nu}_e$	1.96804×10^{-34}	3.9409×10^{-35}
$e^+ e^-$	h,H,A,Z	$\tilde{e}_{L,R}$	3.67648×10^{-33}	2.18089×10^{-31}
$\nu_\mu \bar{\nu}_\mu$	h,H,A,Z	$\tilde{\nu}_\mu$	1.96723×10^{-34}	3.99257×10^{-35}
$\mu^+ \mu^-$	h,H,A,Z	$\tilde{\mu}_{L,R}$	3.67588×10^{-33}	3.97164×10^{-27}
$\nu_\tau \bar{\nu}_\tau$	h,H,A,Z	$\tilde{\nu}_\tau$	1.32008×10^{-35}	1.04916×10^{-35}
$\tau^+ \tau^-$	h,H,A,Z	$\tilde{\tau}_{L,R}$	4.73294×10^{-34}	4.7614×10^{-34}
$u\bar{u}$	h,H,A,Z	$\tilde{u}_{L,R}$	3.16611×10^{-33}	4.75398×10^{-34}
$d\bar{d}$	h,H,A,Z	$\tilde{d}_{L,R}$	2.2194×10^{-34}	9.52563×10^{-35}
$c\bar{c}$	h,H,A,Z	$\tilde{c}_{L,R}$	3.1661×10^{-33}	4.75927×10^{-34}
$s\bar{s}$	h,H,A,Z	$\tilde{s}_{L,R}$	2.26255×10^{-34}	9.87178×10^{-35}
$t\bar{t}$	h,H,A,Z	$\tilde{t}_{L,R}$	3.21770×10^{-35}	2.42824×10^{-34}
$b\bar{b}$	h,H,A,Z	$\tilde{b}_{L,R}$	3.47445×10^{-33}	3.59457×10^{-33}

Table 8.3: Thermally averaged annihilation cross section $\langle \sigma v \rangle$ for Neutralino pair-annihilation into tree level two body final states (YZ). The indices $i=1,..4$. and $k=1,2$.

Process: $\chi_1^0 \tilde{\mu}_R \rightarrow YZ$	Exchanged Particles X			$\langle \sigma v \rangle (cm^3 s^{-1})$
YZ	s channel	t channel	u channel	Soln.2
$Z\mu_R$	μ_R	$\tilde{\mu}_{R,L}$	χ_i^0	8.57919×10^{-27}
$\gamma\mu_R$	μ_R	$\tilde{\mu}_{R,L}$		3.26385×10^{-26}
$h^0\mu_R$	μ_R	$\tilde{\mu}_{R,L}$	χ_i^0	6.95715×10^{-29}
$H^0\mu_R, A\mu_R$	μ_R	$\tilde{\mu}_{R,L}$	χ_i^0	0.00000
$W^- \bar{\nu}_\mu$	$\mu_{R,L}$	$\tilde{\nu}_\mu$	χ_k^\pm	7.44170×10^{-32}
$H^- \bar{\nu}_\mu$	$\mu_{R,L}$	$\tilde{\nu}_\mu$	χ_k^\pm	0.00000

Table 8.4: Thermally averaged annihilation cross section $\langle \sigma v \rangle$ for Neutralino Smuon coannihilation into tree level two body final states (YZ). The indices $i=1,..4$. and $k=1,2$.

8.8 Conclusion and discussion

The NMSGUT can give Neutralino as a dark matter candidate and can account for right relic density i.e. $\Omega h^2 = .11$, if mass spectrum of s-particles have at least one particle whose mass is comparable to that of Neutralino and there is also coannihilation channel. In one case (all s-particles $\sim O(100\text{TeV})$) we get large value of relic density which is not acceptable. For the second case (light $\tilde{\mu}_R$ mass equal to Neutralino mass within 10%) we get a relic density in the right ballpark. In this way relic density calculations constrain the parameter space of NMSGUT. However this is just a start and a preliminary check. The most suitable way is to interface the DarkSusy library with the NMSGUT search criteria. In this way relic density calculations will guide the search engine to look into a region where it fulfills the DM relic density constraints.

Chapter 9

NMSGUT RGEs

9.1 Introduction

Renormalization Group Equations (RGE) are a mathematical tool to investigate the evolution of the scale dependent (“running”) parameters (couplings and masses) of a quantum field theory at different energy scales. It involves loop (1-loop, 2-loop and so on) corrections to the parameters in terms of powers of logarithms of the ratio of running scale (Q) to definitional scale (Q_0). The best known example is the evolution of three gauge couplings of SM with energy. They tend to meet roughly around energy $10^{16.33}$ GeV, pointing to the possibility of “Grand Unification”, the motivating idea of this thesis. Coupling unification suggests that the SM is an effective theory of some larger theory below the GUT scale. The sensitivity of SM Higgs mass to the GUT scale due to corrections $\Delta m_H^2 \sim \alpha M_{GUT}^2$ indicates a structural instability in the SM. However the introduction of supersymmetry solves this problem of naturalness. With supersymmetry and one pair of Higgs the three MSSM gauge couplings meet almost exactly at a point [113]. The two loop RGEs for minimal supersymmetric standard model are available [38] and are being used by many who work on grand unified theories. The RGEs are important to check the viability of GUTs i.e. whether they are able to produce low energy data by downward RG flow of GUT predictions at unification scale. For example to do a

fit at scale M_Z using NMSGUT superpotential parameters and Soft Susy breaking parameters of Sugra-NUHM type $(m_0, m_{1/2}, A_0, m_{H,\bar{H}}^2)$, we need two loop MSSM RGEs given in [38] to run the parameters down from M_X^0 . To do this we randomly throw these parameters at GUT scale. However just like SM is an effective theory of GUT scale, NMSGUT can also be an effective theory of some higher theory at Planck scale. After the Planck scale the gravity becomes strong so we restrict ourselves to the energy range up to the Planck scale $((8\pi G_N)^{-1/2} = 10^{18.34} \text{ GeV})$. Now above the GUT scale MSSM RGEs will not work so we need NMSGUT RGEs which had so far not been computed. Although seemingly straightforward, automated calculation programs like [114] fail because their brute force approach generates too many terms to sum. At Planck scale, with canonical kinetic terms, gravitino mass parameter $(m_{3/2})$ and the universal trilinear scalar parameter A_0 ($\sim m_{3/2}$) will be the only free parameters. The soft Susy breaking parameters at GUT scale $10^{16.33} \text{ GeV}$ are determined by running down soft parameters of NMSGUT with just these two soft parameters in input. In this chapter we present two loop RGEs for soft Susy parameters of NMSGUT. The motive of this work is to produce the type of soft Susy parameters via NMSGUT RGE running from Planck scale to GUT scale $10^{16.33} \text{ GeV}$ that our search program finds are necessary for successful fermion data fitting. Especially we hope to find an explanation for the negative Higgs mass squared parameters $m_{H,\bar{H}}^2$ which are found in NMSGUT fits (at least at large $\tan\beta$) whereas supergravity predicts that all soft scalar masses squared are positive and equal to $m_{3/2}^2$ (at the scale where they are generated : presumably the Planck scale). This final chapter presents our calculation of RGE's and a preliminary exploration of the RGE flows. We derive the 2-loop RGEs for NMSGUT parameters using general RGE formulae given in [38] and gauge invariance as guiding principle to develop methods to overcome combinatorial complexity. The calculation was done in collaboration and part of the results can be found in [30, 116]. The sample tables we generate are for distinct parameter sets.

9.2 Generalized RGEs

The general two loop running of a parameter X is defined as

$$\frac{dX}{dt} = \frac{1}{16\pi^2}\beta_X^{(1)} + \frac{1}{(16\pi^2)^2}\beta_X^{(2)} \quad (9.1)$$

Here β_X^1 and β_X^2 are the beta functions for couplings and masses. In Susy theories the running of couplings arises entirely from anomalous dimensions. The form of generic renormalizable Superpotential is given by

$$W = \frac{1}{6}Y_{ijk}\Phi_i\Phi_j\Phi_k + \frac{1}{2}\mu_{ij}\Phi_i\Phi_j \quad (9.2)$$

Here Φ is the chiral superfield which contains a complex scalar ϕ_i and a Weyl fermion ψ_i . The generic lagrangian corresponding to Soft Susy breaking terms is given by

$$L_{Susy} = -\frac{1}{6}h_{ijk}\phi_i\phi_j\phi_k - \frac{1}{2}b_{ij}\phi_i\phi_j - \frac{1}{2}(m^2)_j^i\phi^{*i}\phi_j - \frac{1}{2}M\lambda\lambda + h.c. \quad (9.3)$$

M is the gaugino mass parameter. We give here the general form of 2-loop beta function for the soft susy breaking parameters $h_{ijk}, b_{ij}, (m^2)_j^i, M$ and gauge coupling g from [38].

$$\frac{dg}{dt} = \frac{1}{16\pi^2}\beta_g^{(1)} + \frac{1}{(16\pi^2)^2}\beta_g^{(2)} \quad (9.4)$$

Where

$$\beta_g^{(1)} = g^3[S(R) - 3C(G)] \quad (9.5)$$

$$\begin{aligned} \beta_g^{(2)} = g^5[-6C(G)^2 + 2C(G)S(R) + 4S(R)C(R)] \\ g^3Y^{ijk}Y_{ijk}C(k)/d(G) \end{aligned} \quad (9.6)$$

$$\frac{dM}{dt} = \frac{1}{16\pi^2}\beta_M^{(1)} + \frac{1}{(16\pi^2)^2}\beta_M^{(2)} \quad (9.7)$$

Where

$$\beta_M^{(1)} = g^2[2S(R) - 6C(G)]M \quad (9.8)$$

i.e. just double of $\beta_g^{(1)}$.

$$\begin{aligned} \beta_M^{(2)} = & g^4[-24C(G)^2 + 8C(G)S(R) + 16S(R)C(R)]M + \\ & 2g^2[h^{ijk} - MY^{ijk}]Y_{ijk}C(k)/d(G) \end{aligned} \quad (9.9)$$

Here g is the gauge coupling of the group under consideration. $Y_{ijk}=(Y^{ijk})^*$. $S(R)$ is the Dynkin index for representation R and $C(G)$ is the Casimir invariant of group. $S(R)C(R)$ is the weighted sum of Dynkin index over Casimir operator. $d(G)$ is the dimensionality of the group.

$$\frac{dh^{ijk}}{dt} = \frac{1}{16\pi^2}[\beta_h^{(1)}]^{ijk} + \frac{1}{(16\pi^2)^2}[\beta_h^{(2)}]^{ijk} \quad (9.10)$$

Where

$$\begin{aligned} [\beta_h^{(1)}]^{ijk} = & \frac{1}{2}h^{ijl}Y_{lmn}Y^{mnk} + Y^{ijl}Y_{lmn}h^{mnk} - 2(h^{ijk} - 2MY^{ijk})g^2C(k) \\ & + (k \longleftrightarrow i) + (k \longleftrightarrow j) \end{aligned} \quad (9.11)$$

$$\begin{aligned} [\beta_h^{(2)}]^{ijk} = & -\frac{1}{2}h^{ijl}Y_{lmn}Y^{npq}Y_{pqr}Y^{mrk} \\ & -Y^{ijl}Y_{lmn}Y^{npq}Y_{pqr}h^{mrk} - Y^{ijl}Y_{lmn}h^{npq}Y_{pqr}Y^{mrk} \\ & + (h^{ijl}Y_{lpq}Y^{pqk} + 2Y^{ijl}Y_{lpq}Y^{pqk} - 2MY^{ijl}Y_{lpq}Y^{pqk})g^2[2C(p) - C(k)] \\ & + (2h^{ijk} - 8MY^{ijk})g^4[C(k)S(R) + 2C(k)^2 - C(G)C(k)] \\ & + (k \longleftrightarrow i) + (k \longleftrightarrow j) \end{aligned} \quad (9.13)$$

Here $C(k)$ represents the Casimir invariant of the representation carried by the chiral superfield.

$$\frac{db^{ij}}{dt} = \frac{1}{16\pi^2}[\beta_b^{(1)}]^{ij} + \frac{1}{(16\pi^2)^2}[\beta_b^{(2)}]^{ij} \quad (9.14)$$

Where

$$[\beta_b^{(1)}]^{ij} = \frac{1}{2}b^{il}Y_{lmn}Y^{mnj} + \frac{1}{2}Y^{ijl}Y_{lmn}b^{mn} + \mu^{il}Y_{lmn}h^{mnj} \quad (9.15)$$

$$-2(b^{ij} - 2M\mu^{ij})g^2C(i) + (i \longleftrightarrow j)$$

$$[\beta_b^{(2)}]^{ij} = -\frac{1}{2}b^{ij}Y_{lmn}Y^{pqn}Y_{pqr}Y^{mrj} - \frac{1}{2}Y^{ijl}Y_{lmn}b^{mr}Y^{pqr}Y_{pqn} \quad (9.16)$$

$$-\frac{1}{2}Y^{ijl}Y_{lmn}\mu^{mr}Y_{pqr}h^{pqn} - \mu^{il}Y_{lmn}h^{npq}Y_{pqr}Y^{mrj}$$

$$-\mu^{il}Y_{lmn}Y^{npq}Y_{pqr}h^{mrj} + 2Y^{ijl}Y_{ipq}(b^{pq} - \mu^{pq}M)g^2C(p)$$

$$+(b^{il}Y_{lpq}Y^{pqj} + 2\mu^{il}Y_{lpq}h^{pqj} - 2M\mu^{il}Y_{lpq}Y^{pqj})g^2[2C(p) - C(i)]$$

$$+(2b^{ij} - 8M\mu^{ij})g^4[C(i)S(R) + 2C(i)^2 - 3C(G)C(i)]$$

$$+(i \longleftrightarrow j) \quad (9.17)$$

$$\frac{d(m^2)_j^i}{dt} = \frac{1}{16\pi^2}[\beta_{(m^2)}^{(1)}]_j^i + \frac{1}{(16\pi^2)^2}[\beta_{(m^2)}^{(2)}]_j^i \quad (9.18)$$

Where

$$[\beta_{(m^2)}^{(1)}]_j^i = \frac{1}{2}Y_{ipq}Y^{pqn}(m^2)_n^j + \frac{1}{2}Y^{jipq}Y_{pqn}(m^2)_i^n + 2Y_{ipq}Y^{jpr}(m^2)_r^q \quad (9.19)$$

$$h_{ipq}h^{jpr} - 8\delta_j^i M\tilde{M}^\dagger g^2 c(i) + 2g^2 t_i^A Tr[t^A m^2]$$

$$[\beta_{(m^2)}^{(2)}]_j^i = -\frac{1}{2}(m^2)_i^l Y_{lmn}Y^{mrj}Y_{pqr}Y^{pqn} - \frac{1}{2}(m^2)_i^j Y^{lmn}Y_{mri}Y^{pqr}Y_{pqn} \quad (9.20)$$

$$-Y_{ilm}Y^{jnm}(m^2)_r^l Y_{pqn}Y^{rpq} - Y^{ilm}Y_{jnm}(m^2)_n^r Y^{rpq}Y_{lpq}$$

$$-Y_{ilm}Y^{jnr}(m^2)_n^l Y_{pqr}Y^{pqm} - 2Y^{ilm}Y_{jln}Y^{npq}Y_{mpr}(m^2)_r^q$$

$$-h_{ilm}Y^{jlm}Y_{npq}h^{mpq} - Y_{ilm}h^{jln}h_{npq}Y^{mpq}$$

$$+[(m^2)_i^l Y_{lpq}Y^{jpr} + Y_{ipq}Y^{lpq}(m^2)_l^j + 4Y_{ipq}Y^{jpl}(m^2)_l^q + 2h_{ipq}h^{jpr}]$$

$$-2h_{ipq}Y^{jpr} - 2Y_{ipq}h^{jpr}M^\dagger + 4Y_{ipq}Y^{jpr}M\tilde{M}^\dagger]g^2[C(p) + C(q) - C(i)]$$

$$\begin{aligned}
& -2g^2 t_i^{Aj} (t^A m^2)_r^l Y_{lpq} Y^{rpq} + 8g^4 t_j^{Ai} \text{Tr}[t^A C(r) m^2] \\
& + \delta_j^i g^4 M M^\dagger [24C(i)S(R) + 48C(i)^2 - 72C(G)C(i)] \\
& + 8\delta_j^i g^4 C(i)(\text{Tr}[S(R)m^2] - C(G)M\tilde{M}^\dagger)
\end{aligned} \tag{9.21}$$

The β functions given above are in the \overline{DR} scheme [115]. The corresponding equations for hard parameters can be found in [38] and the results for the NMSGUT RGE's can be found in [30, 116]. In the next section we present the NMSGUT RGE's for soft parameters and the way to calculate the anomalous dimensions.

9.3 SO(10) RGEs for soft parameters

Superpotential of NMSGUT with terms bearing contraction on SO(10) indices is :

$$\begin{aligned}
W = & \frac{1}{2}\mu_H H_i^2 + \frac{\mu_\Theta}{4!}\Phi_{ijkl}\Phi_{ijkl} + \frac{\lambda}{4!}\Phi_{ijkl}\Phi_{klmn}\Phi_{mnij} + \frac{\mu_{\Sigma,\bar{\Sigma}}}{5!}\Sigma_{ijklm}\bar{\Sigma}_{ijklm} \\
& + \frac{\eta}{4!}\Phi_{ijkl}\Sigma_{ijmno}\bar{\Sigma}_{klmno} + \frac{1}{4!}H_i\Phi_{jklm}(\gamma\Sigma_{ijklm} + \bar{\gamma}\bar{\Sigma}_{ijklm}) \\
& + \frac{\mu_\Theta}{2(3!)}\Theta_{ijk}\Theta_{ijk} + \frac{k}{3!}\Theta_{ijk}H_m\Phi_{mijk} + \frac{\rho}{4!}\Theta_{ijk}\Theta_{mnk}\Phi_{ijmn} \\
& + \frac{1}{2(3!)}\Theta_{ijk}\Phi_{klmn}(\zeta\Sigma_{lmnij} + \bar{\zeta}\bar{\Sigma}_{lmnij}) + h_{AB}\Psi_A^T C_2^{(5)}\gamma_i\Psi_B H_i \\
& + \frac{1}{5!}f_{AB}\Psi_A^T C_2^{(5)}\gamma_{i_1}\dots\gamma_{i_5}\Psi_B\bar{\Sigma}_{i_1\dots i_5} + \frac{1}{3!}g_{AB}\Psi_A^T C_2^{(5)}\gamma_{i_1}\gamma_{i_2}\gamma_{i_3}\Psi_B\Theta_{i_1 i_2 i_3} \tag{9.22}
\end{aligned}$$

Here i, j, k, l, m, n run over 1 to 10. Corresponding to each term in superpotential we have soft term (each soft trilinear coupling corresponding to hard coupling bears tilde on it). First we need to calculate the anomalous dimensions for each superfield. Anomalous dimensions are calculated from wave function renormalization only due to “non-renormalization” theorems of supersymmetry which prevent coupling constant renormalization in the superpotential [52]. For example if we want to calculate the 1-loop β function for $\tilde{\lambda}$ (soft term corresponding to trilinear coupling λ) we need to follow steps given below:

1. Identify the superfields in the λ coupling term (just 210-plet components Φ_{ijkl}

in this case).

2. Then identify the gauge invariant combinations of Φ with other superfields.
3. Then taking any independent component say Φ_{1234} as the (conserved by SO(10)) external line of the propagator, (the other two superfields from the trilinear combination will run inside the loop) calculate the number of ways it gets wave function corrections from the fields this chosen external component couples to in the λ vertices. Since it must emerge with the same SO(10) quantum numbers as it entered with and the counting will apply equally to every such field component, a little practice suffices to get all 1-loop anomalous dimensions. It is clear from Eqn. (9.24) that it gets corrections from $\eta, \kappa, \lambda, \rho, \gamma, \bar{\gamma}, \zeta, \bar{\zeta}$ trilinear coupling terms. The β functions at one loop can be read off from Eqn.(9.11).

thus the one-loop beta function for the soft parameter $\tilde{\lambda}$ is:

$$\beta_{\tilde{\lambda}}^{(1)} = 3\tilde{\lambda}\bar{\gamma}_{\Phi}^{(1)} + 6\lambda\tilde{\gamma}_{\Phi}^{(1)} - 72g_{10}^2(\tilde{\lambda} - 2M\lambda) \quad (9.23)$$

where $\bar{\gamma}_{\Phi}^{(1)} = \frac{1}{2}Y_{\Phi mn}Y^{mn\Phi}$ and $\tilde{\gamma}_{\Phi}^{(1)} = \frac{1}{2}Y_{\Phi mn}h^{mn\Phi}$ are anomalous dimensions

$$\bar{\gamma}_{\Phi}^{(1)} = 4|\kappa|^2 + 180|\lambda|^2 + 2|\rho|^2 + 240|\eta|^2 + 6(|\gamma|^2 + |\bar{\gamma}|^2) + 60(|\zeta|^2 + |\bar{\zeta}|^2) \quad (9.24)$$

$$\tilde{\gamma}_{\Phi}^{(1)} = 4\tilde{\kappa}\kappa^* + 180\tilde{\lambda}\lambda^* + 2\tilde{\rho}\rho^* + 240\tilde{\eta}\eta^* + 6(\tilde{\gamma}\gamma^* + \tilde{\bar{\gamma}}\bar{\gamma}^*) + 60(\tilde{\zeta}\zeta^* + \tilde{\bar{\zeta}}\bar{\zeta}^*) \quad (9.25)$$

The numbers appearing in the above equations can be calculated as follows. Say we want to find β function for the $\tilde{\lambda}^{1234,3456,5612}$. For this we need to calculate the anomalous dimension for fields $\Phi_{1234}, \Phi_{3456}, \Phi_{5612}$. Let's calculate for Φ_{1234} . The first term in $\bar{\gamma}_{\Phi}^{(1)}$ gives the number of ways Φ_{1234} field line gets loop correction from κ trilinear coupling term. It is calculated as follows:

$$\begin{aligned} \frac{\kappa}{3!}H_i\Theta_{jkl}\Phi_{ijkl} &= \kappa\Phi_{1234}(H_1\Theta_{234} - H_2\Theta_{134} + H_3\Theta_{124} - H_4\Theta_{123}) \\ &+ \text{terms without } \Phi_{1234} \end{aligned} \quad (9.26)$$

So we have four terms which will give 1-loop wave function correction to Φ_{1234} from κ term. Similarly we can calculate the other factors. Care must be taken in the calculation of the factor corresponding to η term as there will be doubling of counted terms due to (anti) self-duality of $(\bar{\Sigma})\Sigma$.

1-loop β functions for the SO(10) gauge coupling constant and gaugino mass parameter are

$$\beta_{g_{10}}^{(1)} = 137g_{10}^3 \quad (9.27)$$

$$\beta_M^{(1)} = 274Mg_{10}^2 \quad (9.28)$$

Here $S(R)-3C(G)=137$ with $S(R)=161$ and $C(G)=C(45)=S(45)=8$. The Table 9.1 gives the Dynkin index and Casimir invariant for different representations of NMSGUT. We get a total index $S(R)=1+(3 \times 2)+28+35+35+56=161$.

d	S(R)	C(R) = 45S(R)/d(R)
10	1	9/2
16	2	45/8
120	28	21/2
126	35	25/2
$\overline{126}$	35	25/2
210	56	12

Table 9.1: Dynkin index and Casimir invariant for different field representations of NMSGUT.

The anomalous dimensions for 2-loop beta functions can be calculated once the anomalous dimensions for 1-loop are in hand by extending the summation techniques explained above. For example, the anomalous dimensions for 2-loop beta functions for $\tilde{\lambda}$ (given below) contains anomalous dimensions for all fields at 1-loop.

$$\begin{aligned} \beta_{\tilde{\lambda}}^{(2)} = & 3(-\tilde{\lambda}\bar{\gamma}_{\Phi}^{(2)} - \lambda\tilde{\gamma}_{\Phi}^{(2)} - \lambda\hat{\gamma}_{\Phi}^{(2)} + 2g_{10}^2((\tilde{\lambda} - 2M\lambda)(3120|\eta|^2 + 12|\kappa|^2 + 2160|\lambda|^2 \\ & + 18|\rho|^2 + 30|\gamma|^2 + 30|\bar{\gamma}|^2 + 660|\zeta|^2 + 660|\bar{\zeta}|^2) + 2\lambda(3120\tilde{\eta}\eta^* + 12\tilde{\kappa}\kappa^* + 18\tilde{\rho}\rho^* \\ & + 2160\tilde{\lambda}\lambda^* + 30\tilde{\gamma}\gamma^* + 30\tilde{\bar{\gamma}}\bar{\gamma}^* + 660\tilde{\zeta}\zeta^* + 660\tilde{\bar{\zeta}}\bar{\zeta}^*)) \\ & + 1932g_{10}^4(2\tilde{\lambda} - 8M\lambda) \end{aligned} \quad (9.29)$$

Where the anomalous dimensions $\bar{\gamma}_\Phi^{(2)} = -\frac{1}{2}Y_{\Phi mn}Y^{npq}Y_{pqr}Y^{mr\Phi}$, $\tilde{\gamma}_\Phi^{(2)} = Y_{\Phi mn}Y^{npq}Y_{pqr}h^{mr\Phi}$ and $\hat{\gamma}_\Phi^{(2)} = Y_{\Phi mn}h^{npq}Y_{pqr}Y^{mr\Phi}$ are given by

$$\begin{aligned}\bar{\gamma}_\Phi^{(2)} &= 240|\eta|^2(\bar{\gamma}_\Sigma^{(1)} + \bar{\gamma}_{\bar{\Sigma}}^{(1)}) + 4|\kappa|^2(\bar{\gamma}_H^{(1)} + \bar{\gamma}_\Theta^{(1)}) + 360|\lambda|^2\bar{\gamma}_\Phi^{(1)} + 4|\rho|^2\bar{\gamma}_\Theta^{(1)} \\ &\quad + 6|\gamma|^2(\bar{\gamma}_H^{(1)} + \bar{\gamma}_\Sigma^{(1)}) + 6|\bar{\gamma}|^2(\bar{\gamma}_H^{(1)} + \bar{\gamma}_{\bar{\Sigma}}^{(1)}) + 60|\zeta|^2(\bar{\gamma}_\Theta^{(1)} + \bar{\gamma}_{\bar{\Sigma}}^{(1)}) \\ &\quad + 60|\bar{\zeta}|^2(\bar{\gamma}_\Theta^{(1)} + \bar{\gamma}_{\bar{\Sigma}}^{(1)})\end{aligned}\quad (9.30)$$

$$\begin{aligned}\tilde{\gamma}_\Phi^{(2)} &= 480\tilde{\eta}\eta^*(\bar{\gamma}_\Sigma^{(1)} + \bar{\gamma}_{\bar{\Sigma}}^{(1)}) + 8\tilde{\kappa}\kappa^*(\bar{\gamma}_H^{(1)} + \bar{\gamma}_\Theta^{(1)}) + 720\tilde{\lambda}\lambda^*\bar{\gamma}_\Phi^{(1)} \\ &\quad + 8\tilde{\rho}\rho^*\bar{\gamma}_\Theta^{(1)} + 12\tilde{\gamma}\gamma^*(\bar{\gamma}_H^{(1)} + \bar{\gamma}_\Sigma^{(1)}) + 12\tilde{\bar{\gamma}}\bar{\gamma}^*(\bar{\gamma}_H^{(1)} + \bar{\gamma}_{\bar{\Sigma}}^{(1)}) \\ &\quad + 120\tilde{\zeta}\zeta^*(\bar{\gamma}_\Theta^{(1)} + \bar{\gamma}_{\bar{\Sigma}}^{(1)}) + 120\tilde{\bar{\zeta}}\bar{\zeta}^*(\bar{\gamma}_\Theta^{(1)} + \bar{\gamma}_{\bar{\Sigma}}^{(1)})\end{aligned}\quad (9.31)$$

$$\begin{aligned}\hat{\gamma}_\Phi^{(2)} &= 480|\eta|^2(\tilde{\gamma}_\Sigma^{(1)} + \tilde{\gamma}_{\bar{\Sigma}}^{(1)}) + 8|\kappa|^2(\tilde{\gamma}_H^{(1)} + \tilde{\gamma}_\Theta^{(1)}) + 720|\lambda|^2\tilde{\gamma}_\Phi^{(1)} \\ &\quad + 8|\rho|^2\tilde{\gamma}_\Theta^{(1)} + 12|\gamma|^2(\tilde{\gamma}_H^{(1)} + \tilde{\gamma}_\Sigma^{(1)}) + 12|\tilde{\gamma}|^2(\tilde{\gamma}_H^{(1)} + \tilde{\gamma}_{\bar{\Sigma}}^{(1)}) \\ &\quad + 120|\zeta|^2(\tilde{\gamma}_\Theta^{(1)} + \tilde{\gamma}_{\bar{\Sigma}}^{(1)}) + 120|\bar{\zeta}|^2(\tilde{\gamma}_\Theta^{(1)} + \tilde{\gamma}_{\bar{\Sigma}}^{(1)})\end{aligned}\quad (9.32)$$

The rest of the anomalous dimensions and β functions for 1-loop and 2-loop are given in Appendix A.

9.4 Illustrative run down values of soft parameters at one loop

In this section we present an example for run down soft Susy breaking parameters of NMSGUT at 1-loop. The soft Susy parameters chosen at M_{Planck} scale in terms of $m_{3/2}$ are [117]:

$$A_0 = 3m_{3/2}; \quad m_0^2 = m_{3/2}^2; \quad B = A_0 - m_{3/2}; \quad M = 0 \quad (9.33)$$

and we take $m_{3/2}=10$ TeV at M_{Planck} scale. The choice of $M = 0$ is valid if we assume canonical gauge/gaugino kinetic terms in the Lagrangian. At one loop it comes out zero at GUT scale too. However even $M(M_X^0)=0$ is acceptable in NMSGUT [29] as

we are able to get the acceptable gaugino masses at M_S with 2-loop MSSM RGE running from GUT scale. The main motive of this preliminary study is to see the variation in the soft sector parameters. In Figure 9.1 we present the running of various squared Higgs mass parameters. This is the main result as in NMSGUT the negative Higgs mass square are required for fermion fitting and are the reason for the normal hierarchy for the s-fermions [28]. Table 9.2 contains the sample values of hard parameters of NMSGUT superpotential and Table 9.3 contains the soft Susy breaking parameters at M_{Planck} and M_{GUT} respectively.

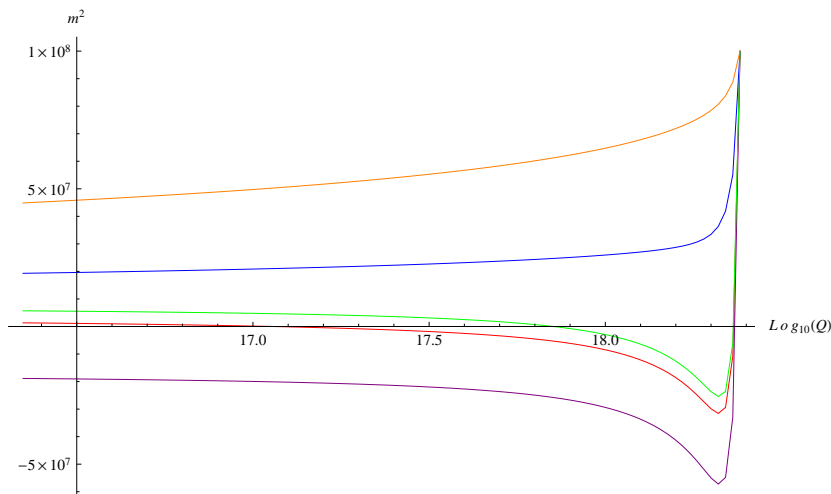


Figure 9.1: Variation of Different Higgs masses squared (m_{Φ}^2 (purple), m_{Σ}^2 (red), m_{Σ}^2 (green), m_{Θ}^2 (blue), m_H^2 (orange)) from $t = \text{Log}_{10}(10^{18.38})$ to $t = \text{Log}_{10}(10^{16.33})$.

The soft masses ($b_H, b_{\Theta}, b_{\Phi}, b_{\Sigma, \bar{\Sigma}}$) for different NMSGUT Higgs representations ($b_{ij} = B \mu_{ij}$) comes out to be very large $O(10^{16}) \text{ GeV}^2$ i.e. $O(m_{3/2} M_X)$ since the hard mass parameters μ_{ij} have GUT scale mass. So the fine tuning condition (discussed in Chapter 2) to determine a pair of light MSSM Higgs will need to be supplemented. The soft masses will also contribute to $m_{H, \bar{H}}^2(M_S)$ that are $O(m_{3/2} M_X) \gg M_S$. So we need to impose an additional condition that the contribution from the soft terms to $b_{H, \bar{H}}$ is $O(m_{3/2}^2)$. One important point to mention is that the value of m_H^2 given in Table 9.3 is the soft squared mass for 10-plet Higgs of NMSGUT and not the $m_{H, \bar{H}}^2$ which is soft squared mass parameters for effective MSSM light Higgs doublets. The running of trilinear soft coupling and s-fermion mass squared parameters ($m_{\frac{2}{3}}^2$) may give distinct values at GUT scale for the three generations: which was considered

Parameter	Value at $M_{Pl} = 10^{18.39} GeV$	Value at $M_X = 10^{16.33} GeV$
g_{10}	1.252	0.336
$h_{11}/10^{-5}$	5.81	6.84
$h_{12}/10^{-7}$	0.0	$3.281 - .088i$
$h_{13}/10^{-7}$	0.0	$0.039 - 1.095i$
$h_{22}/10^{-3}$	-5.86	-6.902
$h_{23}/10^{-7}$	0.0	$-.002 + .12i$
h_{33}	0.0141	0.0166
$f_{11}/10^{-6}$	$0.236 + 1.62i$	$.158 + 1.083i$
$f_{12}/10^{-6}$	$-2.50 - 1.78i$	$-1.668 - 1.191$
$f_{13}/10^{-6}$	$0.55 + 5.15i$	$36.745 + 3.437i$
$f_{22}/10^{-6}$	$6.76 + 0.18i$	$4.51 + .12i$
$f_{23}/10^{-4}$	$-1.26 - .52i$	$-.842 + .349i$
$f_{33}/10^{-4}$	$3.89 + .178i$	$2.599 + .119i$
$g_{12}/10^{-4}$	$-0.784 + 1.53i$	$-0.777 + 1.515i$
$g_{13}/10^{-3}$	$-1.2 + .163i$	$-1.188 + 0.161i$
g_{23}	$-0.0116 - 0.014i$	$-.0115 - 0.004i$
η	$1.21 + 0.013i$	$0.16 + 0.002i$
λ	$0.22 + 0.025i$	$0.02 + 0.002i$
γ	$0.241 + 0.046i$	$0.058 + 0.011i$
$\bar{\gamma}$	$0.251 + 0.053i$	$0.058 + 0.012i$
κ	$0.361 + 0.02i$	$0.123 + 0.007i$
ρ	$0.53 + .031i$	$0.15 + .009i$
ζ	$0.711 + 0.065i$	$0.143 + 0.013i$
$\bar{\zeta}$	$0.801 + 0.072i$	$0.155 + 0.014i$
Parameter	Value (in GeV)	Value (in GeV)
μ_Φ	10^{14}	2.033×10^{13}
μ_Θ	10^{14}	6.381×10^{13}
μ_H	10^{14}	8.997×10^{13}
$\mu_{\Sigma, \bar{\Sigma}}$	10^{14}	3.018×10^{13}

Table 9.2: Variation of hard parameters of NMSGUT superpotential at 1-loop level.

same in our studies of NMSGUT in previous chapters. This will be studied hereafter.

9.5 Discussion

The NMSGUT RGEs are important because they give us the soft Susy breaking parameters at GUT scale derived from the Gravitino mass parameter $m_{3/2}$ and the soft trilinear A_0 at the Planck scale where they may have their origin. They give

Parameter	Value (in GeV) <i>at</i> $M_{Pl} = 10^{18.39} GeV$	Value (in GeV) <i>at</i> $M_X = 10^{16.33} GeV$
\tilde{h}_{11}	1.74	1.84
\tilde{h}_{12}	0.0	$0.025 - 0.007i$
\tilde{h}_{13}	0.0	$0.003 - 0.008i$
\tilde{h}_{22}	-176.07	-185.16
\tilde{h}_{23}	0.0	$-0.0002 + 0.0009i$
\tilde{h}_{33}	423.0	444.64
\tilde{f}_{11}	$0.007 + 0.049i$	$0.003 + 0.022i$
\tilde{f}_{12}	$-0.075 - 0.054i$	$-0.034 - 0.024i$
\tilde{f}_{13}	$1.649 + 0.154i$	$0.742 + 0.069i$
\tilde{f}_{22}	$0.203 + 0.005i$	$0.091 + 0.002i$
\tilde{f}_{23}	$-3.78 + 1.569i$	$-1.696 + 0.704i$
\tilde{f}_{33}	$11.67 + 0.534i$	$5.236 + 0.239i$
\tilde{g}_{12}	$-2.352 + 4.59i$	$-1.826 + 3.564i$
\tilde{g}_{13}	$-36.0 + 4.89i$	$-27.95 + 3.796i$
\tilde{g}_{23}	$-348.0 - 43.08i$	$-270.14 - 33.44i$
$\tilde{\eta}$	$36300.0 + 397.5i$	$-140.48 - 1.54i$
$\tilde{\lambda}$	$6600.0 + 757.5i$	$-104.24 - 11.96i$
$\tilde{\gamma}$	$7218.0 + 1387.5i$	$335.37 + 64.47i$
$\tilde{\bar{\gamma}}$	$7518.0 + 1597.5i$	$309.26 + 65.72i$
$\tilde{\kappa}$	$10818.0 + 607.80i$	$1074.31 + 60.36i$
$\tilde{\rho}$	$15900.0 + 930.0$	$825.58 + 48.68i$
$\tilde{\zeta}$	$21318.0 + 1957.77i$	$360.24 + 33.08i$
$\tilde{\bar{\zeta}}$	$24018.0 + 2167.77i$	$318.26 + 28.72i$
M	0.0	0.0
Parameter	Value (in GeV^2)	Value (in GeV^2)
b_Φ	2×10^{18}	-7.01×10^{16}
b_Θ	2×10^{18}	4.553×10^{17}
b_H	2×10^{18}	1.237×10^{18}
$b_{\Sigma, \bar{\Sigma}}$	2×10^{18}	2.624×10^{16}
m_Φ^2	10^8	-1.88×10^7
m_Θ^2	10^8	1.93×10^7
m_H^2	10^8	4.47×10^7
m_Σ^2	10^8	5.71×10^6
$m_{\bar{\Sigma}}^2$	10^8	1.36×10^6
Eval[$m_{\tilde{\Psi}}^2$]	$\{10^8, 10^8, 10^8\}$	$\{9.999, 9.92, 9.91\} \times 10^7$

Table 9.3: Variation of Soft Susy breaking parameters of NMSGUT at 1-loop level.

negative mass squared for one NMSGUT Higgs multiplet which is required for the explanation of the negative Higgs mass squared found by NMSGUT in random searches for fits of the entire fermion spectra for large $\tan\beta$. We found the results at 1-loop only, so the consistency checks at 2-loops are remaining. The incorporation of NMSGUT RGE's to our fitting code is a big project as it will impose an additional next to leading order fine tuning condition for having one pair of light Higgs doublets in effective MSSM from NMSGUT. We can have different soft trilinear coupling parameter A_0 and masses for different generations of sfermions, which were assumed same in the previous work [27–29]. Thus using our results one can calculate soft Susy breaking parameters by RGE runs of soft parameters from Planck scale and then use the resulting values at GUT scale for further fitting procedure. We note that the techniques we have used to actually evaluate the 2-loop RGEs have overcome the combinatorial complexity that prevented their calculation by automated means. They can be used for any Susy theory.

9.6 Appendix A

Anomalous dimension associated with different superfields for 1-loop β functions are:

$$\bar{\gamma}_{\Sigma}^{(1)} = 200|\eta|^2 + 10|\gamma|^2 + 100|\zeta|^2 \quad (9.34)$$

$$\bar{\gamma}_{\bar{\Sigma}}^{(1)} = 200|\eta|^2 + 10|\bar{\gamma}|^2 + 100|\bar{\zeta}|^2 + 32\text{Tr}[f^\dagger \cdot f] \quad (9.35)$$

$$\bar{\gamma}_H^{(1)} = 84|\kappa|^2 + 126(|\gamma|^2 + |\bar{\gamma}|^2) + 8\text{Tr}[h^\dagger \cdot h] \quad (9.36)$$

$$\bar{\gamma}_{\Theta}^{(1)} = 7(|\kappa|^2 + |\rho|^2) + 105(|\zeta|^2 + |\bar{\zeta}|^2) + 8\text{Tr}[g^\dagger \cdot g] \quad (9.37)$$

$$\bar{\gamma}_{\Psi}^{(1)} = 252f^\dagger \cdot f + 120g^\dagger \cdot g + 10h^\dagger \cdot h \quad (9.38)$$

$$\bar{\gamma}_i^{(1)j} = \frac{1}{2}Y_{ipq}h^{jpa} \quad (9.39)$$

$$\tilde{\gamma}_{\Sigma}^{(1)} = 200\tilde{\eta}\eta^* + 10\tilde{\gamma}\gamma^* + 100\tilde{\zeta}\zeta^* \quad (9.40)$$

$$\tilde{\gamma}_{\bar{\Sigma}}^{(1)} = 200\tilde{\eta}\eta^* + 10\tilde{\gamma}\gamma^* + 100\tilde{\zeta}\zeta^* + 32\text{Tr}[f^\dagger \cdot \tilde{f}] \quad (9.41)$$

$$\tilde{\gamma}_H^{(1)} = 84\tilde{\kappa}\kappa^* + 126(\tilde{\gamma}\gamma^* + \tilde{\gamma}\gamma^*) + 8\text{Tr}[h^\dagger \cdot \tilde{h}] \quad (9.42)$$

$$\tilde{\gamma}_{\Theta}^{(1)} = 7(\tilde{\kappa}\kappa^* + \tilde{\rho}\rho^*) + 105(\tilde{\zeta}\zeta^* + \tilde{\zeta}\zeta^*) + 8\text{Tr}[g^\dagger \cdot \tilde{g}] \quad (9.43)$$

$$\tilde{\gamma}_{\psi}^{(1)} = 252f^\dagger \cdot \tilde{f} + 120g^\dagger \cdot \tilde{g} + 10h^\dagger \cdot \tilde{h} \quad (9.44)$$

$$\hat{\gamma}_i^{(1)j} = \frac{1}{2}h_{ipq}h^{jpa} \quad (9.45)$$

$$\hat{\gamma}_{\Phi}^{(1)} = 240|\tilde{\eta}|^2 + 4|\tilde{\kappa}|^2 + 180|\tilde{\lambda}|^2 + 2|\tilde{\rho}|^2 + 6(|\tilde{\gamma}|^2 + |\tilde{\gamma}|^2) + 60(|\tilde{\zeta}|^2 + |\tilde{\zeta}|^2) \quad (9.46)$$

$$\hat{\gamma}_{\Sigma}^{(1)} = 200|\tilde{\eta}|^2 + 10|\tilde{\gamma}|^2 + 100|\tilde{\zeta}|^2 \quad (9.47)$$

$$\hat{\gamma}_{\Sigma}^{(1)} = 200|\tilde{\eta}|^2 + 10|\tilde{\gamma}|^2 + 100|\tilde{\zeta}|^2 + 32\text{Tr}[\tilde{f}^\dagger \cdot \tilde{f}] \quad (9.48)$$

$$\hat{\gamma}_H^{(1)} = 84|\tilde{\kappa}|^2 + 126(|\tilde{\gamma}|^2 + |\tilde{\zeta}|^2) + 8\text{Tr}[\tilde{h}^\dagger \cdot \tilde{h}] \quad (9.49)$$

$$\hat{\gamma}_{\Theta}^{(1)} = 7(|\tilde{\kappa}|^2 + |\tilde{\rho}|^2) + 105(|\tilde{\zeta}|^2 + |\tilde{\zeta}|^2) + 8\text{Tr}[\tilde{g}^\dagger \cdot \tilde{g}] \quad (9.50)$$

$$\hat{\gamma}_{\Psi}^{(1)} = 252\tilde{f}^\dagger \cdot \tilde{f} + 120\tilde{g}^\dagger \cdot \tilde{g} + 10\tilde{h}^\dagger \cdot \tilde{h} \quad (9.51)$$

One-loop beta functions for the soft parameters:

$$\beta_{\tilde{\eta}}^{(1)} = \tilde{\eta}(\tilde{\gamma}_{\Phi}^{(1)} + \tilde{\gamma}_{\Sigma}^{(1)} + \tilde{\gamma}_{\Theta}^{(1)}) + 2\eta(\tilde{\gamma}_{\Phi}^{(1)} + \tilde{\gamma}_{\Sigma}^{(1)} + \tilde{\gamma}_{\Theta}^{(1)}) - 74g_{10}^2(\tilde{\eta} - 2M\eta) \quad (9.52)$$

$$\beta_{\tilde{\gamma}}^{(1)} = \tilde{\gamma}(\tilde{\gamma}_{\Phi}^{(1)} + \tilde{\gamma}_{\Sigma}^{(1)} + \tilde{\gamma}_H^{(1)}) + 2\gamma(\tilde{\gamma}_{\Phi}^{(1)} + \tilde{\gamma}_{\Sigma}^{(1)} + \tilde{\gamma}_H^{(1)}) - 58g_{10}^2(\tilde{\gamma} - 2M\gamma) \quad (9.53)$$

$$\beta_{\tilde{\gamma}}^{(1)} = \tilde{\tilde{\gamma}}(\tilde{\gamma}_{\Phi}^{(1)} + \tilde{\gamma}_{\Sigma}^{(1)} + \tilde{\gamma}_H^{(1)}) + 2\tilde{\gamma}(\tilde{\gamma}_{\Phi}^{(1)} + \tilde{\gamma}_{\Sigma}^{(1)} + \tilde{\gamma}_H^{(1)}) - 58g_{10}^2(\tilde{\tilde{\gamma}} - 2M\tilde{\gamma}) \quad (9.54)$$

$$\beta_{\tilde{\kappa}}^{(1)} = \tilde{\kappa}(\tilde{\gamma}_{\Phi}^{(1)} + \tilde{\gamma}_{\Theta}^{(1)} + \tilde{\gamma}_H^{(1)}) + 2\kappa(\tilde{\gamma}_{\Phi}^{(1)} + \tilde{\gamma}_{\Theta}^{(1)} + \tilde{\gamma}_H^{(1)}) - 54g_{10}^2(\tilde{\kappa} - 2M\kappa) \quad (9.55)$$

$$\beta_{\tilde{\rho}}^{(1)} = \tilde{\rho}(\tilde{\gamma}_{\Phi}^{(1)} + 2\tilde{\gamma}_{\Theta}^{(1)}) + 2\rho(\tilde{\gamma}_{\Phi}^{(1)} + 2\tilde{\gamma}_{\Theta}^{(1)}) - 66g_{10}^2(\tilde{\rho} - 2M\rho) \quad (9.56)$$

$$\beta_{\tilde{\zeta}}^{(1)} = \tilde{\zeta}(\tilde{\gamma}_{\Phi}^{(1)} + \tilde{\gamma}_{\Sigma}^{(1)} + \tilde{\gamma}_{\Theta}^{(1)}) + 2\zeta(\tilde{\gamma}_{\Phi}^{(1)} + \tilde{\gamma}_{\Sigma}^{(1)} + \tilde{\gamma}_{\Theta}^{(1)}) - 70g_{10}^2(\tilde{\zeta} - 2M\zeta) \quad (9.57)$$

$$\beta_{\tilde{\zeta}}^{(1)} = \tilde{\tilde{\zeta}}(\tilde{\gamma}_{\Phi}^{(1)} + \tilde{\gamma}_{\Sigma}^{(1)} + \tilde{\gamma}_{\Theta}^{(1)}) + 2\tilde{\zeta}(\tilde{\gamma}_{\Phi}^{(1)} + \tilde{\gamma}_{\Sigma}^{(1)} + \tilde{\gamma}_{\Theta}^{(1)}) - 70g_{10}^2(\tilde{\tilde{\zeta}} - 2M\tilde{\zeta}) \quad (9.58)$$

$$\beta_{\tilde{h}}^{(1)} = \tilde{\gamma}_H^{(1)}\tilde{h} + \tilde{h} \cdot \tilde{\gamma}_{\Psi}^{(1)} + (\tilde{\gamma}_{\Psi}^{(1)})^T \cdot \tilde{h} + 2\tilde{\gamma}_H^{(1)}h + 2(h \cdot \tilde{\gamma}_{\Psi}^{(1)} + (\tilde{\gamma}_{\Psi}^{(1)})^T \cdot h) - \frac{63}{2}g_{10}^2(\tilde{h} - 2Mh) \quad (9.59)$$

$$\beta_{\tilde{g}}^{(1)} = \tilde{\gamma}_{\Theta}^{(1)}\tilde{g} + \tilde{g} \cdot \tilde{\gamma}_{\Psi}^{(1)} + (\tilde{\gamma}_{\Psi}^{(1)})^T \cdot \tilde{g} + 2\tilde{\gamma}_{\Theta}^{(1)}g + 2(g \cdot \tilde{\gamma}_{\Psi}^{(1)} - (\tilde{\gamma}_{\Psi}^{(1)})^T \cdot g) - \frac{87}{2}g_{10}^2(\tilde{g} - 2Mg) \quad (9.60)$$

$$\beta_{\tilde{f}}^{(1)} = \bar{\gamma}_{\Sigma}^{(1)} \tilde{f} + \tilde{f} \cdot \bar{\gamma}_{\Psi}^{(1)} + (\bar{\gamma}_{\Psi}^{(1)})^T \cdot \tilde{f} + 2\bar{\gamma}_{\Sigma}^{(1)} \cdot f + 2(f \cdot \bar{\gamma}_{\Psi}^{(1)} + (\bar{\gamma}_{\Psi}^{(1)})^T \cdot f) - \frac{95}{2} g_{10}^2 (\tilde{f} - 2Mf) \quad (9.61)$$

$$\beta_{b_{\Phi}}^{(1)} = 2b_{\Phi} \bar{\gamma}_{\Phi}^{(1)} + 4\mu_{\Phi} \tilde{\gamma}_{\Phi}^{(1)} - 48g_{10}^2 (b_{\Phi} - 2M\mu_{\Phi}) \quad (9.62)$$

$$\beta_{b_H}^{(1)} = 2b_H \bar{\gamma}_H^{(1)} + 4\mu_H \tilde{\gamma}_H^{(1)} - 18g_{10}^2 (b_H - 2M\mu_H) \quad (9.63)$$

$$\beta_{b_{\Theta}}^{(1)} = 2b_{\Theta} \bar{\gamma}_{\Theta}^{(1)} + 4\mu_{\Theta} \tilde{\gamma}_{\Theta}^{(1)} - 42g_{10}^2 (b_{\Theta} - 2M\mu_{\Theta}) \quad (9.64)$$

$$\beta_{b_{\Sigma}}^{(1)} = b_{\Sigma} (\bar{\gamma}_{\Sigma}^{(1)} + \bar{\gamma}_{\Sigma}^{(1)}) + 2\mu_{\Sigma} (\tilde{\gamma}_{\Sigma}^{(1)} + \tilde{\gamma}_{\Sigma}^{(1)}) - 50g_{10}^2 (b_{\Sigma} - 2M\mu_{\Sigma}) \quad (9.65)$$

$$\begin{aligned} \beta_{m_{\Phi}^2}^{(1)} &= 2\bar{\gamma}_{\Phi}^{(1)} m_{\Phi}^2 + 720m_{\Phi}^2 |\lambda|^2 + m_H^2 (12|\gamma|^2 + 12|\bar{\gamma}|^2 + 8|\kappa|^2) \\ &\quad + m_{\Theta}^2 (8|\rho|^2 + 120(|\zeta|^2 + |\bar{\zeta}|^2) + 8|\kappa|^2) + m_{\Sigma}^2 (480|\eta|^2 + 12|\gamma|^2 + 120|\zeta|^2) \\ &\quad + m_{\Sigma}^2 (480|\eta|^2 + 12|\bar{\gamma}|^2 + 120|\bar{\zeta}|^2) + 2\hat{\gamma}_{\Phi}^{(1)} - 96|M|^2 g_{10}^2 \end{aligned} \quad (9.66)$$

$$\begin{aligned} \beta_{m_H^2}^{(1)} &= 2\bar{\gamma}_H^{(1)} m_H^2 + m_{\Phi}^2 (252(|\gamma|^2 + |\bar{\gamma}|^2) + 168|\kappa|^2) + 168m_{\Theta}^2 |\kappa|^2 + 252m_{\Sigma}^2 |\gamma|^2 \\ &\quad + 252m_{\Sigma}^2 |\bar{\gamma}|^2 + 2\hat{\gamma}_H^{(1)} - 36|M|^2 g_{10}^2 + 32\text{Tr}[h^{\dagger} \cdot m_{\Psi}^2 \cdot h] \end{aligned} \quad (9.67)$$

$$\begin{aligned} \beta_{m_{\Theta}^2}^{(1)} &= 2\bar{\gamma}_{\Theta}^{(1)} m_{\Theta}^2 + m_{\Phi}^2 (14(|\kappa|^2 + |\rho|^2) + 210(|\zeta|^2 + |\bar{\zeta}|^2)) + 14m_{\Theta}^2 |\rho|^2 + 14m_H^2 |\kappa|^2 \\ &\quad + 210m_{\Sigma}^2 |\zeta|^2 + 210m_{\Sigma}^2 |\bar{\zeta}|^2 + 2\hat{\gamma}_{\Theta}^{(1)} - 84|M|^2 g_{10}^2 + 32\text{Tr}[g^{\dagger} \cdot m_{\Psi}^2 \cdot g] \end{aligned} \quad (9.68)$$

$$\begin{aligned} \beta_{m_{\Sigma}^2}^{(1)} &= 2\bar{\gamma}_{\Sigma}^{(1)} m_{\Sigma}^2 + m_{\Phi}^2 (400|\eta|^2 + 20|\gamma|^2 + 200|\zeta|^2) + 200m_{\Theta}^2 |\zeta|^2 + 20m_H^2 |\gamma|^2 \\ &\quad + 400m_{\Sigma}^2 |\eta|^2 + 2\hat{\gamma}_{\Sigma}^{(1)} - 100|M|^2 g_{10}^2 \end{aligned} \quad (9.69)$$

$$\begin{aligned} \beta_{m_{\Xi}^2}^{(1)} &= 2\bar{\gamma}_{\Xi}^{(1)} m_{\Xi}^2 + m_{\Phi}^2 (400|\eta|^2 + 20|\bar{\gamma}|^2 + 200|\bar{\zeta}|^2) + 200m_{\Theta}^2 |\bar{\zeta}|^2 + 20m_H^2 |\bar{\gamma}|^2 \\ &\quad + 400m_{\Sigma}^2 |\eta|^2 + 2\hat{\gamma}_{\Xi}^{(1)} - 100|M|^2 g_{10}^2 + 128\text{Tr}[f^{\dagger} \cdot m_{\Psi}^2 \cdot f] \end{aligned} \quad (9.70)$$

$$\begin{aligned} \beta_{m_{\Psi}^2}^{(1)} &= \bar{\gamma}_{\Psi}^{(1)} \cdot m_{\Psi}^2 + m_{\Psi}^2 \cdot \bar{\gamma}_{\Psi}^{(1)} + 10h^{\dagger} \cdot m_{\Psi}^2 \cdot h + 120g^{\dagger} \cdot m_{\Psi}^2 \cdot g + 252f^{\dagger} \cdot m_{\Psi}^2 \cdot f + 10m_H^2 h^{\dagger} \cdot h \\ &\quad + 120m_{\Theta}^2 g^{\dagger} \cdot g + 252m_{\Sigma}^2 f^{\dagger} \cdot f + 2\hat{\gamma}_{\Psi}^{(1)} - 45|M|^2 g_{10}^2 \end{aligned} \quad (9.71)$$

The anomalous dimensions associated with the 2-loop beta functions are given as:

$$\bar{\gamma}_i^{(2)j} = -\frac{1}{2}Y_{imn}Y^{npq}Y_{pqr}Y^{mrj} \quad (9.72)$$

$$\bar{\gamma}_\Sigma^{(2)} = 200|\eta|^2(\bar{\gamma}_\Phi^{(1)} + \bar{\gamma}_\Sigma^{(1)}) + 10|\gamma|^2(\bar{\gamma}_H^{(1)} + \bar{\gamma}_\Phi^{(1)}) + 100|\zeta|^2(\bar{\gamma}_\Theta^{(1)} + \bar{\gamma}_\Phi^{(1)}) \quad (9.73)$$

$$\begin{aligned} \bar{\gamma}_\Sigma^{(2)} &= 200|\eta|^2(\bar{\gamma}_\Phi^{(1)} + \bar{\gamma}_\Sigma^{(1)}) + 10|\bar{\gamma}|^2(\bar{\gamma}_H^{(1)} + \bar{\gamma}_\Phi^{(1)}) + 100|\bar{\zeta}|^2(\bar{\gamma}_\Theta^{(1)} + \bar{\gamma}_\Phi^{(1)}) \\ &\quad + \text{Tr}[f^\dagger \cdot \bar{\gamma}_\Psi^{(1)} \cdot f] \end{aligned} \quad (9.74)$$

$$\begin{aligned} \bar{\gamma}_H^{(2)} &= 84|\kappa|^2(\bar{\gamma}_\Phi^{(1)} + \bar{\gamma}_\Theta^{(1)}) + 126|\gamma|^2(\bar{\gamma}_\Phi^{(1)} + \bar{\gamma}_\Sigma^{(1)}) + 126|\bar{\gamma}|^2(\bar{\gamma}_\Phi^{(1)} + \bar{\gamma}_\Sigma^{(1)}) \\ &\quad + \text{Tr}[h^\dagger \cdot \bar{\gamma}_\Psi^{(1)} \cdot h] \end{aligned} \quad (9.75)$$

$$\begin{aligned} \bar{\gamma}_\Theta^{(2)} &= 7|\kappa|^2(\bar{\gamma}_\Phi^{(1)} + \bar{\gamma}_H^{(1)}) + 7|\rho|^2(\bar{\gamma}_\Theta^{(1)} + \bar{\gamma}_\Phi^{(1)}) + 105|\zeta|^2(\bar{\gamma}_\Sigma^{(1)} + \bar{\gamma}_\Phi^{(1)}) \\ &\quad + 105|\bar{\zeta}|^2(\bar{\gamma}_\Sigma^{(1)} + \bar{\gamma}_\Phi^{(1)}) + \text{Tr}[g^\dagger \cdot \bar{\gamma}_\Psi^{(1)} \cdot g] \end{aligned} \quad (9.76)$$

$$\bar{\gamma}_\Psi^{(2)} = h^\dagger \cdot \bar{\gamma}_\Psi^{(1)T} \cdot h - g^\dagger \cdot \bar{\gamma}_\Psi^{(1)T} \cdot g + f^\dagger \cdot \bar{\gamma}_\Psi^{(1)T} \cdot f + h^\dagger \cdot h \gamma_H^{(1)} - g^\dagger \cdot g \gamma_\Theta^{(1)} + f^\dagger \cdot f \gamma_\Sigma^{(1)} \quad (9.77)$$

$$\tilde{\gamma}_i^{(2)j} = Y_{imn}Y^{npq}Y_{pqr}h^{mrj} \quad (9.78)$$

$$\tilde{\gamma}_\Sigma^{(2)} = 400\tilde{\eta}\eta^*(\bar{\gamma}_\Phi^{(1)} + \bar{\gamma}_\Sigma^{(1)}) + 20\tilde{\gamma}\gamma^*(\bar{\gamma}_H^{(1)} + \bar{\gamma}_\Phi^{(1)}) + 200\tilde{\zeta}\zeta^*(\bar{\gamma}_\Theta^{(1)} + \bar{\gamma}_\Phi^{(1)}) \quad (9.79)$$

$$\begin{aligned} \tilde{\gamma}_\Sigma^{(2)} &= 400\tilde{\eta}\eta^*(\bar{\gamma}_\Phi^{(1)} + \bar{\gamma}_\Sigma^{(1)}) + 20\tilde{\gamma}\gamma^*(\bar{\gamma}_H^{(1)} + \bar{\gamma}_\Phi^{(1)}) + 200\tilde{\zeta}\zeta^*(\bar{\gamma}_\Theta^{(1)} + \bar{\gamma}_\Phi^{(1)}) \\ &\quad + 2\text{Tr}[f^\dagger \cdot \bar{\gamma}_\Psi^{(1)} \cdot \tilde{f}] \end{aligned} \quad (9.80)$$

$$\begin{aligned} \tilde{\gamma}_H^{(2)} &= 168\tilde{\kappa}\kappa^*(\bar{\gamma}_\Phi^{(1)} + \bar{\gamma}_\Theta^{(1)}) + 252\tilde{\gamma}\gamma^*(\bar{\gamma}_\Phi^{(1)} + \bar{\gamma}_\Sigma^{(1)}) + 252\tilde{\gamma}\gamma^*(\bar{\gamma}_\Phi^{(1)} + \bar{\gamma}_\Sigma^{(1)}) \\ &\quad + 2\text{Tr}[h^\dagger \cdot \bar{\gamma}_\Psi^{(1)} \cdot \tilde{h}] \end{aligned} \quad (9.81)$$

$$\begin{aligned} \tilde{\gamma}_\Theta^{(2)} &= 14\tilde{\kappa}\kappa^*(\bar{\gamma}_\Phi^{(1)} + \bar{\gamma}_H^{(1)}) + 14\tilde{\rho}\rho^*(\bar{\gamma}_\Theta^{(1)} + \bar{\gamma}_\Phi^{(1)}) + 210\tilde{\zeta}\zeta^*(\bar{\gamma}_\Sigma^{(1)} + \bar{\gamma}_\Phi^{(1)}) \\ &\quad + 210\tilde{\zeta}\zeta^*(\bar{\gamma}_\Sigma^{(1)} + \bar{\gamma}_\Phi^{(1)}) + 2\text{Tr}[g^\dagger \cdot \bar{\gamma}_\Psi^{(1)} \cdot \tilde{g}] \end{aligned} \quad (9.82)$$

$$\tilde{\gamma}_{\Psi}^{(2)} = 2h^{\dagger} \cdot \tilde{\gamma}_{\Psi}^{(1)T} \cdot \tilde{h} + 2g^{\dagger} \cdot \tilde{\gamma}_{\psi}^{(1)T} \cdot \tilde{g} + 2f^{\dagger} \cdot \tilde{\gamma}_{\psi}^{(1)T} \cdot \tilde{f} + 2h^{\dagger} \cdot \tilde{h} \tilde{\gamma}_H^{(1)} + 2g^{\dagger} \cdot \tilde{g} \tilde{\gamma}_{\Theta}^{(1)} + 2f^{\dagger} \cdot \tilde{f} \tilde{\gamma}_{\Sigma}^{(1)} \quad (9.83)$$

$$\hat{\gamma}^{(2)} = Y_{imn} h^{npq} Y_{pqr} Y^{mrj} \quad (9.84)$$

$$\hat{\gamma}_{\Sigma}^{(2)} = 400|\eta|^2(\tilde{\gamma}_{\Phi}^{(1)} + \tilde{\gamma}_{\Sigma}^{(1)}) + 20|\gamma|^2(\tilde{\gamma}_H^{(1)} + \tilde{\gamma}_{\Phi}^{(1)}) + 200|\zeta|^2(\tilde{\gamma}_{\Theta}^{(1)} + \tilde{\gamma}_{\Phi}^{(1)}) \quad (9.85)$$

$$\begin{aligned} \hat{\gamma}_{\Sigma}^{(2)} &= 400|\eta|^2(\tilde{\gamma}_{\Phi}^{(1)} + \tilde{\gamma}_{\Sigma}^{(1)}) + 20|\bar{\gamma}|^2(\tilde{\gamma}_H^{(1)} + \tilde{\gamma}_{\Phi}^{(1)}) + 200|\bar{\zeta}|^2(\tilde{\gamma}_{\Theta}^{(1)} + \tilde{\gamma}_{\Phi}^{(1)}) \\ &\quad + 2\text{Tr}[f^{\dagger} \cdot \tilde{\gamma}_{\Psi}^{(1)} \cdot f] \end{aligned} \quad (9.86)$$

$$\begin{aligned} \hat{\gamma}_H^{(2)} &= 168|\kappa|^2(\tilde{\gamma}_{\Phi}^{(1)} + \tilde{\gamma}_{\Theta}^{(1)}) + 252|\gamma|^2(\tilde{\gamma}_{\Phi}^{(1)} + \tilde{\gamma}_{\Sigma}^{(1)}) + 252|\bar{\gamma}|^2(\tilde{\gamma}_{\Phi}^{(1)} + \tilde{\gamma}_{\Sigma}^{(1)}) \\ &\quad + 2\text{Tr}[h^{\dagger} \cdot \tilde{\gamma}_{\Psi}^{(1)} \cdot h] \end{aligned} \quad (9.87)$$

$$\begin{aligned} \hat{\gamma}_{\Theta}^{(2)} &= 14|\kappa|^2(\tilde{\gamma}_{\Phi}^{(1)} + \tilde{\gamma}_H^{(1)}) + 14|\rho|^2(\tilde{\gamma}_{\Theta}^{(1)} + \tilde{\gamma}_{\Phi}^{(1)}) + 210|\zeta|^2(\tilde{\gamma}_{\Sigma}^{(1)} + \tilde{\gamma}_{\Phi}^{(1)}) \\ &\quad + 210|\bar{\zeta}|^2(\tilde{\gamma}_{\Sigma}^{(1)} + \tilde{\gamma}_{\Phi}^{(1)}) + 2\text{Tr}[g^{\dagger} \cdot \tilde{\gamma}_{\Psi}^{(1)} \cdot g] \end{aligned} \quad (9.88)$$

$$\hat{\gamma}_{\Psi}^{(2)} = 2h^{\dagger} \cdot \tilde{\gamma}_{\Psi}^{(1)T} \cdot h + 2g^{\dagger} \cdot \tilde{\gamma}_{\psi}^{(1)T} \cdot g + 2f^{\dagger} \cdot \tilde{\gamma}_{\psi}^{(1)T} \cdot f + 2h^{\dagger} \cdot h \tilde{\gamma}_H^{(1)} + 2g^{\dagger} \cdot g \tilde{\gamma}_{\Theta}^{(1)} + 2f^{\dagger} \cdot f \tilde{\gamma}_{\Sigma}^{(1)} \quad (9.89)$$

$$\tilde{\gamma} = Y_{ilm} Y^{jln} h_{npq} h^{mpq} \quad (9.90)$$

$$\begin{aligned} \tilde{\gamma}_{\Phi}^{(2)} &= 480|\eta|^2(\hat{\gamma}_{\Sigma}^{(1)} + \hat{\gamma}_{\Sigma}^{(1)}) + 8|\kappa|^2(\hat{\gamma}_H^{(1)} + \hat{\gamma}_{\Theta}^{(1)}) + 720|\lambda|^2 \hat{\gamma}_{\Phi}^{(1)} \\ &\quad + 8|\rho|^2 \hat{\gamma}_{\Theta}^{(1)} + 12|\gamma|^2(\hat{\gamma}_H^{(1)} + \hat{\gamma}_{\Sigma}^{(1)}) + 12|\bar{\gamma}|^2(\hat{\gamma}_H^{(1)} + \hat{\gamma}_{\Sigma}^{(1)}) \\ &\quad + 120|\zeta|^2(\hat{\gamma}_{\Theta}^{(1)} + \hat{\gamma}_{\Sigma}^{(1)}) + 120|\bar{\zeta}|^2(\hat{\gamma}_{\Theta}^{(1)} + \hat{\gamma}_{\Sigma}^{(1)}) \end{aligned} \quad (9.91)$$

$$\tilde{\gamma}_{\Sigma}^{(2)} = 400|\eta|^2(\hat{\gamma}_{\Phi}^{(1)} + \hat{\gamma}_{\Sigma}^{(1)}) + 20|\gamma|^2(\hat{\gamma}_H^{(1)} + \hat{\gamma}_{\Phi}^{(1)}) + 200|\zeta|^2(\hat{\gamma}_{\Theta}^{(1)} + \hat{\gamma}_{\Phi}^{(1)}) \quad (9.92)$$

$$\begin{aligned} \tilde{\gamma}_{\Sigma}^{(2)} &= 400|\eta|^2(\hat{\gamma}_{\Phi}^{(1)} + \hat{\gamma}_{\Sigma}^{(1)}) + 20|\bar{\gamma}|^2(\hat{\gamma}_H^{(1)} + \hat{\gamma}_{\Phi}^{(1)}) + 200|\bar{\zeta}|^2(\hat{\gamma}_{\Theta}^{(1)} + \hat{\gamma}_{\Phi}^{(1)}) \\ &\quad + 2\text{Tr}[f^{\dagger} \cdot \hat{\gamma}_{\Psi}^{(1)} \cdot f] \end{aligned} \quad (9.93)$$

$$\begin{aligned}\tilde{\gamma}_H^{(2)} &= 168|\kappa|^2(\hat{\gamma}_\Phi^{(1)} + \hat{\gamma}_\Theta^{(1)}) + 252|\gamma|^2(\hat{\gamma}_\Phi^{(1)} + \hat{\gamma}_\Sigma^{(1)}) + 252|\bar{\gamma}|^2(\hat{\gamma}_\Phi^{(1)} + \hat{\gamma}_\Sigma^{(1)}) \\ &\quad + 2\text{Tr}[h^\dagger \cdot \hat{\gamma}_\Psi^{(1)} \cdot h]\end{aligned}\quad (9.94)$$

$$\begin{aligned}\tilde{\gamma}_\Theta^{(2)} &= 14|\kappa|^2(\hat{\gamma}_\Phi^{(1)} + \hat{\gamma}_H^{(1)}) + 14|\rho|^2(\hat{\gamma}_\Theta^{(1)} + \hat{\gamma}_\Phi^{(1)}) + 210|\zeta|^2(\hat{\gamma}_\Sigma^{(1)} + \hat{\gamma}_\Phi^{(1)}) \\ &\quad + 210|\bar{\zeta}|^2(\hat{\gamma}_\Sigma^{(1)} + \hat{\gamma}_\Phi^{(1)}) + 2\text{Tr}[g^\dagger \cdot \hat{\gamma}_\Psi^{(1)} \cdot g]\end{aligned}\quad (9.95)$$

$$\tilde{\gamma}_\Psi^{(2)} = 2h^\dagger \cdot \hat{\gamma}_\Psi^{(1)T} \cdot h + 2g^\dagger \cdot \hat{\gamma}_\Psi^{(1)T} \cdot g + 2f^\dagger \cdot \hat{\gamma}_\Psi^{(1)T} \cdot f + 2h^\dagger \cdot h \hat{\gamma}_H^{(1)} + 2g^\dagger \cdot g \hat{\gamma}_\Theta^{(1)} + 2f^\dagger \cdot f \hat{\gamma}_\Sigma^{(1)} \quad (9.96)$$

$$\dot{\gamma}^{(2)} = h_{ilm} h^{jln} Y_{npq} Y^{mpq} \quad (9.97)$$

$$\begin{aligned}\dot{\gamma}_\Phi^{(2)} &= 480|\tilde{\eta}|^2(\bar{\gamma}_\Sigma^{(1)} + \bar{\gamma}_\Sigma^{(1)}) + 8|\tilde{\kappa}|^2(\bar{\gamma}_H^{(1)} + \bar{\gamma}_\Theta^{(1)}) + 720|\tilde{\lambda}|^2\bar{\gamma}_\Phi^{(1)} \\ &\quad + 8|\tilde{\rho}|^2\bar{\gamma}_\Theta^{(1)} + 12|\tilde{\gamma}|^2(\bar{\gamma}_H^{(1)} + \bar{\gamma}_\Sigma^{(1)}) + 12|\tilde{\tilde{\gamma}}|^2(\bar{\gamma}_H^{(1)} + \bar{\gamma}_\Sigma^{(1)}) \\ &\quad + 120|\tilde{\zeta}|^2(\bar{\gamma}_\Theta^{(1)} + \bar{\gamma}_\Sigma^{(1)}) + 120|\tilde{\tilde{\zeta}}|^2(\bar{\gamma}_\Theta^{(1)} + \bar{\gamma}_\Sigma^{(1)})\end{aligned}\quad (9.98)$$

$$\dot{\gamma}_\Sigma^{(2)} = 400|\tilde{\eta}|^2(\bar{\gamma}_\Phi^{(1)} + \bar{\gamma}_\Sigma^{(1)}) + 20|\tilde{\gamma}|^2(\bar{\gamma}_H^{(1)} + \bar{\gamma}_\Phi^{(1)}) + 200|\tilde{\zeta}|^2(\bar{\gamma}_\Theta^{(1)} + \bar{\gamma}_\Phi^{(1)}) \quad (9.99)$$

$$\begin{aligned}\dot{\gamma}_\Sigma^{(2)} &= 400|\tilde{\eta}|^2(\bar{\gamma}_\Phi^{(1)} + \bar{\gamma}_\Sigma^{(1)}) + 20|\tilde{\tilde{\gamma}}|^2(\bar{\gamma}_H^{(1)} + \bar{\gamma}_\Phi^{(1)}) + 200|\tilde{\tilde{\zeta}}|^2(\bar{\gamma}_\Theta^{(1)} + \bar{\gamma}_\Phi^{(1)}) \\ &\quad + 2\text{Tr}[\tilde{f}^\dagger \cdot \bar{\gamma}_\Psi^{(1)} \cdot \tilde{f}]\end{aligned}\quad (9.100)$$

$$\begin{aligned}\dot{\gamma}_H^{(2)} &= 168|\tilde{\kappa}|^2(\bar{\gamma}_\Phi^{(1)} + \bar{\gamma}_\Theta^{(1)}) + 252|\tilde{\gamma}|^2(\bar{\gamma}_\Phi^{(1)} + \bar{\gamma}_\Sigma^{(1)}) + 252|\tilde{\tilde{\gamma}}|^2(\bar{\gamma}_\Phi^{(1)} + \bar{\gamma}_\Sigma^{(1)}) \\ &\quad + 2\text{Tr}[\tilde{h}^\dagger \cdot \bar{\gamma}_\Psi^{(1)} \cdot \tilde{h}]\end{aligned}\quad (9.101)$$

$$\begin{aligned}\dot{\gamma}_\Theta^{(2)} &= 14|\tilde{\kappa}|^2(\bar{\gamma}_\Phi^{(1)} + \bar{\gamma}_H^{(1)}) + 14|\tilde{\rho}|^2(\bar{\gamma}_\Theta^{(1)} + \bar{\gamma}_\Phi^{(1)}) + 210|\tilde{\zeta}|^2(\bar{\gamma}_\Sigma^{(1)} + \bar{\gamma}_\Phi^{(1)}) \\ &\quad + 210|\tilde{\tilde{\zeta}}|^2(\bar{\gamma}_\Sigma^{(1)} + \bar{\gamma}_\Phi^{(1)}) + 2\text{Tr}[\tilde{g}^\dagger \cdot \bar{\gamma}_\Psi^{(1)} \cdot \tilde{g}]\end{aligned}\quad (9.102)$$

$$\dot{\gamma}_\Psi^{(2)} = 2\tilde{h}^\dagger \cdot \bar{\gamma}_\Psi^{(1)T} \cdot \tilde{h} + 2\tilde{g}^\dagger \cdot \bar{\gamma}_\Psi^{(1)T} \cdot \tilde{g} + 2\tilde{f}^\dagger \cdot \bar{\gamma}_\Psi^{(1)T} \cdot \tilde{f} + 2\tilde{h}^\dagger \cdot \tilde{h} \bar{\gamma}_H^{(1)} + 2\tilde{g}^\dagger \cdot \tilde{g} \bar{\gamma}_\Theta^{(1)} + 2\tilde{f}^\dagger \cdot \tilde{f} \bar{\gamma}_\Sigma^{(1)} \quad (9.103)$$

$$\dot{\gamma}^{(2)} = h_{ilm} Y^{jln} Y_{npq} h^{mpq} \quad (9.104)$$

$$\begin{aligned}
\dot{\gamma}_{\Phi}^{(2)} &= 480\tilde{\eta}^*\eta(\tilde{\gamma}_{\Sigma}^{(1)} + \tilde{\gamma}_{\bar{\Sigma}}^{(1)}) + 8\tilde{\kappa}^*\kappa(\tilde{\gamma}_H^{(1)} + \tilde{\gamma}_{\Theta}^{(1)}) + 720\tilde{\lambda}^*\lambda\tilde{\gamma}_{\Phi}^{(1)} \\
&\quad + 8\tilde{\rho}^*\rho\tilde{\gamma}_{\Theta}^{(1)} + 12\tilde{\gamma}^*\gamma(\tilde{\gamma}_H^{(1)} + \tilde{\gamma}_{\Sigma}^{(1)}) + 12\tilde{\bar{\gamma}}^*\bar{\gamma}(\tilde{\gamma}_H^{(1)} + \tilde{\gamma}_{\bar{\Sigma}}^{(1)}) \\
&\quad + 120\tilde{\zeta}^*\zeta(\tilde{\gamma}_{\Theta}^{(1)} + \tilde{\gamma}_{\Sigma}^{(1)}) + 120\tilde{\bar{\zeta}}^*\bar{\zeta}(\tilde{\gamma}_{\Theta}^{(1)} + \tilde{\gamma}_{\bar{\Sigma}}^{(1)})
\end{aligned} \tag{9.105}$$

$$\dot{\gamma}_{\Sigma}^{(2)} = 400\tilde{\eta}^*\eta(\tilde{\gamma}_{\Phi}^{(1)} + \tilde{\gamma}_{\bar{\Sigma}}^{(1)}) + 20\tilde{\gamma}^*\gamma(\tilde{\gamma}_H^{(1)} + \tilde{\gamma}_{\Phi}^{(1)}) + 200\tilde{\zeta}^*\zeta(\tilde{\gamma}_{\Theta}^{(1)} + \tilde{\gamma}_{\Phi}^{(1)}) \tag{9.106}$$

$$\begin{aligned}
\dot{\gamma}_{\bar{\Sigma}}^{(2)} &= 400\tilde{\eta}^*\eta(\tilde{\gamma}_{\Phi}^{(1)} + \tilde{\gamma}_{\Sigma}^{(1)}) + 20\tilde{\bar{\gamma}}^*\bar{\gamma}(\tilde{\gamma}_H^{(1)} + \tilde{\gamma}_{\Phi}^{(1)}) + 200\tilde{\bar{\zeta}}^*\bar{\zeta}(\tilde{\gamma}_{\Theta}^{(1)} + \tilde{\gamma}_{\Phi}^{(1)}) \\
&\quad + 2\text{Tr}[\tilde{f}^\dagger \cdot \tilde{\gamma}_{\Psi}^{(1)} \cdot f]
\end{aligned} \tag{9.107}$$

$$\begin{aligned}
\dot{\gamma}_H^{(2)} &= 168\tilde{\kappa}^*\kappa(\tilde{\gamma}_{\Phi}^{(1)} + \tilde{\gamma}_{\Theta}^{(1)}) + 252\tilde{\gamma}^*\gamma(\tilde{\gamma}_{\Phi}^{(1)} + \tilde{\gamma}_{\Sigma}^{(1)}) + 252\tilde{\bar{\gamma}}^*\bar{\gamma}(\tilde{\gamma}_{\Phi}^{(1)} + \tilde{\gamma}_{\bar{\Sigma}}^{(1)}) \\
&\quad + 2\text{Tr}[\tilde{h}^\dagger \cdot \tilde{\gamma}_{\Psi}^{(1)} \cdot h]
\end{aligned} \tag{9.108}$$

$$\begin{aligned}
\dot{\gamma}_{\Theta}^{(2)} &= 14\tilde{\kappa}^*\kappa(\tilde{\gamma}_{\Phi}^{(1)} + \tilde{\gamma}_H^{(1)}) + 14\tilde{\rho}^*\rho(\tilde{\gamma}_{\Theta}^{(1)} + \tilde{\gamma}_{\Phi}^{(1)}) + 210\tilde{\zeta}^*\zeta(\tilde{\gamma}_{\Sigma}^{(1)} + \tilde{\gamma}_{\Phi}^{(1)}) \\
&\quad + 210\tilde{\bar{\zeta}}^*\bar{\zeta}(\tilde{\gamma}_{\bar{\Sigma}}^{(1)} + \tilde{\gamma}_{\Phi}^{(1)}) + 2\text{Tr}[\tilde{g}^\dagger \cdot \tilde{\gamma}_{\Psi}^{(1)} \cdot g]
\end{aligned} \tag{9.109}$$

$$\dot{\gamma}_{\Psi}^{(2)} = 2\tilde{h}^\dagger \cdot \tilde{\gamma}_{\Psi}^{(1)T} \cdot h + 2\tilde{g}^\dagger \cdot \tilde{\gamma}_{\Psi}^{(1)T} \cdot g + 2\tilde{f}^\dagger \cdot \tilde{\gamma}_{\Psi}^{(1)T} \cdot f + 2\tilde{h}^\dagger \cdot h \tilde{\gamma}_H^{(1)} + 2\tilde{g}^\dagger \cdot g \tilde{\gamma}_{\Theta}^{(1)} + 2\tilde{f}^\dagger \cdot f \tilde{\gamma}_{\bar{\Sigma}}^{(1)} \tag{9.110}$$

$$\check{\gamma}_i^{j(2)} = Y_{ilm} Y^{jln} Y_{npq} Y^{mpr} (m^2)_r^q \tag{9.111}$$

$$\begin{aligned}
\check{\gamma}_{\Phi}^{(2)} &= m_H^2 (720|\kappa|^2|\lambda|^2 + 14|\kappa|^2|\rho|^2 + 28|\kappa|^4 + 420|\kappa|^2|\zeta|^2 + 420|\kappa|^2|\bar{\zeta}|^2 \\
&\quad + 1080|\lambda|^2|\gamma|^2 + 1080|\lambda|^2|\bar{\gamma}|^2 + 2400|\eta|^2|\gamma|^2 + 2400|\eta|^2|\bar{\gamma}|^2 + 60|\gamma|^4 \\
&\quad + 60|\bar{\gamma}|^4 + 600|\zeta|^2|\gamma|^2 + 600|\bar{\zeta}|^2|\bar{\gamma}|^2) \\
&\quad + m_{\Theta}^2 (720|\lambda|^2|\kappa|^2 + 28|\rho|^2|\kappa|^2 + 360|\rho|^2|\lambda|^2 + 14|\rho|^4 + 420|\zeta|^2|\rho|^2 \\
&\quad + 10800|\zeta|^2|\lambda|^2 + 10800|\bar{\zeta}|^2|\lambda|^2 + 420|\bar{\zeta}|^2|\rho|^2 + 336|\kappa|^4 + 504|\kappa|^2|\gamma|^2 \\
&\quad + 504|\kappa|^2|\bar{\gamma}|^2 + 600|\zeta|^2|\gamma|^2 + 600|\bar{\zeta}|^2|\bar{\gamma}|^2 + 24000|\eta|^2|\zeta|^2 + 24000|\eta|^2|\bar{\zeta}|^2 \\
&\quad + 600|\zeta|^4 + 600|\bar{\zeta}|^4)
\end{aligned}$$

$$\begin{aligned}
& +m_{\Phi}^2(1008|\kappa|^2|\gamma|^2 + 1008|\kappa|^2|\bar{\gamma}|^2 + 364|\kappa|^4 + 816|\gamma|^4 + 1512|\gamma|^2|\bar{\gamma}|^2 \\
& +816|\bar{\gamma}|^4 + 64800|\lambda|^4 + 42|\rho|^2|\kappa|^2 + 14|\rho|^4 + 630|\rho|^2|\zeta|^2 \\
& +630|\rho|^2|\bar{\zeta}|^2 + 840|\kappa|^2|\zeta|^2 + 840|\kappa|^2|\bar{\zeta}|^2 + 12300|\zeta|^4 + 12600|\zeta|^2|\bar{\zeta}|^2 \\
& +12300|\bar{\zeta}|^4 + 96000|\eta|^4 + 3600|\eta|^2|\gamma|^2 + 36000|\eta|^2|\zeta|^2 + 1200|\gamma|^2|\zeta|^2 \\
& +3600|\eta|^2|\bar{\gamma}|^2 + 36000|\eta|^2|\bar{\zeta}|^2 + 1200|\bar{\gamma}|^2|\bar{\zeta}|^2) \\
& +m_{\Sigma}^2(1080|\gamma|^2|\lambda|^2 + 1200|\gamma|^2|\eta|^2 + 10800|\zeta|^2|\lambda|^2 + 12000|\zeta|^2|\eta|^2 \\
& +43200|\eta|^2|\lambda|^2 + 48000|\eta|^4 + 210|\zeta|^2|\rho|^2 + 420|\zeta|^2|\kappa|^2 + 6300|\zeta|^4 \\
& +6300|\zeta|^2|\bar{\zeta}|^2 + 756|\gamma|^4 + 756|\gamma|^2|\bar{\gamma}|^2 + 504|\gamma|^2|\kappa|^2) \\
& +m_{\bar{\Sigma}}^2(1080|\bar{\gamma}|^2|\lambda|^2 + 1200|\bar{\gamma}|^2|\eta|^2 + 10800|\bar{\zeta}|^2|\lambda|^2 + 12000|\bar{\zeta}|^2|\eta|^2 \\
& +43200|\eta|^2|\lambda|^2 + 48000|\eta|^4 + 210|\bar{\zeta}|^2|\rho|^2 + 420|\bar{\zeta}|^2|\kappa|^2 + 6300|\bar{\zeta}|^2|\bar{\zeta}|^2 \\
& +6300|\bar{\zeta}|^4 + 756|\bar{\gamma}|^2|\gamma|^2 + 756|\bar{\gamma}|^4 + 504|\bar{\gamma}|^2|\kappa|^2) \tag{9.112}
\end{aligned}$$

$$\begin{aligned}
\check{\gamma}_H^{(2)} = & m_H^2(924|\kappa|^4 + 1008|\gamma|^2|\kappa|^2 + 1008|\bar{\gamma}|^2|\kappa|^2 + 2016|\gamma|^4 + 1512|\bar{\gamma}|^2|\gamma|^2 \\
& +2016|\bar{\gamma}|^4 + 10\text{Tr}[h^\dagger.h.h^\dagger.h]) \\
& +m_{\theta}^2(336|\kappa|^4 + 924|\kappa|^2|\rho|^2 + 5040|\kappa|^2|\zeta|^2 + 5040|\kappa|^2|\bar{\zeta}|^2 + 504|\kappa|^2|\gamma|^2 \\
& +504|\rho|^2|\gamma|^2 + 20160|\zeta|^2|\gamma|^2 + 7560|\bar{\zeta}|^2|\gamma|^2 + 504|\kappa|^2|\bar{\gamma}|^2 + 504|\rho|^2|\bar{\gamma}|^2 \\
& +7560|\zeta|^2|\bar{\gamma}|^2 + 20160|\bar{\zeta}|^4 + 120\text{Tr}[h^\dagger.h.g^\dagger.g]) \\
& +m_{\Phi}^2(30240|\kappa|^2|\lambda|^2 + 45360|\gamma|^2|\lambda|^2 + 45360|\bar{\gamma}|^2|\lambda|^2 + 588|\kappa|^4 \\
& +588|\kappa|^2|\rho|^2 + 1260|\gamma|^4 + 1260|\bar{\gamma}|^4 + 12600|\zeta|^2|\gamma|^2 + 12600|\bar{\zeta}|^2|\bar{\gamma}|^2 \\
& +8820|\kappa|^2|\zeta|^2 + 8820|\kappa|^2|\bar{\zeta}|^2 + 25200|\eta|^2|\gamma|^2 + 25200|\eta|^2|\bar{\gamma}|^2) \\
& +m_{\Sigma}^2(504|\kappa|^2|\gamma|^2 + 20160|\kappa|^2|\eta|^2 + 13860|\kappa|^2|\zeta|^2 + 30240|\bar{\gamma}|^2|\eta|^2 \\
& +55440|\gamma|^2|\eta|^2 + 7560|\gamma|^2|\zeta|^2 + 756|\gamma|^4 + 7560|\bar{\gamma}|^2|\zeta|^2 + 756|\gamma|^2|\bar{\gamma}|^2) \\
& +m_{\bar{\Sigma}}^2(504|\kappa|^2|\bar{\gamma}|^2 + 20160|\kappa|^2|\eta|^2 + 13860|\kappa|^2|\bar{\zeta}|^2 + 30240|\gamma|^2|\eta|^2 + 756|\gamma|^2|\bar{\gamma}|^2 \\
& +7560|\gamma|^2|\bar{\zeta}|^2 + 756|\bar{\gamma}|^4 + 55440|\bar{\gamma}|^2|\eta|^2 + 7560|\bar{\gamma}|^2|\bar{\zeta}|^2 + 252\text{Tr}[h^\dagger.h.f^\dagger.f]) \\
& +\text{Tr}[(h.h^\dagger(10h.m_{\Psi}^2.h^\dagger + 252f.m_{\Psi}^2.f^\dagger + 120g.m_{\Psi}^2.g^\dagger) + 31752|\bar{\gamma}|^2f^\dagger.f.m_{\Psi}^2 \\
& +10080|\kappa|^2g^\dagger.g.m_{\Psi}^2)] \tag{9.113}
\end{aligned}$$

$$\begin{aligned}
\check{\gamma}_{\Theta}^{(2)} = & m_H^2(28|\kappa|^4 + 77|\kappa|^2|\rho|^2 + 420|\kappa|^2|\zeta|^2 + 420|\kappa|^2|\bar{\zeta}|^2 + 42|\kappa|^2|\gamma|^2 \\
& + 42|\rho|^2|\gamma|^2 + 1680|\zeta|^2|\gamma|^2 + 630|\bar{\zeta}|^2|\gamma|^2 + 42|\kappa|^2|\bar{\gamma}|^2 + 42|\rho|^2|\bar{\gamma}|^2 \\
& + 630|\zeta|^2|\bar{\gamma}|^2 + 1680|\bar{\zeta}|^2|\bar{\gamma}|^2 + 10\text{Tr}[g^\dagger.g.h^\dagger.h]) \\
& + m_\Theta^2(42|\kappa|^2|\rho|^2 + 63|\rho|^4 + 630|\zeta|^2|\rho|^2 + 630|\bar{\zeta}|^2|\rho|^2 + 616|\kappa|^4 \\
& + 630|\zeta|^2|\kappa|^2 + 630|\bar{\zeta}|^2|\kappa|^2 + 16800|\zeta|^4 + 12600|\bar{\zeta}|^2|\zeta|^2 \\
& + 16800|\bar{\zeta}|^4 + 120\text{Tr}[g^\dagger.g.g^\dagger.g]) \\
& + m_\Phi^2(49|\kappa|^2|\rho|^2 + 10500(|\zeta|^2|\gamma|^2 + |\bar{\zeta}|^2|\bar{\gamma}|^2) + 49|\rho|^4 + 588|\kappa|^4 \\
& + 10500(|\zeta|^4 + |\bar{\zeta}|^4) + 1260|\lambda|^2|\kappa|^2 + 1260|\lambda|^2|\rho|^2 + 18900|\lambda|^2|\zeta|^2 \\
& + 18900|\lambda|^2|\bar{\zeta}|^2 + 21000|\eta|^2|\zeta|^2 + 21000|\eta|^2|\bar{\zeta}|^2 + 882|\kappa|^2|\gamma|^2 + 882|\kappa|^2|\bar{\gamma}|^2 \\
& + 735|\rho|^2|\zeta|^2 + 735|\rho|^2|\bar{\zeta}|^2) \\
& + m_\Sigma^2(924|\kappa|^2|\gamma|^2 + 42|\rho|^2|\gamma|^2 + 630|\zeta|^2|\gamma|^2 + 630|\bar{\zeta}|^2|\gamma|^2 + 420|\kappa|^2|\zeta|^2 \\
& + 1155|\rho|^2|\zeta|^2 + 6300|\zeta|^4 + 6300|\bar{\zeta}|^2|\zeta|^2 + 1680|\kappa|^2|\eta|^2 + 1680|\rho|^2|\eta|^2 \\
& + 25200|\zeta|^2|\eta|^2 + 46200|\bar{\zeta}|^2|\eta|^2) \\
& + m_\Xi^2(924|\kappa|^2|\bar{\gamma}|^2 + 42|\rho|^2|\bar{\gamma}|^2 + 630|\zeta|^2|\bar{\gamma}|^2 + 630|\bar{\zeta}|^2|\bar{\gamma}|^2 + 420|\kappa|^2|\bar{\zeta}|^2 \\
& + 1155|\rho|^2|\bar{\zeta}|^2 + 6300|\zeta|^2|\bar{\zeta}|^2 + 6300|\bar{\zeta}|^4 + 1680|\kappa|^2|\eta|^2 + 1680|\rho|^2|\eta|^2 \\
& + 46200|\zeta|^2|\eta|^2 + 25200|\bar{\zeta}|^2|\eta|^2 + 252\text{Tr}[g^\dagger.g.f^\dagger.f]) + \text{Tr}[(g.g^\dagger(h.m_\Psi^2.h^\dagger \\
& + f.m_\Psi^2.f^\dagger + g.m_\Psi^2.g^\dagger) + 70|\kappa|^2h^\dagger.h.m_\Psi^2 \\
& + 840|\rho|^2g^\dagger.g.m_\Psi^2 + 26460|\bar{\zeta}|^2f^\dagger.f.m_\Psi^2)]
\end{aligned} \tag{9.114}$$

$$\begin{aligned}
\check{\gamma}_{\Sigma}^{(2)} = & m_H^2(800|\eta|^2|\kappa|^2 + 40|\gamma|^2|\kappa|^2 + 1100|\zeta|^2|\kappa|^2 + 1200|\eta|^2|\gamma|^2 + 60|\gamma|^4 \\
& + 600|\zeta|^2|\gamma|^2 + 3200|\eta|^2|\bar{\gamma}|^2 + 60|\gamma|^2|\bar{\gamma}|^2 + 600|\zeta|^2|\bar{\gamma}|^2) \\
& + m_{\Theta}^2(400|\eta|^2|\rho|^2 + 800|\eta|^2|\kappa|^2 + 12000|\eta|^2|\zeta|^2 + 32000|\eta|^2|\bar{\zeta}|^2 \\
& + 20|\gamma|^2|\rho|^2 + 880|\gamma|^2|\kappa|^2 + 600|\gamma|^2|\zeta|^2 + 600|\gamma|^2|\bar{\zeta}|^2 + 900|\zeta|^2|\rho|^2 \\
& + 400|\zeta|^2|\kappa|^2 + 6000|\zeta|^4 + 6000|\bar{\zeta}|^2|\zeta|^2) \\
& + m_{\Phi}^2(700|\kappa|^2|\zeta|^2 + 2000|\bar{\gamma}|^2|\eta|^2 + 840|\kappa|^2|\gamma|^2 + 20000|\eta|^2|\bar{\zeta}|^2 \\
& + 36000|\eta|^2|\lambda|^2 + 1800|\gamma|^2|\lambda|^2 + 18000|\zeta|^2|\lambda|^2 + 1260|\gamma|^2(|\gamma|^2 + |\bar{\gamma}|^2) \\
& + 10500|\zeta|^4 + 10500|\zeta|^2|\bar{\zeta}|^2 + 40000|\eta|^4) + \\
& m_{\Sigma}^2(3600|\eta|^2|\gamma|^2 + 1320|\gamma|^4 + 1200|\zeta|^2|\gamma|^2 + 36000|\eta|^2|\zeta|^2 \\
& + 16500|\zeta|^4 + 88000|\eta|^4) + m_{\Xi}^2(1200|\eta|^2|\bar{\gamma}|^2 + 1320|\bar{\gamma}|^2|\gamma|^2 \\
& + 600|\zeta|^2|\bar{\gamma}|^2 + 12000|\eta|^2|\bar{\zeta}|^2 + 600|\gamma|^2|\bar{\zeta}|^2 + 16500|\bar{\zeta}|^2|\zeta|^2 \\
& + 48000|\eta|^4 + 2400|\gamma|^2|\eta|^2 + 24000|\zeta|^2|\eta|^2) \tag{9.115}
\end{aligned}$$

$$\begin{aligned}
\check{\gamma}_{\Sigma}^{(2)} = & m_H^2(800|\eta|^2|\kappa|^2 + 40|\bar{\gamma}|^2|\kappa|^2 + 1100|\bar{\zeta}|^2|\kappa|^2 + 3200|\eta|^2|\gamma|^2 + 60|\gamma|^2|\bar{\gamma}|^2 \\
& + 600|\bar{\zeta}|^2|\gamma|^2 + 1200|\eta|^2|\bar{\gamma}|^2 + 60|\bar{\gamma}|^4 + 600|\bar{\zeta}|^2|\bar{\gamma}|^2 + 10\text{Tr}[f^\dagger \cdot f \cdot h^\dagger \cdot h]) \\
& + m_{\Theta}^2(400|\eta|^2|\rho|^2 + 800|\eta|^2|\kappa|^2 + 32000|\eta|^2|\zeta|^2 + 12000|\eta|^2|\bar{\zeta}|^2 + 20|\bar{\gamma}|^2|\rho|^2 \\
& + 880|\bar{\gamma}|^2|\kappa|^2 + 600|\bar{\gamma}|^2|\zeta|^2 + 600|\bar{\gamma}|^2|\bar{\zeta}|^2 + 900|\bar{\zeta}|^2|\rho|^2 + 400|\bar{\zeta}|^2|\kappa|^2 \\
& + 6000|\bar{\zeta}|^4 + 6000|\bar{\zeta}|^2|\zeta|^2 + 120\text{Tr}[f^\dagger \cdot f \cdot g^\dagger \cdot g]) \\
& + m_{\Phi}^2(700|\kappa|^2|\bar{\zeta}|^2 + 2000|\gamma|^2|\eta|^2 + 840|\kappa|^2|\bar{\gamma}|^2 + 20000|\eta|^2|\zeta|^2 + 36000|\eta|^2|\lambda|^2 \\
& + 1800|\bar{\gamma}|^2|\lambda|^2 + 18000|\bar{\zeta}|^2|\lambda|^2 + 1260|\bar{\gamma}|^2(|\gamma|^2 + |\bar{\gamma}|^2) + 10500|\bar{\zeta}|^2(|\zeta|^2 + |\bar{\zeta}|^2) \\
& + 40000|\eta|^4) + m_{\Xi}^2(1200|\eta|^2|\gamma|^2 + 1320|\bar{\gamma}|^2|\gamma|^2 + 600|\bar{\zeta}|^2|\gamma|^2 + 12000|\eta|^2|\zeta|^2 \\
& + 600|\bar{\gamma}|^2|\zeta|^2 + 16500|\bar{\zeta}|^2|\zeta|^2 + 48000|\eta|^4 + 2400|\bar{\gamma}|^2|\eta|^2 + 24000|\bar{\zeta}|^2|\eta|^2) \\
& + m_{\Sigma}^2(3600|\eta|^2|\bar{\gamma}|^2 + 1320|\bar{\gamma}|^4 + 1200|\bar{\zeta}|^2|\bar{\gamma}|^2 + 36000|\eta|^2|\bar{\zeta}|^2 + 16500|\bar{\zeta}|^4 \\
& + 88000|\eta|^4 + 252\text{Tr}[f^\dagger \cdot f \cdot f^\dagger \cdot f]) + \text{Tr}[(f \cdot f^\dagger)(10h \cdot m_{\Psi}^2 \cdot h^\dagger + 252f \cdot m_{\Psi}^2 \cdot f^\dagger \\
& + 120g \cdot m_{\Psi}^2 \cdot g^\dagger) + 100|\bar{\gamma}|^2 h^\dagger \cdot h \cdot m_{\Psi}^2 + 12000|\bar{\zeta}|^2 g^\dagger \cdot g \cdot m_{\Psi}^2] \tag{9.116}
\end{aligned}$$

$$\begin{aligned}
\check{\gamma}_{\Psi}^{(2)} = & 10h^\dagger \cdot (10h \cdot m_{\Psi}^2 \cdot h^\dagger + 120g \cdot m_{\Psi}^2 \cdot g^\dagger + 252f \cdot m_{\Psi}^2 \cdot f) \cdot h + 120g^\dagger \cdot (10h \cdot m_{\Psi}^2 \cdot h^\dagger \\
& + 120g \cdot m_{\Psi}^2 \cdot g^\dagger + 252f \cdot m_{\Psi}^2 \cdot f) \cdot g + 252f^\dagger \cdot (10h \cdot m_{\Psi}^2 \cdot h^\dagger + 120g \cdot m_{\Psi}^2 \cdot g^\dagger + 252f \cdot m_{\Psi}^2 \cdot f) \cdot f \\
& + 10h^\dagger \cdot (10m_H^2 h \cdot h^\dagger + 120m_{\Theta}^2 g \cdot g^\dagger + 252m_{\Sigma}^2 f \cdot f^\dagger) \cdot h + 120g^\dagger \cdot (10m_H^2 h \cdot h^\dagger \\
& + 120m_{\Theta}^2 g \cdot g^\dagger + 252m_{\Sigma}^2 f \cdot f^\dagger) \cdot g + 252f^\dagger \cdot (10m_H^2 h \cdot h^\dagger + 120m_{\Theta}^2 g \cdot g^\dagger + 252m_{\Sigma}^2 f \cdot f^\dagger) \cdot f \\
& + 10\text{Tr}[h^\dagger \cdot h](84m_{\Phi}^2 |\kappa|^2 + m_{\Theta}^2(84|\kappa|^2 + 126|\gamma|^2 + 126|\bar{\gamma}|^2) + 126(|\gamma|^2 m_{\Sigma}^2 + |\bar{\gamma}|^2 m_{\Sigma}^2) \\
& + \text{Tr}[h^\dagger \cdot m_{\Psi}^2 \cdot h]) + 120\text{Tr}[g^\dagger \cdot g](7m_{\Theta}^2 |\rho|^2 + 7m_H^2 |\kappa|^2 + m_{\Phi}^2(7|\rho|^2 + 7|\kappa|^2 + 105|\zeta|^2 \\
& + 105|\bar{\zeta}|^2) + 105(m_{\Sigma}^2 |\zeta|^2 + \tilde{m}_{\Sigma}^2 |\bar{\zeta}|^2) + \text{Tr}[g^\dagger \cdot m_{\Psi}^2 \cdot g]) + 252\text{Tr}[f^\dagger \cdot f](10m_H^2 |\bar{\gamma}|^2 \\
& + 100m_{\Theta}^2 |\bar{\zeta}|^2 + m_{\Phi}^2(200|\eta|^2 + 100|\bar{\zeta}|^2 + 10|\bar{\gamma}|^2) + 200m_{\Sigma}^2 |\eta|^2 + \text{Tr}[f^\dagger \cdot m_{\Psi}^2 \cdot f]) \quad (9.117)
\end{aligned}$$

Two-loop beta functions for the soft parameters:

$$\begin{aligned}
\beta_{\tilde{\eta}}^{(2)} = & -\tilde{\eta}(\tilde{\gamma}_{\Sigma}^{(2)} + \tilde{\gamma}_{\Sigma}^{(2)} + \tilde{\gamma}_{\Phi}^{(2)}) - \eta(\tilde{\gamma}_{\Sigma}^{(2)} + \tilde{\gamma}_{\Sigma}^{(2)} + \tilde{\gamma}_{\Phi}^{(2)}) - \eta(\hat{\gamma}_{\Sigma}^{(2)} + \hat{\gamma}_{\Sigma}^{(2)} + \hat{\gamma}_{\Phi}^{(2)}) \\
& + 2g_{10}^2((\tilde{\eta} - 2M\eta)(7920|\eta|^2 + 70|\gamma|^2 + 1660|\zeta|^2 + 70|\bar{\gamma}|^2 + 1660|\bar{\zeta}|^2 \\
& + 12|\kappa|^2 + 2160|\lambda|^2 + 18|\rho|^2 - 40\text{Tr}[f^\dagger \cdot f]) + 2\eta(7920\tilde{\eta}\eta^* + 70\tilde{\gamma}\gamma^* \\
& + 1660\tilde{\zeta}\zeta^* + 70\tilde{\gamma}\bar{\gamma}^* + 1660\tilde{\zeta}\bar{\zeta}^* + 12\tilde{\kappa}\kappa^* + 2160\tilde{\lambda}\lambda^* + 18\tilde{\rho}\rho^* - 40\text{Tr}[f^\dagger \cdot \tilde{f}])) \\
& + 5982g_{10}^4(2\tilde{\eta} - 8M\eta) \quad (9.118)
\end{aligned}$$

$$\begin{aligned}
\beta_{\tilde{\gamma}}^{(2)} = & -\tilde{\gamma}(\tilde{\gamma}_H^{(2)} + \tilde{\gamma}_{\Sigma}^{(2)} + \tilde{\gamma}_{\Phi}^{(2)}) - \gamma(\tilde{\gamma}_H^{(2)} + \tilde{\gamma}_{\Sigma}^{(2)} + \tilde{\gamma}_{\Phi}^{(2)}) - \gamma(\hat{\gamma}_H^{(2)} + \hat{\gamma}_{\Sigma}^{(2)} + \hat{\gamma}_{\Phi}^{(2)}) \\
& + 2g_{10}^2((\tilde{\gamma} - 2M\gamma)(1524|\kappa|^2 + 2590|\gamma|^2 + 2550|\bar{\gamma}|^2 + 54\text{Tr}[h^\dagger \cdot h] \\
& + 5520|\eta|^2 + 1660|\zeta|^2 + 2160|\lambda|^2 + 18|\rho|^2 + 660|\bar{\zeta}|^2) \\
& + 2\gamma(1524\tilde{\kappa}\kappa^* + 2590\tilde{\gamma}\gamma^* + 2550\tilde{\gamma}\bar{\gamma}^* + 54\text{Tr}[h^\dagger \cdot \tilde{h}] + 5520\tilde{\eta}\eta^* \\
& + 1660\tilde{\zeta}\zeta^* + 2160\tilde{\lambda}\lambda^* + 18\tilde{\rho}\rho^* + 660\tilde{\zeta}\bar{\zeta}^*)) + 4614g_{10}^4(2\tilde{\gamma} - 8M\gamma) \quad (9.119)
\end{aligned}$$

$$\begin{aligned}
\beta_{\tilde{\gamma}}^{(2)} = & -\tilde{\gamma}(\tilde{\gamma}_H^{(2)} + \tilde{\gamma}_\Sigma^{(2)} + \tilde{\gamma}_\Phi^{(2)}) - \bar{\gamma}(\tilde{\gamma}_H^{(2)} + \tilde{\gamma}_\Sigma^{(2)} + \tilde{\gamma}_\Phi^{(2)}) - \bar{\gamma}(\hat{\gamma}_H^{(2)} + \hat{\gamma}_\Sigma^{(2)} + \hat{\gamma}_\Phi^{(2)}) \\
& + 2g_{10}^2((\tilde{\gamma} - 2M\bar{\gamma})(1524|\kappa|^2 + 2550|\gamma|^2 + 2590|\bar{\gamma}|^2 + 54\text{Tr}[h^\dagger \cdot h] \\
& - 40\text{Tr}[f^\dagger \cdot f] + 1660|\bar{\zeta}|^2 + 5520|\eta|^2 + 2160|\lambda|^2 + 18|\rho|^2 + 660|\zeta|^2) \\
& + 2\bar{\gamma}(1524\tilde{\kappa}\kappa^* + 2550\tilde{\gamma}\gamma^* + 2590\tilde{\gamma}\bar{\gamma}^* + 54\text{Tr}[h^\dagger \cdot \tilde{h}] - 40\text{Tr}[f^\dagger \cdot \tilde{f}] \\
& + 1660\tilde{\zeta}\bar{\zeta}^* + 5520\tilde{\eta}\eta^* + 2160\tilde{\lambda}\lambda^* + 18\tilde{\rho}\rho^* + 660\tilde{\zeta}\zeta^*) \\
& + 4614g_{10}^4(2\tilde{\gamma} - 8M\bar{\gamma}) \tag{9.120}
\end{aligned}$$

$$\begin{aligned}
\beta_{\tilde{\kappa}}^{(2)} = & -\tilde{\kappa}(\tilde{\gamma}_H^{(2)} + \tilde{\gamma}_\Theta^{(2)} + \tilde{\gamma}_\Phi^{(2)}) - \kappa(\tilde{\gamma}_H^{(2)} + \tilde{\gamma}_\Theta^{(2)} + \tilde{\gamma}_\Phi^{(2)}) - \kappa(\hat{\gamma}_H^{(2)} + \hat{\gamma}_\Theta^{(2)} + \hat{\gamma}_\Phi^{(2)}) \\
& + 2g_{10}^2((\tilde{\kappa} - 2M\kappa)(1566|\kappa|^2 + 2550|\gamma|^2 + 2550|\bar{\gamma}|^2 + 54\text{Tr}[h^\dagger \cdot h] \\
& + 102|\rho|^2 + 2130|\zeta|^2 + 2130|\bar{\zeta}|^2 + 6\text{Tr}[g^\dagger \cdot g] + 3120|\eta|^2 + 2160|\lambda|^2) \\
& + 2\kappa(1566\tilde{\kappa}\kappa^* + 2550\tilde{\gamma}\gamma^* + 2550\tilde{\gamma}\bar{\gamma}^* + 54\text{Tr}[h^\dagger \cdot \tilde{h}] + 102\tilde{\rho}\rho^* \\
& + 2130\tilde{\zeta}\zeta^* + 2130\tilde{\bar{\zeta}}\bar{\zeta}^* + 6\text{Tr}[g^\dagger \cdot \tilde{g}] + 3120\tilde{\eta}\eta^* + 2160\tilde{\lambda}\lambda^*) \\
& + 4248g_{10}^4(2\tilde{\kappa} - 8M\kappa) \tag{9.121}
\end{aligned}$$

$$\begin{aligned}
\beta_{\tilde{\zeta}}^{(2)} = & -\tilde{\zeta}(\tilde{\gamma}_\Theta^{(2)} + \tilde{\gamma}_\Sigma^{(2)} + \tilde{\gamma}_\Phi^{(2)}) - \zeta(\tilde{\gamma}_\Theta^{(2)} + \tilde{\gamma}_\Sigma^{(2)} + \tilde{\gamma}_\Phi^{(2)}) - \zeta(\hat{\gamma}_\Theta^{(2)} + \hat{\gamma}_\Sigma^{(2)} + \hat{\gamma}_\Phi^{(2)}) \\
& + 2g_{10}^2((\tilde{\zeta} - 2M\zeta)(54|\kappa|^2 + 102|\rho|^2 + 3130|\zeta|^2 + 2130|\bar{\zeta}|^2 + 6\text{Tr}[g^\dagger \cdot g] \\
& + 5520|\eta|^2 + 70|\gamma|^2 + 2160|\lambda|^2 + 30|\bar{\gamma}|^2) + 2\zeta(54\tilde{\kappa}\kappa^* + 102\tilde{\rho}\rho^* + 3130\tilde{\zeta}\zeta^* \\
& + 2130\tilde{\bar{\zeta}}\bar{\zeta}^* + 6\text{Tr}[g^\dagger \cdot \tilde{g}] + 5520\tilde{\eta}\eta^* + 70\tilde{\gamma}\gamma^* + 2160\tilde{\lambda}\lambda^* + 30\tilde{\gamma}\bar{\gamma}^*) \\
& + 5616g_{10}^4(2\tilde{\zeta} - 8M\zeta) \tag{9.122}
\end{aligned}$$

$$\begin{aligned}
\beta_{\tilde{\bar{\zeta}}}^{(2)} = & -\tilde{\bar{\zeta}}(\tilde{\gamma}_\Theta^{(2)} + \tilde{\gamma}_\Sigma^{(2)} + \tilde{\gamma}_\Phi^{(2)}) - \bar{\zeta}(\tilde{\gamma}_\Theta^{(2)} + \tilde{\gamma}_\Sigma^{(2)} + \tilde{\gamma}_\Phi^{(2)}) - \bar{\zeta}(\hat{\gamma}_\Theta^{(2)} + \hat{\gamma}_\Sigma^{(2)} + \hat{\gamma}_\Phi^{(2)}) \\
& + 2g_{10}^2((\tilde{\bar{\zeta}} - 2M\bar{\zeta})(54|\kappa|^2 + 102|\rho|^2 + 2130|\zeta|^2 + 3130|\bar{\zeta}|^2 + 6\text{Tr}[g^\dagger \cdot g] \\
& - 40\text{Tr}[f^\dagger \cdot f] + 5520|\eta|^2 + 70|\bar{\gamma}|^2 + 2160|\lambda|^2 + 30|\gamma|^2) + 2\bar{\zeta}(54\tilde{\kappa}\kappa^* + 102\tilde{\rho}\rho^* \\
& + 2130\tilde{\zeta}\zeta^* + 3130\tilde{\bar{\zeta}}\bar{\zeta}^* + 6\text{Tr}[g^\dagger \cdot \tilde{g}] - 40\text{Tr}[f^\dagger \cdot \tilde{f}] + 5520\tilde{\eta}\eta^* + 70\tilde{\gamma}\bar{\gamma}^* \\
& + 2160\tilde{\lambda}\lambda^* + 30\tilde{\gamma}\gamma^*) + 5616g_{10}^4(2\tilde{\bar{\zeta}} - 8M\bar{\zeta}) \tag{9.123}
\end{aligned}$$

$$\begin{aligned}
\beta_{\tilde{\rho}}^{(2)} = & -\tilde{\rho}(2\tilde{\gamma}_{\Theta}^{(2)} + \tilde{\gamma}_{\Phi}^{(2)}) - \rho(2\tilde{\gamma}_{\Theta}^{(2)} + \tilde{\gamma}_{\Phi}^{(2)}) - \rho(2\hat{\gamma}_{\Theta}^{(2)} + \hat{\gamma}_{\Phi}^{(2)}) \\
& + 2g_{10}^2((\tilde{\rho} - 2M\rho)(96|\kappa|^2 + 186|\rho|^2 + 3600|\zeta|^2 + 3600|\bar{\zeta}|^2 + 6Tr[g^\dagger \cdot g] \\
& + 3120|\eta|^2 + 2160|\lambda|^2 + 30|\gamma|^2 + 30|\bar{\gamma}|^2) + 2\rho(96\tilde{\kappa}\kappa^* + 186\tilde{\rho}\rho^* \\
& + 3600\tilde{\zeta}\zeta^* + 3600\tilde{\bar{\zeta}}\bar{\zeta}^* + 6Tr[g^\dagger \cdot \tilde{g}] + 3120\tilde{\eta}\eta^* + 2160\tilde{\lambda}\lambda^* + 30\tilde{\gamma}\gamma^* \\
& + 30\tilde{\bar{\gamma}}\bar{\gamma}^*)) + 5250g_{10}^4(2\tilde{\rho} - 8M\rho)
\end{aligned} \tag{9.124}$$

$$\begin{aligned}
\beta_{\tilde{h}}^{(2)} = & -\tilde{h}\tilde{\gamma}_H^{(2)} - h\tilde{\gamma}_H^{(2)} - h\hat{\gamma}_H^{(2)} \\
& + 2g_{10}^2((\tilde{h} - 2Mh)(1512|\kappa|^2 + 2520(|\gamma|^2 + |\bar{\gamma}|^2) + 54Tr[h^\dagger \cdot h]) \\
& + 2h(1512\tilde{\kappa}\kappa^* + 2520(\tilde{\gamma}\gamma^* + \tilde{\bar{\gamma}}\bar{\gamma}^*) + 54Tr[h^\dagger \cdot \tilde{h}])) + 657g_{10}^4(2\tilde{h} - 8Mh) \\
& - \tilde{h} \cdot \tilde{\gamma}_\Psi^{(2)} - h \cdot \tilde{\gamma}_\Psi^{(2)} - h \cdot \hat{\gamma}_\Psi^{(2)} + 2g_{10}^2((\tilde{h} - 2Mh)(45h^\dagger \cdot h + 1260g^\dagger \cdot g + 3150f^\dagger \cdot f) \\
& + 2h(45h^\dagger \cdot \tilde{h} + 1260g^\dagger \cdot \tilde{g} + 3150f^\dagger \cdot \tilde{f})) + (2\tilde{h} - 8Mh)\frac{26685g_{10}^4}{32} \\
& + (-\tilde{h} \cdot \tilde{\gamma}_\Psi^{(2)} - h \cdot \tilde{\gamma}_\Psi^{(2)} - h \cdot \hat{\gamma}_\Psi^{(2)} + 2g_{10}^2((\tilde{h} - 2Mh)(45h^\dagger \cdot h + 1260g^\dagger \cdot g + 3150f^\dagger \cdot f) \\
& + 2h(45h^\dagger \cdot \tilde{h} + 1260g^\dagger \cdot \tilde{g} + 3150f^\dagger \cdot \tilde{f})) + (2\tilde{h} - 8Mh)\frac{26685g_{10}^4}{32})^T
\end{aligned} \tag{9.125}$$

$$\begin{aligned}
\beta_{\tilde{f}}^{(2)} = & -\tilde{f}\tilde{\gamma}_\Sigma^{(2)} - f\tilde{\gamma}_\Sigma^{(2)} - f\hat{\gamma}_\Sigma^{(2)} \\
& + 2g_{10}^2((\tilde{f} - 2Mf)(2400|\eta|^2 + 40|\bar{\gamma}|^2 + 1000|\bar{\zeta}|^2 - 40Tr[f^\dagger \cdot f]) \\
& + 2f(2400\tilde{\eta}\eta^* + 40\tilde{\gamma}\gamma^* + 1000\tilde{\bar{\zeta}}\bar{\zeta}^* - 40Tr[f^\dagger \cdot \tilde{f}])) + 2025g_{10}^4(2\tilde{f} - 8Mf) \\
& - \tilde{f} \cdot \tilde{\gamma}_\Psi^{(2)} - f \cdot \tilde{\gamma}_\Psi^{(2)} - f \cdot \hat{\gamma}_\Psi^{(2)} + 2g_{10}^2((\tilde{f} - 2Mf)(45h^\dagger \cdot h + 1260g^\dagger \cdot g + 3150f^\dagger \cdot f) \\
& + 2f(45h^\dagger \cdot \tilde{h} + 1260g^\dagger \cdot \tilde{g} + 3150f^\dagger \cdot \tilde{f})) + (2\tilde{f} - 8Mf)\frac{26685g_{10}^4}{32} \\
& + (-\tilde{f} \cdot \tilde{\gamma}_\Psi^{(2)} - f \cdot \tilde{\gamma}_\Psi^{(2)} - f \cdot \hat{\gamma}_\Psi^{(2)} + 2g_{10}^2((\tilde{f} - 2Mf)(45h^\dagger \cdot h + 1260g^\dagger \cdot g + 3150f^\dagger \cdot f) \\
& + 2f(45h^\dagger \cdot \tilde{h} + 1260g^\dagger \cdot \tilde{g} + 3150f^\dagger \cdot \tilde{f})) + (2\tilde{f} - 8Mf)\frac{26685g_{10}^4}{32})^T
\end{aligned} \tag{9.126}$$

$$\begin{aligned}
\beta_{\tilde{g}}^{(2)} = & -\tilde{g}\tilde{\gamma}_{\Theta}^{(2)} - g\tilde{\gamma}_{\Theta}^{(2)} - g\hat{\gamma}_{\Theta}^{(2)} + 2g_{10}^2((\tilde{g} - 2Mg)(42|\kappa|^2 + 84|\rho|^2 + 1470|\zeta|^2 + 1470|\bar{\zeta}|^2 \\
& + 6Tr[g^\dagger \cdot g]) + 2g(42\tilde{\kappa}\kappa^* + 84\tilde{\rho}\rho^* + 1470\tilde{\zeta}\zeta^* + 1470\tilde{\bar{\zeta}}\bar{\zeta}^* + 6Tr[g^\dagger \cdot \tilde{g}])) \\
& + 1659g_{10}^4(2\tilde{g} - 8Mg) \\
& - \tilde{g}\cdot\tilde{\gamma}_{\Psi}^{(2)} - g\cdot\tilde{\gamma}_{\Psi}^{(2)} - g\cdot\hat{\gamma}_{\Psi}^{(2)} + 2g_{10}^2((\tilde{g} - 2Mg)(45h^\dagger \cdot h + 1260g^\dagger \cdot g + 3150f^\dagger \cdot f) \\
& + 2g(45h^\dagger \cdot \tilde{h} + 1260g^\dagger \cdot \tilde{g} + 3150f^\dagger \cdot \tilde{f})) + (2\tilde{g} - 8Mg)\frac{26685g_{10}^4}{32} \\
& + (-\tilde{g}\cdot\tilde{\gamma}_{\Psi}^{(2)} - g\cdot\tilde{\gamma}_{\Psi}^{(2)} - g\cdot\hat{\gamma}_{\Psi}^{(2)} + 2g_{10}^2((\tilde{g} - 2Mg)(45h^\dagger \cdot h + 1260g^\dagger \cdot g + 3150f^\dagger \cdot f) \\
& + 2g(45h^\dagger \cdot \tilde{h} + 1260g^\dagger \cdot \tilde{g} + 3150f^\dagger \cdot \tilde{f})) + (2\tilde{g} - 8Mg)\frac{26685g_{10}^4}{32})^T \quad (9.127)
\end{aligned}$$

$$\begin{aligned}
\beta_{b_\Phi}^{(2)} = & -2b_\Phi\tilde{\gamma}_\Phi^{(2)} - 2\mu_\Phi(\hat{\gamma}_\Phi^{(2)} + \tilde{\gamma}_\Phi^{(2)}) + 4g_{10}^2((b_\Phi - 2\mu_\Phi M)(3120|\eta|^2 + 12|\kappa|^2 \\
& + 2160|\lambda|^2 + 18|\rho|^2 + 30|\gamma|^2 + 30|\bar{\gamma}|^2 + 660|\zeta|^2 + 660|\bar{\zeta}|^2) \\
& + 4\mu_\Phi(3120\tilde{\eta}\eta^* + 12\tilde{\kappa}\kappa^* + 2160\tilde{\lambda}\lambda^* + 18\tilde{\rho}\rho^* + 30\tilde{\gamma}\gamma^* + 30\tilde{\bar{\gamma}}\bar{\gamma}^* \\
& + 660\tilde{\zeta}\zeta^* + 660\tilde{\bar{\zeta}}\bar{\zeta}^*)) + 3864g_{10}^4(2b_\Phi - 8\mu_\Phi M) \quad (9.128)
\end{aligned}$$

$$\begin{aligned}
\beta_{b_H}^{(2)} = & -2b_H\tilde{\gamma}_H^{(2)} - 2\mu_H(\hat{\gamma}_H^{(2)} + \tilde{\gamma}_H^{(2)}) + 4g_{10}^2((b_H - 2\mu_H M)(1512|\kappa|^2 + 2520|\gamma|^2 \\
& + 2520|\bar{\gamma}|^2 + 54Tr[h^\dagger \cdot h]) + 4\mu_H(1512\tilde{\kappa}\kappa^* + 2520\tilde{\gamma}\gamma^* + 2520\tilde{\bar{\gamma}}\bar{\gamma}^* \\
& + 54Tr[h^\dagger \cdot \tilde{h}])) + 1314g_{10}^4(2b_H - 8\mu_H M) \quad (9.129)
\end{aligned}$$

$$\begin{aligned}
\beta_{b_\Sigma}^{(2)} = & -b_\Sigma(\tilde{\gamma}_\Sigma^{(2)} + \tilde{\bar{\gamma}}_\Sigma^{(2)}) - \mu_\Sigma(\hat{\gamma}_\Sigma^{(2)} + \tilde{\gamma}_\Sigma^{(2)} + \hat{\gamma}_\Sigma^{(2)} + \tilde{\bar{\gamma}}_\Sigma^{(2)}) + 2g_{10}^2((b_\Sigma - 2\mu_\Sigma M) \\
& (4800|\eta|^2 + 40|\gamma|^2 + 1000|\zeta|^2 + 40|\bar{\gamma}|^2 + 1000|\bar{\zeta}|^2 - 40Tr[f^\dagger \cdot f]) \\
& + 2\mu_\Sigma(4800\tilde{\eta}\eta^* + 40\tilde{\gamma}\gamma^* + 1000\tilde{\zeta}\zeta^* + 40\tilde{\bar{\gamma}}\bar{\gamma}^* + 1000\tilde{\bar{\zeta}}\bar{\zeta}^* - 40Tr[f^\dagger \cdot \tilde{f}])) \\
& + 8100g_{10}^4(2b_\Sigma - 8\mu_\Sigma M) \quad (9.130)
\end{aligned}$$

$$\begin{aligned}
\beta_{b_\Theta}^{(2)} = & -2b_\Theta\tilde{\gamma}_\Theta^{(2)} - 2\mu_\Theta(\hat{\gamma}_\Theta^{(2)} + \tilde{\gamma}_\Theta^{(2)}) + 4g_{10}^2((b_\Theta - 2\mu_\Theta M)(42|\kappa|^2 + 84|\rho|^2 \\
& + 1470|\zeta|^2 + 1470|\bar{\zeta}|^2 + 6Tr[g^\dagger \cdot g]) + 4\mu_\Theta(42\tilde{\kappa}\kappa^* + 84\tilde{\rho}\rho^* + 1470\tilde{\zeta}\zeta^* \\
& + 1470\tilde{\bar{\zeta}}\bar{\zeta}^* + 6Tr[g^\dagger \cdot \tilde{g}])) + 3318g_{10}^4(2b_\Theta - 8\mu_\Theta M) \quad (9.131)
\end{aligned}$$

$$\begin{aligned}
\beta_{m_\Phi^2}^{(2)} = & -2\bar{\gamma}_\Phi^{(2)} m_\Phi^2 - 4(360m_\Phi^2 \bar{\gamma}_\Phi^{(1)} |\lambda|^2 + m_H^2 \bar{\gamma}_H^{(1)} (4|\kappa|^2 + 6(|\gamma|^2 + |\bar{\gamma}|^2))) \\
& + 6m_\Theta^2 \bar{\gamma}_\Theta^{(1)} (4|\rho|^2 + 4|\kappa|^2 + 60(|\zeta|^2 + |\bar{\zeta}|^2)) + m_\Sigma^2 \bar{\gamma}_\Sigma^{(1)} (6|\gamma|^2 + 240|\eta|^2 + 60|\zeta|^2) \\
& + m_\Sigma^2 \bar{\gamma}_\Sigma^{(1)} (6|\bar{\gamma}|^2 + 240|\eta|^2 + 60|\bar{\zeta}|^2) - 2(\bar{\gamma}_\Sigma^{(1)} (240|\eta|^2 m_\Sigma^2 + 6|\bar{\gamma}|^2 m_H^2 + 60|\bar{\zeta}|^2 m_\Theta^2) \\
& + \bar{\gamma}_\Sigma^{(1)} (240|\eta|^2 m_\Sigma^2 + 6|\gamma|^2 m_H^2 + 60|\zeta|^2 m_\Theta^2) + \bar{\gamma}_H^{(1)} (4|\kappa|^2 m_\Theta^2 + 6|\gamma|^2 m_\Sigma^2 + 6|\bar{\gamma}|^2 m_\Sigma^2) \\
& + \bar{\gamma}_\Theta^{(1)} (4|\kappa|^2 m_H^2 + 2|\rho|^2 m_\Theta^2 + 60|\zeta|^2 m_\Sigma^2 + 60|\bar{\zeta}|^2 m_\Sigma^2) + 360m_\Phi^2 |\lambda|^2 \bar{\gamma}_\Phi^{(1)}) \\
& - 2\check{\gamma}_\Phi^{(2)} - \check{\gamma}_\Phi^{(2)} - \dot{\gamma}_\Phi^{(2)} - 2\text{Re}[\dot{\gamma}_\Phi^{(2)}] \\
& + 2g_{10}^2 (2m_\Phi^2 (3120|\eta|^2 + 12|\kappa|^2 + 2160|\lambda|^2 + 18|\rho|^2 + 30|\gamma|^2 + 30|\bar{\gamma}|^2 + 660|\zeta|^2 \\
& + 660|\bar{\zeta}|^2) + 2(3120|\tilde{\eta}|^2 + 12|\tilde{\kappa}|^2 + 2160|\tilde{\lambda}|^2 + 18|\tilde{\rho}|^2 + 30|\tilde{\gamma}|^2 + 30|\tilde{\gamma}|^2 \\
& + 660|\tilde{\zeta}|^2 + 660|\tilde{\bar{\zeta}}|^2) - 2(3120\tilde{\eta}\eta^* + 12\tilde{\kappa}\kappa^* + 2160\tilde{\lambda}\lambda^* + 18\tilde{\rho}\rho^* + 30\tilde{\gamma}\gamma^* + 30\tilde{\gamma}\bar{\gamma}^* \\
& + 660\tilde{\zeta}\zeta^* + 660\tilde{\bar{\zeta}}\bar{\zeta}^*)M^\dagger - 2(3120\tilde{\eta}^*\eta + 12\tilde{\kappa}^*\kappa + 2160\tilde{\lambda}^*\lambda + 18\tilde{\rho}^*\rho + 30\tilde{\gamma}^*\gamma \\
& + 30\tilde{\gamma}^*\bar{\gamma} + 660\tilde{\zeta}^*\zeta + 660\tilde{\bar{\zeta}}^*\bar{\zeta})M + 4(3120|\eta|^2 + 12|\kappa|^2 + 2160|\lambda|^2 + 18|\rho|^2 \\
& + 30|\gamma|^2 + 30|\bar{\gamma}|^2 + 660|\zeta|^2 + 660|\bar{\zeta}|^2)MM^\dagger + 4(2160m_\Phi^2 |\lambda|^2 \\
& + m_H^2 (12|\kappa|^2 + 30|\gamma|^2 + 30|\bar{\gamma}|^2) + m_\Theta^2 (18|\rho|^2 + 12|\kappa|^2 + 660(|\zeta|^2 + |\bar{\zeta}|^2)) \\
& + m_\Sigma^2 (30|\gamma|^2 + 3120|\eta|^2 + 660|\zeta|^2) + m_\Sigma^2 (30|\bar{\gamma}|^2 + 3120|\eta|^2 + 660|\bar{\zeta}|^2)) \\
& + 46368g_{10}^4 |M|^2 + 96g_{10}^4 (56m_\Phi^2 - 8|M|^2) \tag{9.132}
\end{aligned}$$

$$\begin{aligned}
\beta_{m_H^2}^{(2)} = & -2\bar{\gamma}_H^{(2)} m_H^2 - 4(m_\Phi^2 \bar{\gamma}_\Phi^{(1)} (126(|\gamma|^2 + |\bar{\gamma}|^2) + 84|\kappa|^2) + 84m_\Theta^2 \bar{\gamma}_\Theta^{(1)} |\kappa|^2 + 126(m_\Sigma^2 \bar{\gamma}_\Sigma^{(1)} |\gamma|^2 \\
& + m_\Sigma^2 \bar{\gamma}_\Sigma^{(1)} |\bar{\gamma}|^2)) - 2\text{Tr}[h \cdot \bar{\gamma}_\Psi^{(1)} \cdot \tilde{m}_\Psi^2 \cdot h^\dagger] - 2\text{Tr}[h \cdot \tilde{m}_\Psi^2 \cdot \bar{\gamma}_\Psi^{(1)} \cdot h^\dagger] \\
& - 2(\tilde{m}_\Phi^2 (126(|\gamma|^2 \bar{\gamma}_\Sigma^{(1)} + |\bar{\gamma}|^2 \bar{\gamma}_\Sigma^{(1)}) + 84|\kappa|^2 \bar{\gamma}_\Theta^{(1)}) \\
& + \bar{\gamma}_\Phi^{(1)} (126(|\gamma|^2 m_\Sigma^2 + 126(|\bar{\gamma}|^2 m_\Sigma^2 + 84|\kappa|^2 m_\Theta^2) + \text{Tr}[\tilde{m}_\Psi^2 \cdot h^\dagger \cdot \bar{\gamma}_\Psi^{(1)} \cdot h]) - 2\check{\gamma}_H^{(2)} - \check{\gamma}_H^{(2)} \\
& - \dot{\gamma}_H^{(2)} - 2\text{Re}[\dot{\gamma}_H^{(2)}] + 2g_{10}^2 (2m_H^2 (1512|\kappa|^2 + 2520|\gamma|^2 + 2520|\bar{\gamma}|^2 + 54\text{Tr}[h^\dagger \cdot h]) \\
& + 2(1512|\tilde{\kappa}|^2 + 2520|\tilde{\gamma}|^2 + 2520|\tilde{\gamma}|^2 + 54\text{Tr}[h^\dagger \cdot h]) - 2(1512\tilde{\kappa}\kappa^* + 2520\tilde{\gamma}\gamma^* \\
& + 2520\tilde{\gamma}\bar{\gamma}^* + 54\text{Tr}[\tilde{h} \cdot h^\dagger])M^\dagger - 2(1512\tilde{\kappa}^*\kappa + 2520\tilde{\gamma}^*\gamma + 2520\tilde{\gamma}^*\bar{\gamma} + 54\text{Tr}[\tilde{h}^\dagger \cdot h])M \\
& + 4(1512|\kappa|^2 + 2520|\gamma|^2 + 2520|\bar{\gamma}|^2 + 54\text{Tr}[h \cdot h^\dagger])MM^\dagger + 4(m_\Phi^2 (5040(|\gamma|^2 + |\bar{\gamma}|^2) \\
& + 3024|\kappa|^2) + 3024m_\Theta^2 |\kappa|^2 + 5040(m_\Sigma^2 |\gamma|^2 + m_\Sigma^2 |\bar{\gamma}|^2) + 108\text{Tr}[h^\dagger \cdot h \cdot \tilde{m}_\Psi^2])) \\
& + 15768g_{10}^4 |M|^2 + 36g_{10}^4 (m_H^2 - 8|M|^2) \tag{9.133}
\end{aligned}$$

$$\begin{aligned}
\beta_{m_\Theta^2}^{(2)} = & -2\bar{\gamma}_\Theta^{(2)}m_\Theta^2 - 4(m_\Phi^2\bar{\gamma}_\Phi^{(1)}(105(|\zeta|^2 + |\bar{\zeta}|^2) + 7(|\kappa|^2 + |\rho|^2)) + 7m_H^2\bar{\gamma}_H^{(1)}|\kappa|^2 \\
& + 7m_\Theta^2\bar{\gamma}_\Theta^{(1)}|\rho|^2 + 105(m_\Sigma^2\bar{\gamma}_\Sigma^{(1)}|\zeta|^2 + m_\Sigma^2\bar{\gamma}_\Sigma^{(1)}|\bar{\zeta}|^2)) \\
& - 2\text{Tr}[g.\bar{\gamma}_\Psi^{(1)}.\tilde{m}_\Psi^2.g^\dagger] - 2\text{Tr}[g.\tilde{m}_\Psi^2.\bar{\gamma}_\Psi^{(1)}.g^\dagger] - 2(\bar{\gamma}_\Phi^{(1)}(7|\kappa|^2m_H^2 + 7|\Theta|^2m_\Theta^2 \\
& + 105|\zeta|^2m_\Sigma^2 + 105|\bar{\zeta}|^2m_\Sigma^2) + 7|\kappa|^2m_\Phi^2\bar{\gamma}_H^{(1)} + 7|\rho|^2m_\Phi^2\bar{\gamma}_\Theta^{(1)} + 105|\zeta|^2m_\Phi^2\bar{\gamma}_\Sigma^{(1)} \\
& + 105|\bar{\zeta}|^2m_\Phi^2\bar{\gamma}_\Sigma^{(1)} + \text{Tr}[\tilde{m}_\Psi^2.g^\dagger.\bar{\gamma}_\Psi^{(1)}.g]) - 2\check{\gamma}_\Theta^{(2)} - \check{\gamma}_\Theta^{(2)} - \check{\gamma}_\Theta^{(2)} - 2\text{Re}[\check{\gamma}_\Theta^{(2)}] \\
& + 2g_{10}^2(2\tilde{m}_\Theta^2(42|\kappa|^2 + 84|\rho|^2 + 1470|\zeta|^2 + 1470|\bar{\zeta}|^2 + 6\text{Tr}[g^\dagger.g]) \\
& + 2(42|\tilde{\kappa}|^2 + 84|\tilde{\rho}|^2 + 1470|\tilde{\zeta}|^2 + 1470|\tilde{\bar{\zeta}}|^2 + 6\text{Tr}[g^\dagger.g]) \\
& - 2(42\tilde{\kappa}\kappa^* + 84\tilde{\rho}\rho^* + 1470\tilde{\zeta}\zeta^* + 1470\tilde{\bar{\zeta}}\bar{\zeta}^* + 6\text{Tr}[\tilde{g}.g^\dagger])M^\dagger \\
& - 2(42\tilde{\kappa}^*\kappa + 84\tilde{\rho}^*\rho + 1470\tilde{\zeta}^*\zeta + 1470\tilde{\bar{\zeta}}^*\bar{\zeta} + 6\text{Tr}[\tilde{g}^\dagger.g])M \\
& + 4(42|\kappa|^2 + 84|\rho|^2 + 1470|\zeta|^2 + 1470|\bar{\zeta}|^2 + 6\text{Tr}[g.g^\dagger])MM^\dagger \\
& + 4(m_\Phi^2(1470(|\zeta|^2 + |\bar{\zeta}|^2) + 42|\kappa|^2 + 84|\rho|^2) + 42m_H^2|\kappa|^2 + 84m_\Theta^2|\rho|^2 \\
& + 1470(m_\Sigma^2|\zeta|^2 + m_\Sigma^2|\bar{\zeta}|^2) + 6\text{Tr}[g^\dagger.g.\tilde{m}_\Psi^2]) + 39816g_{10}^4|M|^2 \\
& + 84g_{10}^4(28m_\Theta^2 - 8|M|^2)
\end{aligned} \tag{9.134}$$

$$\begin{aligned}
\beta_{m_\Sigma^2}^{(2)} = & -2\bar{\gamma}_\Sigma^{(2)}m_\Sigma^2 - 4(m_\Phi^2\bar{\gamma}_\Phi^{(1)}(200|\eta|^2 + 100|\zeta|^2 + 10|\gamma|^2) + 10m_H^2\bar{\gamma}_H^{(1)}|\gamma|^2 \\
& + 100m_\Theta^2\bar{\gamma}_\Theta^{(1)}|\zeta|^2 + 200m_\Sigma^2\bar{\gamma}_\Sigma^{(1)}|\eta|^2) - 2(\bar{\gamma}_\Phi^{(1)}(10|\gamma|^2m_H^2 + 100|\zeta|^2m_\Theta^2) \\
& + \bar{\gamma}_\Theta^{(1)}(200|\eta|^2m_\Sigma^2 + 100|\zeta|^2m_\Phi^2) + 200|\eta|^2m_\Theta^2\bar{\gamma}_\Sigma^{(1)} + 10|\gamma|^2m_\Phi^2\bar{\gamma}_H^{(1)}) \\
& - 2\check{\gamma}_\Sigma^{(2)} - \check{\gamma}_\Sigma^{(2)} - \check{\gamma}_\Sigma^{(2)} - 2\text{Re}[\check{\gamma}_\Sigma^{(2)}] \\
& + 2g_{10}^2(2m_\Sigma^2(2400|\eta|^2 + 40|\gamma|^2 + 1000|\zeta|^2) + 2(2400|\tilde{\eta}|^2 + 40|\tilde{\gamma}|^2 + 1000|\tilde{\zeta}|^2) \\
& - 2(2400\tilde{\eta}\eta^* + 40\tilde{\gamma}\gamma^* + 1000\tilde{\zeta}\zeta^*)M^\dagger - 2(2400\tilde{\eta}^*\eta + 40\tilde{\gamma}^*\gamma + 1000\tilde{\zeta}^*\zeta)M \\
& + 4(2400|\eta|^2 + 40|\gamma|^2 + 1000|\zeta|^2)MM^\dagger + 4(m_\Phi^2(2400|\eta|^2 + 1000|\zeta|^2 + 40|\gamma|^2) \\
& + 40m_H^2\bar{\gamma}_H^{(1)}|\kappa|^2 + 1000m_\Theta^2\bar{\gamma}_\Theta^{(1)}|\zeta|^2 + 2400m_\Sigma^2\bar{\gamma}_\Sigma^{(1)}|\eta|^2) + 48600g_{10}^4|M|^2 \\
& + 100g_{10}^4(35m_\Sigma^2 - 8|M|^2)
\end{aligned} \tag{9.135}$$

$$\begin{aligned}
\beta_{m_\Sigma^2}^{(2)} = & -2\bar{\gamma}_\Sigma^{(2)} m_\Sigma^2 - 4(m_\Phi^2 \bar{\gamma}_\Phi^{(1)} (200|\eta|^2 + 100|\bar{\zeta}|^2 + 10|\bar{\gamma}|^2) + 10m_H^2 \bar{\gamma}_H^{(1)} |\bar{\gamma}|^2 \\
& + 100m_\Theta^2 \bar{\gamma}_\Theta^{(1)} |\bar{\zeta}|^2 + 200m_\Sigma^2 \bar{\gamma}_\Sigma^{(1)} |\eta|^2) - 2\text{Tr}[f \cdot \bar{\gamma}_\Psi^{(1)} \cdot \tilde{m}_\Psi^2 \cdot f^\dagger] - 2\text{Tr}[f \cdot \tilde{m}_\Psi^2 \cdot \bar{\gamma}_\Psi^{(1)} \cdot f^\dagger] \\
& - 2(\bar{\gamma}_\Phi^{(1)} (10|\bar{\gamma}|^2 m_H^2 + 100|\bar{\zeta}|^2 m_\Theta^2) + \bar{\gamma}_\Theta^{(1)} (200|\eta|^2 m_\Sigma^2 + 100|\bar{\zeta}|^2 m_\Phi^2)) + 200|\eta|^2 m_\Theta^2 \bar{\gamma}_\Sigma^{(1)} \\
& + 10|\bar{\gamma}|^2 m_\Phi^2 \bar{\gamma}_H^{(1)} + \text{Tr}[\tilde{m}_\Psi^2 \cdot f^\dagger \cdot \bar{\gamma}_\Psi^{(1)} \cdot f]) - 2\check{\gamma}_\Sigma^{(2)} - \check{\gamma}_\Sigma^{(2)} - \check{\gamma}_\Sigma^{(2)} - 2\text{Re}[\dot{\lambda}_\Sigma^{(2)}] \\
& + 2g_{10}^2 (2\tilde{m}_\Sigma^2 (2400|\eta|^2 + 40|\bar{\gamma}|^2 + 1000|\bar{\zeta}|^2) + 2(2400|\tilde{\eta}|^2 + 40|\tilde{\gamma}|^2 + 1000|\tilde{\zeta}|^2) \\
& - 2(2400\tilde{\eta}\eta^* + 40\tilde{\gamma}\gamma^* + 1000\tilde{\zeta}\zeta^*)M^\dagger - 2(2400\tilde{\eta}^*\eta + 40\tilde{\gamma}^*\gamma + 1000\tilde{\zeta}^*\zeta)M \\
& + 4(2400|\eta|^2 + 40|\bar{\gamma}|^2 + 1000|\bar{\zeta}|^2)MM^\dagger + 4(m_\Phi^2 (2400|\eta|^2 + 1000|\bar{\zeta}|^2 + 40|\bar{\gamma}|^2) \\
& + 40m_H^2 |\bar{\gamma}|^2 + 1000m_\Theta^2 |\bar{\zeta}|^2 + 2400m_\Sigma^2 \bar{\gamma}_\Sigma^{(1)} |\eta|^2 - 40\text{Tr}[f^\dagger \cdot f \cdot \tilde{m}_\Psi^2]) \\
& + 48600g_{10}^4 |M|^2 + 100g_{10}^4 (35m_\Sigma^2 - 8|M|^2) \tag{9.136}
\end{aligned}$$

$$\begin{aligned}
\beta_{m_\Psi^2}^{(2)} = & -\tilde{m}_\Psi^2 \cdot \bar{\gamma}_\Psi^{(2)} - \bar{\gamma}_\Psi^{(2)T} \cdot m_\Psi^2 - 4(20m_H^2 \bar{\gamma}_H^{(1)} h^\dagger \cdot h + 240m_\Theta^2 \bar{\gamma}_\Theta^{(1)} g^\dagger \cdot g + 504\tilde{m}_\Sigma^2 \bar{\gamma}_\Sigma^{(1)} f^\dagger \cdot f \\
& + 10h^\dagger \cdot m_\Psi^2 \cdot \bar{\gamma}_\Psi^{(1)} \cdot h + 120g^\dagger \cdot m_\Psi^2 \cdot \bar{\gamma}_\Psi^{(1)} \cdot g + 252f^\dagger \cdot m_\Psi^2 \cdot \bar{\gamma}_\Psi^{(1)} \cdot f + 10h^\dagger \cdot \bar{\gamma}_\Psi^{(1)T} \cdot m_\Psi^2 \cdot h \\
& + 120g^\dagger \cdot \bar{\gamma}_\Psi^{(1)T} \cdot m_\Psi^2 \cdot g + 252f^\dagger \cdot \bar{\gamma}_\Psi^{(1)T} \cdot m_\Psi^2 \cdot f) - 2(10m_H^2 h^\dagger \bar{\gamma}_\Psi^{(1)T} \cdot h + 120m_\Theta^2 g^\dagger \bar{\gamma}_\Psi^{(1)T} \cdot g \\
& + 252m_\Sigma^2 f^\dagger \bar{\gamma}_\Psi^{(1)T} \cdot f \\
& + m_\Psi^2 (10\bar{\gamma}_H^{(1)} h^\dagger h + 120\bar{\gamma}_\Theta^{(1)} g^\dagger g + 252\bar{\gamma}_\Sigma^{(1)} f^\dagger f)) - 2\check{\gamma}_\Psi^{(2)} - \check{\gamma}_\Psi^{(2)} - \check{\gamma}_\Psi^{(2)} - \dot{\gamma}_\Psi^{(2)} - \dot{\gamma}_\Psi^{(2)\dagger} \\
& + 2g_{10}^2 (\tilde{m}_\Psi^2 (45h^\dagger \cdot h + 1260g^\dagger \cdot g + 3150f^\dagger \cdot f) + (45h^\dagger \cdot h + 1260g^\dagger \cdot g + 3150f^\dagger \cdot f) \tilde{m}_\Psi^{2T} \\
& + 4(45m_H^2 h^\dagger h + 1260m_\Theta^2 g^\dagger g + 3150m_\Sigma^2 f^\dagger f + m_\Psi^2 (45h^\dagger \cdot h + 1260g^\dagger \cdot g + 3150f^\dagger \cdot f)) \\
& + 2(45\tilde{h}^\dagger \cdot \tilde{h} + 1260\tilde{g}^\dagger \cdot \tilde{g} + 3150\tilde{f}^\dagger \cdot \tilde{f}) - 2(45\tilde{h}^\dagger \cdot h + 1260\tilde{g}^\dagger \cdot g + 3150\tilde{f}^\dagger \cdot f)M \\
& + 2(45h^\dagger \cdot \tilde{h} + 1260g^\dagger \cdot \tilde{g} + 3150f^\dagger \cdot \tilde{f})M^\dagger + 4(45h^\dagger \cdot h + 1260g^\dagger \cdot g + 3150f^\dagger \cdot f)MM^\dagger) \\
& + \frac{80055}{4} g_{10}^4 MM^\dagger + 45g_{10}^4 (2m_\Psi^2 - 8MM^\dagger) \tag{9.137}
\end{aligned}$$

Chapter 10

Summary

The new minimal supersymmetric SO(10) GUT (NMSGUT) based on Higgs system $10+120+210+126+\overline{126}$, 16 dimensional matter fermion representation and 45 dimensional gauge field representation is a promising candidate theory of particle physics beyond standard model. The structural features of NMSGUT e.g. symmetry breaking scheme of GUT (in terms of a single complex parameter), calculable GUT scale spectra, GUT scale threshold effects etc. make this theory very appealing. The successful embedding of Seesaw mechanism to explain neutrino masses compatible with the neutrino oscillations, t-b- τ Yukawa unification in the large $\tan\beta$ regime, facilitation of LSP WIMP as a dark matter candidate due to preservation of R-parity at weak scale etc are other features of NMSGUT.

Present work is basically a step towards the promotion of this structurally rich theory. This dissertation comprises the study of various problems like effect of GUT scale threshold corrections on SO(10) Yukawa and consequently suppression of d=5, $\Delta B \neq 0$ operator, Supersymmetric seesaw inflection point inflation (SSI), reheating in context of SSI, embedding of SSI in NMSGUT and BICEP2 revolution, relic density calculation using DarkSusy for NMSGUT generated soft spectra and finally the NMSGUT RGEs for the evolution between M_{Planck} and M_{GUT} .

In Chapter 2, we reviewed the NMSGUT, its complete superpotential, Higgs system, symmetry breaking scheme, GUT scale spectrum, importance of GUT scale

threshold corrections to α_3, α_s, M_X and $d=5, \Delta B \neq 0$ operator responsible for proton decay. But with these operators the resulting proton decay rate comes out 6-7 orders of magnitude faster than experimental bound.

In Chapter 3, we presented a generic mechanism for suppression of $\Delta B \neq 0$ operators. The GUT scale threshold corrections to fermion, anti-fermion and Higgs line leading to SO(10) Yukawa vertex play an important role in fermion fitting. The corrections to Higgs line are large which results in the lowering of SO(10) Yukawa required to match with MSSM Yukawa while fitting. These lowered Yukawas then determine the $\Delta B \neq 0$ operators which gives proton decay rates $O(10^{-34} yr s^{-1})$.

After reviewing inflation and inflection point inflation in the Dirac-neutrino-inflation scenario in Chapter 4, we showed that the Majorana-neutrino-inflation scenario is not only possible but more plausible than the Dirac neutrino based inflection in Chapter 5. In Majorana-neutrino-inflation scenario, the inflation parameters and thus the inflation conditions are determined in terms of Seesaw superpotential parameters. Fine tuning conditions are less severe and more stable. Reheating in such scenario can occur via instant preheating. After the end of inflation the inflaton can decay non-perturbatively in the modes which get inflaton vev induced mass. These modes further decay into MSSM degrees of freedom which gets thermalized due to scattering leading to a temperature of $10^{11} - 10^{13}$ GeV.

In Chapter 7, the embedding of SSI in NMSGUT is studied. The required number of e-folds for sufficient reheating requires small quartic coupling which seems hard to achieve in NMSGUT along with fermion fitting. An important outcome of this study was that the fermion fitting in NMSGUT is possible even with small value of $\tan\beta \approx 2.50$. It implies that NMSGUT is viable on the entire range of $\tan\beta$.

In Chapter 8 we showed that the lightest neutralino (Bino in our case) relic density calculations for dark matter put constraints on NMSGUT generated s-particle spectrum. For a heavy spectrum with all s-fermion of $O(10 \text{ TeV})$ relic density comes out to be very large. But with spectrum having one light s-fermion like smuon having mass comparable to Bino gives reasonable relic density for smuon since it provides

a viable co-annihilation channel.

In the Final Chapter 9 we presented the importance of NMSGUT RGEs is in the region between Planck and GUT scale. The soft parameters for the Higgs mass squares comes out to be negative which is a very peculiar behavior of NMSGUT soft parameters at GUT scale and it needs at least one of the mass square of a Higgs representation out of six to be negative. We see from the RGE flow for soft parameters from Planck scale (throwing value of $m_{3/2}$) to GUT scale gives negative mass squares for some Higgs representations. Thus negative NUHM proceeding from a SUGRA seed of universal soft scalar masses may be an inherent property of NMSGUT.

Our work has further strengthened the viability of the NMSGUT by solving the longstanding d=5 fast B violation problem. It has widened the ambit of the theory even further by showing its relevance for inflationary and dark matter cosmology.

The SO(10) RGE's for this complex model have been calculated to two loops for the first time and shown to justify the negative Higgs squared soft masses assumed in our NMSGUT fits.

These explorations have defined a number of problems for continued research which we are pursuing.

Bibliography

- [1] ATLAS Collaboration, G. Aad et al., Phys.Lett. **B716**, 1 (2012), [arXiv:hep-ph/1207.7214].
- [2] CMS Collaboration, S. Chatrchyan et al., Phys.Lett. **B716**, 30 (2012) , [arXiv:hep-ph/1207.7235].
- [3] J. Beringer et al. (Particle Data Group), Phys. Rev. D **86**, 010001(2012).
- [4] K. S. Hirata et al. [Kamiokande-II collaboration], Phys. Rev. Lett. **63**, 16 (1989); Phys. Rev. Lett. **65**, 1297 (1990); Phys. Rev. Lett. **65**, 1301 (1990).
- [5] S. Fukuda et al. [Super-Kamiokande Collaboration], Phys. Rev. Lett. **86**, 5651 (2001) [arXiv:hep-ex/0103032]; Phys. Rev. Lett. **86**, 5656 (2001) [arXiv:hep-ex/0103033].
- [6] J. C. Pati and Salam, “Lepton number as the fourth color”, Phys. Rev. D **10**,275 (1974).
- [7] H. Georgi and S. L. Glashow, “Unity of all elementary particle forces”, Phys. Rev. Lett. **32**, 438 (1974).
- [8] H. Fritzsch and P. Monkowski, “Unified interactions of Leptons and Hadrons”, Annals Phys. **93**, 193 (1975).
- [9] P. Minkowski, Phys. Lett. **B67**,110 (1977); M. Gell-Mann, P. Ramond and R. Slansky, in *Supergravity*, eds. P. van Nieuwenhuizen and D.Z. Freedman (North Holland 1979); T. Yanagida, in Proceedings of *Workshop on Unified Theory and*

- Baryon number in the Universe*, eds. O. Sawada and A. Sugamoto (KEK 1979); R.N. Mohapatra and G. Senjanović, Phys. Rev. Lett. **44**, 912 (1980); R.N. Mohapatra and G. Senjanović, Phys. Rev. **D23**,165 (1981); G. Lazarides, Q. Shafi and C. Wetterich, Nucl. Phys. **B181**, 287 (1981).
- [10] M.S. Carena, M. Olechowski, S. Pokorski and C. E. M. Wagner, Nucl. Phys. B **426**, 269 (1994) [arXiv:hep-ph/9402253]; B. Ananthanarayan, Q. Shafi and X. M. Wang, Phys. Rev. D **50**, 5890 (1994) [arXiv:hep-ph/9311225]; R. Rattazzi, U. Sarid and L.J. Hall, [arXiv:hep-ph/9405313];
- [11] L.J. Hall, R. Rattazzi and U. Sarid, Phys. Rev. D **50**, 7048 (1994) [arXiv:hep-ph/9306309]; R. Hempfling, Phys. Rev. D **49**, 6168 (1994).
- [12] C. S. Aulakh, K. Benakli and G. Senjanovic, Phys. Rev. Lett. **79**, 2188 (1997) [arXiv:hep-ph/9703434]
- [13] C. S. Aulakh, A. Melfo and G. Senjanovic, Phys. Rev. D **57**,4174 (1998) [arXiv:hep-ph/9707256];
- [14] C. S. Aulakh, A. Melfo, A. Rasin and G. Senjanovic, Phys. Lett. B **459**, 557 (1999) [arXiv:hep-ph/9902409].
- [15] C. S. Aulakh, B. Bajc, A. Melfo, A. Rasin and G. Senjanovic, Nucl. Phys. B **597**, 89 (2001) [arXiv:hep-ph/0004031].
- [16] C. S. Aulakh and R.N. Mohapatra, CCNY-HEP-82-4 April 1982, CCNY-HEP-82-4-REV, Jun 1982 , Phys. Rev. **D28**, 217 (1983).
- [17] T. E. Clark, T. K. Kuo, and N. Nakagawa, Phys. Lett. **115B**, 26 (1982).
- [18] K. S. Babu and R. N. Mohapatra, Phys. Rev. Lett. **70**,2845 (1993).
- [19] C. S. Aulakh, B. Bajc, A. Melfo, G. Senjanovic and F. Vissani, Phys. Lett. B **588**, 196 (2004) [arXiv:hep-ph/0306242].
- [20] B. Bajc, A. Melfo, G. Senjanovic and F. Vissani, Phys. Rev. D **70**, 035007 (2004) [arXiv:hep-ph/0402122].

- [21] B. Bajc, A. Melfo, G. Senjanovic and F. Vissani, Phys. Lett. B **634** (2006) 272 [hep-ph/0511352].
- [22] B. Bajc, G. Senjanovic and F. Vissani, Phys. Rev. Lett. **90** (2003) 051802 [hep-ph/0210207].
- [23] C. S. Aulakh and A. Girdhar, hep-ph/0204097; v2 August 2003; v4, 9 February, 2004; Int. J. Mod. Phys. A **20**, 865 (2005).
- [24] C. S. Aulakh and A. Girdhar, Nucl. Phys. B **711**, 275 (2005).
- [25] T. Fukuyama, A. Ilakovac, T. Kikuchi, S. Meljanac and N. Okada, Eur. Phys. J. C **42**, 191 (2005) [arXiv:hep-ph/0401213v1.,v2].
- [26] V.V. Dixit and M. Sher, Phys. Rev. D **40**, 3765 (1989).
- [27] C. S. Aulakh and S. K. Garg, Nucl.Phys. **B857**,101-142 (2012); C. S. Aulakh and S. K. Garg, *NMSGUT II: Fermion Fits and Soft spectra*, arXiv:hep-ph/0807.0917v2.
- [28] C. S. Aulakh, “NMSGUT III: Grand Unification Upended” [arXiv:hep-ph/1107.2963v1].
- [29] C. S. Aulakh, I. Garg and C. K. Khosa, Nucl. Phys. B **882**, 397 (2014) [arXiv:hep-ph/1311.6100].
- [30] Charanjit Kaur, “Study of Baryon Number and Lepton Flavor Violation in the New Minimal Supersymmetric SO(10) GUT”, Ph.D Thesis, Panjab Uni. Chandigarh, 2014.
- [31] C. S. Aulakh and I. Garg, Phys. Rev. D. **86**, 065001 (2012) [arXiv:hep-ph/1201.0519v4].
- [32] C. S. Aulakh, B. Bajc, A. Melfo, A. Rasin and G. Senjanovic, Phys. Lett. B **460** (1999) 325 [hep-ph/9904352].

- [33] C. S. Aulakh and S. K. Garg, Nucl. Phys. B **757**, 47 (2006) [arXiv:hep-ph/0512224].
- [34] C. S. Aulakh, *From germ to bloom* [arXiv:hep-ph/0506291].
- [35] M. Fukugita and T. Yanagida, Phys. Lett. B **174**, 45 (1986).
- [36] S. Weinberg, Phys. Lett. **91B**, 5 (1980).
- [37] L.J. Hall, Nucl. Phys. **B178**, 75 (1981).
- [38] S. P. Martin, M. T. Vaughn, Phys. Rev. **D50** 2282, (1994) [arXiv:hep-ph/9311340].
- [39] S. Antusch and M. Spinrath, Phys. Rev. D **78**, 075020 (2008) [arXiv:0804.0717 [hep-ph]].
- [40] Numerical Recipes in Fortran 90, Second Edition(1996), Cambridge Univ. Press, W. H. Press, S. A. Teukolsky, W. T. Vetterling, and B. P. Flannery.
- [41] L. Lavoura, H Kühböck, W. Grimus, Nucl. Phys. B **754**,1 (2006) [arXiv:0603259 [hep-ph]].
- [42] D. M. Pierce, J. A. Bagger, K. T. Matchev and R. j. Zhang, Nucl. Phys. B **491**, 3 (1997) [arXiv:hep-ph/9606211].
- [43] W. Porod, Comput. Phys. Commun. **153**, 275 (2003) [arXiv:hep-ph/0301101].
- [44] H. E. Haber et al. Phys.Lett. B **306**, 327-334 (1993) [arXiv:hep-ph/9302228]; H. E. Haber [arXiv:hep-ph/9505240], A. Arbey et al. Phys.Lett. B **708**, 162-169 (2012) [arXiv:hep-ph/1112.3028]; A. Arbey et al. JHEP **1209**,107 (2012) [arXiv:hep-ph/1207.1348].
- [45] A. Arvanitaki, N. Craig, S. Dimopoulos and G. Villadoro, JHEP **1302**, 126 (2013) [arXiv:1210.0555 [hep-ph]].
- [46] Y. Hayato *et al.* [Super-Kamiokande Collaboration], Phys. Rev. Lett. **83**, 1529 (1999) [hep-ex/9904020].

- [47] S. Weinberg, Phys. Rev. Lett. **43**, 1566 (1979).
- [48] N. Sakai and T. Yanagida, Nucl. Phys. B **197**, 533 (1982).
- [49] V. Lucas and S. Raby, Phys. Rev. D **55**, 6986 (1997) [arXiv:hep-ph/9610293].
- [50] T. Goto and T. Nihei, Phys. Rev. D **59**, 115009 (1999) [arXiv:hep-ph/9808255].
- [51] B. D. Wright [arXiv:hep-ph/9404217] (1994).
- [52] J. Wess and B. Zumino, Phys. Lett. B **37**, 95 (1971); J. Iliopoulos and B. Zumino, Nucl. Phys. B **76**, 310, (1974); S. Ferrara, J. Iliopoulos and B. Zumino, Nucl. Phys. B **77**, 413, (1974); B. Zumino, Nucl. Phys. B **89**, 535, (1975); S. Ferrara and O. Piguet, Nucl. Phys. B **93**, 261, (1975); M. Grisaru, W. Siegel, and M. Rocek, Nucl. Phys. B **159**, 429, (1979).
- [53] P. Langacker and N. Polonsky, Phys. Rev. D **47**, 4028 (1993) [arXiv:hep-ph/9210235]; P. Langacker and N. Polonsky, Phys. Rev. D **52**, 3081 (1995) [arXiv:hep-ph/9503214].
- [54] J. Ellis, G. Ridolfi, F. Zwirner, Phys. Lett. **B262**, 477 (1991).
- [55] ATLAS and CMS results reported at SUSY2013, ICTP Trieste, August 2013.
- [56] A. Kusenko, P. Langacker and G. Segre, Phys. Rev. D **54**, 5824 (1996) [hep-ph/9602414].
- [57] A. A. Penzias and R.W. Wilson Ap.J. **142**,419-421 (1965).
- [58] A. H. Guth, Phys. Rev. **D 23**, 347356 (1981).
- [59] A. Albrecht and P. J. Steinhardt, Phys. Rev. Lett. **48**,1220 (1982).
- [60] S. W. Hawking, Phys. Lett. **B115**, 295 (1982)
- [61] A. A. Starobinsky, Phys. Lett. **B117**, 175 (1982)
- [62] A. H. Guth and S.-Y. Pi, Phys. Rev. Lett. **49**, 1110 (1982).

- [63] Andrew Liddle, “An Introduction to Modern Cosmology” (John Wiley and Sons Ltd. 2003).
- [64] G. F. Smoot, C. L. Bennett, A. Kogut, E. L. Wright, J. Aymon, N. W. Boggess, E. S. Cheng and G. De Amici *et al.*, *Astrophys. J.* **396**, L1 (1992) ; G. F. Smoot *et al.*, *Astroph J.* 396, L1 (1992).
- [65] E. Komatsu *et. al.* [WMAP Coallaboration], *Astrophys. J. Suppl.* **192**, 18 (2011)[arXiv:1001.4538[astro-ph.CO]].
- [66] P. A. R. Ade *et al.* [BICEP2 Collaboration], *Phys. Rev. Lett.* **112**, 241101 (2014) [arXiv:1403.3985 [astro-ph.CO]].
- [67] R. Allahverdi, K. Enqvist, J. Garcia-Bellido and A. Mazumdar, *Phys. Rev. Lett.* **97**, 191304 (2006) [arXiv:hep-ph/0605035]
- [68] R. Allahverdi, B. Dutta, A. Mazumdar, *Phys. Rev. D***75**, 075018 (2007)[arXiv:hep-ph/0702112].
- [69] R. Allahverdi, B. Dutta, Y. Santoso, *Phys. Rev. D***82**, 035012 (2010)[arXiv:hep-ph/1004.2741].
- [70] K. Enqvist and A. Mazumdar, *Phys. Rept.* **380**, 99 (2003).
- [71] M. Dine and A. Kusenko, *Rev. Mod. Phys.* **76**, 1 (2004).
- [72] A. Mazumdar, J. Rocher, *Phys. Rept.* **497**, 85-215 (2011)[arXiv:1001.0993 [hep-ph]].
- [73] F. Buccella, J. P. Derendinger, S. Ferrara and C. A. Savoy, *Phys. Lett.* **B115**, 375 (1982).
- [74] I. Affleck, M. Dine, and N. Seiberg, *Nucl. Phys.* **B241** , 493 (1984) ; *Nucl. Phys.* **B256**,557 (1985).
- [75] T. Gherghetta, C. F. Kolda and S. P. Martin, *Nucl. Phys. B* **468**,37 (1996) [hep-ph/9510370].

- [76] M. A. Luty and W. Taylor, Phys. Rev. D **53**,3399 (1996)[hep-th/9506098].
- [77] R. Allahverdi, A. Kusenko and A. Mazumdar, JCAP **0707**, 018 (2007) [arXiv:hep-ph/0608138]; R. Allahverdi, B. Dutta and A. Mazumdar, Phys. Rev. Lett. **99**, 261301 (2007) [arXiv:0708.3983 [hep-ph]].
- [78] S. Hotchkiss, A. Mazumdar and S. Nadathur, JCAP **1106**,002 (2011) [arXiv:1101.6046 [astro-ph.CO]].
- [79] J. C. Bueno Sanchez, K. Dimopoulos and D. H. Lyth, JCAP **0701**,015 (2007) [hep-ph/0608299]; R. Allahverdi, K. Enqvist, J. Garcia-Bellido, A. Jokinen and A. Mazumdar, JCAP **0706**, 019 (2007) [arXiv:hep-ph/0610134].
- [80] D. H. Lyth and E. D. Stewart, Phys. Lett. B **283**,189 (1992).
- [81] A. R Liddle and S. M Leach, Phys. Rev. D **68**, 103503 (2003) [astro-ph/0305263].
- [82] H. Murayama, H. Suzuki, T. Yanagida and J. Yokoyama, Phys. Rev. Lett. **70**,1912 (1993).
- [83] J. R. Ellis, M. Raidal and T. Yanagida, Phys. Lett. B **581**,9 (2004) [hep-ph/0303242].
- [84] G. Felder, L. Kofman and A. Linde, Phys. Rev. D **59**,123523-1 (1999) [arXiv:hep-ph/9812289].
- [85] E. J. Ahn and E. W. Kolb, Phys. Rev. D **74**, 103503 (2006) [astro-ph/0508399].
- [86] R. Allahverdi, A. Ferrantelli, J. Gracia-Bellido and A. Mazumdar, Phys. Rev.D **83**, 123507 (2011).
- [87] L. Kofman, A. Linde and A. A. Starobinsky, Phys. Rev. Lett. **73**, 3195 (1994) ;Phys. Rev. D **56**, 06 (1997).
- [88] Y. Shtanov, J. H. Traschen and R. H. Brandenberger, Phys. Rev.D **51**, 5438 (1995) [arXiv:hep-ph/9407247].

- [89] S. Davidson and S. Sarkar, JHEP 0011, 012 (2000)[arXiv:hep-ph/0009078].
- [90] M. Kawasaki, K. Kohri and T. Moroi , Phys. Rev. D **71**,083502 (2005).
- [91] Amjad Ashoorioon, P. S. Bhupal Dev and Anupam Mazumdar, Mod. Phys. Lett. A **29**, 1450163 (2014) [arXiv:1211.4678v2]
- [92] L. M. Krauss and F. Wilczek, Phys. Rev. D **89**, 047501 (2014) [arXiv:1309.5343].
- [93] PLANCK Collaboration [arXiv:1405.0871v1]; [arXiv:1405.0872v1]; [arXiv:1405.0873v1]; [arXiv:1405.0874v2].
- [94] R. Flauger, J. C. Hill, and D. N. Spergel, [astro-ph.CO/arXiv:1405.7351v1].
- [95] M. J. Mortonson and U. Seljak, [astro-ph.CO/arXiv:1405.5857v1].
- [96] D. H. Lyth, Phys. Rev. Lett. **78**,1861 (1997)[hep-ph/9606387].
- [97] S. Antusch and D. Nolde, JCAP **1405**, 035 (2014) [arXiv:1404.1821 [hep-ph]].
- [98] P. A. R. Ade et al. [Planck Collaboration], 2013 [arXiv:1303.5076v1[astro-ph.CO]].
- [99] D. Hanson *et al.*, Phys. Rev. Lett. **111**, 141301 (2013).
- [100] P. Gondolo et. al.,JCAP **07**,008 (2004) [arXiv:astro-ph/0406204]
<http://www.fysik.su.se/edsjo/darksusy/>
- [101] J. H. Oort, Bulletin of the Astronomical Institute of the Netherlands. **6**, 249 (1932).
- [102] F. Zwicky Ap.J. **86**, 217-246 (1937).
- [103] V. Rubin, Scientific American **248**,96-108 (1983).
- [104] D. Clowe et. al., Ap.J.**648**, 109 (2006).

-
- [105] R. Bernabei et al., [DAMA collaboration] *Eur.Phys.J* **C56**, 333-355 (2008)[arXiv:0804.2741 [astro-ph]].
- [106] K. N. Abazajian et al., *JCAP* **11**, 041 (2010).
- [107] S. P. Martin, hep-ph/9709356(2008).
- [108] K. Griest and D. Seckel, *Phys. Rev. D* **43**, 3191 (1991).
- [109] P. Gondolo and G. Gelmini, *Nucl. Phys. B* **360**, 145 (1991).
- [110] J. Edsjö and P. Gondolo, *Phys. Rev.* **D56**, 1879 (1997) [arXiv:hep-ph/1311.6100].
- [111] P. Skands et. al. *JHEP* **07**, 036 (2004) [arXiv:hep-ph/0311123v4].
- [112] G. Jungman et al. *Physics Reports* **267**,195-373 (1996).
- [113] W. J. Marciano and G. Senjanovic, *Phys. Rev. D* **25**, 3092 (1982); U. Amaldi, W. de Boer and H. Furstenau, *Phys. Lett. B* **260**, 447 (1991).
- [114] R. M. Fonseca, *Comput. Phys. Commun.* **183**, 2298 (2012) [arXiv:1106.5016 [hep-ph]].
- [115] W. Siegel, *Phys. Lett. B* **84**, 193, (1979); D. M. Capper, D. R. T. Jones and P. van Nieuwenhuizen, *Nucl. Phys. B* **167**, 479, (1980).
- [116] C. S. Aulakh, I. Garg and C. K. Khosa, to Appear.
- [117] M. Drees, R. Godbole and P. Roy, “Theory and Phenomenology of Sparticles”, World Scientific Publishing Co. Pte. Ltd.